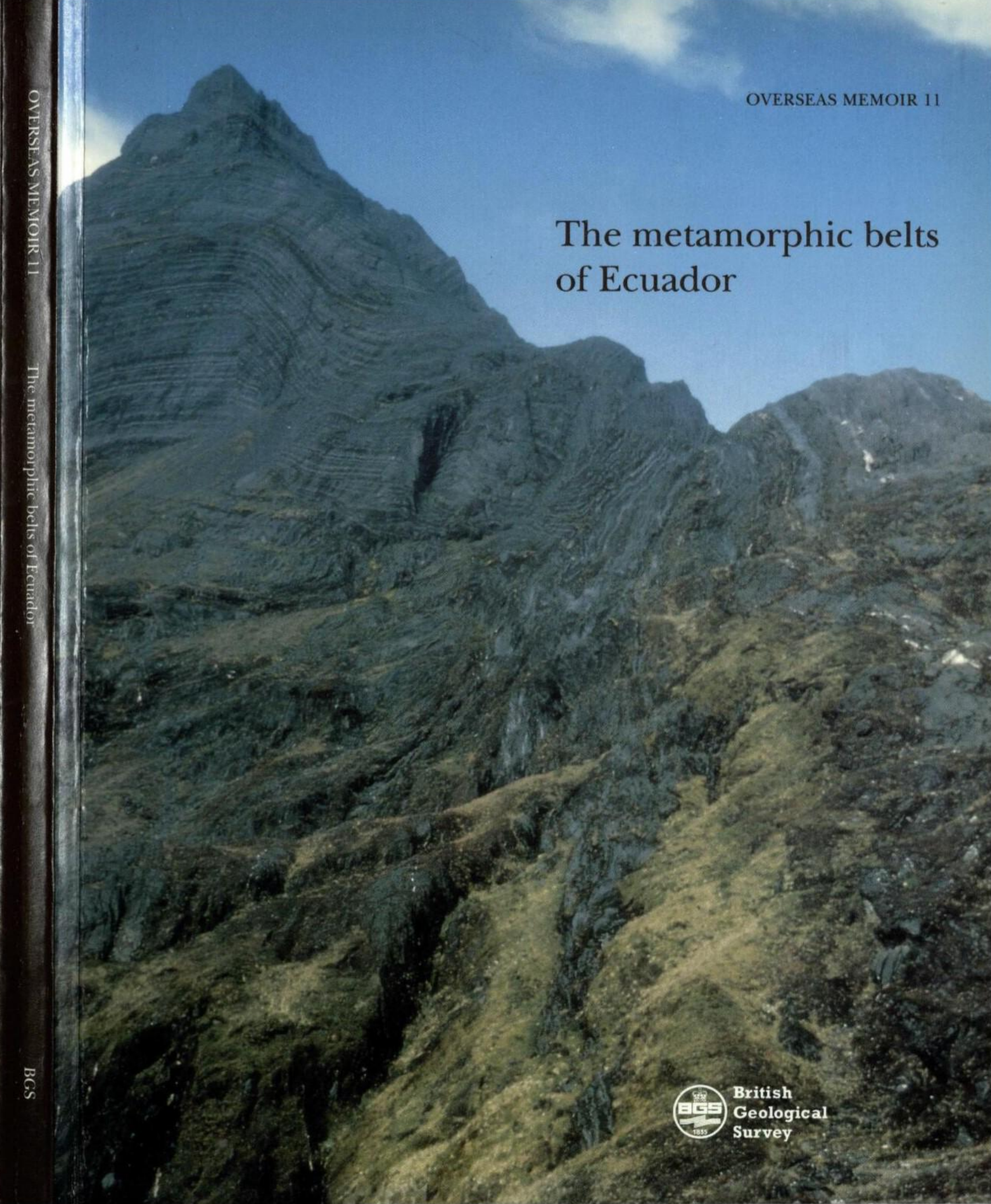

OVERSEAS MEMOIR 11

The metamorphic belts of Ecuador

British Geological Survey

OVERSEAS MEMOIR 11 The metamorphic belts of Ecuador BGS

The metamorphic belts of Ecuador

Cover photograph

Cerro Hermoso in the Llanganates mountains, a folded and metamorphosed carbonate sequence, recently glaciated

Cerro Hermoso (4571m) from the south-west, a folded carbonate sequence and the highest point in the Llanganates mountains (photo: M. L.)

Project field party negociating the Río Parcayacu tributary along the Río Mulatos traverse (photo: M. L.).

Martin Litherland (left) and Gonzalo Viteri (‘The man with one hand’) (right) eating at camp. ֍

A camp by the Río Mulatos. ֍

Unloading the Land Rover, the Antisana volcano in the background. ֍

Nambija in 1988, polluted with mercury and arsenic, where pigs and children wade. ֍

Resting in the Río Mulatos. From left to right, Ramiro, David y Manuel.

Building a makeshift bridge to cross the Río Cascabel.

BRITISH GEOLOGICAL SURVEY

OVERSEAS MEMOIR 11

The metamorphic belts of Ecuador

M. Litherland, J. A. Aspden y

R. A. Jemielita

Keyworth, Nottingham British Geological Survey 1994

Primera publicación 1994

Bibliographic reference

LITHERLAND M., ASPDEN J. A. and JEMIELITA R. A. (1994) The metamorphic belts of Ecuador. *Overseas memoir of the British Geological Survey*, No. 11.

Authors

Martin Litherland, OBE, BSc, PhD, CGeol, MIMM
John A. Aspden, BSc, PhD
British Geological Survey

Richard A. Jemielita, BSc, PhD, MIMM
formerly of the British Geological Survey

BRITISH GEOLOGICAL SURVEY

Keyworth, Nottingham NG12 5GG

(0115) 936 3100

Murchison House, West Mains Road, Edinburgh
EH9 3LA 0131-667 1000

London Information Office, Natural History Museum
Earth Galleries, Exhibition Road, London SW7 2DE
0171-589 4090

The full range of Survey publications is available from the BGS Sales Desk at the Survey headquarters, Keyworth, Nottingham. The more popular maps and books may be purchased from BGS-approved stockists and agents and over the counter at the Bookshop, Gallery 37, Natural History Museum, Cromwell Road, (Earth Galleries), London. Sales Desks are also located at the BGS London Information Office, and at Murchison House, Edinburgh. The London Information Office maintains a reference collection of BGS publications including maps for consultation. Some BGS books and reports may also be obtained from HMSO Publications Centre or from HMSO bookshops and agents.

The British Geological Survey carries out the geological survey of Great Britain and Northern Ireland (the latter as an agency service for the government of Northern Ireland), and of the surrounding continental shelf, as well as its basic research projects. It also undertakes programmes of British technical aid in geology in developing countries as arranged by the Overseas Development Administration.

The British Geological Survey is a component body of the Natural Environment Research Council.

C13 12/94

ISBN 0 85272 239 7

Printed in England by Linney Colour Print Ltd

CONTENTS

PLATES

FIGURES

TABLES

MAPS

PREFACE

This Overseas Memoir reports on geological and mineral studies of the metamorphic rocks of Ecuador which are essentially confined to the Cordillera Real and El Oro metamorphic belts. The objectives were the elucidation of their nature, structure, relationships, genesis, and mineralisation, in response to the need for a geological and mineral database to support and promote a viable national mining industry. The work was carried out under the Cordillera Real Geological Research Project (1986-1993), a bilateral Technical Cooperation project between the Governments of Ecuador (Ministry of Energy and Mines) and the United Kingdom (Overseas Development Administration – ODA), using geoscientists from the Ecuadorian Mining Institute (INEMIN), replaced in 1991 by the Geological and Mining Corporation (CODIGEM); and the British Geological Survey (BGS).

ODA and BGS participation in the geological and mineral development of Ecuador began in 1969 and during the 1970s British and Ecuadorian geologists carried out the primary mapping and mineral exploration of the coastal area and the Western Cordillera. The present work thus completes the reconnaissance studies of the Ecuadorian Andes by Anglo-Ecuadorian teams, and provides the springboard for the regional plate tectonic interpretations outlined in this text and on the national maps (Geologic and Tectonometallogenic) prepared by ODA/BGS in conjunction with CODIGEM.

BGS staff were contracted by ODA to serve on the project. Dr. M. Litherland (Project Leader) and Dr. J. A. Aspden (Senior Geologist) were resident in Quito for the duration of the project and undertook the reconnaissance studies of the Cordillera Real from 1986 to 1990. From mid-1990 to 1993 Dr. Aspden covered the El Oro metamorphic district whilst Dr. R. A. Jemielita (Economic Geologist) carried out follow-up mineral studies over the Cordillera Real. During the same period Dr. Litherland compiled the national maps. In addition to the residential staff and their counterparts, other INEMIN/CODIGEM and BGS geoscientists carried out geochemical, petrographic, geochronological and palaeontological studies on project samples. Dr. Litherland was responsible for the compilation of this Memoir and accompanying maps.

Peter J. Cook, DSc

Director

Kingsley Dunham Centre

British Geological Survey

Keyworth

Nottingham NG12 5GG

October 1994

ONE
Introduction

PHYSIOGRAPHY

Considering its small size (283520 km^2), mainland Ecuador is physiographically very varied. The Andean range or Sierra, is at its narrowest here (120 km), being bounded to the west by the coastal lowlands (*Costa*) and to the east by the upper Amazon basin (*Oriente*). The Sierra comprises two parallel ranges, the *Cordillera Occidental* (Western Cordillera) and the *Cordillera Real* or *Cordillera Oriental* (Eastern Cordillera) (Figure 1). The highest peak is Chimborazo (6310m). The two cordilleras trend approximately NNE-SSW, separated in central and northern Ecuador by the Inter-Andean valley which contains most of the major cities.

The Cordillera Real, the main subject of this memoir, is about 650km long and 60km wide within Ecuador. Elevations along its watershed are controlled in the north by a chain of Plio-Quaternary volcanoes (Plate 1). From north to south the major peaks are Cayambe (5790m), Antisana (5704m), Cotopaxi (5897m), Tungurahua (5016m), Altar (5319m) and Sangay (5230m). To the west the floor of the Inter-Andean Valley occurs at 2000-3500m, while the sub-Andean foothills of the eastern slope are at altitudes of about 1000m. The highest peaks of metamorphic rocks are Cerro Soroche (4730m), Sara Urcu (4670m) and Cerro Hermoso (4571m). Project expeditions visited these areas; Hermoso was climbed (Cover and Frontispiece).

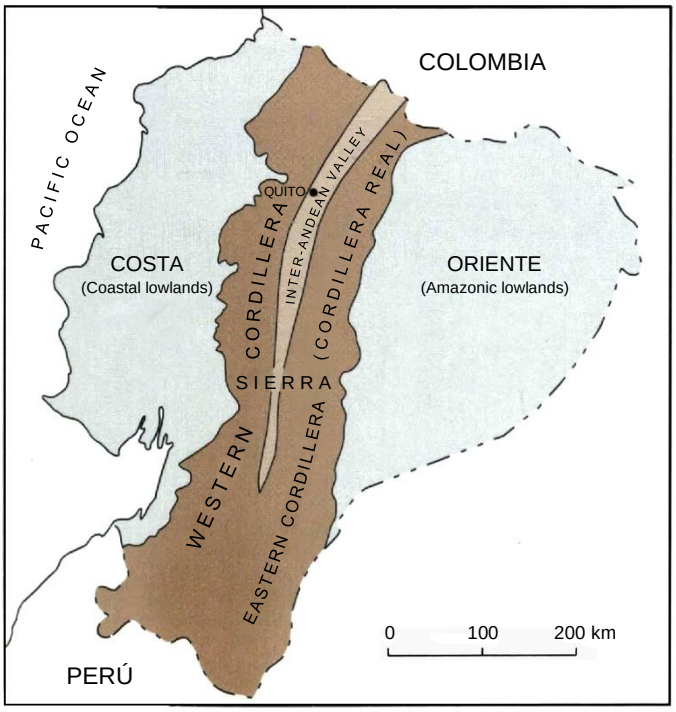

In the south of the Cordillera Real, the watershed levels fall to 3000-3500m; the Inter-Andean valley disappears and the two cordilleras merge. West of this massif, and trending east-west, at right angles to the Andes, is the coastal foothills range of the El Oro metamorphic district, the other smaller project study area (Figure 2).

The Cordillera Real and the Sierra as a whole are deeply dissected by major perennial rivers. The Sierra is a major watershed dividing Amazon (Atlantic)-directed from Pacific-directed drainage. However, the following four rivers drain eastwards to the Amazon from the Western Cordillera crossing the Cordillera Real and forming important lines of communication: the Chingual in the north, and, further south, the Pastaza, Paute and Zamora.

CLIMATE AND VEGETATION

Ecuador is an equatorial country with snow-peaked mountains. Crossing the Cordillera Real from west to east there is a tremendous variation in climate and vegetation. The Inter-Andean Valley in the west is temperate with grassland vegetation and rainfall in the region of 700mm per year (see rainfall for Quito and Cuenca, Table 1). Ascending the western slopes to the watershed one crosses cold, wet, windy mountainous moorlands (*páramos*) scarred by recent glaciations and generally enshrouded in clouds, the snow line lies at about 4500m. On the sheltered eastern side, the tree line of the montane forest is at about 3500m, and as one descends to the Amazonic lowlands the climate and vegetation become more tropical. Rainfall is high over this eastern slope region due to rising hot air masses from the Oriente; figures for Puyo and Tena are 4632mm and 3304mm respectively, falling to 1374mm at Zamora further south (Table 1). The rainfall figures for the cordillera indicate no dry season, only that the period from October to March is slightly less wet. Indeed, the precipitation during Puyo's driest month is four times Quito's wettest.

The Vilcabamba and El Oro areas near Perú have a more extreme dry season between May and November due to the influence of the Humboldt current (Table 1), whilst between December and June rainfall is high due to the El Niño current. With the low altitude, this produces hot, sticky conditions. This area supports only scrubby woodland.

Figure 1. Geomorphological framework of Ecuador.

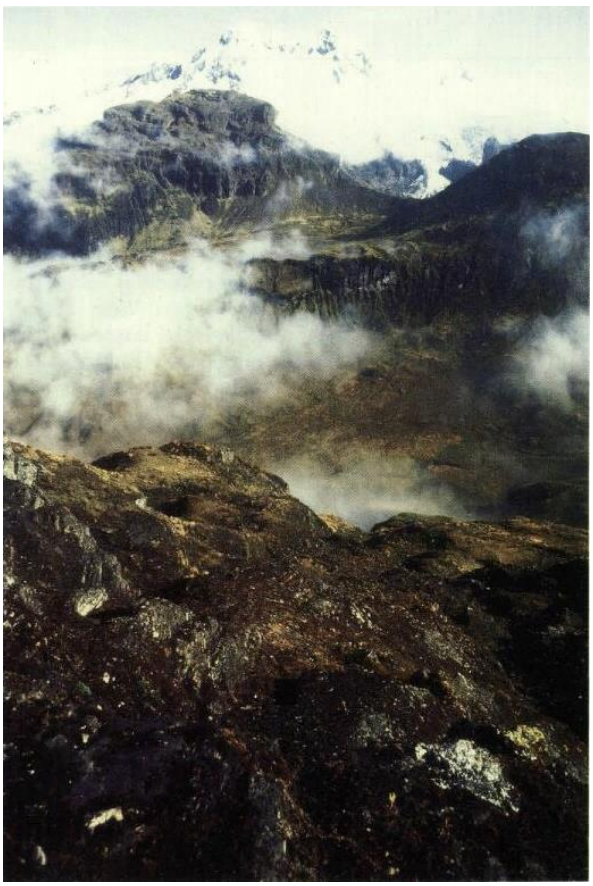

a

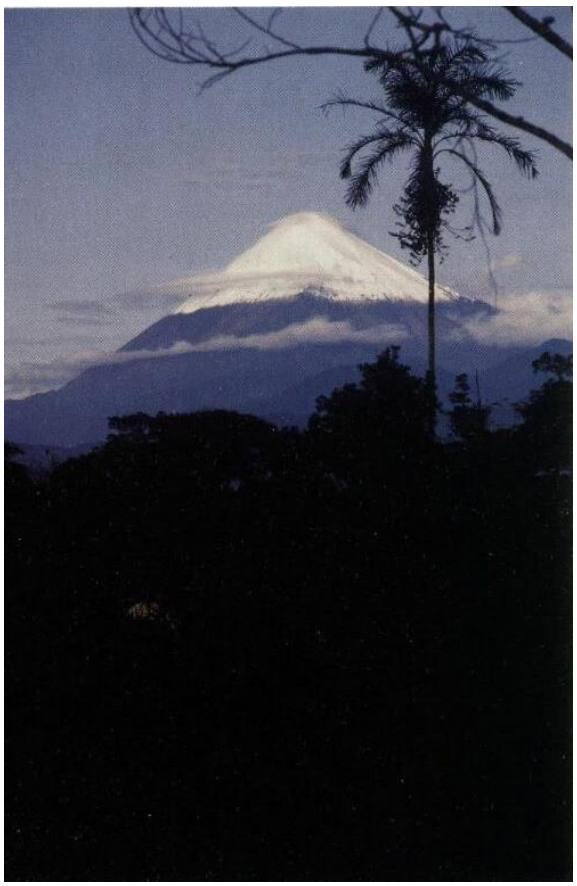

b

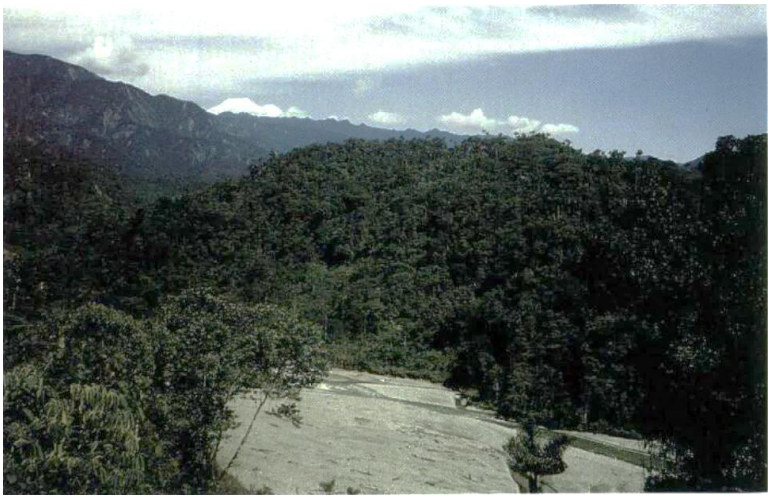

c

Plate 1. Cordillera Real scenery

(a) El Altar volcano (5319m): view of the volcanic cover sequence from the basement schists (photo: R. A. J.).

(b) Sangay (5230m): one of the highest active volcanoes in the world, which straddles the Cordillera Real (photo: R. A. J.).

(c) The Cordillera Real range: view from the Río Salado in the subtropical, sub-Andean lowlands, to the snow-capped Cayambe volcano (5790m) in the far distance (photo: M. L.).

Table 1. Average monthly rainfall figures in millimetres (Data from INAMHI).

Location	Jan	Feb	March	April	May	June	July	Aug	Sept	Oct	Nov	Dec	Total
CORDILLERA REAL													
Tulcán	59.67	82.87	90.22	120.26	62.96	56.74	44.30	49.57	63.44	99.97	132.88	102.44	**965.32**
Quito	50.20	72.20	69.20	71.30	48.40	30.30	22.90	29.80	54.10	52.20	55.40	64.20	**620.20**
Papallacta	63.27	107.67	108.01	108.65	159.06	180.08	193.05	107.81	109.31	95.48	84.13	82.98	**1399.50**
Cotopaxi	68.75	106.60	142.06	123.80	143.70	77.27	58.20	62.85	103.73	98.58	93.37	84.72	**1163.63**
Tena	147.75	167.66	269.77	343.40	325.54	380.56	246.95	268.62	287.57	310.34	343.31	212.20	**3303.67**
Baños	50.58	84.30	98.56	132.41	123.81	162.58	157.72	144.40	115.68	70.06	56.96	41.55	**1238.61**
Puyo	271.55	277.43	454.90	450.08	429.95	486.80	412.97	361.72	384.78	394.78	366.93	340.47	**4632.36**
Sucúa	41.06	90.86	127.41	125.12	130.92	171.81	115.40	114.67	123.15	99.80	84.12	36.91	**1261.23**
Paute	42.22	67.94	93.80	83.72	44.55	58.80	51.75	36.52	48.37	60.65	65.18	66.22	**719.72**
Cuenca	40.38	70.14	95.82	98.60	56.10	45.01	35.20	30.24	50.21	72.33	67.62	62.62	**724.27**
Loja	77.30	103.55	120.17	82.96	31.41	53.65	44.01	38.13	31.66	57.42	45.67	56.44	**742.37**
Zamora	90.71	97.43	147.95	124.00	104.76	146.25	126.08	114.83	95.68	85.10	115.30	125.47	**1373.56**
Vilcabamba	76.76	96.74	150.60	99.37	44.36	19.57	11.87	18.18	20.82	47.88	43.95	70.10	**700.20**
EL ORO													
Marcabelí	190	286.30	322.60	275.70	107.70	40.60	7.80	9.40	17.10	21.40	30.20	117.40	**1426.20**
Santa Rosa	92.40	149.00	148.40	73.50	24.70	12.50	17.80	11.30	15.10	18.60	51.10	23.50	**637.90**
Zaruma	212.40	237.00	307.40	221.80	108.90	25.40	6.80	6.50	25.70	40.50	34.70	142.90	**1370.00**

HUMAN ASPECT

The population of Ecuador is approximately 11 million and rising fast, with a density of 37 per km^2, the highest in South America. About 40 per cent are Indians, many of whom are Quechua-speaking descendents of the inhabitants of the Incan Empire. They live mainly in remote regions of the Sierra, whilst whites and *mestizos* inhabit the towns.

The Inter-Andean highway links the main towns of the Sierra from Tulcán (pop. 33000) in the north, through Ibarra (80000), Quito (1250000), Ambato (140000), Riobamba (148000), Cuenca (250000) to Loja (160000) in the south. Over the Cordillera Real the population is sparse; sizable towns (e.g. Baños) exist only along the main access routes. In the east, the unsurfaced sub-Andean 'highway' links smaller towns, the largest of which are Puyo, Zamora, Macas and Tena. Population is relatively dense over the El Oro metamorphic district, with towns such as Portovelo and Piñas in the mapped area, bordered by Arenillas, Santa Rosa, Pasaje and the city of Machala (158000) on the adjacent coastal plain.

Subsistence farming is the traditional livelihood of the Indians in their lands and of the more recent mestizo colonisers who clear the forests along new access routes. Cash crops such as potatoes are also produced. Gold panning is a common source of seasonal income and there is an embryonic hard-rock mining industry. The Cordillera Real is also the source of Ecuador's hydroelectric power from the plants at Agoyán, Pisayambo and Paute. Large inaccessible areas have been designated as National Parks.

ACCESS

There are five all-weather routes across the Cordillera Real connecting the Inter-Andean and Sub-Andean 'highways'. From north to south these are: Papallacta-Baeza, Baños-Puyo, Cuenca-Limón, Loja-Zamora and Loja-Zumba. The Guamote-Macas road is still under construction; the Tulcán-Lago Agrio road has reached La Bonita, and the Salcedo-Tena road has long been abandoned as a viable project.

South of the Río Paute there are a number of mule trails across the cordillera, but to the north extensive segments are without access. These include the 120km of cordillera between the Papallacta and Baños roads which contains the Llanganates mountains, recently traversed by the mountaineer MacInnes (1984); and the stretch between the Papallacta and La Bonita roads, inaccessible since the destruction of the Oyacachi-El Chaco trail by the March 1987 earthquake. A foot traverse across the heart of this area (e.g. Sigsigpamba-Río Dorado-Río Cofanes-Puerto Libre) would take three or four weeks and would thus require at least one supply cache.

Whilst rock outcrop is abundant along the road cuttings and over the *páramos*, it is generally sparse through the montane forest and often inaccessible along river gorge sections. Over many areas stream or talus blocks were used to identify the geology.

PREVIOUS GEOLOGICAL WORK

The metamorphic rocks of the Cordillera Real and El Oro (Figure 2), the subject of this memoir, were depicted on the national geological maps of Theodoro Wolf (1892) and Walter Sauer (1957). Wolf's descriptions incorporated economic geology as part of this naturalist's *magnum opus*. Sauer (1965) was very detailed and objective, representing some of the observations he made whilst traversing the country to its most inaccessible quarters. He recognised most of the metamorphic lithologies including ophiolites; distinguished the para- from the ortho-gneisses, and located and named many of the post-tectonic plutonic phases. His study was the most exhaustive before the present survey. In his review of the Sub-Andean region, he utilised the pioneering works of Wasson and Sinclair (1923), Colony and Sinclair (1932) and Tschopp (1953).

Reconnaissance mapping of the metamorphic rocks aided by photogeological interpretation began with the studies of Kennerley of the British Geological Survey over the Llanganates area (Kennerley, 1971) and Loja Province (Kennerley, 1973). Feininger (1978, 1980) continued the mapping of the El Oro metamorphic belt westward, discovering the blueschist/eclogite/ophiolite complex at Raspas. Reconnaissance sheet mapping by DGGM/INEMIN/CODIGEM at a scale of 1:100000 has continued over the years with little differentiation of the metamorphic rocks; the overlying Plio-Quaternary volcanic sequences have attracted more detailed studies.

Individual attempts to understand the metamorphic rocks of the Cordillera Real have also been undertaken along the few road sections. These include the petrological and geochemical studies of Herbert (1977, 1983), the petrological and structural studies of Trouw (1976), a review by Feininger (1982), and unpublished metamorphic studies by Duque.

Some K-Ar geochronology was undertaken (Kennerley, 1980; Aly, 1980; Feininger and Silberman, 1982; Hall and Calle, 1982; Baldock, 1982; Herbert and Pichler, 1983; Pichler and Aly, 1983); the available Rb-Sr geochronology was statistically invalid.

Regional summaries of the metamorphic rocks in a national context (Kennerley, 1980; Baldock, 1982, 1985), whilst providing descriptions of the lithologies and dividing them longitudinally into various 'Groups', could only speculate on their age and correlation since there was only a range of metamorphic K-Ar ages from Precambrian to Tertiary and no palaeontological data. Whilst most authors agreed with Sauer (1965) that the metamorphic rocks are of Paleozoic or Precambrian age as indicated by their equivalents along strike in either Perú or Colombia, Feininger (1975, 1982), claimed the bulk of the Cordillera Real to comprise deeper-water equivalents of the Amazonic Cretaceous sequence to the east. This supported the hypothesis of Bristow (1973), who, resurrecting an earlier suggestion by Liddle and Palmer (1941), claimed that the Upper Cretaceous sequences of the Cuenca area could be traced eastwards into their metamorphic equivalents. The Cordillera Real rocks thus appeared to be laterally Cretaceous and longitudinally Palaeozoic!

MINING HISTORY

At the time of the Spanish conquest, the Incan kingdom of Quito was known for its gold, silver and platinum jewellery which, in those times, was without commercial importance. The Spanish rapidly located the alluvial mines and hard-rock sources of much of the alluvial gold, e.g. the Nambija and Zaruma districts. Indeed, such was the gold fever that, of the thirty settlements they established, twenty were alluvial gold mining towns along the sub-Andean zone of the Cordillera Real (Navarro, 1986 Vol. 1). However, due to Indian revolts, disease and economic factors, mining ceased at the beginning of the 17th century, with the exception of the Zaruma district, which was worked at reduced production levels. But even this area was virtually abandoned in the 19th century.

Foreign investors helped to reopen the Zaruma mines in the late 19th century and gold-polymetallic mines were also worked in the project area at Pilzhum, Peggy and San Bartolomé. More recently, a hunting party rediscovered the forgotten mines of Nambija which triggered an intense search for other deposits. Thus, during the disastrous 'El Niño' rainy season of 1982-1983, which destroyed almost all the harvest of the fertile coastal area, the impoverished *campesinos* dedicated themselves to the search for gold, first locating the Ponce Enríquez field. From this time an ever-increasing gold fever has seized wide sections of the poorer parts of the population.

Gold production figures for 1990 were in the region of 13 tonnes: five tonnes from Nambija, three from Zaruma-Portovelo, two from Ponce Enríquez and the remainder from Chinapintza, Guaysimi, Campanilla and alluvial workings.

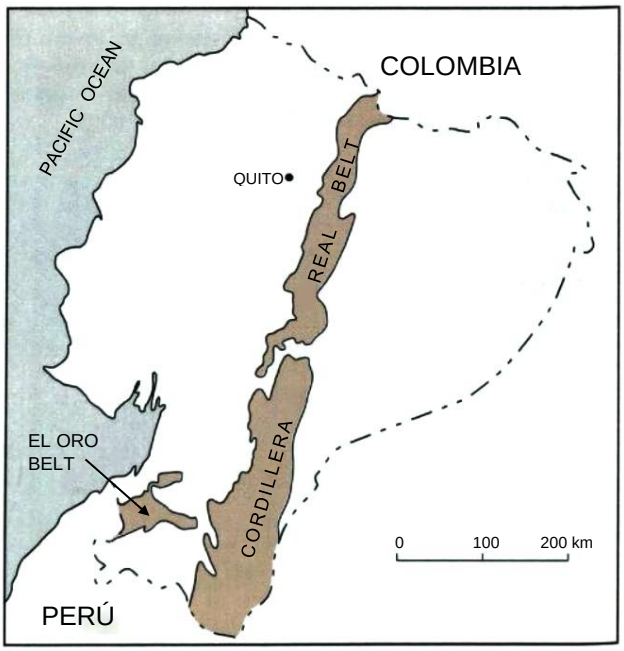

Figure 2. Location of the metamorphic/plutonic belts described in the text

PROJECT OPERATIONS

The area of study was initially limited to the metamorphic rocks of the Cordillera Real and El Oro. Later it was decided to include the unmetamorphosed Zamora batholith and its envelope rocks on the accompanying map in order to augment the study of the pre-Cretaceous history of Ecuador and also include the important Nambija mining area. However, the field surveys over this, the Sub-Andean belt, were not as detailed as over the rest of the project area.

The reconnaissance survey of the Cordillera Real (1986-1990) was undertaken along a series of geotraverses using roads and trails where available. Litherland, with counterparts Bermúdez or Pozo, mapped the area north of the Río Pastaza, and Aspden, with counterparts Viteri or Bermúdez, mapped the area south of the Río Paute; the intervening ground was shared. The survey of the El Oro metamorphic belt (1990-1992) was undertaken by Aspden, with counterparts Silva, Bermúdez or Bonilla.

Outcrops and river boulders were sampled and geological observations made. Stream sediment samples (sieved in the field to 175 mesh grain size) and panned heavy-mineral concentrates were collected where convenient.

In terms of specialised field studies, the major economic follow-up programme was conducted by Jemielita and counterpart Bolaños. There was an economic investigation by Clarke and Viteri in 1988, regional geochronological studies by Rundle in 1987 and Harrison in 1989, and a palaeontological investigation by Woods in 1991.

Microscopic petrographic studies and some stream, mineral and heavy-mineral geochemistry were undertaken in Quito, whilst geochronological, palaeontological, rock and most of the mineral analyses were carried out in the BGS laboratories (UK). Consultant's reports are listed on pp. 107-108.

REPORTS AND MAPS

Geological field maps were constructed using IGM (Instituto Geográfico Militar) base maps, normally on a 1:50000 scale. These became increasingly available for the Cordillera Real, replacing the old 'Census' maps drawn from uncontrolled airphoto mosaics. The 1:500000 scale topographic base for the accompanying maps was compiled by project staff from IGM maps and satellite images.

Annual reports were produced for the first four years of the project. These bilingual reports include appendices of specific field reports (in Spanish), laboratory analyses, reports by project consultants, and geotraverse maps.

A summary of the first four years' work on the Cordillera Real together with 1:500000 scale geology and metal maps were produced. The work on the El Oro region, with a 1:100000 scale geological map, and the results of the economic follow-up of the Cordillera Real were produced as unpublished reports. All these are available as open-file reports at BGS (in English) and CODIGEM (in Spanish).

Published and unpublished project-related reports and maps are listed separately on pp. 107-109.

ACKNOWLEDGEMENTS

Throughout its existence the project has been strongly supported, financially and administratively, by both the governments of Ecuador and the UK. The British representatives were the successive ODA desk officers for Ecuador: Mr. D. Lawless, Mr. G. Roberts, Mr. R. Russell and Mr. J. M. Harris; and their representatives in the British Embassy, Quito: Redmond Norton, Douglas de Wilton and Caroline Blake: under ambassadors Michael Atkinson and Frank Wheeler. The Ecuadorian Government was represented by the successive Mining Subsecretaries: Sr. F. Navarro, Sr. M. Horra and Sr. E. Núñez del Arco; and INEMIN/CODIGEM directors: Horacio Rueda, Guillermo Bixby, Leonardo Elizalde, Edgar López and Carlos Muirragui.

Regarding the scientific studies, we have appreciated the support given by the successive BGS regional geologists: Clive Jones, John Bennett and Barrie Page, who have monitored the project for ODA. Equally we thank the INEMIN/CODIGEM technical directors: Edgar Salazar and Wilson Santamaría. Barrie Page has edited the text of this memoir, whilst Niall Spencer was responsible for the preparation of the maps and diagrams. Typesetting and page make-up was by Jackie Norman; copy editing by Molly Simmons.

The Ecuadorian project staff must be congratulated for their enthusiasm and dedication in spite of their increasingly difficult personal circumstances. Important contributions were made by geologists Ramiro Bermúdez, Francisco Viteri and Miguel Pozo and later by Johnson Bolaños, Wilson Bonilla, Alfredo Zamora and Kleber Silva. The project secretary in Quito, Fabiola Alcocer, handled the project administration and bilingual reports admirably, as did Victor Acitimbay, the project cartographer, in producing the project diagrams and maps.

Many ODA consultants also made important contributions to the Project. These included Martin Clarke (Economic Geologist), Neil Fortey (Petrologist), Steve Harrison (Geochronologist), Chris Rundle (Geochronologist) and Mark Woods (Palaeontologist), all of whom visited Ecuador. Clarke and Viteri's mineral survey was one of the epic field campaigns of the entire project. These consultants also undertook studies in the UK, along with others listed on pp. 107-108. This list highlights some important contributions: for example, palaeontologists of the BGS Biostratigraphy Unit identified Jurassic biota in the Cordillera Real and the first Triassic fossils from Ecuador; Neil Fortey and Martin Gillespie of the BGS Mineralogy and Petrology Unit interpreted the rock chemistry; whilst members of the NERC Isotope Geology Centre were able to date the rocks of the metamorphic belts by different isotopic methods, including the most recent lead isotope studies by Steve Noble.

We are equally grateful to the staff in the INEMIN, Quito Polytechnic and BGS laboratories who undertook the analytical work for the project, and to the scientific institutions and mining companies who collaborated with the project and who helped to make it a success within Ecuador. In this respect special thanks are due to Napoleón Báez, David Coochey, Pablo Duque, Arturo Egüez, Minard Hall, Alex Hirtz, Luis Torres, Phil Townsend and Frank Van Thournout. We also appreciate the important contributions made by Río Tinto Zinc (formerly BP Minerals).

In the field, locally recruited guides and porters carried, cut, chopped, cooked and fished, and tried to ensure that the geologists arrived in one piece at the bottom of the Andes.

Last, but not least, there is Manuel Célleri (Plate 15b), our CODIGEM field assistant, who also acted as driver, cook, panner and sergeant, who knows the Cordillera Real and remembers everything that happened.

Brian Kennerley launched the ODA and BGS participation in Ecuadorian geology leading the first investigations and the first project team. Following his untimely death in 1976, he now lies peacefully in a Quito cemetary. This memoir is dedicated to his memory which is still treasured by many Ecuadorians.

TWO
Geological Setting

ANDEAN PLATE TECTONICS

Andean metamorphic rocks

Regionally metamorphosed rocks comprising schists and gneisses similar to those described in this memoir are known throughout the Andean chain (Zeil, 1979). These range in age from the Lower Proterozoic Arequipa massif of coastal Perú (Shackleton et al., 1979), through the Middle Proterozoic Grenvillian granulite and gneiss massifs of Colombia (Kroonenberg, 1982), the Upper Proterozoic Central Andean basement of Perú (Dalmayrac et al., 1980), to Palaeozoic. The Palaeozoic rocks comprise not only belts of metamorphic rocks but also non-metamorphosed cover sequences (Dalmayrac et al., 1980). Major belts of even younger schists and gneisses, i.e. of Mesozoic-Cenozoic age, have been reported from Ecuador (Feininger, 1987), and are confirmed in this memoir. Only recently have attempts been made to account for these metamorphic rocks within the framework of the crustal growth of South America.

Growth of South America

The Andean metamorphic basement has been interpreted as a collage of terranes, the accretion of which relates to the periodic breakup and reformation of Pangaea.

Following the most recent speculations (Hoffman, 1991; Hartnady, 1991; Storey, 1993), the earliest Pangaea so far recognised comprises pre-1300 Ma cratons sutured together by a single Grenvillian (1300-900Ma) collision belt. In this model the Grenvillian rocks of the Sunsas and San Ignacio belts recognised over the Brazilian Shield of Bolivia (Litherland et al., 1985; 1989) are thought to have formed in that part of the belt close to the type locality in Canada (Figure 3a).

This Grenville-sutured Pangaea, as with later ones, acted as a large surface insulator that inhibited the escape of heat from the mantle. Heat build-up resulted in large-scale convection and eventual splitting of the lithosphere leading to continental breakup and the destruction of Pangaea.

Between the breakup of Grenvillian Pangaea (800 Ma) and the formation of Pan African Pangaea (600 Ma), it appears that the Amazonic cratonic area adjacent to the present northern Andes remained in position *vis-à-vis* North America whilst the bulk of southern South America was formed by the amalgamation of old cratonic blocks. This amalgamation occurred during a series of late Precambrian collisions with island arcs and oceanic and continental fragments, thus producing the pattern of Brazilide (Pan-African) fold belts (Ramos, 1989). Of these accreted terranes, those of Arequipa and Pampeanas form the basement to parts of the present Andes (Figure 3b).

The breakup of the Pan-African Pangaea in the Cambrian precipitated the separation of North America from Gondwanaland and the opening of the Iapetus and Pacific oceans. Southern South America was formed by the suturing of Patagonia and smaller Palaeozoic terranes along the Chilean 'Andean' margin (Ramos, 1989).

The continents drifted together again in the late Carboniferous (Figure 3c) to form the Hercynian Pangaea, only to break up once more with the opening of the Tethys Ocean at the beginning of the Jurassic. Since then, subduction of the Pacific Ocean along the edge of the South American Plate has produced the type example of the destructive plate margin providing a model for the sedimentary, tectonic and magmatic processes of a subduction regime (Dewey and Bird, 1970). During this period the only well-defined region of continental accretion has been the Northern Andes (see below) (Figure 3d), a small area relative to that of the suspect terranes of the North American cordillera emplaced during the same period (Coney et al., 1980). The subduction of the Farallon and Nazca oceanic plates since about 70 Ma has proceeded along a vector similar to that of the present day (Figure 4) (Daly, 1989).

Terranes in the Northern Andes

The most striking geological change along the whole Andean belt occurs between the Central and Northern Andes (Gansser, 1973), coinciding seaward with the Carnegie Ridge and landward with the Amazon lineament (de Loczy, 1968). The north-west striking Central Andes are replaced by the north-north-east-striking Northern Andes, referred to as the Amotape zone or Huancabamba deflection (Gerth, 1955). In addition to the change in strike, the Northern Andes is also characterised by the appearance of basic igneous rocks along the coast (Goossens, 1968; Goossens and Rose, 1973). Gravimetric studies (Case et al., 1973; Feininger and Seguin, 1983) led to the proposal that the Andean crust here was oceanic, taking the form of an allochthonous terrane (Feininger and Bristow, 1980; McCourt et al., 1984; Lebrat et al., 1985; Roperch et al., 1987) accreted in either late Cretaceous or early Tertiary times. This event was followed by the 'normal' subduction process and accompanying magmatism characteristic of the Peruvian Andes since the Cretaceous.

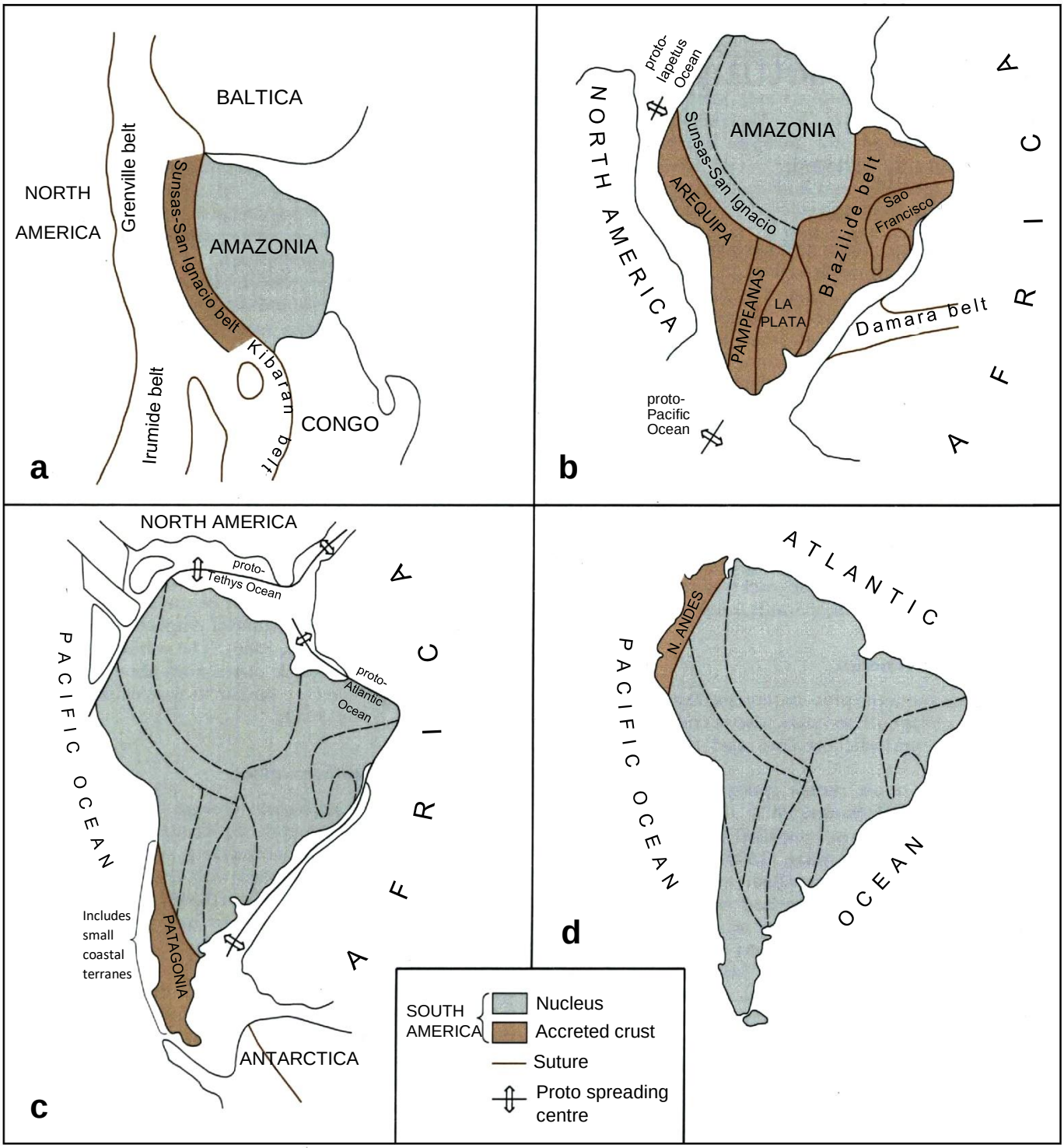

Figure 3. The geotectonic growth of South America

(a) c.900 Ma 'Grenville-sutured Pangaea'; **(b)** c.600 Ma 'Pan-African sutured Pangaea';

(c) c.200 Ma 'Hercynian sutured Pangaea'; **(d)** present day.

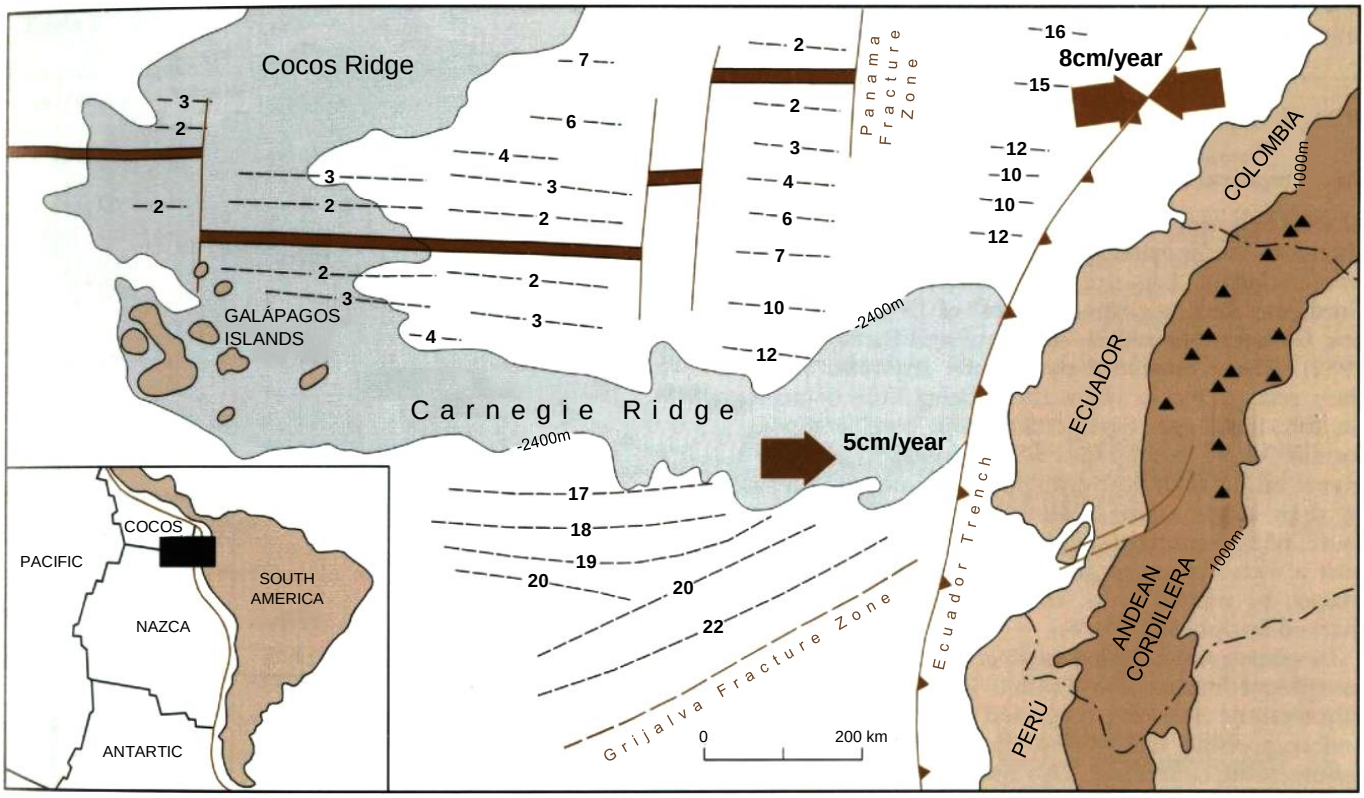

Figure 4. Present-day plate tectonics of the equatorial east Pacific area between the Galápagos Islands and Northern Andes, after Barberi et al. (1988). The age (Ma) of the oceanic crust is indicated, as well as the direction and rate (cm/yr) of plate motion (double vector = relative motion); triangles = mainland active volcanoes.

This oceanic, or Piñón terrane of the Northern Andes is sutured eastwards against metamorphic basement comprising the north-north-east-trending Central Cordillera of Colombia and the Cordillera Real of Ecuador; and southwards against the discordant east-west trending Amotape massif of northern Perú and southern Ecuador. In Colombia (McCourt et al., 1984; Aspden and McCourt, 1986; Restrepo and Toussaint, 1988; Forero, 1990; Restrepo-Pace, 1992) and in Ecuador (Aspden et al, 1987, 1988; Feininger, 1987; Mourier et al., 1988; Litherland and Zamora, 1991; Aspden and Litherland, 1992) these rocks have been variably interpreted as suspect terranes. This memoir presents the results of seven years' work on these metamorphic rocks of Ecuador and assesses their status in terms of global tectonics.

Andean metallogenesis

The Andean chain is well endowed with a variety of mineral deposits, which, in Perú and Chile, appear to show a systematic change in types across the belt (Sillitoe, 1972), generally interpreted as closely related to the Mesozoic-Cenozoic evolution of the orogen (Frutos, 1982). In the west, closest to the trench, is the iron-apatite belt of the early, primitive island arcs. Further east, and associated with a later, more evolved stage of the continental margin, with thicker crust, are the Cu-Mo porphyries and polymetallic (Ag-Pb-Zn) deposits. Finally, furthest east and associated with the thickest and most evolved crust are the Sn-Bi-Sb-W deposits: the 'tin belt'. This progression also marks an increasing atomic size in the metals involved.

Although the metallogenic belts are ascribed to mantle-derived (I-type) magmas, Frutos (1982) points out that these Mesozoic-Cenozoic provinces are also closely related to those of the pre-Mesozoic basement, suggesting some degree of remobilisation. In particular, it is remarkable that the Cenozoic tin belt of Bolivia is precisely situated over the Lower Palaeozoic metasedimentary strata-bound tin deposits (Schneider and Lehman, 1977). In New Mexico epithermal gold deposits have been demonstrated as remobilised from Precambrian volcanogenic sulphides of greenstone belt affinity (Fulp and Woodward, 1990), indicating that metal deposits need not automatically be assigned a mantle source simply because they are associated with I-type magmatism.

The metallogenesis of Ecuador has been reviewed by Goossens (1972b) and Paladines (1989). Despite a general paucity of information over the inaccessible regions, especially the Cordillera Real, the metallogenic belts identified in Perú and further south are not apparent, and particular emphasis is placed on east-west transverse faults and their intersection with major Andean structures. Alternatively, these differences may be accounted for by the interpretation of the Northern Andes as a collage of terranes, the continental margin of which only stabilised in the Lower or Middle Tertiary.

METAMORPHIC ROCKS OF ECUADOR

Stratigraphical nomenclature

At the beginning of the current project, it was decided to abandon the previously formalised lithostratigraphical nomenclature for the metamorphic rocks of the Cordillera Real, e.g. the 'Groups' of Llanganates, Zamora, Cofanes, Margajitas, Ambuquí and Paute (Baldock, 1982). There appeared to be little scientific basis for their recognition as units, there being little or no data on thickness, age, type section, top, base, component formations or stratigraphical relations. Some were regional rather than lithostratigraphical units as illustrated by their name changes along the cordillera. Furthermore, field reconnaissance showed the groups to encompass a wide variety of original lithotypes, separated, in places, by major faults, one of which (Peltetec) was marked by ophiolitic rocks.

In place of the abandoned nomenclature, the metamorphic complex was divided into Andean-trending lithotectonic divisions, separated by fundamental faults, and comprising subdivisions which showed a degree of lithotectonic coherence. This system was kept non-lithostratigraphical, informal and objective so that it could be amended in the light of new geochronological and palaeontological ages and field relationships. The successive Annual Reports (1987-1990) illustrate this evolution. Eventually it settled into a framework which formed an adequate basis for description of the metamorphic rocks of the cordillera (Litherland and Aspden, 1990; Aspden and Litherland 1992).

Metamorphic terranes

The major lithotectonic divisions of the Cordillera Real fulfill the requirements of suspect terranes (Coney et al., 1980; Jones et al., 1983) in that they show internal homogeneity and continuity of stratigraphy whilst the boundaries between them separate distinct temporal or physical rock sequences. Thus, for the purposes of this memoir, the rocks of the Cordillera Real will be described by age and metamorphic terrane (Figure 5), whilst those of the geotectonically isolated El Oro complex, mapped in greater detail, are allocated a separate chapter. In Chapter eight, models are presented to account for the nature and accretion of the terranes. It is noticeable that certain terrane boundaries (Figure 5) follow fundamental geomorphological boundaries (Figure 1).

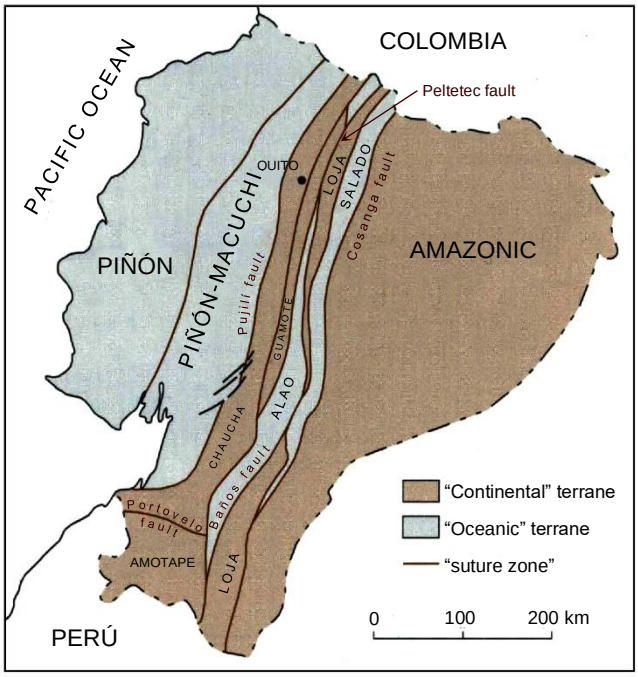

Figure 5. Provisional terrane map of Ecuador after Litherland and Zamora (1991).

Table 2 summarises the geological history of the metamorphic rocks of Ecuador linked to important phases of mineralisation. It introduces some of the terminology used in the succeeding chapters and anticipates some of the major conclusions.

Table 2. Summary of geological history

ERA / EPOCH	STRATIGRAPHICAL UNIT(S)	GEOTECTONIC SETTING	MINERALISATION
Upper Cenozoic	Continental magmatic arc	Subduction of Nazca plate; uplift	**Au** placers; **Au-polymetallic** porphyry/epithermal
Lower Cenozoic	Magmatic arc; back arc sediments	Subduction; accretion of Piñón terrane	Granodiorite-related **Au-polymetallic; PGM** in Tampanchi mafic complex; **Au** palaeoplacers
Upper Cretaceous	Tena, Yunguilla and Alamor Units; plutons	Subduction; uplift; unroofing	**Au** palaeoplacers
Lower Cretaceous	Ophiolites	Peltetec-Palenque tectonometamorphic accretionary event of thrusting/transpression	**Au** in mesothermal shear zone quartz veins; **polymetallics** in skarn klippen
Upper Jurassic	Alao and Salado terranes; Palenque Unit, Misahuallí Unit	Island arc; marginal basin; accretionary prism; continental arc respectively	Primary massive sulphides **(polymetallic)**
Lower Jurassic	Zamora and Azafrán plutonic chains	I-type magmatic arc	**Au** skarns (Nambija), porphyry and epithermal **Au-polymetallics**
Triassic	Tres Lagunas-Moromoro S-type granites	Tres Lagunas-Moromoro tectonometamorphic event: major shear zone	**Sn-W** in S-type granites; **Au-Sb** in shear-zone-hosted quartz veins
Palaeozoic	Premetamorphic sediments of Loja, Amotape and Chaucha terranes and Amazonic craton	? Intracontinental basins	

THREE

Cordillera Real: Precambrian, Palaeozoic and Triassic rocks

AMAZONIC CRATON

During the Palaeozoic and Triassic, the Precambrian Amazonic craton was the site of deposition of the Pumbuiza and Macuma formations and the Piuntza unit. This region of deposition underwent no subsequent orogenic event and thus contrasts with Palaeozoic/Triassic metamorphic terranes of Loja and El Oro further west. The metamorphic Isimanchi unit is included in this group since it is associated with the undeformed Jurassic Zamora batholith, part of the Amazonic craton since Jurassic times.

Precambrian basement

The Phanerozoic sequences of the Amazonic craton are underlain by an unexposed metamorphic basement complex (Baldock, 1982) recorded in various boreholes; samples from the Tapi well were dated by Rb-Sr (one point) at about 1600 Ma (oral communication, F. Ramírez).

Within the Jurassic Zamora batholith (p.26) there are large 'rafts' of older migmatitic gneiss (oral communication, David Coochey), the largest of which are shown on the accompanying map and indicated as Precambrian. They are unlikely to be blocks of the Triassic Sabanilla migmatites, since Triassic rocks of the Piuntza unit with no regional tectono-metamorphic history are also found as rafts in the same batholith.

Pumbuiza Formation (Palaeozoic)

This unit (named by K. T. Goldschmid of Shell Co., in 1940) of highly folded, grey to black slates with fine grained quartzitic sandstones crops out in the northern Cutucú Mountains (Tschopp, 1953) to the east of the accompanying map. It may also be present in the core of the Cutucú Uplift anticline of the Río Santiago (oral communication, F. Ramírez). It is not considered to be present within the (now disbanded) Margajitas Formation along the Sub-Andean belt of the Cordillera Real as suggested by Tschopp (1953). The unit is unconformably overlain by the Macuma Formation of Upper Carboniferous age and is generally ascribed to the Devonian.

Macuma Formation (Carboniferous)

The Macuma Formation (named by J. J. Dozy of Shell Co., in 1940) comprises a 200m-thick unit of blue-grey bioclastic limestones and black shales, overlain by about 1250m of white to dark grey, cliff-forming limestones and shales (Tschopp, 1953). Gradations from sandy limestones to greenish brown sandstones are common in both units. The palaeontology indicates rocks of Lower Pennsylvanian age, with the possibility that the uppermost beds are Permian (Tschopp, 1953).

The formation crops out in the cores of major anticlines where it is associated with the Pumbuiza Formation. It may also occur in the form of the Isimanchi unit (see below), Seismic studies over the Oriente (Bankwill et al., 1991) indicate that the Macuma limestones are contained mainly in fault-bounded half-grabens.

Isimanchi unit (?Carboniferous)

This is a new unit comprising the low-grade phyllites and marbles noted around the village of Isimanchi in the extreme south of the cordillera and further north along a traverse east of Valladolid to Porvenir. Although similar in metamorphic grade to the Chigüinda unit (p.15), the lithologies are markedly different. The Isimanchi unit forms a belt which wedges out to the north, being overthrust in the west by the Sabanilla migmatites and bounded to the east by the undeformed Zamora batholith, of Jurassic age, along the contact of which the Isimanchi rocks are intensely silicified and hornfelsed.

A palaeontological analysis of marble samples from east of Valladolid (British Geological Survey, 1989) indicates fish remains resembling Carboniferous to Late Triassic forms, and a possible conodont element which, if confirmed, would imply a pre-Jurassic age.

The unit comprises black and green phyllites, off white metamorphosed tuffs and volcanic breccias, and marbles. The latter are blue to off white in colour and form a series of spectacular hills some of which have developed typical karstic scenery. Dips of bedding/cleavage are generally steep but close to the Sabanilla migmatites the cleavage is shallow and dips to the west. The thickness of the unit is unknown.

East of this main belt, similar 'schists' have been reported as large rafts in the Zamora batholith (oral communication, P. Jeffcock) and these are shown as the Isimanchi unit of the accompanying map. In places the schists are reported (oral communication, P. Jeffcock) to be unconformably overlain by the Triassic Piuntza unit.

The above information indicates a pre-Jurassic, possibly Carboniferous sequence. This and the presence of the marble horizons would suggest a correlation with the Macuma Formation to the east. However, the volcanic component and tectono-metamorphic overprint is lacking at Cerro Macuma.

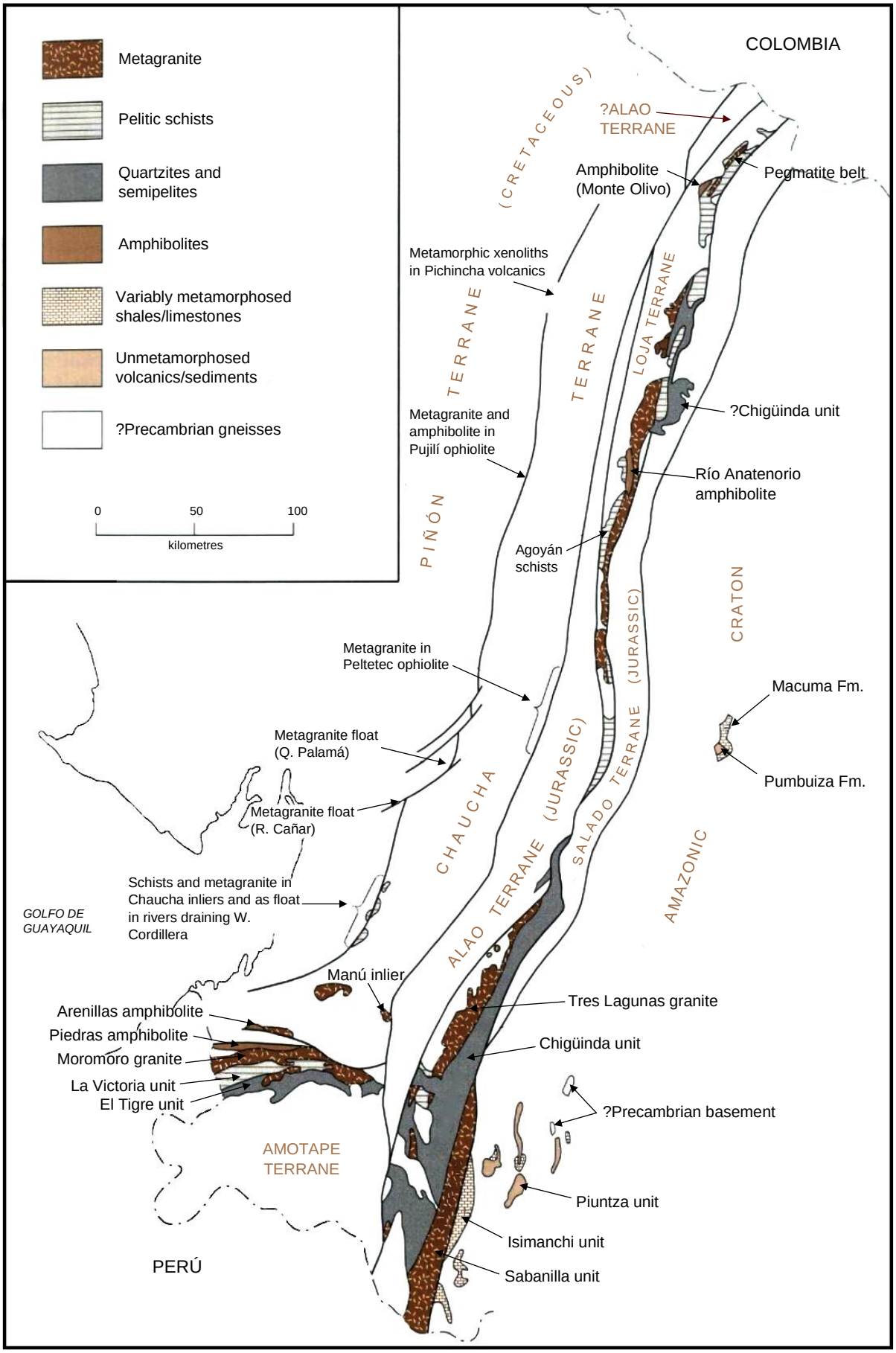

Figure 6 Precambrian, Palaeozoic and Triassic rocks and terranes of Ecuador

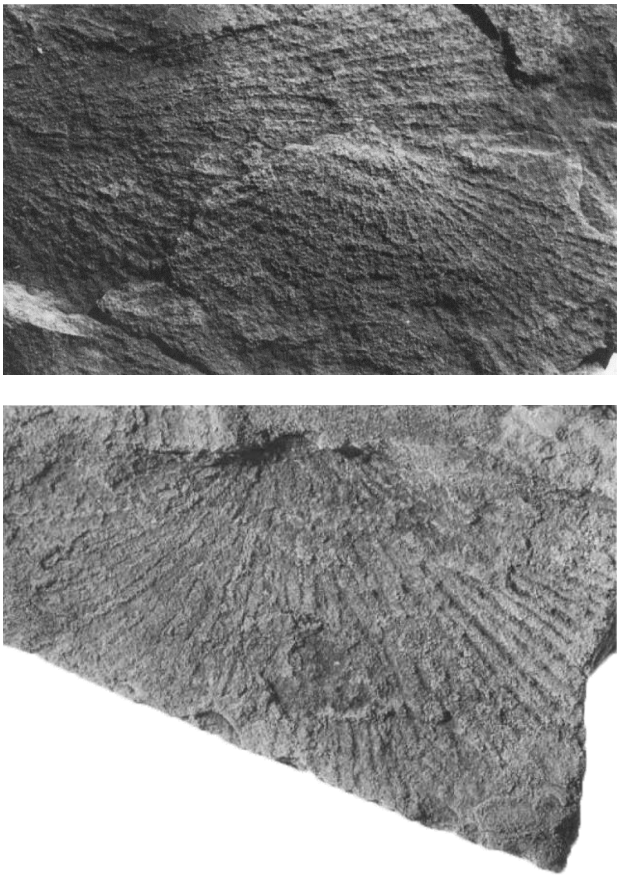

Plate 2. Triassic fossil: the bivalve? *Entomonotis richmondiana* (Zittel) from the Río Timbara, (×1), BGS specimen No. FOR 4822

Piuntza unit (Triassic)

The Piuntza unit is the first Triassic stratigraphical unit recognised to crop out in Ecuador. It occurs as shallow-dipping, volcano-sedimentary rocks, lying within the bounds of the Jurassic Zamora batholith, the contact metamorphism of which produced the gold-bearing iron skarns of the Nambija, Piuntza and María Elena mining areas. It unconformably overlies the Isimanchi unit (oral communication, P. Jeffcock).

The identification of the unit on the accompanying map is based mainly on mining company reports and maps; over some areas it is difficult to differentiate the Piuntza unit from the volcanic Misahuallí unit of Jurassic age, regarded as contemporaneous with the batholith. The Piuntza unit is shown as cropping out over interfluves, with the plutonic rocks forming the valley floors, suggesting the form of an eroded roof to the batholith. The common occurrence of skarn rocks along the ridges may relate to their greater resistance to erosion compared to the unmetamorphosed protolith.

Bivalve fossils (Plate 2) from a sequence of partially skarnified grey calcareous siltstones of the Río Timbara, near Piuntza, and from the area of Guaysimi, near Nambija, were identified by the project as 'all either *Halobia*, *Daonella* or *Entomonotis* and are therefore late Middle to Upper Triassic in age. They are most likely *Entomonotis richmondiana* (Zittel), and therefore possible Norian' (Ivimey-Cook and Morris, 1989). This identification confirmed the presence of Triassic rocks in Ecuador and provides the type locality for the sequence.

Mr. M. Turner, of Zamora, has in his mineral collection a sample of gold skarn with a fossil impression (Plate 5b), reported to have been collected from Guaysimi Alto mine, south of Nambija in the main skarn belt. This bivalve was identified as *Costatoria* sp. of Middle-Upper Triassic age (Woods and Morris, 1992), thus confirming the age and regional extent of the Piuntza unit, as well as identifying the skarn protolith, variously considered to have been limestones belonging to the Macuma, Santiago or Napo Formations (Tschopp, 1953).

The Piuntza lithologies comprise limestones, a variety of calcareous shales and sandstones, fine-grained tuffs, and volcanic flows and breccias of andesite-dacite composition; the thickness in the Campanilla/Nambija sector is a minimum of 300m (oral communication, A. Warden). It is suggested (oral communication, D. Coochey) that within the Nambija belt the volcanic fraction increases northwards and the marble fraction southwards. Although the rocks are heavily skarnified, there is no sign of any regional tectonometamorphic imprint.

The Piuntza unit is a continental/marine volcanosedimentary sequence. It is not found at the stratigraphic contact between the Macuma and Santiago Formations further north in Ecuador, which would suggest a restricted basin, perhaps corresponding to the area of the Zamora batholith itself. Such a basin could be the source of the gold concentrated later in the Jurassic skarn deposits. In this context it is interesting to note the apparent mutual exclusivity of the Piuntza Unit and Santiago Formation (see p.22), there being no indication of the latter over the batholith. Further east, Triassic spores have been found in well samples of the redbed 'Sacha Formation' (Bankwill et al., 1991), correlated tentatively with the Permo-Triassic Mitu Group of Perú.

It appears that the Piuntza unit has many similarities with other Triassic sedimentary basins in South America, which have been interpreted as rift basins (Suárez and Bell, 1992). However, whilst the Piuntza Unit is essentially undeformed and 'cratonic', it must be pointed out that high-grade migmatites of similar Upper Triassic age crop out only a few kilometres to the west in the form of the Sabanilla complex, part of the Tres Lagunas granite suite (p.19). This indicates the fundamental nature of the intervening Palanda fault.

LOJA TERRANE

This metamorphic lithotectonic division is named after the city of Loja, over which region it is at its widest, 35km, spanning most of the Cordillera Real. It is defined by the close association of metamorphosed Palaeozoic semipelitic sedimentary rocks of the Chigüinda and Agoyán units with the Triassic Tres Lagunas 'blue quartz' granite. Amphibolites and the Sabanilla migmatites are also included in the terrane. The western boundary of the Loja terrane is the Baños fault against the Alao metamorphic terrane of Jurassic age. In the east there are tectonic contacts with the Jurassic Salado metamorphic terrane and the Amazonic craton over which Palaeozoic rocks are unmetamorphosed. The Loja terrane forms the topographic 'spine' of the Cordillera Real and is continuous along it except for the Río Paute section.

Chigüinda unit (Palaeozoic)

This unit dominates the geology of the southern Cordillera Real and the road sections across it: Cuenca-Limón, Catamayo-Loja-Zamora, Loja-Zumba, and Sigsig-Chigüinda; the latter settlement gives its name to the unit. It constitutes part of Kennerley's (1973) undifferentiated Zamora Series.

The Chigüinda unit comprises essentially quartzites and black phyllites as a semipelitic sequence. In the southern cordillera it forms a belt of rocks up to 30km wide, wedging out to the north, which is flanked westwards by metagranites of Tres Lagunas and eastwards by Sabanilla migmatites and Upano schists. Contacts are tectonic. Similar semipelitic rocks have been mapped as the Chigüinda unit in the north of the cordillera, over the Cuyuja nappe complex. A special feature of the unit is its close association with the Tres Lagunas granites.

Kennerley (1973) regarded the rocks as Palaeozoic, in view of their continuity with Peruvian sequences that are unconformably overlain by the Permo-Triassic Mitu Group. These metamorphic rocks of the Olmos massif of northern Perú comprise little-studied Precambrian and Palaeozoic sequences (Cobbing et al., 1981), which have yielded Ordovician-Silurian fauna (Mourier, 1988). During the present survey the phyllites and slates of lowest grade were sampled on a regional basis for palynological analysis. Two samples collected from the Loja-Zamora road (7126-95605 and 7132-95610) contain a small number of poorly preserved miospores of a type of organisation suggesting nothing more diagnostic than a post-Silurian age (Owens, 1992). Taking the above into account, along with the association with the Triassic Tres Lagunas granite, the age of the Chigüinda unit is indicated as Devonian to Permian.

Samples of low-grade phyllites from the Río Ingenio, 4km west of San José de Yacuambí, yielded the Early Jurassic-Cretaceous pollen *Perinopollenites elatoides* (Riding, 1989b). Rather than suggesting this younger age for the entire Chigüinda unit, it is thought more likely that these rocks belong to the Jurassic Upano unit of the Salado terrane which is difficult to distinguish lithologically without the volcanic component. The unit therefore excludes these rocks.

The Chigüinda unit comprises a monotonous sequence of generally impure, fine- to medium-grained quartzites, metasiltstones, graphitic schists, phyllites, slates and rare metagreywackes, the thickness of which is unknown but must be measured in kilometres. There is and overall absence of greenish rocks of metavolcanic affinity, and, east of Cuenca such rocks in ?tectonic association have been assigned to the adjacent Alao-Paute, El Pan or Upano units of Jurassic age.

The rocks are recrystallised and no sedimentary structures were noted. Metamorphic minerals are generally of low grade and include ubiquitous sericite and chlorite, with biotite and garnet noted particularly over a locally flat-lying 'schistose' sector along the Gualaceo-Limón road. Chloritoid and stilpnomelane have been observed and staurolite was seen in one sample from the Catamayo-Loja road.

The bedding and primary cleavage are generally subparallel, steeply dipping and Andean-trending, with evidence of more than one phase of deformation. Certain sectors, particularly the Cuyuja nappes in the north, and near the watershed along the Gualaceo-Limón road, exhibit 'flat belts' of cleavage.

The Chigüinda unit is a thick sequence derived from a continental source, probably in an intracratonic basin or passive margin setting. In terms of pre-metamorphic lithologies and age, the unit is similar to the Devonian and Carboniferous rocks of the Perú-Bolivia trough further south (Laubacher and Megard, 1985).

Agoyán unit (?Palaeozoic)

This unit of pelitic schists and paragneiss crops out mainly in the north of the cordillera; in the south there are small occurrences north of Loja. The most accessible outcrops are along the road just east of the Agoyán tunnel near Baños, where Sauer (1965) made the first petrological descriptions, and from which the unit is named; others occur near Monte Olivo and Papallacta.

The overall outcrop pattern of the unit is narrower than that of the Chigüinda and more disrupted by folding and faulting; contacts with adjacent units are regarded as tectonic and the overall thickness is not known. The unit is closely associated with the Tres Lagunas granite and essentially replaces the Chigüinda unit in this role in the north of the cordillera. At certain localities the presence of thin slivers of Tres Lagunas granite in the Agoyán schists was used to distinguish these schists from similar pelitic schists of the Upano unit. As with the Chigüinda unit, greenish meta-igneous rocks are rare; those noted are described under Monte Olivo amphibolites.

The metamorphic grade of these rocks is too high for fossil preservation and attempts have been made to date them by K-Ar geochronology. These have indicated ages of 417 Ma (Evernden, 1961) and 57 ± 2 Ma (Herbert and Pichler, 1983). Muscovite ages determined by Rundle (1988) and Harrison (1990) are Late Cretaceous, whilst those of biotite (from Papallacta) are Precambrian (p.119), but since the two metamorphic minerals are probably the same age, the younger ages may be due to argon release (age resetting) (p.62) and the older to local enrichment of radiogenic argon. The actual depositional age of the Agoyán unit is probably Palaeozoic, similar to Chigüinda.

Typical lithologies are medium-grained, garnet-muscovite schists and coarser-grained gneisses. These latter carry garnet crystals over 1cm in size at the type area near the Agoyán tunnel and reach over 2cm at Monte Olivo. In most areas the schists and gneisses are well mixed, but over the Monte Olivo sector they can be mapped as discrete divisions separated by a pegmatitic belt. East of Papallacta, gneiss boulders in the Río Chalpi contain small granitoid veins: evidence of incipient migmatisation.

Black graphitic schists may be present, and west of the Monte Olivo amphibolite there is a belt of feldspathic metapsammites. Thin, fine-grained orthoquartzites, garnet quartzites and quartz schists also occur. Certain sequences are essentially semipelitic, although over a wide area the quartzite fraction never approaches that found in the Chigüinda unit. Biotite, albite, chlorite and chloritoid may also be developed, and kyanite has been noted in associated veins. In the south of the cordillera, near Masaca, the unit is represented by quartz-rich biotite schists. The rocks are invariably steeply dipping, with schistosity the primary planar surface and with bedding indicated only where quartzitic or graphitic horizons are present.

The Agoyán unit is more pelitic and thus, in the strict sense, it is not the higher-grade equivalent of the Chigüinda semipelites. However, there is no evidence to indicate that they did not form within a common basin.

Monte Olivo amphibolites (?Palaeozoic)

This term includes all the amphibolites found in the Loja terrane, from the major belts, up to 2km wide, at Monte Olivo and Río Anatenorio, to small dykes and lenses. Such rocks are found associated with the four major Loja terrane units: Chigüinda, Agoyán, Tres Lagunas and Sabanilla, and, where not strongly tectonised, contacts can be identified as discordant or concordant.

K-Ar dates on hornblendes from an amphibolite dyke near Papallacta with relict igneous texture (p.119) (Rundle, 1988) are Upper Devonian in age (363 ± 9 Ma and 371 ± 10 Ma), whilst dates from an adjacent, more metamorphosed, garnet amphibolite yield Carboniferous ages (306 ± 10 Ma and 342 ± 23 Ma) (Harrison, 1990). It is possible that these indicate the age of intrusion or amphibolitisation.

Regarding the two main outcrops, that at Monte Olivo appears to represent a stratigraphical formation between metapsammites and pelitic schists with a well-exposed concordant or transitional contact with the former. Lithologies are dominated by amphibolitic schists of mafic metabasaltic affinity with hornblende-quartz-calcite-epidote-biotite assemblages. Fine- to coarse-grained gneissic types with quartzofeldspathic segregations, are present, associated in places with fine-grained, grey-green quartzites. In contrast, the Río Anatenorio outcrops show massive, fine- to medium-grained garnet amphibolites with schistose margins against the Agoyán schists; smaller bands are entirely schistose.

Many outcrops are too small to show on the accompanying map. In certain cases, such amphibolites reveal discordant (intrusive) relationships *vis-à-vis* original compositional layering in the schists yet are affected by a common schistosity. Many also show relict dolerite textures, e.g. Papallacta. Below the Agoyán Dam in the Río Pastaza, large outcrops and boulders of Tres Lagunas metagranite contain disrupted amphibolite dykes with sharp intrusive contacts, the margins of which are only slightly foliated by the tectonic fabric in the granite indicating a late-plutonic, syntectonic emplacement (Plate, 13). From a distance it appears that one such dyke cuts the granite further downstream across the face of the Agoyán Falls. (The stretch of the Río Pastaza below the dam and including the Agoyán Falls is now bypassed by the hydro-electric tunnel and is essentially dry).

The Monte Olivo amphibolites represent a phase of mafic dykes which cut, or are concordant with, the premetamorphic Agoyán and Chigüinda sediments; at Monte Olivo, an original intrusive sill, or basalt lavas are present. However, the Devonian and Carboniferous K-Ar ages of these dykes at Papallacta could indicate the postsedimentary/premetamorphic phase of intrusion older than the disrupted amphibolite dykes within the Upper Triassic Tres Lagunas granite.

Tres Lagunas granites (Upper Triassic)

This, the ‘blue quartz’ granite, is the principal igneous unit of the Loja Terrane (Aspden et al., 1992b). It is found associated with the metasedimentary rocks of Chigüinda and Agoyán throughout the Cordillera Real in forms ranging from batholithic to detached tectonic lenses a few centimetres wide. The granite had previously been recognised at Papallacta (Colony and Sinclair, 1932), Sigsig (Harrington, 1957) and Tres Lagunas (Kennerley, 1973), and the present study has linked these occurrences into a semicontinuous belt. The unit is named after the Tres Lagunas area, east of Saraguro, where it attains batholithic proportions, 100km long and over 10km wide. Accessible outcrops occur at Peggy Mine, near Sigsig; below the Agoyán dam near Baños; and around the Malacatus basin area.

Although the bulk of the granite is found within the Loja terrane, thin tectonic lenses, not more than a metre wide, have been identified within the Peltetec ophiolitic mélange (p.45), the Cuyuja nappes, and reported from the Alao terrane (oral communication, M. Mora). The granite also forms xenoliths within the Tertiary Alao pluton, which cuts the Alao terrane (Figure 16). These occurrences outside the Loja terrane, however small, are important in any tectonic model of the cordillera.

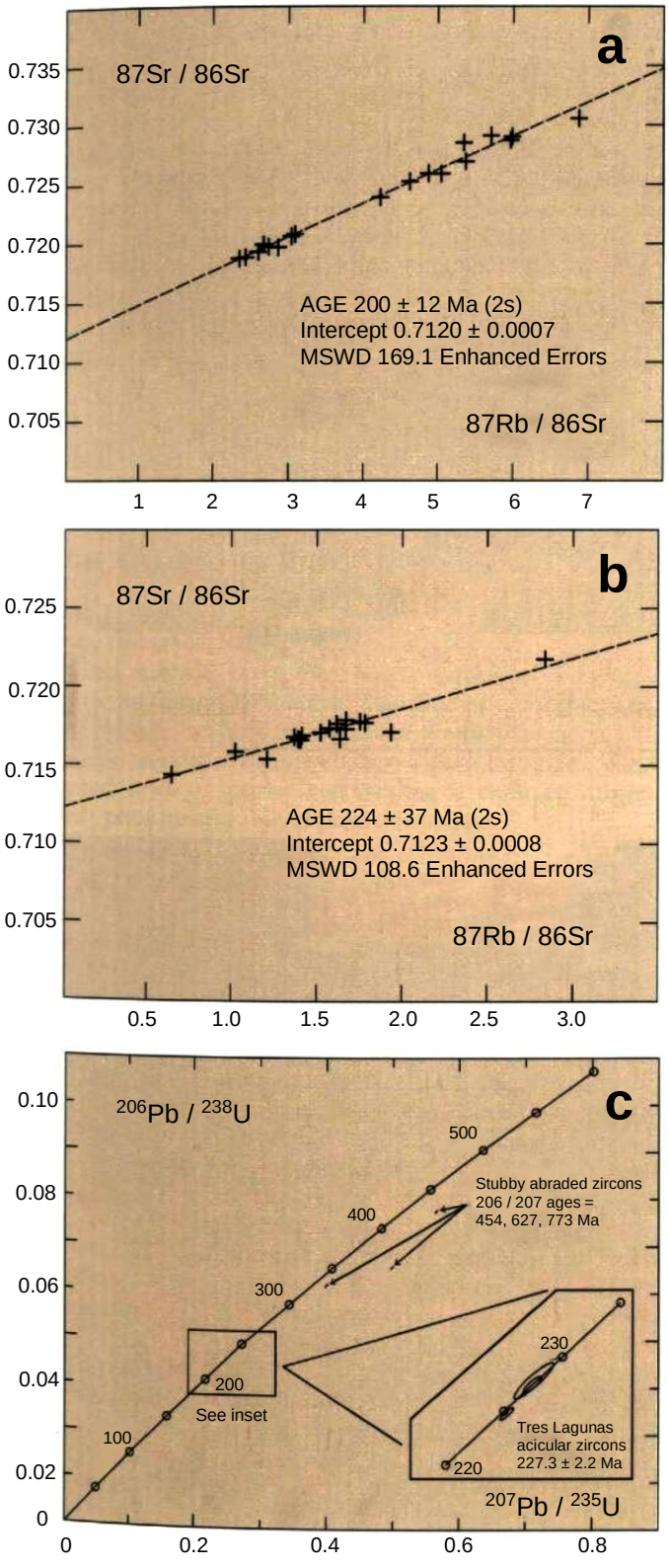

Figure 7. Geochronological plots for the Tres Lagunas granite and Sabanilla unit.

(a) Rb-Sr plot of 19 Tres Lagunas granite samples from the Tres Lagunas and Malacatus sectors; **(b)** Rb-Sr plot of 18 samples of the Sabanilla migmatite; **(c)** U-Pb concordia diagram for the Tres Lagunas granite. The crystallisation age of 227.3±2.2 Ma is defined by analyses of acicular zircons. Abraded, rounded zircons have inherited ages as old as Upper Proterozoic.

Previous K-Ar dating of rocks now ascribed to this unit gave 173 ± 4 Ma and 78 ± 1 Ma (Kennerley, 1980) and 60 ± 2 Ma (Herbert and Pichler, 1983). The project's age dating programme has concentrated heavily on this unit. 14 K-Ar ages (p.119) gave the range of 60-100 Ma, which, whilst interesting in terms of resetting events, was regarded as too young. Combined Rb-Sr whole rock data (17 points) produced an errorchron age of 200 ± 12 Ma (MSWD = 169; Ri = 0.712) (Figure 7a) (Harrison, 1990). Sm-Nd analysis of garnets yielded a poorly constrained isochron of 257 ± 125 Ma (Harrison, 1990). Finally, the age of intrusion was more precisely determined as 227.3±2.2 Ma using lead isotope analysis of zircons and based on a concordant point for good quality needles (Figure 7c) (written communication, S. Noble). Rounded zircon grains from the same sample showed older inherited ages probably derived from the Chigüinda sediments.

The field appearance of the granite varies from massive to sheared and schistose (Plate 3). Over areas relatively undeformed, and where primary igneous textures are essentially preserved, the granite is medium to coarse grained and carries prominent smoky-grey alkali feldspar megacrysts which can attain lengths up to 14cm. Many samples also contain brightly coloured, pale blue quartz crystals, along with colourless ones, and this is the most diagnostic feature of the granite in the field. The origin of this colouration is uncertain, but it may relate to the effects of internal strain in individual crystals. Modal quartz is in the region of 35-59 per cent and K-feldspar, 1-13 per cent. Plagioclase (albite-oligoclase) (13-41 per cent mode) is cream coloured and may be included in, or rimmed by, the alkali feldspar; rapakivi overgrowths also occur. The major mafic mineral is biotite (9-18 per cent mode), which is typically of foxy red colour in thin section; hornblende has not been recorded. The rocks are monzogranites and granodiorites after Streckeisen (1976) (Figure 8); more mafic associates, e.g. diorites, were not noted.

Garnet is a common accessory mineral reaching up to 30 per cent of the mode along a mappable belt of garnet granite between Papallacta and Oyacachi. Here, original granite textures have been destroyed save for the irregular, re-entrant forms of pink garnet crystals (Fortey, 1990). Cordierite has been recorded but is rare. Muscovite is common (1-9 per cent mode) but mostly it is subordinate to biotite which it generally replaces. Other mineral parageneses include the formation of epidote; sericite/zoisite alteration of feldspars; recrystallisation and/or chloritisation of biotite; and the growth of tourmaline.

Contacts with adjacent Agoyán or Chigüinda unit rocks are seen or inferred as tectonic; no intrusive contact has yet been seen. However, xenoliths of greenschist, quartzite, semipelite and aplite phases have been noted, but are rare. A pregranite phase of folding is present in a small, partially assimilated, semipelitic xenolith in river blocks above the Agoyán falls. In the same boulders there are disrupted amphibolite dykes (p.53). Large xenocrysts of quartz, up to 5cm across, are common in the Malacatus area.

a

b

Plate 3. Tres Lagunas granites.

(a) Weakly metamorphosed granite with characteristic blue quartz.

(b) Tres Lagunas granite as mylonitic augen gneiss cut by post-tectonic pegmatite

The granite invariably shows evidence of deformation, metamorphism and recrystallisation, ranging from incipient alteration in massive rocks with preserved igneous textures to the formation of gneissic and mylonitic granites and augen gneisses (Plates 3 and 14). Such mylonitic textures were previously noted at Papallacta (Colony and Sinclair, 1932) and Tres Lagunas (Kennerley, 1973). The tectonic foliation is generally steeply dipping but may also form 'flat belts' within the enveloping Chigüinda or Agoyán units. The common rock types are foliated or schistose granite, biotite gneiss or augen gneiss, which contain augens up to 4cm across of blue-grey alkali feldspar + quartz; blue quartz may also be present in these rocks. The granite can be traced across the strike into high-strain zones in which the igneous texture of the protolith is progressively destroyed. In particular, the grain size is mechanically reduced by an increase in the number of millimeter-scale, diastomising microshears and the typical end-product of this process is a relatively fine-grained, pale, micro-augen schistose rock of S-C mylonite type (Lister and Snoke, 1984).

The progressive cataclastic deformation in these rocks has been documented petrographically by Dangerfield (1988) in the form of the following stages:

1. Some recrystallised quartz mosaic; plagioclase sericitised and altering to zoisite.

2. Considerable development of recrystallised quartz mosaic; biotite ragged and marginally recrystallised, its cleavage distorted.

3. Quartz mosaic complete; mica cleavage distorted, some recrystallisation; feldspar lamellar twinning bent or broken; non-penetrative mica foliae developed.

4. Quartz mosaic forms well-developed laminae; mica disrupted and/or partly recrystallised; definite augen formed; penetrating mica foliae developed.

5. Continuous quartz laminae developed; mica foliae complete; augen well-formed commonly with pressure shadows; complete schistosity developed.

Pegmatites are associated with the granite and in most cases cut the mylonitic fabric (Figure 3b). They comprise quartz-feldspar-muscovite-tourmaline veins with quartz-tourmaline veins and balls. True greisens have not been identified, but the presence of topaz in heavy minerals from the Río Sangurima, near Chigüinda, could indicate their proximity. In the extreme north, the Monte Olivo pegmatite belt is a concordant unit, up to 2km in thickness, of massive pegmatite or pegmatised schist which follows the local schist/paragneiss contact in the Agoyán unit. Megacrysts of perthite, muscovite, tourmaline, titanite and green zoisite occur and dumortierite has been noted (Fortey, 1990). In this area there is evidence that tectonic processes have partially destroyed the pegmatite textures.

GEOCHEMISTRY

Analytical data is given on pp.140-143 and plotted on Figure 8, along with data from the Sabanilla unit, the Moromoro granites and the Zamora granitoids.

Based on the CIPW normative values almost all the Tres Lagunas granite samples from Valladolid, Malacatus, Peggy, Saraguro and Baños plot in the quartz-rich part of the monzogranite field in the QAP ternary diagram (Figure 8a). The same granites plot in the volcanic arc granites field on the Rb against Y + Nb plot (Pearce et al., 1984) (Figure 8b) but are somewhat enriched and fall close to the boundary with within-plate granites.

Compared with the Zamora granitoids the Tres Lagunas granites are enriched in various elements and depleted in Na_2O on the scatter plots against SiO_2 (Aspden et al., 1992b). Whereas Th, Ce, Y and Nb rise with increasing SiO_2 in the I-type Zamora granitoids they fall with increasing SiO_2 in the Tres Lagunas granites which are thus a separate group and could not have formed by fractionation of I-type magmas (Aspden et al., 1992b).

On the K_2O v. Na_2O and Al/(Na+K+Ca/2) v. SiO_2 plots (Figures 8c and 8d), the Tres Lagunas granites fall into the S-type of Chappell and White (1974). They are peraluminous (A/NKC> 1.1). Equally on the ACF plot (Aspden et al., 1992b), the granites straddle the plagioclase-biotite tie line and extend into the Al-rich part of the diagram. An S-type parentage was also suggested on a petrographic basis by Atherton (1987) and by Clarke (1989), based on plots of preliminary analytical results.

The Chappell and White (1974) classification of granites into S- and I-types is broadly similar to the ilmenite- and magnetite series of Ishihara (1977) in that all S-types belong to the ilmenite-series, and the majority of I-types correspond with the magnetite series. The Fe_2O_3/FeO v. SiO_2 plot (Lehmann and Harmanto, 1990) shows the separation of the Tres Lagunas granites and Zamora granitoids into the ilmenite- and magnetite-series respectively (Figure 8e).

On a number of plots, it can also be seen that granites collected from different sectors of the Tres Lagunas outcrop form individual clusters of compositional subgroups. These subgroups are apparent in diagrams which involve Cr, Ni and SiO_2 as discriminants (Aspden et al., 1992b) and suggest a lack of regional uniformity.

In conclusion, the Tres Lagunas granites can be classified as S-types and their relatively high $^{87}Sr/^{86}Sr$ ratios also indicate a substantial crustal component in their origin. This value, 0.712 (Figure 7a), is greater than the entire range of Ri values from the Zamora and Azafrán granitoids and is similar to that of crustally contaminated modern andesites in Colombia (James, 1984). The significance of the discovery of this regional S-type granite belt which is strongly mylonitised in places, is discussed on p.77.

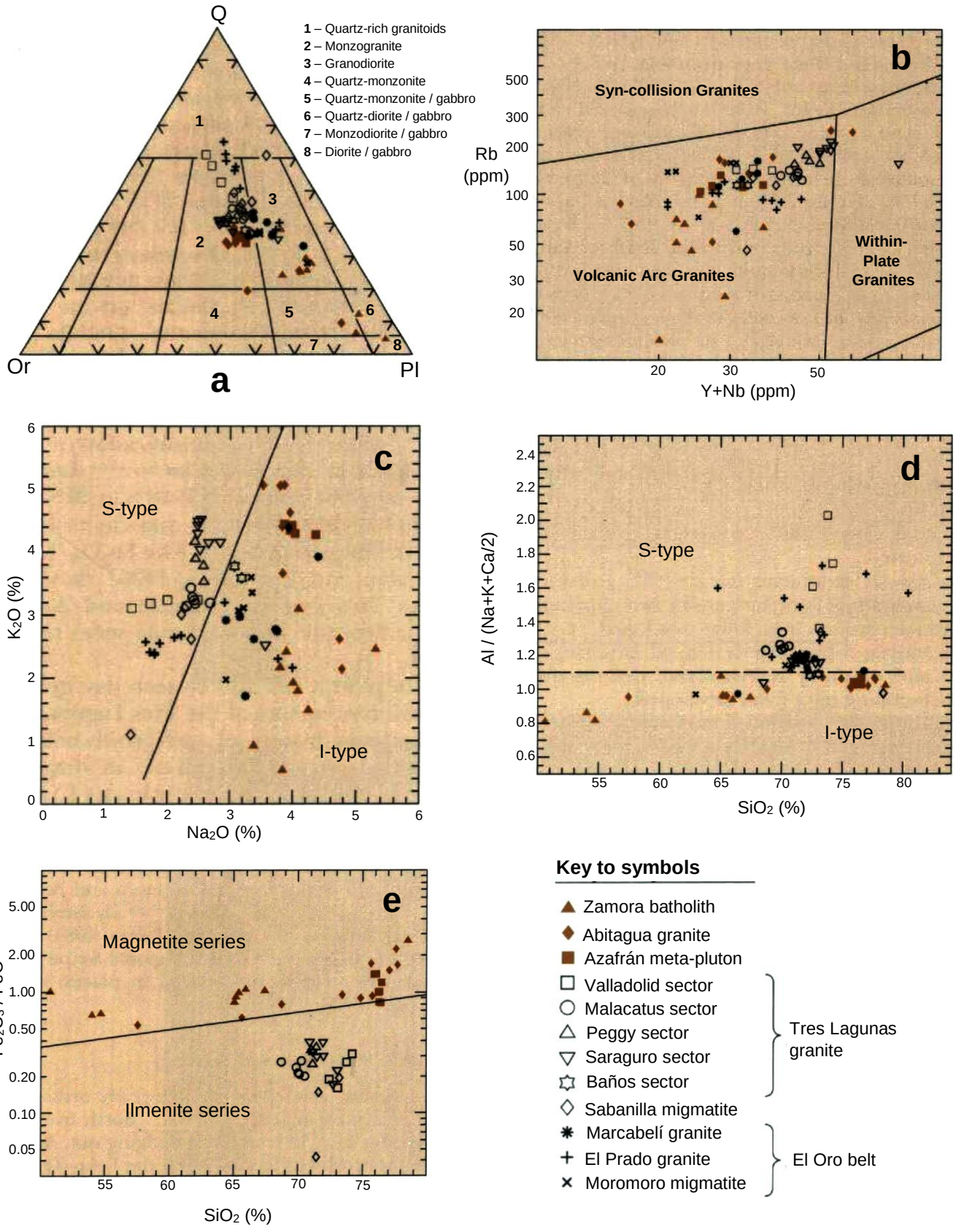

Figure 8. Geochemical plots for granitoid rocks.

(a) QAP ternary plot for all granitoid rocks after Streckeisen (1976) based on CIPW normative values (Q = quartz; Or = orthoclase; Pl = anorthite + albite); **(b)** granitoids on Rb v. Y + Nb discrimination plot of Pearce et al. (1984a); **(c)** K_2O v. Na_2O diagram for all granitoids, I-type and S-type fields after Chappell and White (1974); **(d)** aluminosity index v. SiO_2 for all granitoids, I-type and S-type fields after Chappell and White (1974); **(e)** Fe_2O_3/FeO v. SiO_2 plot for Cordillera Real granitoids, fields after Ishihara et al. (1979) and Lehman and Harmanto (1990)

Sabanilla unit (Palaeozoic and Triassic)

This unit is a suite of medium- to high-grade ortho- and paragneisses forming a 10km-wide belt north from the Peruvian border for 150km before wedging out. Accessible outcrops occur near Sabanilla, on the Loja-Zamora road, which gives its name to the unit, and along the Loja-Zumba road and the track to Pico Toledo. Contacts with the adjacent Chigüinda and Isimanchi units, both of lower metamorphic grade, are tectonic. East of the Isimanchi unit, gneissic rafts in the Zamora batholith, which resemble the Sabanilla unit, have been allocated a Precambrian age.

The geochronology of the metaplutonic phases shows K-Ar muscovite and biotite ages of 60-100 Ma (p.119), and, as in the case of the Tres Lagunas granite, these are regarded as reset. The hornblende K-Ar ages are older at about 130Ma. The Rb-Sr geochronology (p.118) shows an 8-point errorchron of 233 ± 51 Ma (MSWD = 175; Ri = 0.7118) (Rundle, 1987b). A further set of ten samples collected from a single outcrop (Harrison, 1990) gave 198 ± 45 Ma (MSWD = 25.3; Ri = 0.7123). Combining the two datasets gave an errorchron of 224 ± 37 Ma (MSWD = 108) (Figure 7b), an age similar to that of the Tres Lagunas granites.

To the east of Sabanilla and to the south of Yangana the western margin of the unit comprises steeply dipping to vertical gneissic ‘quartzites’, which contain sillimanite, muscovite, biotite and perthite in places, which pass eastwards into granodioritic biotite orthogneisses with prominent muscovite. These gneisses may exhibit a streaky biotite foliation along with incipient migmatisation. Further east, towards Zamora, migmatitic gneisses and streaky biotite gneisses carrying sillimanite and kyanite are present (see also Trouw, 1976). High grade assemblages of sillimanite-biotite-quartz-albite and kyanite-biotite-orthoclase-quartz were noted. Around Valladolid and to the north, amphibolitic gneisses, with or without biotite, are common especially within the metaplutons, and their general form suggests they were originally basic dykes or sheets. Staurolite-bearing gneisses occur to the north of Palanda over an area where muscovite and/or biotite pegmatites are common. There are also minor, unfoliated, muscovite-tourmaline-garnet pegmatitic leucogranites associated with two-mica, garnet-bearing orthogneisses. Gneissic xenoliths are common and, in some outcrops, it can be seen that the progressive digestion of this material produces the biotite-rich schlieren which are themselves streaked out. The field observations indicate plutonic granodiorites (orthogneisses) associated with pelitic sediments now metamorphosed to medium- to high-grade paragneisses.

Geochemically, the Sabanilla unit orthogneisses plot into the S-type granite field along with the Tres Lagunas granites (Figure 8), and are of similar age, with a similar initial strontium ratio of about 0.712 (Figure 7b). In contrast to the Tres Lagunas granites, however, they do not contain blue quartz, are not commonly megacrystic, are more homogeneously foliated, and are associated with high-grade migmatites. It is thus probable that the Sabanilla unit represents a deeper-level, migmatitic phase of the Tres Lagunas granite.

FOUR

Cordillera Real: Jurassic-Lower Cretaceous rocks

AMAZONIC CRATON

During the Jurassic and Lower Cretaceous, the Amazonic craton was the site of deposition (Santiago Formation and Chapiza unit), volcanic extrusion (Misahuallí unit) and magmatic intrusion (Zamora granitoids) over a region which underwent no subsequent tectonometamorphic event and thus contrasts with the Jurassic metamorphic terranes of Salado, Alao and Guamote further west.

Santiago Formation (Lower Jurassic)

This unit, named by K. T. Goldschmid of Shell Co., in 1940, of marine limestones, shales, sandstones and volcanic rocks, forms much of Cordillera Cutucú of southeast Ecuador (Tschopp, 1953; Baldock, 1982), to the east of the accompanying map. Ammonites recovered from it: *Arietites* (Tschopp, 1953), *Arnioceras* and *Coroniceras* (Geyer, 1974); and *Leptechioceras* sp. indet. and *Paltechioceras* sp. indet. (Aspden and Ivimey-Cook, 1992) (Plate 7e and f), indicate a Sinemurian age. The Formation extends southwards into Perú but is absent in boreholes further north and east in Ecuador.

The Formation, about 2000m thick, comprises a low-dipping, unmetamorphosed sequence of grey siliceous limestones, calcareous sandstones, turbiditic in places, and black shales. Westwards, in outcrops along the new road to Santiago, calcareous turbidites of the Santiago Formation grade laterally into a continental-type sequence of tuffaceous grey siltstones and sandstones with basaltic lava flows containing pillow structures in places (Aspden and Litherland, 1992), a sequence which lithologically corresponds to the Chapiza Formation. It thus appears that at least the base of the Chapiza Formation could be the lateral equivalent of the top of the Santiago Formation. A similar transition has been reported in northern Perú (Cobbing et al., 1981; Jaillard et al., 1990).

Chapiza unit (Jurassic-Lower Cretaceous)

The Chapiza Formation (named by K. T. Goldschmid of Shell Co., in 1940) comprised a succession of low-dipping, unmetamorphosed, continental-type, clastic sediments overlain by the volcanic Misahuallí Member (Tschopp, 1953). In this memoir the Misahuallí rocks are described separately and the sediments are referred to as the Chapiza unit.

The Chapiza unit forms much of the Cordillera Cutucú to the east of the accompanying map where it overlies, or is a facies of, the Santiago Formation of Lower Jurassic age. Indeed, the Sinemurian ammonites collected by the project from the Santiago Formation were from the Santiago road close to this facies boundary (Aspden and Ivimey-Cook, 1992). In the Oriente, palynological data from an oil well indicates Neocomian-Aptian rocks at 33m below the Hollín unconformity and the Jurassic/Cretaceous boundary at 213m (Bristow and Hoffstetter, 1977).

The sedimentary Chapiza sequence of Cordillera Cutucú comprises about 2500m of red, pink and grey shales and sandstones with thin horizons of anhydrite, dolomite and gypsum (Tschopp, 1953). There are strong indications (above) that at least part of the sequence is equivalent to the Santiago Formation. Thus, along the road east to Santiago, there are sandstones and grey to reddish tuffaceous siltstones, intercalated with basalt flows, and minor calcareous siltstones and sandstones similar to those in the Santiago Formation. The volcanic component decreases east of Río Undo where the rocks can be classified as Santiago Formation in the strict sense. In both the Chapiza and Santiago facies there are large turbiditic canals 10-20m deep and 100m wide containing poorly sorted material rich in volcaniclasts.

Misahuallí unit (Jurassic-?Cretaceous)

Low-dipping lavas and pyroclastic rocks noted in the Río Misahuallí, east of the accompanying map, were named the 'Misahuallí basalts and tuffs' by Wasson and Sinclair (1927); and these formed the upper Misahuallí Member of the Chapiza Formation (Tschopp, 1953), with a thickness of up to 2000m. In the present memoir the term Misahuallí unit includes all the continental-type volcanic rocks of the sub-Andean belt known, or considered to be, essentially of Jurassic age, overlying the Lower Jurassic Santiago Formation and overlain by the Hollín Formation of Aptian-Albian age. Over the present area these comprise, in the main, the volcanic rocks associated with the major Jurassic batholiths. These rocks are extensively exposed along the sub-Andean zone of the accompanying map, and, with the exception of the extreme north, are limited westwards by the Cosanga fault.

Hall and Calle (1982) quote a K-Ar age of 132 Ma from P. Espín (personal communication) of a sample of the Misahuallí Member from a deep well in the Oriente. In the present survey, rocks assigned to the Misahuallí unit are cut by the Abitagua granite of 162 ± 1 Ma (p. 24), whilst a hornblende andesite dyke intruding the same granite gave a K-Ar age of 168 ± 8 Ma. Further south, the volcanic rocks are related to the Lower to Middle Jurassic Zamora batholith (p. 26), with associated lava and dyke samples giving K-Ar ages of 230 ± 14 Ma and 143 ± 7 Ma respectively (p. 119).

Lithologies comprise green to dark grey basalts, trachytes, grey-green, violet and pink tuffs and tuffaceous breccias, interstratified with red shales, sandstones and conglomerates (Baldock, 1982). Pillow structures have been reported from basalts east of the Río Nangaritza (oral communication, I. Gemuts). Over the present area, green to dark grey or purple andesites and agglomerates have also been noted.

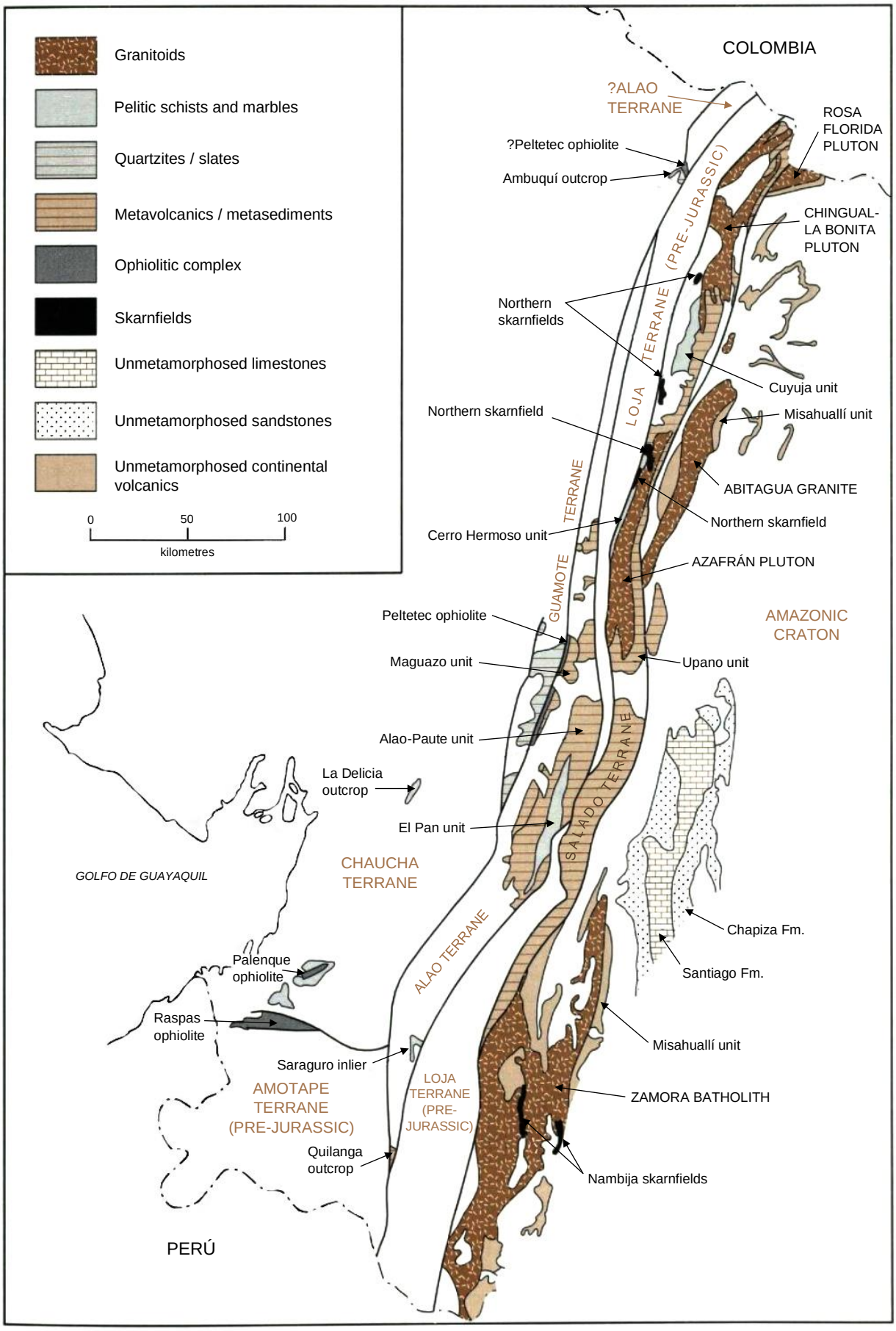

Figure 9. Jurassic-Lower Cretaceous rocks and terranes of Ecuador.

In the north of the area, east of the Cosanga fault, the Misahuallí unit occurs as the highest-level igneous facies of the Rosa Florida pluton. No contacts were noted along the Rosa Florida-Puerto Libre trail, but there is a lessening of grain size south-eastwards from plutonic, through subvolcanic, to volcanic types. Grey-green andesitic lavas, porphyries and greenish banded tuffs are present in outcrop; float blocks in the Río La Chispa show tuffs and agglomerates containing diagnostic pink syenitic clasts derived from the pluton. Further south, in the Río Mulatos west of the Abitagua granite, the main lithologies are siliceous lavas, either off-white or black and glassy, or pink porphyritic types, associated with flow breccias and pyroclastics. Sedimentary intercalations were not noted.

In the south of the area many of the outcrops shown as Misahuallí unit are based on mining company reports and, in certain cases, there may be some confusion with the volcanosedimentary Piuntza unit of Triassic age. However, over those outcrops traversed by the Project, the lithologies comprise hornblende andesites, feldspar microporphyritic andesites, dacites, and andesite-dacite lavas and pyroclastics, with little or no sedimentary phase, but in many places associated with porphyritic subvolcanic intrusions. It is interesting to note that in the eastern extremity of this area, along the Río Tundalne, the Misahuallí unit apparently replaces the Chapiza sediments, exposed further north in the Río Santiago, along the western limb of the Cutucú anticline overlying the Santiago Formation.

In the north of the area, the Misahuallí unit is shown on the accompanying map to crop out west of the Cosanga fault within the metamorphic belt. Thus, around La Bonita there are purple, green, grey or off-white, massive and cleaved metavolcanic rocks of intermediate to acid composition with abundant epidote. Meta-agglomerates were also noted, but a metasedimentary phase is absent. Just north of Rosa Florida, and within this metavolcanic belt, the trail crosses a distinctive formation of fine-grained, siliceous 'cherty', banded rocks of metavolcanic affinity, intercalated with grey slates: lithologies also found as float blocks in the streams further south. Similar banded lithologies occur as blocks in tributaries of the Río Cofanes further west where the laminations are off-white, pink, pale green and black, and in many places studded by garnet. Further south still, along the Río Salado west of Reventador volcano, there are outcrops of deformed and sheared grey andesites, green tuffs and purple porphyries, and river boulders of red and green meta-agglomerates and greenstone vein breccias. Metamorphosed felsitic lavas and agglomerates of Misahuallí-type were also noted tectonically mixed with Upano unit rocks in the Río Cosanga (Figure 19) and along the Gualaceo-Limón road.

These regionally metamorphosed 'Misahuallí-type' rocks occur within the Upano unit of the Salado terrane, thus transgressing the Cosanga fault, a proposed suture. They appear to pass laterally into the volcanosedimentary Upano unit of that terrane (p.27).

It is suggested that the Misahuallí unit represents the volcanic sequences of a continental magmatic arc, the main plutonic phases of which are described below. The volcanic rocks are interpreted to wedge out eastwards within the Oriente basin (Bankwill et al., 1991) and pass laterally westwards across the Cosanga fault into the Upano unit of the Cordillera Real.

Zamora granitoids (Jurassic)

Three major, essentially undeformed and unmetamorphosed granitoid plutons occur over the Amazonic craton forming a sub-Andean chain associated with volcanic rocks attributed to the Misahuallí unit. They are described from north to south.

The **Rosa Florida pluton** is part of the former La Bonita pluton (Baldock, 1982) now separated from the La Bonita plutonic phase by a belt of Misahuallí volcanics and the Cosanga fault. Along the La Bonita-Puerto Libre trail the first outcrops occur close to the village of Rosa Florida. In this region the dominant lithologies are grey, coarse-grained, biotite quartz-monzonite and deep pink, coarse-grained, biotite quartz-syenite; hornblende was noted in places. Further south, these pass into subvolcanic equivalents, finer grained or porphyritic, before passing into the Misahuallí volcanic phase. A diagnostic feature of the pluton is the bright pink colour of the K-feldspar in the syenitic rocks. Volcanic greenstone xenoliths and autobrecciated dykes are common.

On the earlier national map, Baldock (1982) shows a granite inlier lying between the Rosa Florida and Abitagua plutons. Float rock in the Río Borja, presumably derived from this occurrence, was of deep-pink quartz-syenite type, indicating that the Rosa Florida pluton may extend into this area southwards beneath the cover of younger rocks.

The **Abitagua granite,** noted by Colony and Sinclair (1932) and named by Sauer (1950), is an elongate pluton at least 120km long and up to 15km wide. Most contacts appear to be faulted, but the batholith intrudes the Jurassic Misahuallí volcanics in the west along the Río Mulatos, and, in the south, north of the Río Pastaza, it is unconformably overlain by the Cretaceous Hollín Formation. In the north the granite appears to be buried by the Cenozoic Sumaco volcanics.

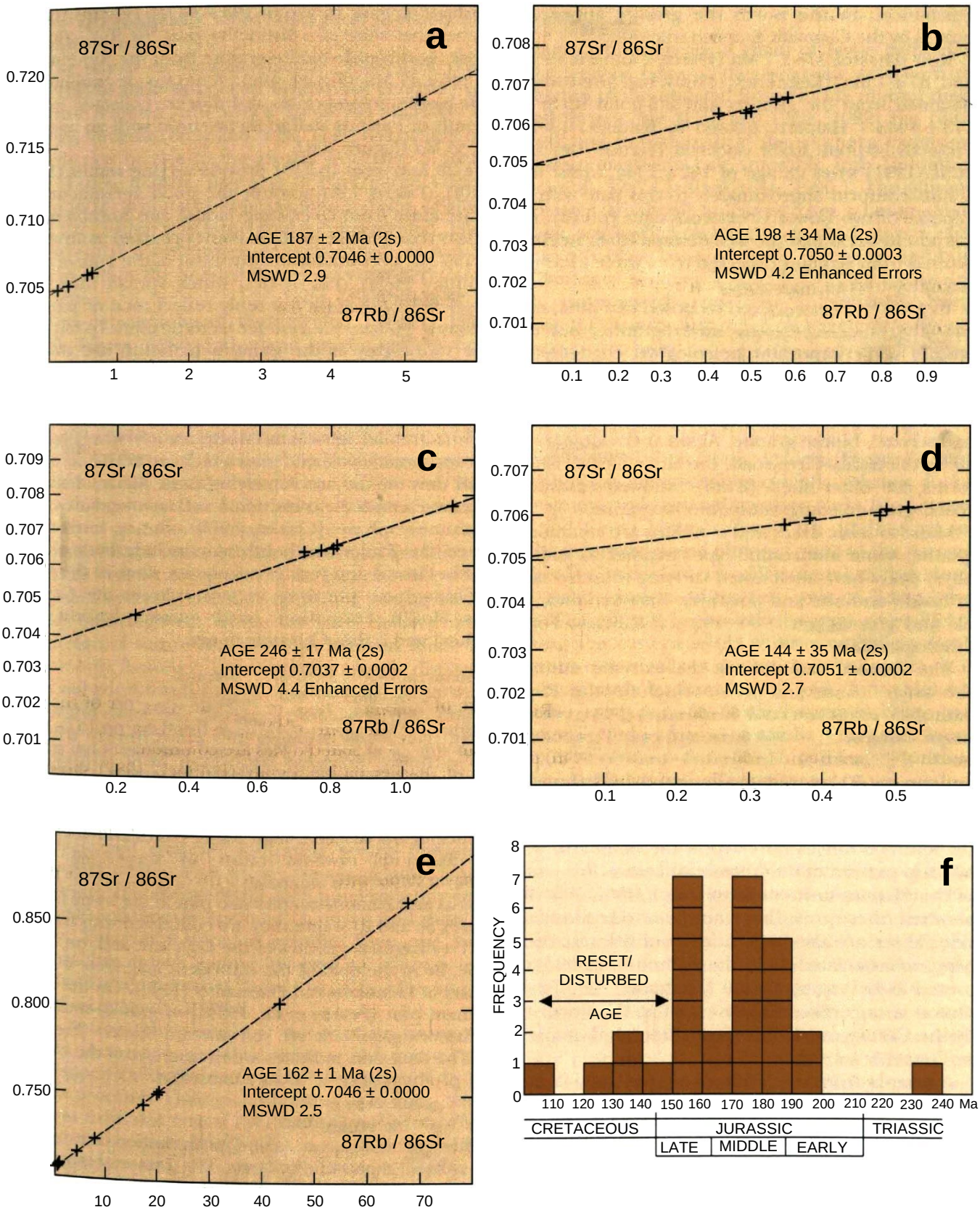

Figure 10. Geochronology of the Zamora granitoids.

(a) Rb-Sr plot of the La Paz sector of the Zamora batholith; **(b)** Rb-Sr plot of the eastern (Paquisha) sector of the Zamora batholith; **(c)** Rb-Sr plot of the Río Pituca (southern) sector of the Zamora batholith; **(d)** Rb-Sr plot of the Río Mayo (Palanda) sector of the Zamora batholith: **(e)** Rb-Sr plot of the Abitagua granite; **(f)** histogram of K-Ar mineral ages from the Zamora batholith.

K-Ar dates of 178 ± 7 Ma (Herbert and Pichler, 1983) and 87 ± 7 Ma (Kennerley, 1980) had previously been obtained from the granite, and a 3-point Rb-Sr plot of 173 ± 5 Ma (Halpern, quoted in Baldock, 1982). The Project's 16-point Rb-Sr isochron (Figure 10e) (Aspden et al., 1991) gives an age of 162 ± 1 Ma, whilst the K-Ar results conform approximately to this date with the exception of two Lower Cretaceous ages (p.119). It is important to stress that the well-defined Rb-Sr isochron was plotted from samples collected from three localities with maximum spacings 100km apart.

In general, the pluton is composed of a pink, medium- or coarse-grained, biotite monzogranite, but detailed studies show important petrological changes. For example, at its western margin along the Río Mulatos the outer 3km of xenolithic, medium-grained, hornblende-biotite granite is intruded by a coarse-grained, K-feldspar megacrystic, biotite granite. Again, at the western margin along the Baños-Puyo road, the latter megacrystic phase forms the outer shell (2km) followed eastward by a coarse-grained equigranular biotite granite.

Mafic to felsic dykes and xenoliths are common in the granite; some monzonitic types weather to kaolin. Porphyry dykes have been noted carrying rounded xenoliths of basalt, andesite and porphyry. Rare xenoliths of marble and greywacke could represent Santiago Formation lithologies.

The **Zamora batholith**, in the extreme south-east of the area, is now defined to include the Río Mayo batholith of Baldock (1982) along with newly discovered major extensions to the north and east. The body as now mapped presents an elongate batholith over 200km long and up to 50km wide, segmented into three by the north-trending La Canela and Nangaritza faults. Outcrops of ?Precambrian gneisses and Palaeozoic Isimanchi schists occur as rafts within the batholith, whilst the outcrop pattern of the Triassic volcanosedimentary rocks of the Piuntza unit conforms to a fairly flat eroded roof pendant; these rocks have not been recorded from outside. There are also large outcrops of volcanic rocks overlying, or associated with the batholith, which are interpreted as belonging to the Misahuallí unit. Finally, the pluton is unconformably overlain in the north and east by the Cretaceous Hollín Formation, and cut, in places, by Cenozoic intrusives.

A sample from the 'Palanda pluton', which is now included as part of the Zamora batholith, showed differing mineral ages with a range of 152-180 Ma (Kennerley, 1980); a K-Ar age of 171 ± 6 Ma was reported by Pichler and Aly (1983). The Project's Rb-Sr geochronological results from five suites of samples (p.118); all gave reasonably good linear correlations with relatively low MSWD values. However, the calculated ages are variable, with high errors due to the small spread of Rb-Sr ratios. Probably the most reliable data are from a suite of five samples from the La Paz area which define an isochron of 187 ± 2 Ma (Figure 10a).

Six samples from the Paquisha area gave an age of 198 ± 34 Ma (Figure 10b), whilst another suite of a distinctive porphyritic, pink, K-feldspar, hornblende-biotite granite from the Río Pituca gave 246 ± 17 Ma (Figure 10c). A group of five hornblende-biotite granodiorites and diorites collected from the south of Palanda define an isochron with an age of 144 ± 35 Ma (Figure 10d).

The 29 K-Ar ages (p.119) provide varying results (Figure 10f). Taking into account the good agreement of separate dates from co-existing biotite and hornblende, it is clear that a major isotopic event occurred at around 170-190 Ma, presumably the intrusion of the bulk of the batholith. The younger dates, which spread into the Cretaceous (Figure 10f) probably reflect total or partial resetting, related to the Peltetec tectonic event (p.63).

The lithologies of the Zamora batholith are dominated by hornblende-biotite granodiorites and diorites; true granites are rare. Porphyritic hornblende granodiorites are common in the Guaysimi area. There are also finer-grained subvolcanic rocks associated probably with co-magmatic piles which are shown as Misahuallí unit on the accompanying map. Many of these centres are seen to be transitional and co-magmatic with the plutonic phase (Clarke, 1989), but as currently mapped the Zamora batholith may include both older (e.g. Río Pituca) and younger elements, since in the east the Chinapintza porphyry metamorphoses the Cretaceous Hollín Formation (oral communication, D. Coochey) and is thus Cenozoic in age.

GEOCHEMISTRY OF THE ZAMORA GRANITOIDS

Major and trace element analyses of samples from the Abitagua and Zamora plutons are listed on pp. 137-139 and plotted on Figure 8. The broad compositional spectrum of the granitoids, manifested by a wide range in SiO_2, are typical of cordilleran I-type plutons (Chappell and White, 1974; Pitcher, 1983), as are the common presence of hornblende, high Na_2O values and low initial strontium isotopic ratios of the order of 0.7034-0.7056 (Rundle, 1987b) (Figure 10). The Abitagua and Zamora samples also plot in the I-type field (Figures 8c and d) where they are contrasted with the S-type Tres Lagunas granites of the Loja unit and, on Figure 8e, lie in the field of the equivalent magnetite-series granites of Lehmann and Harmanto (1990). On the discriminant plot (Pearce et al., 1984a) of granite settings the Zamora granitoids are volcanic arc related (Figure 8b). The data thus indicates a derivation from the magmatic products of ocean plate subduction.

CONTACT ROCKS AND SKARNS

Silicification, epidotisation, and propylitisation are common along the plutonic contacts. The Zamora batholith is also associated with gold-bearing grandite skarns which are currently being worked for gold (p.84).

The main skarn belt, that of Nambija, is about 30km in length and 2km wide, trending north-south. Another, smaller, and less well-defined belt, that of María Elena, occurs to the east; skarn rocks are also known from Piuntza; more skarn rocks probably wait to be discovered.

The skarns of Nambija (Salazar, 1988; Litherland et al., 1992b) form as pockets in the roof pendants of the Triassic Piuntza unit which comprises marbles, sandstones, andesitic lavas and tuffs. The preservation of the skarns may be due to the greater resistance to weathering of these massive, pale grey or pink, garnet rocks, cut by quartz-carbonate-adularia-epidote veins (Plates 5d and 22c) within which the gold is concentrated. There is preferential skarnification of certain beds as narrow as 10cm within the bedded Piuntza sequence of Campanilla Mine.

The petrography of the skarns (Beddoe-Stephens, 1989; Fortey, 1990; Litherland et al., 1992b) shows a variation from monomineralic grandite rocks to incipiently skarnified protolith, comprising predominantly andesitic volcaniclastic rocks that exhibit sericitic and propylitic (chlorite, epidote, prehnite) alteration. Incipient skarnification is indicated by isolated grandite crystals nucleating in chlorite-calcite veinlets and, locally, sprays of pyroxene and clusters of epidote. Subsequent growth of grandite develops on these nucleii such that advanced skarn rocks exhibit a mosaic of grandite cores of small crystals overgrown by larger, clearer, yellowish crystals displaying complex oscillatory zoning and low-order birefringence. Where two such clusters interact, an irregular suture line develops between them. More commonly, however, later grandite crystals display perfect euhedral forms adjacent to interstitial quartz, adularia and calcite. In places quartz forms alternating concentric growth zones with grandite, indicating that this interstitial infill developed penecontemporaneously with grandite growth, possibly as a result of volume reduction during skarnification. In other places later grandite growth develops along veinlets cross-cutting early-formed grandite, indicating several episodes of growth and fracturing. In one sample grandite is associated with clinopyroxene forming numerous tiny equant crystals poikilitically enclosed by quartz and dusty adularia. The composition of grandite from one sample shows that growth zoning involved an increase in the andradite component from $Ad_{46}Gr_{51}$ to $Ad_{69}Gr_{29}$ (Litherland et al., 1992b).

A petrographic feature of the Nambija skarns is the clear, unstrained, poikilitic habit of the quartz, giving the superficial appearance of being unaffected by alteration processes. Fluid inclusion homogenisation temperatures from this quartz (Shepherd, 1988) indicates formation, or recrystallisation and annealing, at relatively low temperatures of about 200°C. Moreover, a pattern in which fluid temperature decreased to around 150°C and salinity increased from about 2 to 24 wt% NaCl equivalents is indicated by comparison of fluid inclusion data for quartz from apparently unretrogressed garnet skarn with that for quartz in auriferous carbonate-adularia-bearing rocks (Shepherd, 1988).

CONCLUSIONS

The Zamora granitoids are a chain of I-type batholiths along the western edge of the Amazonic craton. With the exception of the undated Rosa Florida pluton, their suspected Jurassic age (Hall and Calle, 1982) has been confirmed, and they thus form the southern extension of a Jurassic magmatic belt traceable into Colombia (Aspden et al., 1987; Jaillard et al., 1990). The plutons and associated Misahuallí volcanics form a Lower-Middle Jurassic continental magmatic arc which passes eastwards into a backarc basin of clastic (Chapiza) and bioclastic (Santiago) sediments. The Zamora batholith appears to encompass the previous Upper Triassic basin containing the Piuntza unit, the relics of which contain skarn rocks rich in gold.

SALADO TERRANE

This metamorphic lithotectonic division (Figure 9) comprises within the metamorphosed mafic volcanic rocks, or greenstones, and metasedimentary rocks the Upano, Cuyuja and Cerro Hermoso units. In addition, it includes the metamorphosed plutonic rocks of the Azafrán granitoids. It is named after a well-exposed section along the Río Salado and its tributaries, west of Reventador Volcano. The terrane forms a narrow strip up to 25km wide along the eastern slopes of the Cordillera Real, wedging out tectonically in the south near Zamora. It is bounded eastwards by the important Cosanga-Méndez fault, east of which Jurassic rocks of similar age are unmetamorphosed and compositionally different. Westwards its contacts are tectonic with the Loja metamorphic terrane of Palaeozoic-Triassic age.

Upano unit (?Jurassic)

This is a newly defined lithotectonic subdivision of andesitic greenstones and associated metasedimentary rocks which forms an almost continuous belt up to 15km wide along the eastern slope of the cordillera. Accessible sections include the new Guamote-Macas road along the Río Upano, from which the unit is named, and west of Baeza along the Papallacta-Baeza road. Contacts with other units are generally tectonic, although those with the Cuyuja unit may be transitional. The Cretaceous Hollín Formation is interpreted to overlie the unit unconformably in the east.

Rocks belonging to the Upano unit were described by Sauer (1965) from the Río Upano and Baeza, where Trouw (1976) grouped them into a Baeza Formation. Many of the phyllitic lithologies were grouped into Sauer's (1965) semimetamorphic belt. They were also included in Tschopp's (1948) essentially metasedimentary Margajitas Formation which was originally regarded as Palaeozoic in age, being similar to the Pumbuiza Formation. Later, Baldock (1982) recognised the association with Cretaceous Napo Formation limestones which further confused the issue. However, the metamorphic progression from phyllites to schists westwards across the Sub-Andean fault appears to be a geological reality, and is particularly clear west of Baeza.

a

b

Plate 4. Salado terrane rocks.

(a) Essentially undeformed Chingual granodiorite with mafic xenoliths: river boulder in Río Salado (photo: M. L.).

(b) Strongly deformed, mylonitic, Upano greenstone from Río Oyacachi, close to Río Santamaría confluence (photo: R. A. J.).

The age of the Upano unit is still not well established. Feininger's (1975) hypothesis is that this and adjacent metamorphic units are Cretaceous. This is not supported by the available geochronology and palaeontology (see later), and occurrences of diagnostic Cretaceous formation rocks are regarded here as tectonic infolds related to late-Tertiary shortening and thrusting, although it may be difficult to ascribe isolated outcrops of black slate to either age-unit. Thus, the K-Ar date of 54 ± 2 Ma from a sample close to the Baeza Pumping Station (Feininger and Silberman, 1982) is regarded as a reset age. The Upano unit is associated with the Middle Jurassic Azafrán pluton and it is believed that the metavolcanic rocks can be traced eastwards into the Jurassic Misahuallí unit. Its probable age is thus Lower or Middle Jurassic. The presence of clastic blue quartz could indicate derivation from the Upper Triassic granites of Tres Lagunas. The pollen *Perinopollenites elatoides*, of Early Jurassic-Cretaceous age (Riding, 1989b), was discovered in low-grade pelitic phyllites, originally mapped as the Palaeozoic Chigüinda unit, from the Río Ingenio about 4km west of San José de Yacuambí (Ridding, 1989b). This belt of phyllites west of the Sub-Andean fault has now been assigned to the Upano unit.

The bulk of the Upano unit is formed of meta-andesitic greenstones, greenschists and metagreywackes intercalated with pelitic and graphitic schists. The most characteristic lithology is the greenish, massive, fine-to medium-grained meta-andesite, well exposed near Baeza and especially along the Río Oyacachi near the junction with the Río Santamaría where mylonitic belts are prominent (Plate 4b). In thin section the metamorphic quartz-albite-epidote-chlorite-calcite ± biotite matrix contains rare relics of original feldsparphyric textures. Late epidote veins and pods are common in this lithology. Colony and Sinclair (1932) provide detailed petrographic descriptions from samples collected west of Baeza.

The greenstones are invariably associated with greenschists which generally have higher chlorite along with muscovite and garnet, and are particularly well exposed along the trail down the Río Paute. Some outcrops show precleavage volcaniclastic fragments indicating an andesitic tuff origin. Paler, fine-grained, muscovite-biotite bearing quartzofeldspathic schists may also be present and probably represent a metamorphosed acid tuffs.

Fine, medium-, or coarse-grained, greyish, volcaniclastic metagreywackes are particularly conspicuous at Baeza and the Ríos Upano, Cosanga and Oyacachi sections, where they are intercalated with greenstones and greenschists. The rock varies from massive to well-cleaved and phyllitic. Clastic blue quartz has been noted and primary heavy mineral banding is sometimes preserved. The greywackes are dominated by deformed angular clasts of feldspar and lithic fragments, most of which are volcanic in origin.

The metagreywackes from the Cuyuja unit of Cerro Hermoso, from the Upano unit of the Río Chalupas west of the Sub-Andean fault, and from the Upano unit south of Río Negro de Pastaza, east of the Sub-Andean fault, i.e. from separate localities across the strike of the Salado terrane, exhibit a common feature regarding their content of acid volcanic clasts. Many clasts can be seen, microscopically, to be of fine-grained quartzofeldspathic material with a ferruginous opaque 'peppering' which also serves to pseudomorph the clast when both matrix and grain boundaries are recrystallised.

The schists, phyllites and metalavas generally exhibit a steep tectonic foliation with concordant quartz veins, with calcite veins in the metavolcanic rocks. Flat cleavage belts are notably present over the Cuyuja nappe complex (Figure 19).

In the north of the cordillera some metavolcanic rocks are shown as Misahuallí rather than Upano unit. This is because they resemble the continental volcanic facies of Misahuallí and are lacking in associated sediments. In fact, there are strong indications from river and stream float that the Upano unit passes laterally into the Misahuallí unit in this region. In the south, the Upano rocks of the Gualaceo-Limón and Chigüinda-Gualaquiza trails show a similar mixing with the Misahuallí unit. The large, tectonically isolated area of Upano unit on the accompanying map west of Puyo and north of the Río Palora has not been field-checked and may also be of mixed facies.

In the extreme north of the cordillera, in the area of Santa Bárbara close to the Colombian border, the Upano unit is represented by gneissic rocks. These are fine to medium grained, and biotite rich (± hornblende), and could be derived from a calcareous tuff protolith, thus representing a higher-grade equivalent of the Misahuallí facies. No migmatites were noted over this ground where Salazar et al. (1986) have suggested the extension of Precambrian rocks from Colombia.

Two greenstone samples analysed geochemically (Fortey and Gillespie, 1993) are andesitic on the $Na_2O + K_2O$ v. SiO_2 plot of Le Bas et al. (1986), and plot in the calc-alkaline field on the Ti v. Zr diagram of Pearce and Cann (1973) (Figure 14). On the rock/MORB plot of Pearce (1983) they show a variable degree of subduction-related LIL enrichment and possible crustal contamination as indicated by high Nb (Figure 14). The samples thus indicate less oceanic and more calc-alkaline character compared with the Alao-Paute unit to the east.

The Upano unit is a little-studied metamorphosed volcanosedimentary belt. Greywacke sediments with a probable westward source from the Tres Lagunas granite are mixed with volcanic rocks of possible calc-alkaline affinity which appear to be transitional with the continental Misahuallí volcanics to the east, and may be cogenetic with the Azafrán granitoids within the Salado terrane.

Cuyuja unit (?Jurassic)

This is a metasedimentary subdivision of the Salado terrane which occurs in the north of the Cordillera and is well exposed in the vicinity of Cuyuja on the road from Papallacta to Baeza where the rocks form a 10km-wide belt of flat tectonic stratigraphy within the Cuyuja nappe complex. It also forms the base of the Cerro Hermoso sequence (Figure 11). There is little to distinguish the Cuyuja schists from the adjacent Agoyán schists of the Loja Terrane to the west. K-Ar muscovite and biotite ages have given 82 ± 3 Ma (Kennerley, 1980) and 59 ± 2 (Herbert and Pichler, 1983), but, as with the Upano unit, these are regarded as reset. Contact metamorphic cordierite and sillimanite cut the metamorphic rocks at Cerro Hermoso and these minerals almost certainly relate to the adjacent Azafrán pluton of Jurassic age.

The Cuyuja unit between Papallacta and Baeza can be divided into a series of grey or black, graphite-muscovite schists which tectonically overlie pale muscovite schists (Colony and Sinclair, 1932; Trouw, 1976). In detail the two may be intercalated in places and there are also psammitic bands and greenschist horizons. The schists are medium to coarse grained and, apart from muscovite and graphite, contain quartz and albite, commonly chlorite, chloritoid, biotite, epidote and sulphides, with rare garnet and quartz veins containing kyanite.

In the Cerro Hermoso area (Figure 11), Cuyuja-type pelitic schists form the base of the local sequence of the Cerro Hermoso unit. These contain muscovite and quartz with or without chlorite, biotite, garnet and chloritoid. Close to the contact with the overlying Cerro Hermoso phyllites there are bands of fine- to medium-grained quartz-chloritoid rock and metagreywacke. The overlying grey and black phyllites are muscovite-graphite rocks with or without chloritoid, again with bands of quartz-chloritoid rock and metagreywacke. The latter contains the opaque-'peppered' volcaniclasts identified in the Upano unit (p.29), as well as the local development of contact metamorphic sillimanite and cordierite. Then follows the meta-conglomerate marker horizon which forms the base of the Cerro Hermoso unit.

The Cuyuja unit is almost certainly part of a lithostratigraphical group comprising the Upano and Cerro Hermoso units of the Salado terrane. Within this concept it could represent a westerly, distal deep-water facies of the Upano volcanic/turbidite facies. In this context it is noteworthy that fine-grained metagreywackes with diagnostic Upano-type volcaniclasts pass upwards into the Cerro Hermoso carbonates.

Cerro Hermoso unit (?Jurassic)

This unit refers to the carbonate sequence at Cerro Hermoso, but is also used, for convenience, to describe other marble bands within the Salado terrane. Outcrops are limited to a narrow belt through the Cerro Hermoso area and isolated occurrences elsewhere.

The carbonate rocks of Cerro Hermoso (Litherland et al., 1991) were first noted by Reiss (in Wolf, 1892). They were attributed to the Cretaceous Napo Formation by Wolf (1892), Tschopp (1956) and Kennerley (1971), but Sauer (1958) and Vera and Vivanco (1983) suggested they were older. Microscopic studies of marbles collected during the present survey show partially recrystallised shell fragments and ?spores, but no identifications could be made. However, as in the case of the Upano and Cuyuja units, the Cerro Hermoso rocks are intruded by the Middle Jurassic Azafrán pluton and are probably Lower to Middle Jurassic in age.

The Project's map of the remote Cerro Hermoso area (Cover and Frontispiece) is shown on Figure 11. Due to excellent exposure, the preservation of way-up structures (sedimentary truncations and bottom structures) and a relatively uncomplicated tectonic pattern, a lithostratigraphy can be elucidated over this area, the first of its kind over the Cordillera Real. The western side of Cerro Hermoso mountain corresponds to the western limb of the Cerro Hermoso syncline, where prominent bedding is flat and cut by a single subvertical cleavage.

The lower two formations are attributed to the Cuyuja unit. Then follows a 10m-thick bed comprising meta-conglomerate followed by grey quartzites and metawackes with muscovite and chloritoid. The conglomerate shows local tourmaline-sulphide mineralisation and chloritoid prisms which cut the foliation.

Above this are 450m of metamorphosed black limestone, black calcareous phyllites and paler calc-arenites. The lower marble unit contains beds up to 2m in thickness and has a brownish-weathering base which can be used as a marker horizon for mapping. All the marbles are strongly cleaved but show clear evidence, microscopically, of recrystallised shell fragments and other biota. Close to the Cerro Hermoso fault the marbles may be rich in garnet and the phyllites in chloritoid; andalusite crystals may cut the cleavage. The upper marbles are well banded with premetamorphic shales and sandstones, and resemble a flysch sequence.

The marbles of Cerro Hermoso itself occur as a synclinal outlier (Figure 11). However, further west the Cerro Hermoso unit is shown on the same figure to be present as a steeply dipping belt which can be traced southwards within the metamorphic complex to the Río Pastaza where black phyllites and marbles occur in the region of Río Blanco (Sauer, 1965). To the north, the belt was traced to the Río Parcayacu by Merlyn and Cruz (1986), who also discovered an outlier of marble over the Azafrán pluton further east, interpreted as a tectonic klippe. Sauer (1958) also studied the marbles of the Parcayacu (which drains Yanacocha lake), but he called this river the Mulatos.

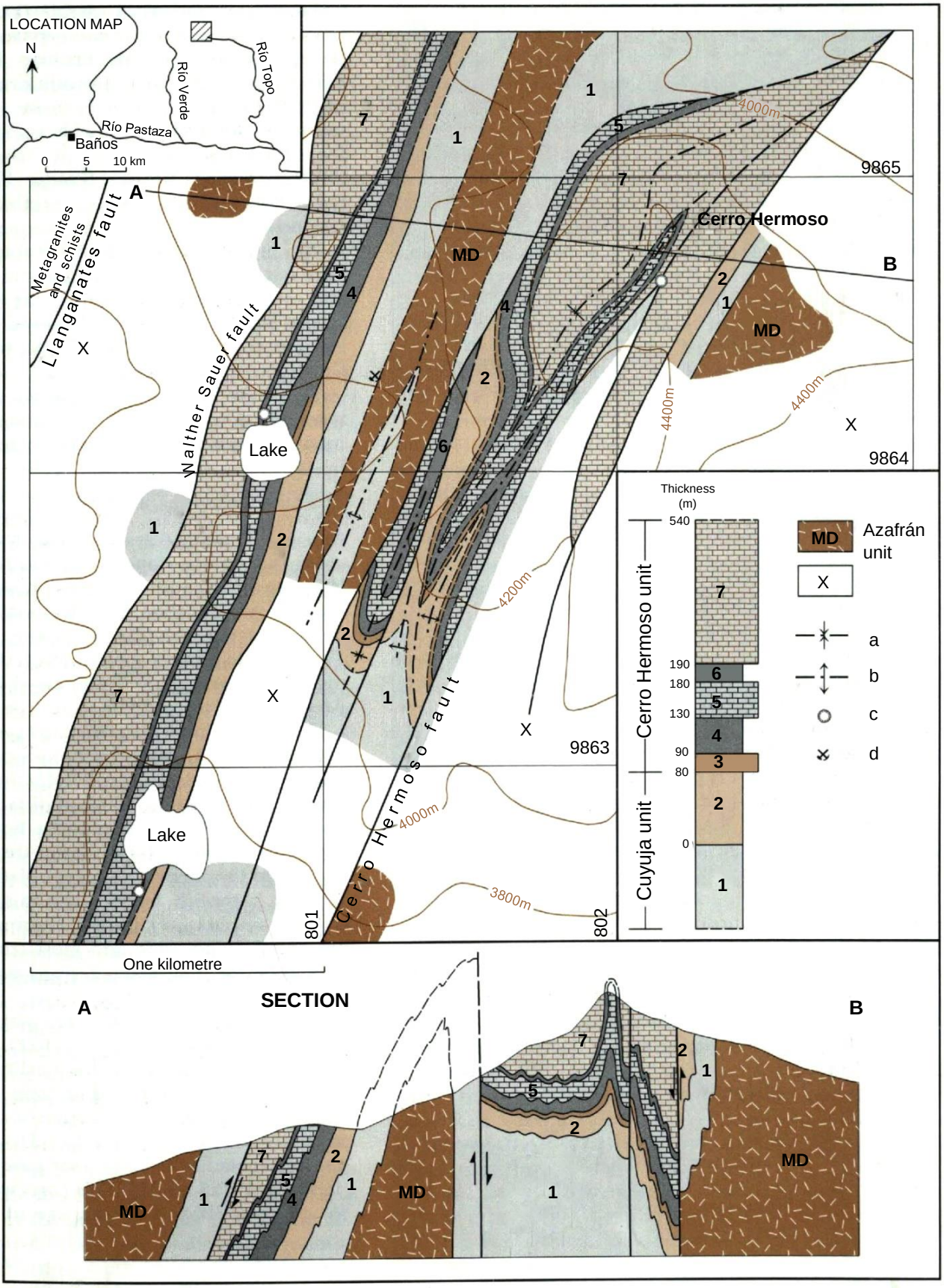

Figure 11. Geological map and section of the area around Cerro Hermoso, after Litherland et al. (1991).

Explanation of symbols: X = unmapped; MD = metadiorite / hornblende gneiss; 1 = muscovite-garnet- chloritoid schist; 2 = grey phyllites and quartzites / metagreywackes with chloritoid; 3 = metaconglomerate / quartzite / metagreywacke with chloritoid; 4 = grey phyllites; 5 = massive bioclastic marbles with brownish weathering base; 6 = dark calc phyllites; 7 = black marbles / black slates / calc arenites; a = syncline; b = anticline; c = karstic pothole; d = old mineral working.

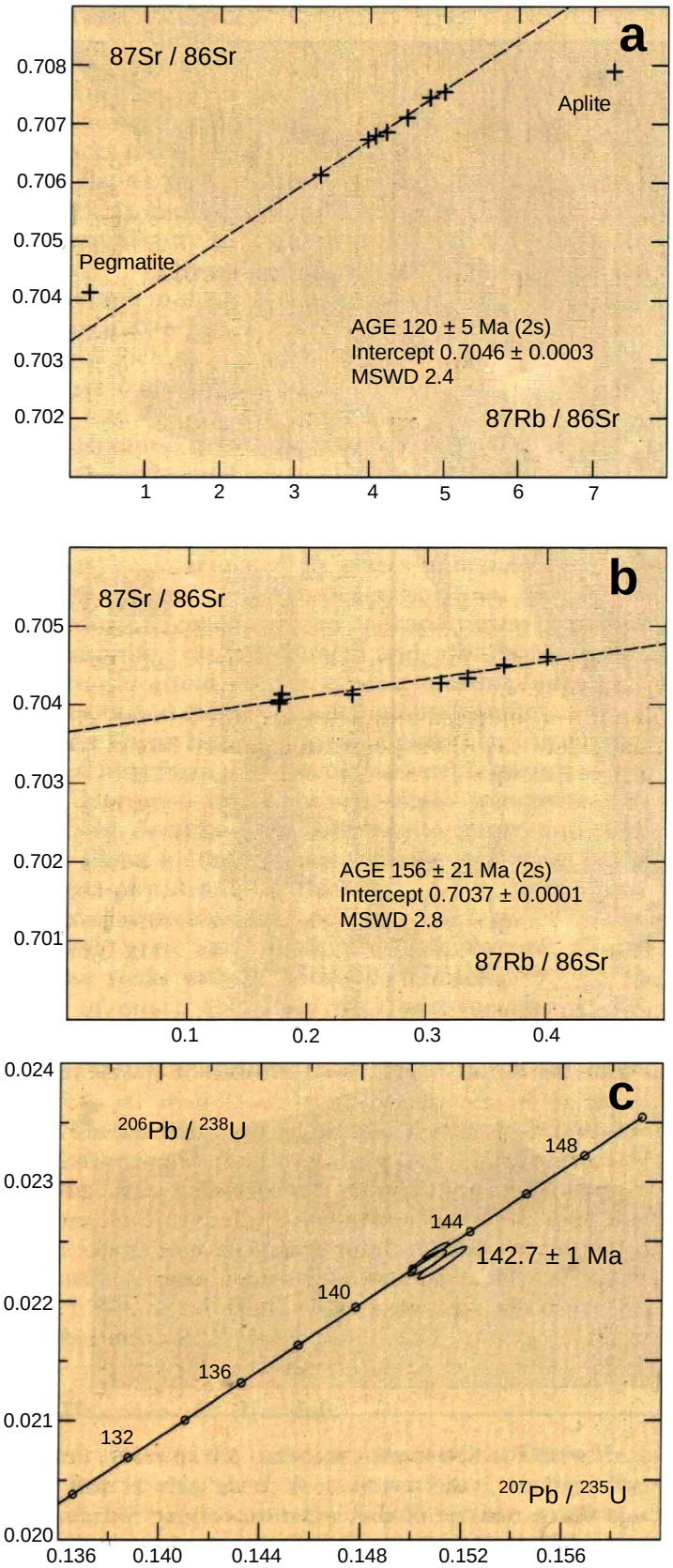

Figure 12. Geochronological plots of the Azafrán and Chingual plutons.

(a) Rb-Sr plot for the Azafrán metapluton; **(b)** Rb-Sr plot for the Chingual metapluton; **(c)** U-Pb concordia diagram for the Azafrán pluton; zircon data give an age of 142.7±1 Ma.

Away from the Cerro Hermoso belt, a narrow marble/calc-silicate formation has been noted in two localities at the same tectonostratigraphical level within the Cuyuja nappe complex at the top of the Cuyuja unit (Figure 19). One locality is along the Río Oyacachi in the north, and the other along the Río Cosanga in the south. Creamy, grey and black marble float blocks in the Río Quijos, below and above the Papallacta confluence, may be derived from the same horizon. The Río Cosanga occurrence comprises rusty-weathering siliceous dolomite with conspicuous green fuchsite. Other marbles are found in the main skarnfields (p.36) and may account for the marble blocks in the Río Diviso and other rivers flowing east into the Río Salado. The black marbles of Sara Urcu superficially resemble those of Cerro Hermoso.

Within the Upano unit in the south, marble horizons were noted along the Río Paute trail east of Guarumales, and along the Río Negro trail just west of Copal. Exposure is insufficient to determine whether these belong to isolated bands within the Upano unit or to a defined Cerro Hermoso carbonate unit.

The Cerro Hermoso and Cuyuja units may represent a more distal westward facies of the Upano volcanosedimentary sequence, or the upper extension of it.

Azafrán granitoids (Jurassic)

A belt of metamorphosed granitoid rocks was discovered along the eastern slope of the northern Cordillera Real. It is associated with metamorphosed sedimentary and volcanic rocks of the Cerro Hermoso, Cuyuja and Upano units, and together they comprise the Salado terrane. The Azafrán unit is named after the previously recognised meta-igneous phase along the Baños-Puyo road. Accessible outcrops occur at Azafrán and La Bonita.

There are two outcrop areas, referred to as the Azafrán and Chingual-La Bonita plutons. The Azafrán pluton extends from the Río Chalupas in the north to the Río Sangay in the south, a distance of some 125km. Further north the Chingual-La Bonita pluton extends for approximately 100km from the Colombian border to the Río Oyacachi. They are probably parts of one continuous batholith buried, tectonically, by the Cuyuja nappe complex over the intervening ground. The belts are about 10km wide and most contacts with the adjacent rocks of the Salado terrane are interpreted to be tectonic.

The pluton at the type area was first recognised by Sauer (1958) and Kennerley (1971). Project K-Ar studies on dioritic samples from this locality gave mixed results. One sample of fresh diorite gave 171 ± 5 Ma and another had concordant hornblende-biotite ages giving a mean of 173 ± 3 Ma (p.120). However, a sample of sheared metadiorite 50m away gave a mean concordant age of 128 ± 3 Ma. This corresponds approximately to a 7-point Rb-Sr isochron age of 120 ± 5 Ma (Figure 12a) from the main granite phase at Azafrán. Two biotite separates from these samples gave K-Ar ages in the region of 50 Ma. Probably the most precise age for the granite intrusion at Azafrán is 142.7 ± 1 Ma given by the U-Pb concordia diagram from the zircon analysis (Figure 12c) (written communication, S. Noble).

In the north, seven samples of the Chingual pluton gave a Rb-Sr isochron age of 156±21 Ma (Figure 12b), whilst K-Ar ages from the Chingual and Sacha phases of this pluton show a range of 19-34 Ma (p.120).

From the above data the Azafrán granitoids are interpreted to have been emplaced at the Jurassic-Cretaceous boundary and then affected by later resetting events, one of which occurred around 130 Ma. It is possible that the dioritic phase was older, around 170 Ma.

In the type area of Azafrán, Sauer (1965) recognised the fresh hornblende diorites of the Río Verde sector and the granites further east, which are quartz-monzonitic in places. Both these lithologies vary from massive rocks with only minor alteration (formation of epidote and sericite) to steeply dipping mylonitic gneisses as noted by Kennerley (1971). Westwards, as far as the Río Blanco, the medium-grained diorites seen near the Río Verde are converted into hornblende-biotite (+garnet) schists and gneisses and may be difficult to distinguish, in their weathered state, from associated metasedimentary rocks, as suggested by Baldock (1982).

Float blocks in the Río Verde also indicate the area to the north-west of Azafrán to be essentially metadioritic, a point confirmed in the survey of Cerro Hermoso (Figure 11). In this sector the metaplutonic phase is predominantly dioritic and it is interesting to note how the tectonometamorphic effects, e.g., the gneissic foliation and presence of metamorphic hornblende, biotite and garnet, increase close to the important faults which affect the sequence. The details of Figure 11 also indicate the Azafrán phase to be associated only with the lowermost pelitic schists with which it is folded, suggesting the possibility of a local sill-like intrusion in this area.

North of Cerro Hermoso the Río Mulatos traverse confirmed the northward extension of the Azafrán pluton from the type area. Outcrops and float blocks indicate a dominance of granodiorite and diorite, with minor gabbro, dolerite, quartz-monzonite, granite and aplogranite, suggesting that the Azafrán granite of the 'type' area is regionally atypical. Both main types carry an abundance of mafic xenoliths. Highly strained gneissic, and essentially undeformed phases were noted within a particular float block.

South of Azafrán the Río Palora traverse confirmed the southern extension of the pluton. Again, the main units are granodiorites and diorites, with biotite-metagranodiorites predominant. Further south, along the Río Upano, the metaplutonic phase is absent. The Río Salado pluton shows the same compositions but it has been allocated a Tertiary age based on its undeformed state.

Veins are common in the pluton. The gneissic phase shows calcite-quartz-biotite-sulphide veins which are parallel to the foliation and probably syntectonic. Post-tectonic epidote-plagioclase veins are also common and related to late shears. Aplites and small tourmaline pegmatites are found associated with the granite phase at Azafrán. Late, undeformed quartz-monzonite veins cut the pluton and surrounding rocks.

In the north, the Chingual-La Bonita pluton is less well-defined. Along the road to La Bonita occur the orthogneiss belts of Sacha and Chingual, and that of La Bonita itself. All are dominated by medium-grained, foliated, biotite (± hornblende) granodiorites and are essentially homogeneous, with the biotite forming porphyroblasts up to 1.5cm across. In the La Bonita sector there are zones of mylonitic augen gneiss; K-feldspar proto-augen gneisses are common throughout the sections. Diorite, gabbro and hornblendite are minor lithologies; there is a 20m-wide pegmatitic metagabbro belt along the southern contact of the Chingual phase.

Further south, the map of the Chingual-La Bonita pluton is based on information from only a few traverses and the map of the central sector around the Río El Dorado is highly interpretive. Suffice it to say that the lithologies are similar to those on the La Bonita road with the exception of the metagranite east of the Río Cedro along the Río Oyacachi. In the Río Diviso tributary of the Río Salado there is an important porphyry phase intruded by diorite prior to the main shearing. Xenolithic metagranodiorites are prominent as river float (Plate 4a) whilst pegmatitic gabbro blocks contain hornblende up to 10cm long.

Chemical analyses for the Azafrán granitic phase are given on p.139. The geochemical plots (Figure 8) indicate it to be an I-type pluton as do the low initial strontium isotopic ratios (Figures 12a and b). Indeed, in terms of lithology, age and origin there is little to distinguish the Azafrán from the Zamora granitoids. It is their tectonic status and nature of host rock lithologies which places them in different terranes.

Contact rocks and skarns

Contact metamorphic andalusite, cordierite and sillimanite were noted at Cerro Hermoso (Figure 11) and elsewhere in metasedimentary rocks near the Azafrán granitoid belt. A belt of 'spongy' garnetiferous marble lies close to the Cerro Hermoso fault (Figure 11), with prismatic chloritoid cutting the regional cleavage in the same area. Such post-tectonic phenomena are attributed to the Azafrán phase despite the fact that the cleavage cut by these minerals also affects the pluton.

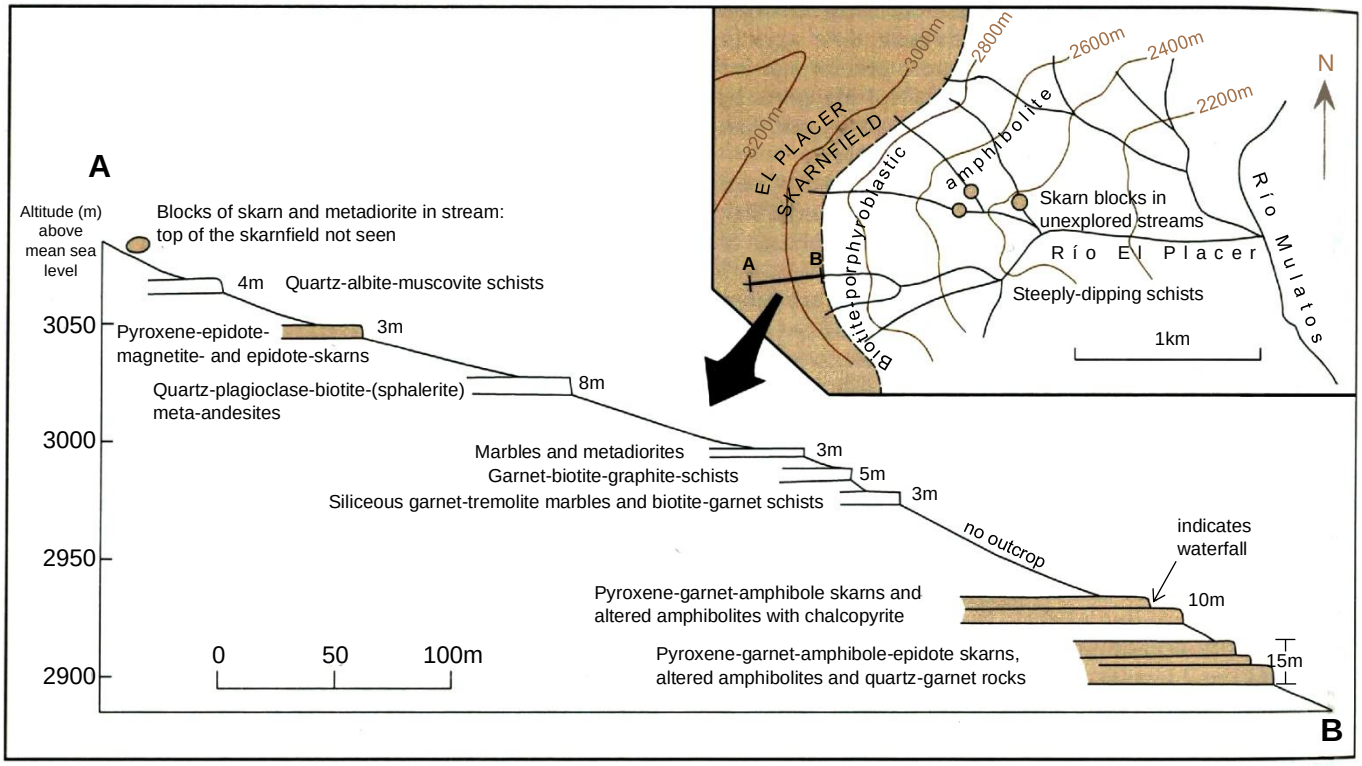

Figure 13. Location map and stream section of the El Placer skarnfield. Skarn rocks are coloured.

Skarn rocks are widespread within the Salado terrane of the northern Cordillera Real (Litherland et al., 1992b). They were first discovered by Project personnel as river boulders in the Río Mulatos in 1986. In 1987 a follow-up expedition traced these blocks to the El Placer skarnfield. In 1988 the Urcucocha skarnfield was discovered, and, in 1989, the Sara Urcu field. Meanwhile the Inga skarn had been discovered across the Río Mulatos from El Placer by Ing. L. Torres, and the Río Verde field by Ing. E. Salazar.

These skarnfields are shown on the accompanying map along with occurrences of skarn river float which indicate the existence of other fields yet to be discovered. For example, new fields can be predicted to crop out between Sara Urcu and the Río Oyacachi, and between the Ríos Oyacachi and Papallacta. There is also a field along the main watershed about 10km south of la Bonita: streams draining east and west contain epidote skarns and skarnified siliceous banded rocks. All these fields, known or suspected, are found at the top of the cordillera watershed at levels of 2000-4500m above sea level, which partly accounts for their previous lack of recognition.

The skarnfields have thicknesses in the region of 200-300m, exhibit tectonic contacts and contain tectonic intercalations of other rocks, mostly regionally metamorphosed. They generally exhibit a subhorizontal foliation and their outcrops are interpreted to be high-level klippen; they form enormous volumes of rock along the cordilleran watershed.

The El Placer field (Figure 13) was discovered by tracing float blocks in the Río El Placer to source, 1000m above its confluence with the Río Mulatos. Some of these blocks are enormous (Plate 5a). The subhorizontal tectonic foliation in the skarns contrasts with the steep foliation of the schists and gneisses in the Río Mulatos. The tectonic sequence in this skarnfield (Figure 13) is underlain by a thick formation of massive biotite porphyroblastic amphibolite with subordinate ultramafic rocks and marbles. The El Placer skarn continues at high levels eastwards across the Río Mulatos in the form of the Inga skarnfield. It terminates westwards along the Llanganates fault, along which, in the Río Parcayacu, there is a thin subvertical skarn occurrence (oral communication, A. Egüez). Further south, near the Río Pastaza, the Río Verde skarn was located at only 2100m above mean sea level (msl).

North of El Placer, the Urcucocha field was discovered in outcrop on the Antisana-Cosanga traverse at about 4000m above msl (Plate 5c). The unit forms a small ridge about 200m high along the main watershed. Four individual tectonic units can be mapped within a gentle synform (Figure 19). The lowermost (150m) and third (50m) units are dominated by massive epidotic skarns (Plate 5c); the second (80m) and fourth (50m) are fine-grained quartz-muscovite-biotite schists of probably felsic volcanic origin. Further north still, the skarns at Sara Urcu, at over 4000m above msl, are steeply dipping and associated with black marbles. It is interesting to note the increasing altitude of the skarnfields northwards.

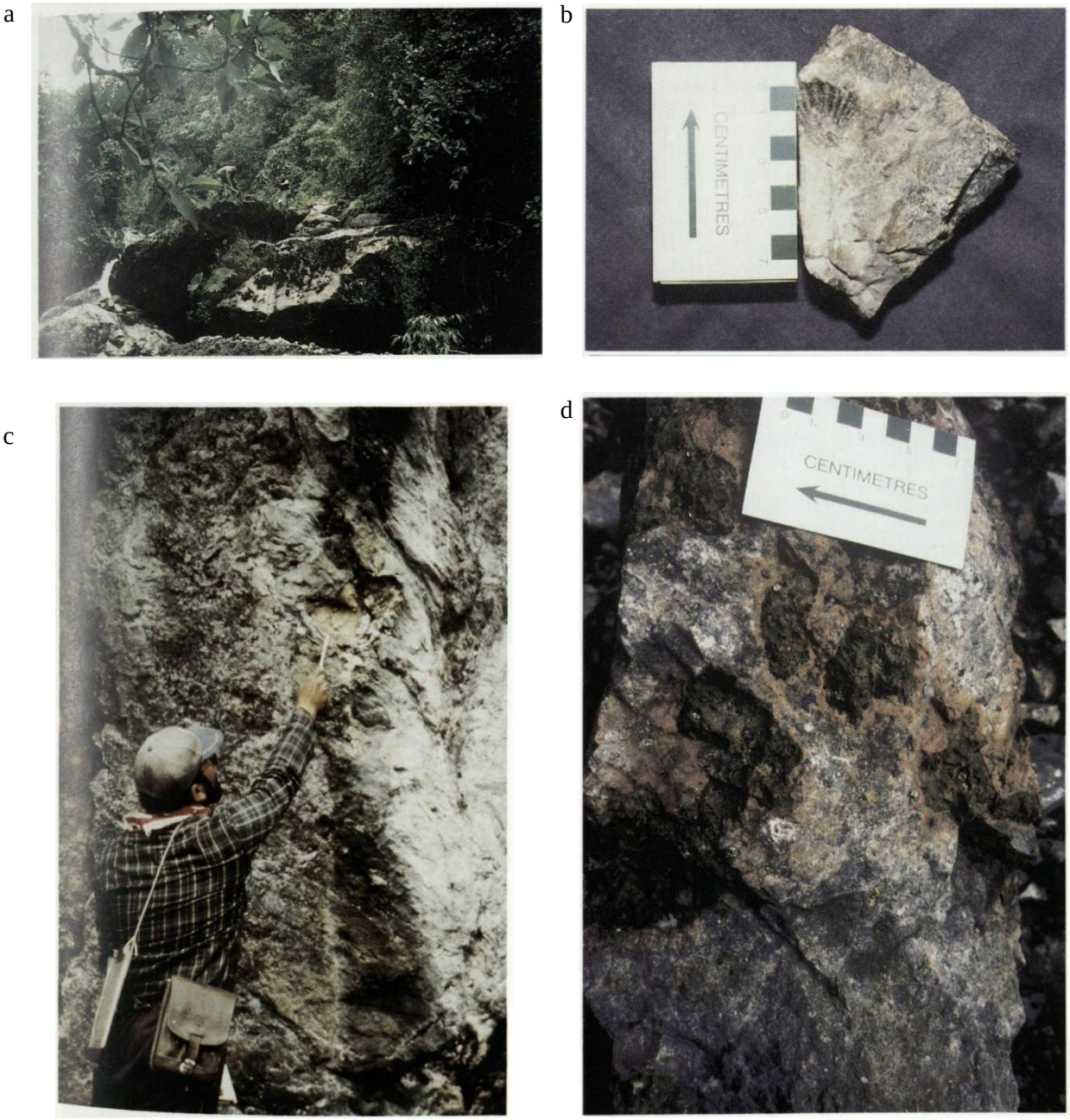

Plate 5. Skarn rocks (see also Plate 19).

(a) Enormous skarn boulder in the Río El Placer (Figure 13) derived from the El Placer skarnfield (photo M. L.).

(**b)** Gold-bearing skarn with Triassic bivalve *Costatoria*, from collection of Mr. M. Turner of Zamora, reportedly from Guaysimi Alto mine, near Nambija (photo R. A. J.).

(c) Discovery of Urcucocha skarnfield. Miguel Pozo is indicating a carbonate inclusion in the massive epidote skarn which forms the summit ridge (Figure 19) (photo: M. L.).

(d) Epidote (green) and adularia (pink) skarn from Campanilla mine near Nambija. Pyrite and chalcopyrite are also present (photo R. A. J.).

Typically, the outcrops and river blocks are massive and multicoloured due to pink garnet, green epidote and pyroxene, and black hornblende and magnetite, with a diagnostic 'elephant-skin' weathering; individual blocks or bands may comprise monomineralic epidote rock or garnet rock. A fracture cleavage or local gneissification (Plate 19b) is parallel to the regional schistosity in adjacent schists or gneisses, which may be accompanied by quartz and calcite veins to produce agmatitic structures.

Petrographic studies (Thompson, 1987; Williams, 1987; Fortey, 1990; Litherland et al., 1992b) indicate that skarnification affected a variety of metamorphosed sedimentary and volcanogenic rocks as well as undeformed high-level dioritic intrusions. Precursor lithologies include graphitic, pelitic and semipelitic schists, marbles, feldspathic schists of probable dacitic composition, and amphibolites.

Several specimens preserve stages of incomplete metasomatic alteration of the parent lithologies. Thus, quartz-rich pelitic schists from Río Oyacachi blocks contain undeformed wollastonite porphyroblasts which probably represent decarbonatisation of original marly rock, and feldspathic metavolcanic schists from this area show patchy alteration to fine-grained biotite which may have resulted from K-metasomatism prior to partial skarnic alteration to diopsidic pyroxene.

Many specimens represent rocks subjected to more complete skarn alteration: monomineralic grandite rock probably formed by alteration of metasediments; pyroxenites and epidotites from basic volcanics. This is indicated in outcrop at Urcucocha, where epidotic skarns preserve relics of andesitic greenstone. Samples of massive, fine-grained tourmaline indicate that boron metasomatism of pelitic metasedimentary rocks was associated, locally at least, with the main skarn formation.

The polymineralic skarns are of more uncertain parentage. In these rocks a multistage pattern of development typical of calcic skarns is apparent. Millimetre-scale grandite crystals and fine granules of clinopyroxene commonly occur in close association: a paragenesis evidently developed at a high-temperature stage of the alteration. The pale garnet is isotropic to weakly birefringent, and electron probe micro-analysis (EPMA) results (Fortey, 1990) indicate grossular-andradite composition of varying Ca/Fe^{+3} ratio (Litherland et al., 1992b). Compositions of accompanying pyroxenes include hedenbergite and diopside of intermediate Mg/Fe^{+2} ratio. Sodic pyroxene more typically forms massive pyroxene skarns and also occurs as relict crystals engulfed in epidote. This latter mineral also appears to represent a later, probably cooler, stage of alteration, associated with second generation garnet and deep blue-green, iron-rich hornblende and traces of biotite. EPMA results for hornblende (Fortey, 1990; Litherland et al., 1992b) indicate edenitic, pargasitic and hastingsitic compositions.

The protolith rocks of the northern skarnfields, and those tectonically associated with them, are identical to the lithologies already described from the Upano, Cuyuja and Cerro Hermoso units, and Azafrán granitoids. It is suggested (Litherland et al., 1992b) that the volcanosedimentary sequence represented by these units was thrust eastwards along the Llanganates fault and skarnified over the hot Azafrán batholith flattening out at higher levels, in the form of a conveyor belt. This model would account for the presence of a thrust sheet of skarn rock extending at least 150km along the cordillera, now eroded to form isolated klippen.

ALAO TERRANE

This metamorphic tectonostratigraphic division comprises metavolcanic and metasedimentary rocks of the Alao-Paute, El Pan and Maguazo units of Jurassic age; unlike the other major terranes there is no plutonic phase. It is named after the west-trending Alao valley (Plate 6) which crosses the terrane and contains an accessible road. The Alao terrane (Figure 9) is essentially a greenstone belt up to 35km wide cropping out along the western slopes of the cordillera, in places as inliers within the Inter-Andean valley; its situation makes it more accessible than the terranes further east. The greater part is buried by Cenozoic volcanic deposits especially to the north and south of the cordillera, leaving a well-exposed central segment 200km in length between Píllaro and Sigsig along which the three subdivisions form continuous parallel strips. However, the isolated southern outcrops near Saraguro and Quilanga are important in any regional appraisal.

The Alao terrane is bounded to the east, across the Baños fault, by the metamorphic Loja terrane of Palaeozoic-Triassic age, and, to the west, across the Peltetec fault, by the Jurassic Guamote Terrane and, further south, the Chaucha and Amotape terranes of Palaeozoic-Triassic age.

Alao-Paute unit (?Jurassic)

This new unit describes the main greenstone belt of the Alao terrane. It is well exposed in road sections along the Ríos Alao, Paute and Pastaza, in the Gualaceo-Sigsig region and on the trail from Atillo to Macas, where it forms a belt over 15km wide. The rocks invariably exhibit a steeply dipping cleavage or schistosity. Contacts with the adjacent El Pan and Maguazo units are regarded as tectonic.

Many geologists have visited and described the accessible sections across this unit (Sheppard and Bushnell, 1933; Liddle and Palmer, 1941; Sauer, 1965; Kennerley, 1971; Bristow, 1973; Trouw, 1976; Herbert, 1977); but the present mapping has established the greenstone belt from the Río Paute to the Río Pastaza.

In the Río Paute area, Bristow (1973) termed the unit the San Francisco metavolcanics, and suggested an Upper Cretaceous age based on evidence of transition with unmetamorphosed rocks of the Yunguilla and Piñón Formations further west.

Plate 6. Alao valley: general view looking west, with the village of Alao in the foreground (photo R. A. J.).

K-Ar ages from samples of intercalated phyllites gave 88 Ma and 92 Ma (Kennerley, 1980) and 61 Ma (Herbert and Pichler, 1983). Project K-Ar ages from igneous hornblendes gave 115 ± 12 Ma and 142 ± 36 Ma (Rundle, 1988). These are probably minimum (reset) ages; the depositional age is more likely to be in the region of 160 Ma, the pollen age of the associated Maguazo unit. The Alao-Paute unit is cut by the Late Cretaceous Magtayán pluton, whilst the gently folded Late Cretaceous Yunguilla Formation of the Cuenca area is now believed to unconformably overlie the vertically foliated metamorphic units of the Alao terrane.

In the Río Paute area between Descanso and Gualaceo and north to Pindilig there are outcrops of massive lavas, amygdaloidal in places, agglomerates and bands of green phyllite of probable tuffitic origin; individual flows can be traced by the presence of calcified tops. Twenty samples from this area are predominantly basaltic with lesser basaltic andesites and andesites when plotted on a $K_2O + Na_2O$ v. SiO_2 plot (Le Bas et al., 1986) (Fortey and Gillespie, 1993). Over this accessible area some of the massive lavas are essentially unmetamorphosed and contrast strongly with the greenstones and greenschists further east and north, an observation which lead to their separation as a younger unit (Sheppard and Bushnell, 1933) or as a stage in a metamorphic transition (Bristow, 1973). Detailed petrographic descriptions of these hornblende andesites can be found in Sheppard and Bushnell (1933).

Over the remainder of the outcrop area, the Alao-Paute unit is generally of higher metamorphic grade with increased quartz or carbonate veining. Metamorphosed lavas crop out as greenstones and there are intercalated greenschists, graphitic schists, pelitic schists, quartzites and marbles: an assemblage difficult to distinguish from the Upano unit, especially across their mutual contact along the Río Paute. In certain sectors, mylonite belts produce a strong uniform schistosity (Plate 14c and d) where ‘massive’ greenstones are no longer visible; this phenomenon can be studied at the accessible outcrops south of Sigsig and at outcrops along the Río Pastaza near Baños.

Mineral assemblages in these rocks are typical of the greenschist facies. The greenstones and greenschists contain quartz + chlorite + albite ± carbonate ± epidote ± actinolite ± biotite; whilst the more pelitic rocks are dominated by muscovite + chlorite ± chloritoid.

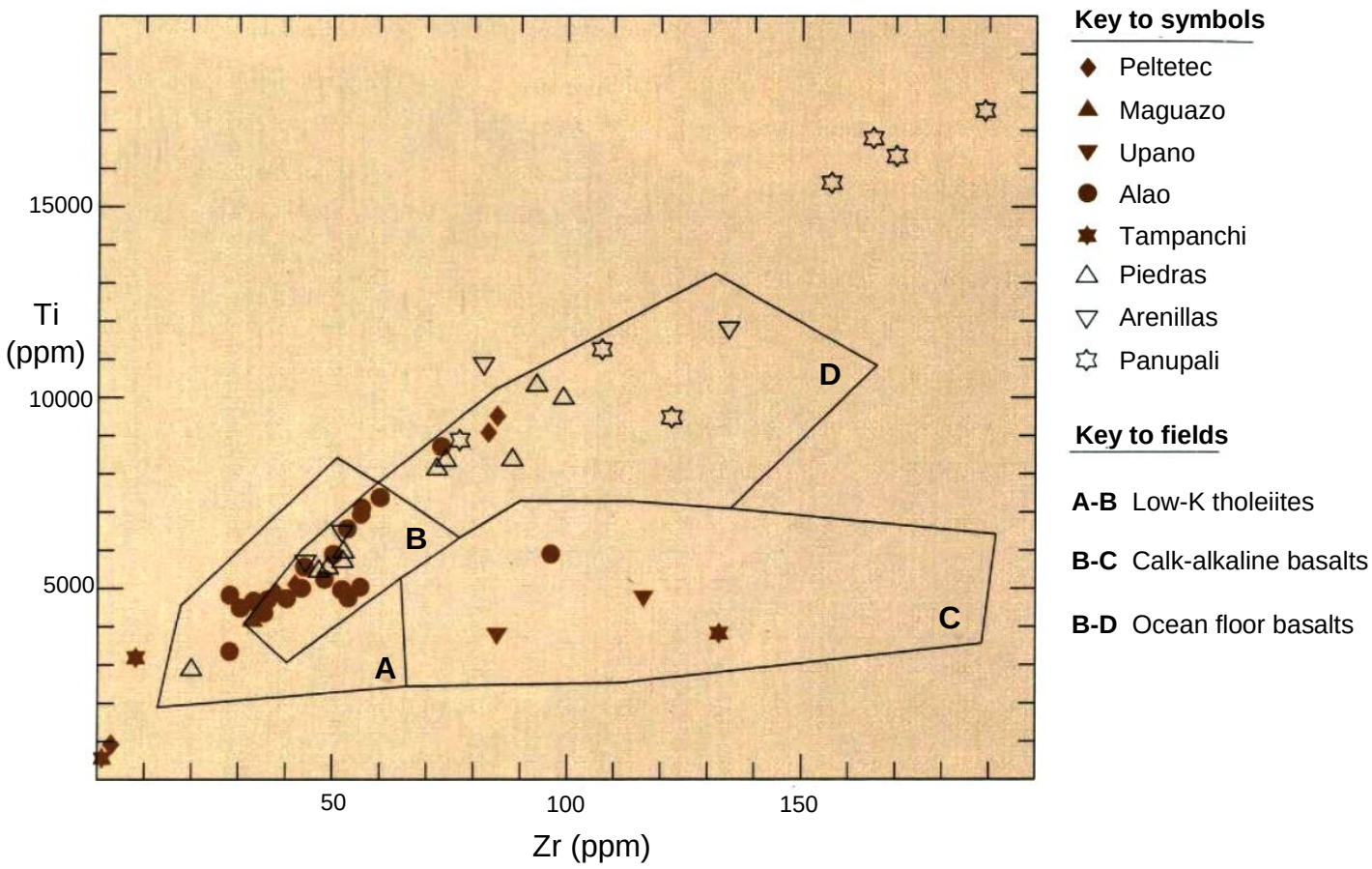

Figure 14. Basic rocks of the Ecuador metamorphic belts plotted on Ti v. Zr diagram of Pearce and Cann (1973).

In terms of their geochemistry, the twenty Alao-Paute samples plot onto the Ocean Floor Basalt trend on the Ti v. Zr plot of Pearce and Cann (1973) (Figure 14) and thus confirm their previous identification as tholeiitic basalts by Herbert (1983). On the rock/MORB plot (Pearce, 1983) (Figure 15a), it is clear that considerable scatter of values exists, notably for LIL elements. Of the general features, values for Nb, Zr, Ti and Y are close to unity, indicating little or no crustal contamination, whilst LIL elements show varying degrees of subduction-related enrichment of ocean ridge basalt. Variable Cr and Ni suggest that fractionation of mafic and ore phases has also been important in the differentiation of the group, but the weakness of the Sr enrichment trend suggests that plagioclase fractionation was of minor significance.

The above data indicates the Alao-Paute unit to be an oceanic island arc with a subordinate deep-water sedimentary component.

El Pan unit (Jurassic)

This is essentially the El Pan schists of Bristow (1973), a metamorphosed volcanosedimentary facies within the Alao terrane outcrop, lacking, in particular, the massive greenstones. The unit occurs as an elongate belt 70km long and up to 7km wide which encompasses the Andean-trending sector of the Río Paute's course; it is also interpreted to occur in the isolated inlier to the south near Saraguro. A sample collected from this latter locality contained a spore tentatively identified as *Uvaesporites* sp. (Riding, 1989b), a genus that is well represented in the Middle Jurassic to Early Cretaceous of Europe.

Lithologies comprise quartz-calcite-chlorite greenschists, graphitic schists and quartz-sericite phyllites with lesser quartzites, quartz-albite-epidote-chlorite schists, actinolite-chlorite schists, black marbles, epidote rich calc-silicate rocks and clinozoisite-tremolite rocks. This suggests metamorphosed calcareous tuffs, clays and marls; there is no evidence that the greenschists are strongly mylonitised lavas.

The El Pan unit could represent a marine backarc sequence to the oceanic Alao-Paute island arc. Particularly significant is the absence of massive turbidite formations, found, for example in the Maguazo unit.

Maguazo unit (Jurassic)

This new subdivision refers to a belt of metamorphosed turbiditic and volcanic rocks traceable from an inlier close to San José de Poaló in the north, to the Río Paute in the south, a distance of about 200km. Accessible outcrops occur near Maguazo bridge along the Río Alao and along the Penipe-Río Blanco, Guamote-Atillo and Guasuntos-Zula roads, as well as the road from Cuenca to Gualaceo. The belt is 5-10km wide and exhibits tectonic contacts with the Peltetec ophiolite in the west and the Alao-Paute unit in the east along the San Antonio fault (Figure 16). Recent detailed studies north-east of Cuenca and west of Pindilig (oral communication, M. Merlyn) indicate the presence of the Maguazo turbidites east of the San Antonio fault where Bristow et al. (1975) mapped the Cretaceous Yunguilla Formation. Accessible outcrops of this section occur along the road which follows Río Dudas.

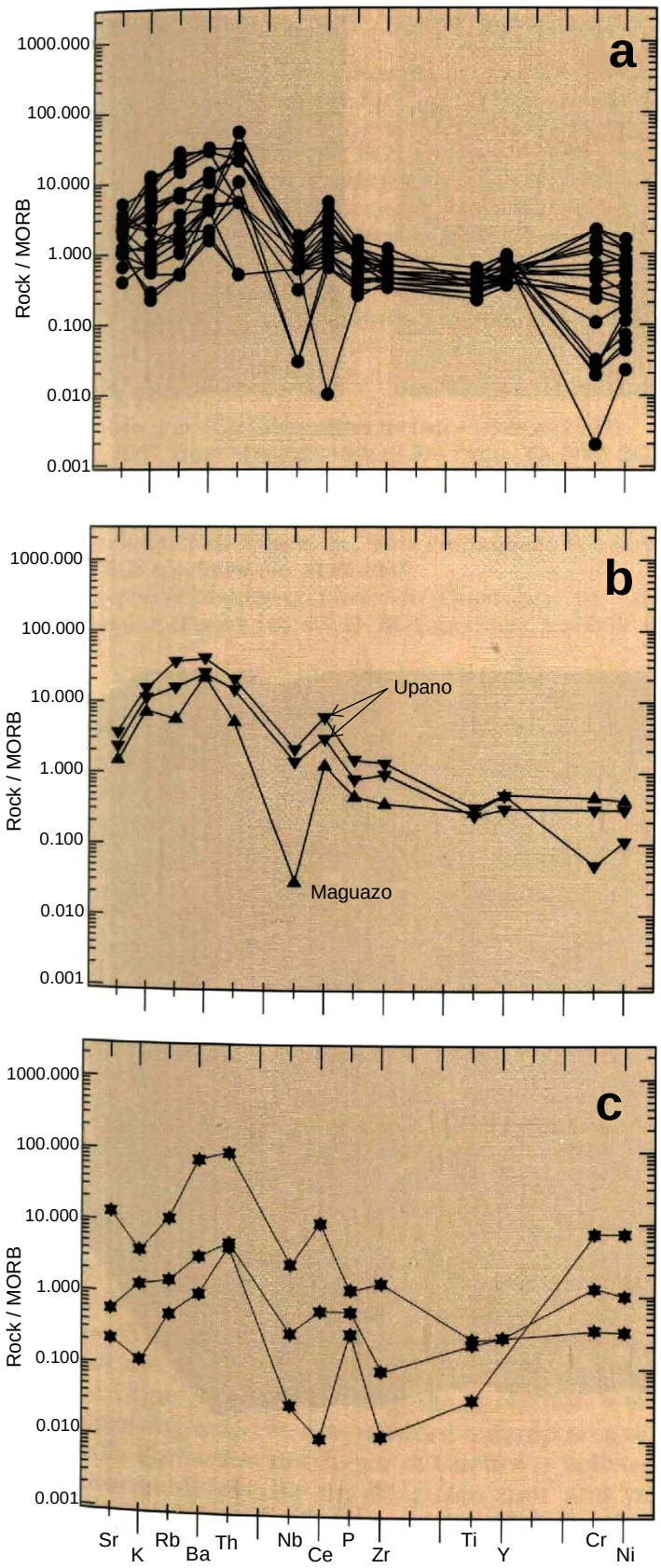

Figure 15. Mafic rocks of the Cordillera Real plotted on MORB normalised 'spider diagrams' of Pearce (1983).

(a) Alao-Paute greenstones; **(b)** Upano and Maguazo greenstones; **(c)** Tampanchi mafic and ultramafic rocks.

The Maguazo unit has yielded important fossil remains (Aspden and Ivimey-Cook, 1992). A river block of calcareous phyllite and chert from the lower reaches of the Río Jadán on the Cuenca-Gualaceo road provided dark brown acritarchs of probable Ordovician age along with Mesozoic pollen, spores and dinoflagellate cysts (Molyneux, 1988b; Riding, 1988). The pollen grains include: *Callialasporites dampieri* (Balme, 1957) Sukh Dev, 1961; *C. segmentatus* (Balme, 1957) Sukh Dev, 1961; *C. turbatus* (Balme, 1961) Schultz, 1967 (Plate 7d); *Cerebropollenites macroverrucosus* (Thiergart, 1949) Schultz, 1967; *Classopollis meyeriana* Klaus, 1960; *Cycadopites* (Wodehouse, 1933) Wilson and Webster sp.; and *Perinopollenites elatoides* Couper, 1958. The spores are of *Cyathidites* sp. Couper, 1953. The dinoflagellate cysts include: *Gonyaulacysta eisenackii* (Deflandre, 1938) Dodekova, 1967 emend. Sarjeant, 1982 (Plate 7a); *G. jurassica* (Deflandre, 1938) Norris and Sarjeant, 1965 emend. Sarjeant, 1982 subsp. *adecta* (Plate 7c); and indeterminate forms of *Gonyaulacoid* and *Sentusidinium* Sarjeant and Stover, 1978 sp. Species of *Micrhystridium* Deflandre, 1937 and *Tasmanites* Newton, 1875 were also noted.

The presence of *G. eisenackii* and *G. jurassica adecta* indicates a Callovian/Oxfordian age. The first of these is confined to these stages in Europe (Berger, 1986; Riding, 1987) and is more common between the Middle Callovian and Middle Oxfordian (166-160 Ma).

The acritarchs include forms corresponding to *Cymatiogalea*, *Acanthodiacrodium* and *Polygonium*. These suggest an Early Ordovician age, having been reworked into the Jurassic sediments of the Maguazo unit.

Samples collected from outcrops of the Maguazo unit from the vicinity of Quebrada Totora Yacu (**7417-96849**), alongside the Cuenca-Gualaceo road east of the Río Jadán, also yielded palynoflora (Riding, 1989a; Aspden and Ivimey-Cook, 1992). These included the pollen *Perinopollenites elatoides* and *Classopollis classoides* (Pflug, 1953) Pocock and Jansonius, 1961; and the dinoflagellate cyst *Sirmiodinium grossii* Alberti, 1961 emend. Warren, 1973. The pollen association indicates a Jurassic-Cretaceous age, but *Sirmiodinium grossii* narrows this down to between Upper Bathonian and Lower Albian (Woollam and Riding, 1983). Acritarchs were also noted, similar to the Ordovician forms described above.

The above palynological data establish a Jurassic age for the Maguazo unit and thus negates the hypothesis of Bristow (1973) which correlated the metasedimentary rocks of the present Alao terrane with the unmetamorphosed Upper Cretaceous Yunguilla Formation. On the accompanying map the now-reduced outcrop area of the Yunguilla Formation north-east of Cuenca is believed to unconformably overlie the Maguazo unit and other rocks of the Alao terrane.

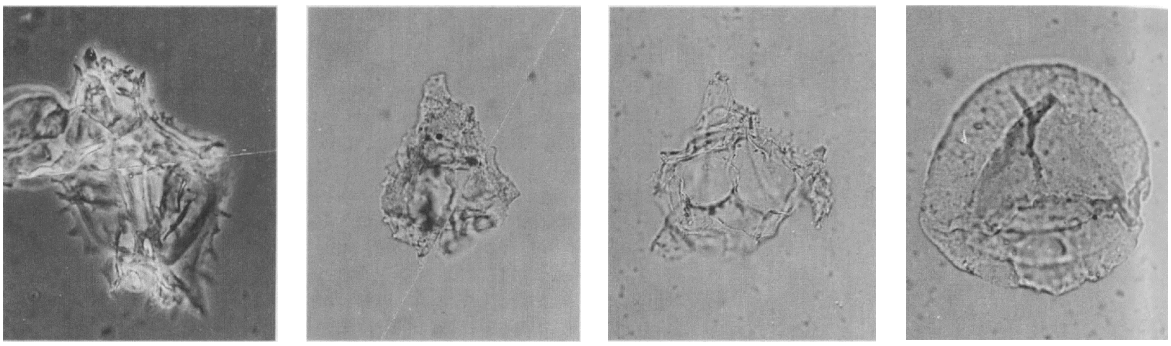

a b c d

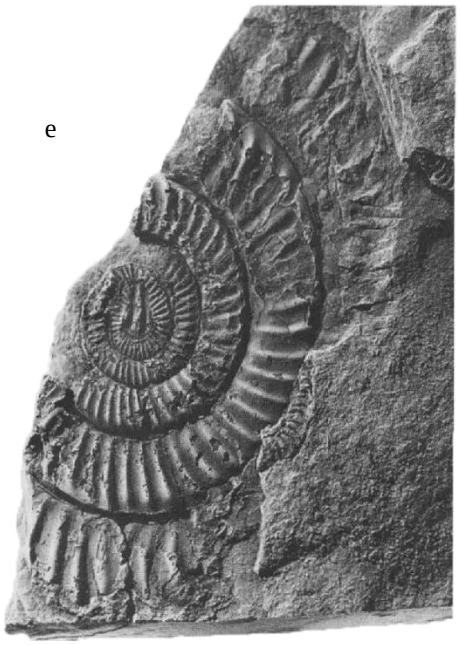

e

f

g

Plate 7. Jurassic fossils.

(a) Dinoflagellate cyst *Gonyaulacysta eisenackii* (Deflandre, 1938) Dodekova, 1967 emend. Sarjeant, 1982, from Maguazo unit of Río Paute. Central view, composite microphotograph using phase contrast, (×500), BGS specimen No. MPK 9456.

(b) Dinoflagellate cyst *Gonyaulacysta jurassica* (Deflandre, 1938) Norris & Sarjeant, 1965 emend. Sarjeant, 1982 (subspecies uncertain), from Maguazo unit of Río Paute. Dorsal view, composite microphotograph, (×500), BGS No. MPK 9457.

(c) Dinoflagellate cyst *Gonyaulacysta jurassica* subspecies *adecta* Sarjeant, 1982 variety *adecta*, from Maguazo unit of Río Paute. Oblique dorsal view, high focus, (×500), BGS specimen No. MPK 9458.

(d) Pollen grain *Callialasporites turbatus* (Balme, 1957) Schultz, 1967, form Maguazo unit of Río Paute. (×500) BGS specimen No. MPK 9459

(e) Ammonite *Leptechioceras* sp., from the Santiago Formation. (×1), BGS specimen No. FOR 4806

(f) Ammonite *Paltechioceras* sp., from the Santiago Formation. (×1), BGS specimen No. FOR 4808

(g) Ammonite *?Arnioceras* cf *ceratoides* (Quenstedt), from the Cebadas unit (Figure 16). (×1), BGS specimen No. FOR 4924

The Maguazo unit is dominated by a slightly metamorphosed turbidite-andesitic basalt sequence. The turbidites are fine grained and siliceous at Río Maguazo (Figure 16) but are more volcaniclastic at Quebrada Totora Yacu (Río Paute) where a first-phase syncline can be observed. In these latter outcrops the turbidites show laminated divisions and non-laminated calcareous tuffs; load casts and ripple marks are present and there are cleaved felsitic sills. The weak metamorphism and the presence of a non-penetrative, steeply dipping, first cleavage ensures the preservation of sedimentary structures useful as way-up indicators. Thus, graded bedding, ripple cross-bedding and bottom structures in the steeply dipping rocks of the type area of the Alao valley also indicate the presence of a first-phase syncline and a rough stratigraphy can be elucidated for the unit (see section on Figure 16), which has a minimum thickness of 3km. These fold structures appear to be coherent and contrast with the tectonic mélange which characterises the Peltetec ophiolite immediately to the west.

The associated andesitic basalts are massive and uncleaved and only slightly metamorphosed in contrast with the greenstones and greenschists of the Alao-Paute unit east of the San Antonio fault (Figure 16). The one sample to be analysed shows geochemical patterns similar to the Alao-Paute unit (Figures 14 and 15b). Agglomerates are associated with tuffs along the Cuenca-Gualaceo road near Quebrada Totora Yacu.

Minor lithologies of the Maguazo unit include purple and black phyllites, ferruginous or pyritic in places; green phyllites of tuffitic origin; reddish, fine-grained orthoquartzites (Atillo, Alao); and cherts. The red cherty blocks in the Río Jadán (Paute Valley) are particularly noteworthy, but the source of these boulders has not been traced and they may be derived from the Peltetec ophiolite. Black and white cherts are exposed along the Río Zula road along with fine siliceous acid volcanic rocks. Dark or pale marbles were also noted along the Huarguallá, Paute and Zula roads, the latter section also exhibiting sedimentary limestone breccias. In the Río Blanco de Patate there is a marker horizon of dark calcareous sandstone of probable turbidite origin.

The Maguazo unit can be interpreted as a possible marine forearc sequence to the Alao-Paute oceanic island arc. The presence of turbidites and reworked acritarchs would indicate a high-energy environment, and the proximity of unmetamorphosed or low-grade Ordovician source rocks.

GUAMOTE TERRANE

This new tectonostratigraphic division (Figure 9) comprises metamorphosed Jurassic-Lower Cretaceous quartzites and slates which crop out in basement inliers along the western slope of the cordillera north of Cuenca, the largest of these being to the east of Guamote. North of Riobamba there are only three outcrops: a possible inlier near Patate; a small inlier in the Río Yanayacu in front of the Pisayambo hydroelectric plant; and the hills east of Ambuquí in the extreme north close to Colombia. Rocks of the unit are readily accessible and there are excellent exposures along the main Pan-American highway just south of Guamote and near Ambuquí in the Chota valley.

The Guamote terrane is bounded to the east, across the Peltetec ophiolite, by the Alao terrane of similar age but different geological environment. To the west it appears to be limited by the Ingapirca fault and thus lies in a fault-controlled belt up to 15km wide. It is possible, however, that west of the Ingapirca fault the Guamote rocks are entirely buried by the younger Cenozoic volcanics. River blocks of Punín-type quartzites were found west of this fault in Quebrada Bashog, 1.5km south of Yaruquíes, but these may be derived from younger conglomerates.

An ammonite fossil was discovered in a small roadside quarry in Cebadas black slates (**7701-97956**) (Figure 16); exhaustive searches failed to yield further material. It is a sheared cast (Plate 7g) most like an *Arnioceras* cf. *ceratoides* (Quenstedt) of Lower Sinemurian age (Ivimey-Cook and Howarth, 1991). The other possibilities considered, *Arieticeras*, *Vermiceras* and *Leptechioceras*, are also of Lower Jurassic age. Several small bivalves were also present in the sample comparable with *Lucina* or small *Homomya*.

An indeterminate ammonite fragment collected from the quarry in Punín quartzites close to the old bridge at Guamote (**7545-97873**) shows a style of ornament resembling the genus *Olcostephanus*, of Upper Valanginian (Lower Cretaceous) age (Woods and Morris, 1992). This sample belonged to the late Ing. Victor Pérez who had also collected a fragment of fossilised wood from the same locality.

Coals and carbonaceous sediments which crop out along the road (**7768-98554**) from the Río Patate to Patate town may be part of the Guamote terrane. Samples collected by the late Dr. F. Dugard contained the microspores cf. *Deltoidospora* sp. and *Cicatricosisporites* sp. (Warrington, 1987). The latter was originally described from Eocene deposits in Hungary and is known to range down to the late Jurassic. The apparent absence of *Angiosperm* pollen, which would be anticipated in association with *Cicatricosisporites* in younger Cretaceous and post-Cretaceous assemblages, may favour a late Jurassic to early Cretaceous age (Warrington, 1987).

The rocks of the Guamote terrane are divided into three units on the accompanying map: the Punín quartzitic unit and the Cebadas and Guasuntos slate units. All show shallow or flat cleavages in marked contrast to the metamorphic rocks of the Peltetec ophiolite and Alao terrane.

The **Punín unit** comprises quartzites and minor slates. It exhibits lithological changes from north to south. In the Punín inlier and Guamote sector the quartzites are off-white to medium grey, pink or red in colour and vary from medium-grained feldspathic types through coarse-grained types to conglomerates with clasts up to 1cm across. These are intercalated with black, grey, purple, green or off-white slates, which, in the small quarry 200m east of Punín, are essentially unmetamorphosed. Other features are the reported fossil wood from the Guamote quarry; the presence of fine ferruginous sandstones; and clay concretions, ferruginous in places, up to 20cm across, in the quartzites. The coarse quartzites show subrounded to angular clasts dominated by milky quartz with subordinate clasts of smoky quartz, mudstone pellets and pyrite-rich, fine-grained, recrystallised acid volcanics, in a matrix of more-rounded fine quartz.

South around Palmira, the conglomerates are also pale grey in colour but the quartzites are grey or black due to the presence of smoky quartz. Clasts of blue quartz were also noted, possibly derived from the Triassic blue quartz granites of Tres Lagunas-type described earlier. The slate fraction is grey to black without the multicolour intercalations of the northern outcrops. Further south along the Ríos Zula, Silante and San Pedro, the Punín unit is entirely grey to black in colour. The quartzites are fine to medium grained, poorly sorted, and dominated by smoky quartz clasts with subordinate blue quartz. Over this area the unit includes the 'Ingapirca Formation' mapped by Bristow et al. (1975) as an extension of the Upper Cretaceous Yunguilla Formation.

Over the Ambuquí inlier, near the Colombian border, the Guamote terrane rocks are dominated by fine-grained, dark, subvitreous quartzites and black graphitic slates. At the western extremity, in the Cachiyacu valley, pale quartzites and phyllites are also present.

The **Cebadas** and **Guasuntos units** are essentially black slate subdivisions with subordinate black or grey, fine- to medium-grained quartzites (Plate 8). The Ambuquí outcrop is included in this unit on the accompanying map, although the black and grey, fine-grained quartzite fraction comprises about half the rocks.

The Guamote terrane is a marine sequence of Lower Jurassic to possibly Lower Cretaceous age which includes shallow-water conglomerates and fossilised trees. In fact, the terrane may comprise a Lower Jurassic marine sequence mixed, tectonically, with shallow-water Lower Cretaceous deposits. The rocks contain smoky and blue quartz, presumably from the erosion of Tres Lagunas-type granites, and some acid volcanics, which were deposited rapidly as witnessed by the preservation of pyrite in the clasts.

OPHIOLITIC ROCKS AND MÉLANGES

Peltetec ophiolitic belt.

This tectonostratigraphic division was discovered during the first year of the project and was recognised as of great significance in any regional geotectonic interpretation (Litherland, 1987; Aspden and Litherland, 1987; Aspden et al., 1987; Aspden et al., 1988; Litherland and Aspden, 1990; Litherland et al., 1990; Aspden and Litherland, 1992; Litherland et al., 1992a). The Peltetec belt is a narrow zone, 1-2km wide, of steeply dipping ophiolitic rocks exposed in inliers along the western slope of the cordillera between Penipe in the north and Río Zula in the south: a distance of about 85km. The eastern part of the basement outcrop at Ambuquí close to Colombia is also included in the regional unit. The belt is tectonically bounded to the west by the shallow-dipping rocks of the Guamote terrane, and to the east by the Maguazo unit of the Alao terrane; outcrops show features of a tectonic mélange. Both the Guamote and Maguazo rocks contain Jurassic fossils and it is possible that the fossiliferous chert blocks from the Río Jadán attributed to the Maguazo unit are actually derived from the Peltetec belt. All three units are interpreted to be unconformably overlain by the outcrop of Upper Cretaceous Yunguilla Formation north-east of Azogues.

The ophiolitic rocks were first recognised along the Licto-Alao road near a stream gulley (**7716-97946**) close to the village of Peltetec (local spelling) (Figure 16). There are outcrops of metagabbro in the stream, and metabasalts eastwards along the road; associated with boulders of other mafic igneous lithologies, including serpentinites and pretectonic serpentinite conglomerates, both in the stream and higher up the steep hillside.

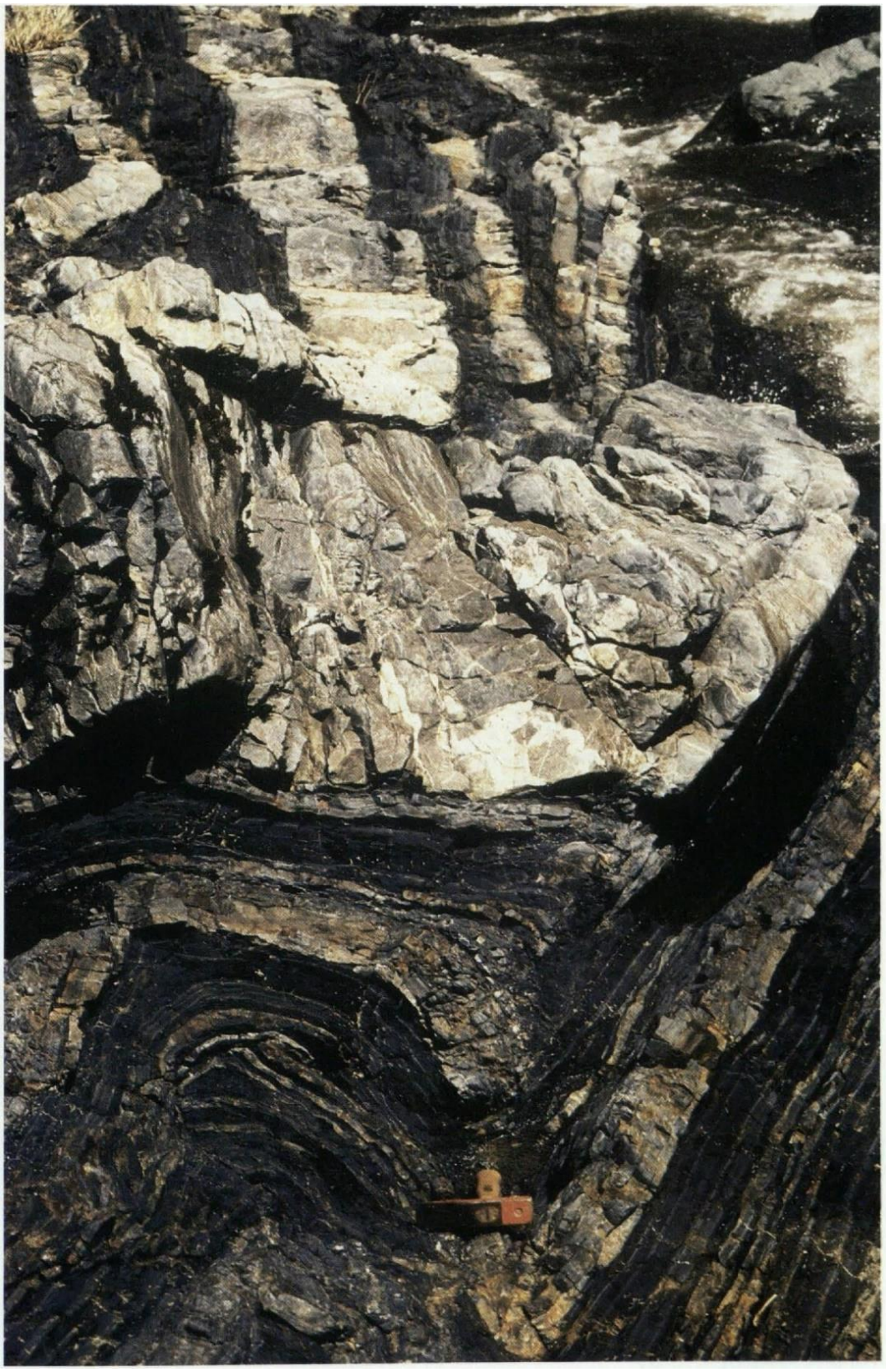

Plate 8. Guamote terrane rocks: folded, banded, black slates and quartzites of the Cebadas unit in the Río Alao (Photo R. A. J.).

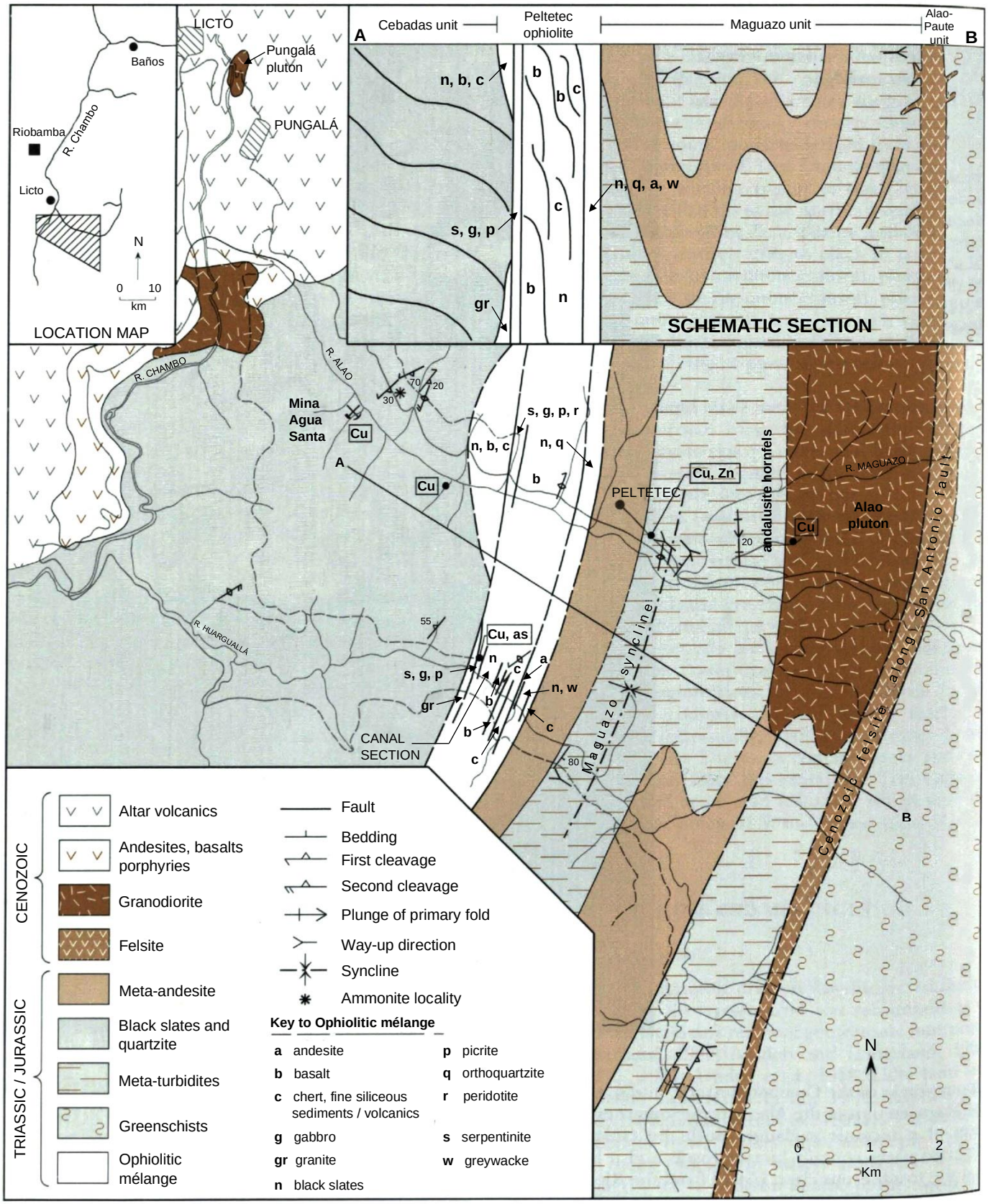

Figure 16. Geological map and section of the lower Alao Valley and environs, after Litherland et al. (1992a). Mineral symbols: Cu = copper, Zn = zinc; as = asbestos

Petrographic studies (Fortey, 1990; Litherland et al., 1992a) indicate a wide variety of rock types. The plutonic rocks can be divided into those in which alteration has destroyed almost all the primary constituents and those in which augite is substantially unaltered. Among the former group are rocks in which primary grain boundaries are preserved indicating static alteration. Alteration products of pyroxene include dark-stained carbonate, probably brucite, and micro-scale tremolite-chlorite intergrowths. Plagioclase alteration products include chalcedonic pseudomorphs and complex quartz-hematite-sericite pseudomorphs. Other alteration products include carbonate and albite. A brucite-rich rock may be an altered norite. Other plutonic rocks with deformed fabrics comprise foliated tremolitic serpentinite and sheared gabbro, rich in brucite (after pyroxene) and periclase (after feldspar).

The less-altered plutonic rocks comprise melanocratic olivine-gabbros and peridotite. In general plagioclase in these rocks has been replaced by pseudomorphs of brown, subopaque, cryptogranular material, possibly made up of quartz and hematite. Olivine is replaced by pseudomorphs of serpentine or of chlorite-quartz. Pyroxene, however, has resisted alteration and displays the strong birefringence and oblique extinction of augite.

Hypabyssal variants include spilitised dolerites and the basalts which comprise microporphyritic types dominated by a dark, incipiently devitrified groundmass; porphyritic vesicular types, with alteration to quartz, albite, carbonate, sericite, chlorite and epidote: compatible with reaction with heated seawater; and hydrothermally brecciated types with late epidote-quartz and carbonate-anthophyllite veins.

There are also basalt-volcanoclastic sedimentary rocks. Some are of immature microbreccias of basalt and dolerite clasts in a groundmass of comminuted basaltic material; others of quartzofeldspathic siltstones fractured and invaded by albite-epidote veins carrying patches of fine-grained ‘mylonitic’ quartz as well as patches of carbonate and brown-hued clay mineral.

North of Peltetec the ophiolitic rocks are exposed along the Río Quishpe and around Penipe. At the latter locality, along the road south to Río Blanco, there are metabasalts, serpentinites, pyroxenites, hornblendites, black phyllites and volcaniclastic rocks. The serpentinite shows an early massive mesh fabric crossed by magnesite veinlets which were later sheared.

South of Peltetec the ophiolitic rocks are well exposed along a recently excavated irrigation canal in the Huarguallá valley (Figure 16). There is an east-dipping black serpentinite (Plate 9a), 15m thick, more sheared and asbestiform towards the base, overlain by 5m of olivine gabbro and olivine-pyroxenite and spillitic basalt lavas. There are sedimentary rocks containing clasts of augite and cherty mudstone set in a muddy matrix, and these are brecciated by later, hydrothermal veins. This canal section of Huarguallá also contains tectonic slices of cherts and mudstones, metabasalts and black slates and andesites which may belong to the adjacent Cebadas and Maguazo units respectively. There is also a thin, 5m, slice of Tres Lagunas-type blue quartz granite of Triassic age. In contrast to the adjacent units this section exhibits a tectonic mélange of differing lithologies.

Further south, along the Guamote-Atillo and Guasuntos-Zula roads, the igneous ophiolitic fraction has not been noted. Over these sections the tectonic mélange comprises slices of black, maroon or pale cherts, somewhat silicified fine-grained sediments and volcanics, and slices of the blue-quartz granite. Greywackes were also noted at Zula.

In the extreme north there is a narrow belt of basaltic greenstones which forms the eastern flank of the Ambuquí inlier. Contacts with the adjacent Guamote-type metasediments are tectonic. No ultramafic rocks were noted despite an extensive search, although serpentinites are carved for ornamental stone in nearby San Gabriel. The metabasalts are tentatively correlated with the Peltetec ophiolite.

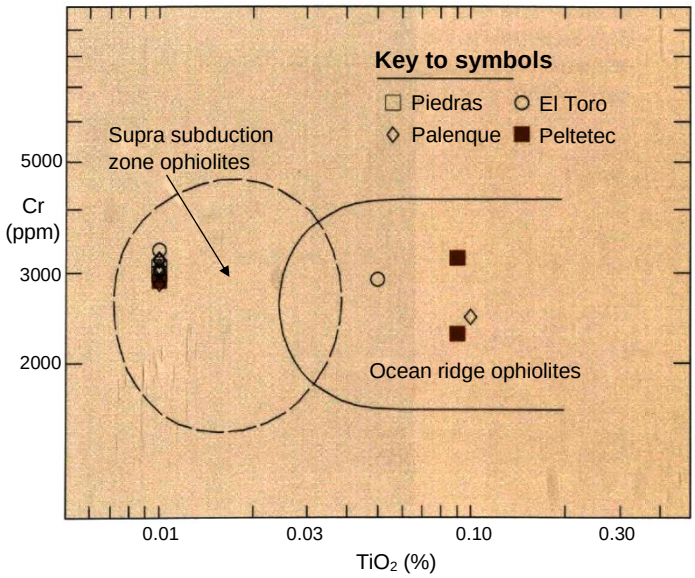

Figure 17. Ultramafic rocks from ophiolitic units plotted on Cr v. TiO_2 diagram of Pearce et al. (1984b).

a

b

Plate 9. Serpentinites.

(a) First field check of the Peltetec serpentinite at the Huarguallá valley irrigation canal (Figure 16). Left to right: Ramiro Bermúdez, Pablo Duque, Francisco Viteri, John Aspden, Martin Litherland, Wilson Santamaría, Clive Jones, Edgar Salazar.

(b) Discovery of the Quebrada Soledad serpentinite outcrop at 4000m in the high cordillera (Figure 19) (photo: M. L.).

Taken as a whole the specimens from the Peltetec belt form a consistent set of ophiolite-related lithologies. The basalts and sedimentary rocks could represent the upper part of the oceanic crust; the dolerites the immediate levels in which dykes are dominant; whilst the plutonic rocks are arguably the subcrustal magma chambers. Other rocks could represent alteration and deformation on shear zones before incorporation into the mélange or during subsequent tectonic movements. It is interesting to note the disappearance of magmatic ophiolitic rocks south of Huarguallá which corresponds to the incoming of tectonic slices of the blue-quartz granite of Tres Lagunas within the mélange.

Of the three analysed samples of Peltetec ultramafic rocks, two plot into the MORB (oceanic crust) field on the Pearce et al. (1984b) diagram (Figure 17), whilst the other falls into the Supra Subduction Zone field which have the geochemical characteristics of island arcs but the structure of oceanic crust and are believed to form by sea floor spreading directly above subducted oceanic lithosphere.

Other Cordillera Real serpentinites

In addition to the Peltetec belt, serpentinites also occur within the Tampanchi complex (p.52), and as outcrops and float blocks of massive and sheared, dark greenish grey to black serpentinite found over the pre-Cretaceous metamorphic basement east of the Baños fault, the locations of which are indicated on the accompanying map.

Sauer (1965) reported serpentinite blocks in the Río Guachalá near Cayambe, and as outcrops in the Río Mulatos. The first occurrence was confirmed by the project but no such outcrops were seen in the Río Mulatos. However, further examination of Sauer's (1958) traverse map and field data indicates that he traversed what is now referred to as the Río El Golpe/Niagara Grande or Parcayacu, a tributary of the present Mulatos, his Río Langoa, and thus his serpentinite outcrops occur close to the main confluence.

The discovery by P. Duque of serpentinite boulders in the Río Chalpi de Papallacta was confirmed; as was the report by A. Hirtz of similar boulders in Río Huagrayacu, near Baeza, which solved the problem of the source of the large blocks in the adjacent Río Quijos first reported by Colony and Sinclair (1932).

The project has discovered the following new serpentinite localities from north to south: river blocks of massive or sheared serpentinites were noted in the Río Cofanes; the Río Cariyacu de Oyacachi (with hornblendites); the Río Quijos, upstream from the Río Papallacta confluence; the Río Bermejo near Baeza; in streams draining east and west from the Urcucocha skarnfields; in the Ríos Aliso and Cosanga; in the Río Mulatos upstream from the Parcayacu; and in the Quebrada de Los Incas, a tributary of the Río Muyo. Of these the entry point of the enormous Cosanga blocks has been given outcrop status on the accompanying map (Figure 19); similarly the Urcucocha blocks are represented as a synformal unit at the base of the skarns.

Serpentinite was found in outcrop close to Quebrada Soledad in the high moorlands south of Antisana volcano (Plate 9b). It forms a west-dipping belt with a maximum thickness of 30m bounded by grey and black phyllites (Figure 19). A small outcrop of green, sheared, fuchsitic serpentinite, 10m thick, was noted along the road 100m west of Río El Carmen close to Monte Olivo.

The petrology of the serpentinite samples collected from the outcrops and river blocks over the northern sector (Fortey, 1990) indicates common characteristics. The serpentinites from Soledad exhibit a massive interlocking antigorite mesh with relict chrome spinel and micro-poikilitic secondary magnesite. This appears to have formed by static alteration of ultrabasic rock, probably peridotite. In sheared samples this is partially replaced by talc, magnesite and tremolite as evidenced in samples from Urcucocha and near Baeza. The Cr and Ni chemistry (Litherland, 1988; 1989) is typical of ophiolites and precludes a sedimentary origin.

Only one serpentinite/ultrabasic locality was reported from the southern sector of the cordillera. This occurs in the extreme south along the main road east of Zumba in the form of a small outcrop along the main fault which divides the Miocene Zumba basin from the Isimanchi unit. Serpentinites, olivine pyroxenites and gabbros are present. Further east, near the junction of the Río Isimanchi and Río Mayo there are xenoliths in the Zamora batholith which include a hypersthene-rich norite hornfels which was probably incorporated into the batholith prior to serpentinisation (Fortey, 1990), suggesting a pre-Jurassic age.

FIVE

Cordillera Real: later Cretaceous and Cenozoic rocks

Whilst the aim of the project was the study of the pre-Cretaceous metamorphic rocks of Ecuador, these have been affected by more recent geological events, producing, for example, important phases of mineralisation within them. In this section the Cretaceous and Cenozoic rock units of the Cordillera are briefly described and details provided where pertinent.

SEDIMENTARY AND VOLCANIC FORMATIONS

In the Oriente the 80-240m thick **Hollín Formation** of Aptian/Albian age, represented by diagnostic whitish sandstones or quartzites, unconformably overlies a widely variable substrate, including Misahuallí volcanics, Sacha sandstones, Macuma limestones, Pumbuiza shales and Precambrian crystalline basement (Bankwill et al., 1991). Then followed a marine transgression and the deposition of the **Napo Formation** which comprises dark grey limestones, black shales and sandstones, 200-650m thick, of mid-Albian to mid Maastrichtian age (Wilkinson, 1982). Both these units were derived from the east (Baldock, 1982). The overlying **Tena Formation,** 250-1000m thick, comprises fluviatile and lacustrine redbeds and represents the withdrawal of the sea and the start of a continental environment of deposition derived from a proto-Andean cordillera (Wilkinson, 1982). Its age is largely Maastrichtian but probably extends into the Palaeocene (Baldock, 1982).

In the Sub-Andean zone, immediately west of the Cosanga fault, these Cretaceous formations are folded and faulted with the basement rocks of the Salado terrane, forming a belt of 'semi-metamorphic' rocks previously termed the Margajitas Group (Baldock, 1982). In this belt, the Napo shales, for example, may occur as slates or phyllites. The Project studies have added to the understanding of this complex belt by differentiating basement and cover sequences, and recognising new Cretaceous outcrops, such as the oolitic Napo Formation limestones in the Río Mulatos west of the Abitagua granite.

Project palaeontological studies (Woods and Morris, 1992) of rocks attributed to the Napo Formation along the road from Gualaquiza to Macas identified the echinoid *Holectypus planatus*, the bivalve *Calva*, and the ammonite *Hysteroceras* cf. *subbinum* Spath, of Upper Albian age (see Bristow and Hoffstetter, 1977, for other Napo Formation species). Ammonites from the Río Upano from the collection of Ing. L. Cevallos were identified as: *Hypengonoceras ?chouberti* Collignon; *Oxytropidoceras cantianum* Spath; *Oxytropidoceras* (*Venezoliceras*) *commune* Renz; *Oxytropidoceras* (*Venezoliceras*) cf. *bitubercalatum* (Collignon); and *Oxytropidoceras* (*Venezoliceras*) cf. *madagascariense* (Collignon) (Plate 10).

In the area of the Zamora batholith, along the Río Vergel, there is a belt of fossiliferous shales shown on the accompanying map as a tectonic slice along the major La Canela fault. Samples (Plate 11) showed the presence of the ammonites: *Oxytropidoceras* sp.; *Adkinsites* sp.; and *Brancoceras* sp., indicating a Middle Albian age and establishing these rocks as belonging to the Napo Formation rather than the Santiago (Ivimey-Cook and Howarth, 1988; Aspden and Ivimey-Cook, 1992). Similar fossils were noted from samples collected at the headwaters of the Río Nangaritza, to the north-east of the Río Vergel. The samples also yielded the pollen *Araucariacites* sp. and *Cycadopites*; and the dinoflagellate cysts *Florentinia ?deanei* (Davey and Williams, 1966); and *Oligosphaeridium ?complex* (Davey and Williams, 1966).

Upper Cretaceous (Maastrichtian) fossils were found in rocks cropping out over the cordillera near Azogues which were correlated with the **Yunguilla Formation** (Bristow, 1973). The unit comprises shales, sandstones, greywackes, tuffs and andesitic sills, with a thickness in the region of 2000m. The outcrop north-east of Azogues has been substantially reinterpreted in recent years so that the western margin is incorporated into the older Punín quartzite unit of the Guamote terrane, whilst the eastern sector is included in the older Maguazo turbiditic unit of the Alao terrane. What is still shown as Yunguilla Formation is thought to unconformably overlie the metamorphic rocks of the Alao and Guamote terranes, although a detailed resurvey of the sector is needed.

In the Oriente the Cretaceous/Palaeocene Tena Formation is overlain by sedimentary formations belong to the Cenozoic continental back-arc basin (Baldock, 1982), overlain in the north by the Plio-Quaternary volcanic formations of the Reventador, Pan de Azúcar and Sumaco volcanoes.

Plate 10. Lower Cretaceous ammonites from the Napo Formation along the Chinimbimi sector of the Río Upano, from the collection of Ing. Luis Cevallos (CODIGEM). (× 0.75), plaster cast BGS Nos. FOR 5014-5018.

(a) *Oxytropidoceras* (*Venezoliceras*) *commune* Renz.

(b) *Oxytropidoceras* (*Venezoliceras*) cf. *bitubercalatum* (Collignon).

(c) *Oxytropidoceras* (*Venezoliceras*) cf. *madagascariense* (Collignon).

(d) *Hypengonoceras ?chouberti* Collignon.

(e) *Oxytropidoceras cantianum* Spath.

a

c

b

d

e

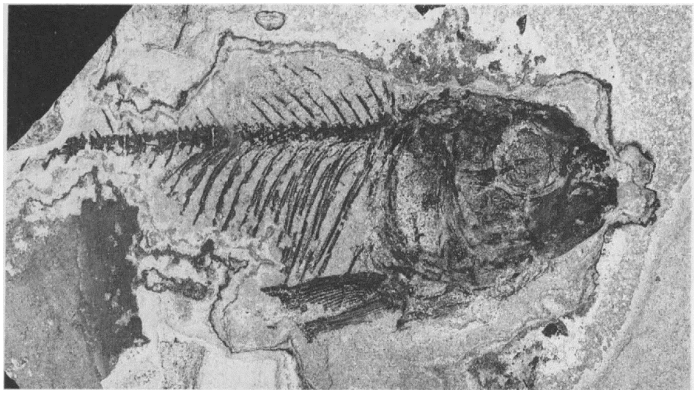

a

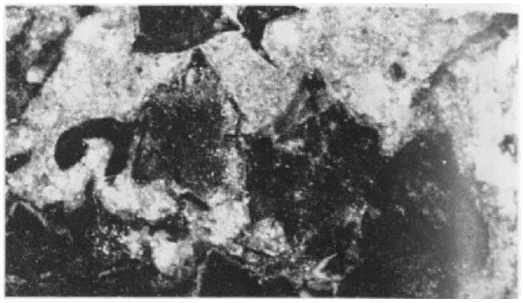

b

c

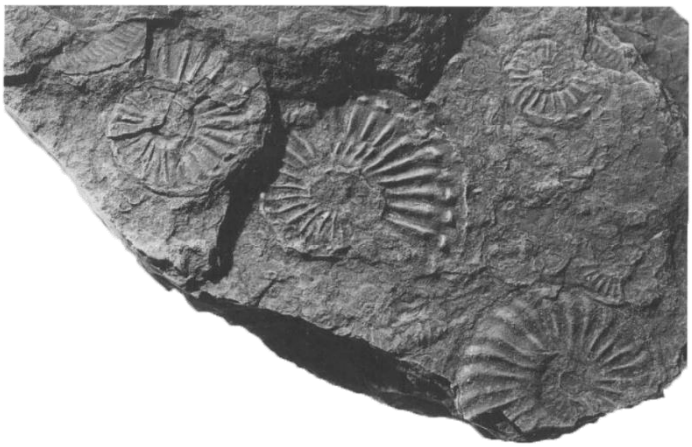

d

e

Plate 11. Cretaceous and Cenozoic fossils.

(a) *Characinae* fish from near Laguna Atillo (×1).

(b) Two tricuspid teeth from its lower mandible (× 10).

(c) Ammonite *Oxytropidoceras* sp. from headwaters of Río Nangaritza, (× 1), BGS specimen No. FOR 4820.

(d) Ammonites *Adkinsites* sp., *Oxytropidoceras* sp. and *Brancoceras* sp. from the Río Vergel, (× 1), BGS specimen No. FOR 4821

(e) Ammonite *Adkinsites* sp. from Río Nangaritza, (× 1), BGS specimen No. FOR 4820

The **Cenozoic** sedimentary and volcanic formations of the cordillera are summarised by Baldock (1982). Recent geochronological studies (Barberi et al., 1988; Lavenu et al., 1992) have clarified this sequence so that four main volcanic events: 'Sacapalca' (Palaeocene-Eocene); 'Saraguro' (Oligocene); 'Pisayambo' (Mio-Pliocene); and 'Cotopaxi' (Plio-Quaternary) are now distinguished on the new national geological map of Ecuador (Litherland et al., 1993a). The volcanic rocks previously indicated as Quaternary Tarqui Formation have been redefined as Tertiary units (Lavenu et al., 1992) and there appears to be little evidence for Plio-Quaternary volcanic activity south of Sangay volcano.

Cenozoic sedimentary rocks in the cordillera are essentially confined to the Mio-Pliocene nonmarine basins (Bristow and Parodiz, 1982; Lavenu and Noblet, 1990), which were largely contemporaneous with the Pisayambo volcanics. A new, small basin was discovered by the Project close to Laguna Atillo, at 3550m above msl, which contained a fossil fish of the subfamily *Characinae* of the family *Characidae* (Patterson, 1990) (Plate 11a and b). Similar forms have been described by Bristow (1973) from the Cuenca basin.

Plate 12. Condué granite: cut by felsite sheets with chilled margins, in the Río Cofanes above the Río Condué confluence (photo: M. L.).

GRANITOIDS AND PORPHYRIES

The **Pimampiro pluton** in the extreme north of the cordillera is an undeformed granodioritic body with megacrystic hornblende. Seven K-Ar dates (p.120) gave a range of 47-94 Ma. Concordant hornblende and biotite ages give 81 ± 3 Ma indicating a Cretaceous age.

The undeformed, hornblende-rich, **Magtayán granodiorite**, exposed as an inlier in the Miocene volcanics east of Alausí, yielded K-Ar ages in the order of 75-80 Ma (p.120) similar to those obtained by Kennerley (1980). This inlier is close to others composed of hornblendite, and the two lithologies could be part of a plutonic complex. These Cretaceous intrusives may represent feeders to the volcaniclastic Yunguilla Formation nearby, and form part of a still poorly recognised Upper Cretaceous/Palaeocene magmatic arc.

In the extreme north of the area, the post-tectonic **Condué granite** has been provisionally allocated a Cretaceous age. This previously unknown pluton occurs over a poorly accessible region but sufficient outcrop (Plate 12) and river float rocks were seen to indicate a large batholith-sized body. The typical rock in the west is a leucocratic, pink, coarse- to very coarse-grained granite, low in biotite, with biotite-free aplitic and pegmatitic phases.

In places there are K-feldspar megacrysts up to 5cm long, and at the confluence of the Ríos Condué and San Jorge, a paler granite, richer in biotite is mixed with the dominant type and may represent an early phase. In the east, there are outcrops in the Río Cofanes and Río Condué near la Sofía. In tributary streams of the Río Cofanes, there are xenoliths of volcanic rocks or biotite-rich vestiges within some of the granite boulders; porphyry sheets may also be present.

The southern extension of the granite is based on samples collected by Ing. W. Santamaría east of Sigsigpamba, and observations by Ing. L. Torres along the Río Agua Clara. However, further studies are required, over this, the least accessible part of the cordillera, to properly define the extent of the granite and determine its age.

Several Cenozoic K-Ar dates have been obtained by the Project from essentially unmetamorphosed and undeformed plutons in the south of the cordillera (p.120). Five ages and four from Kennerley (1980) give an average of around 60 Ma for the granodioritic **San Lucas pluton** (Wolf, 1892). This is close to the age of 58 ± 2 Ma from two samples of the **Catamayo granodiorite** which crops out along the new Catamayo-Loja road, and the age of about 54 Ma for the **Pichinal pluton,** east of Saraguro. These plutons may be feeders to the nearby Palaeocene Sacapalca volcanic unit.

The average of five ages from the **Amaluza pluton** (Kennerley, 1980) along the Río Paute gives 40 Ma, a Late Eocene date similar to 43 ± 2 Ma, the average of four Project ages for the granodioritic **Pungalá pluton** (Figure 16), and 39 ± 3 Ma, the age of the **Ishpingo pluton** on the Gualaceo-Limón road.

Seven K-Ar ages from the large volcanoplutonic **Portachuela batholith** near the Peruvian border gave an average of 20 Ma, whilst the porphyry stock near Baeza was calculated at 0.54 Ma (Herbert and Pichler, 1983). Many of the small, undated, porphyry stocks throughout the cordillera are probably of similar Upper Cenozoic age. The topographically prominent porphyry neck of Cerro Pan de Azúcar is one of these. The Chinapintza porphyry, in the south-east, affects the Cretaceous Hollín Formation (oral communication, D. Coochey) and is thus of Cenozoic age.

There are many post-tectonic plutons and stocks over the cordillera and El Oro which are still undated and many to be discovered, as indicated by the common occurrence of blocks of granitoid, porphyry or andalusite/sillimanite hornfels in unsurveyed rivers. Of the larger undated bodies there is the Condué granite; the granodiorite-porphyry complex of the Río Azuela; the Alao valley pluton (Figure 16); and the Colimbo pluton south of the Atillo-Macas road recognised by marginal aplogranite and dolerite phases along the road and granodiorite-diorite boulders in the rivers draining from the south.

MAFIC AND ULTRAMAFIC INTRUSIVES

The **Tampanchi mafic-ultramafic complex** was recognised along the road east of Taday where Bristow et al. (1975) reported amphibolites. Essentially undeformed ultrabasic rocks, pyroxenites, gabbros, amphibolites and some acid rocks are present and the complex as a whole is assumed to cut Jurassic metamorphic rocks of the Alao-Paute unit. Project K-Ar studies on magmatic hornblendes gave three dates from 60 to 65 Ma, suggesting an Early Palaeocene age (p.120).

The complex is roughly oval in plan, about 8×4 km in dimensions, and the rocks appear to be distributed in the form of concentric shells (Pozo, 1990), although more detailed geological mapping is required to confirm this. The central zone comprises serpentinites and olivine-clinopyroxenites. This is followed by clinopyroxenites which are medium grey-green, medium-to coarse-grained rocks comprising essentially fresh subrounded augite crystals as the cumulate phase, with intercumulate green hornblende and rutile. Partial replacement of augite by hornblende occurs in places; orthopyroxene was not noted. In one sample there is a tongue of interlocking andesine crystals which cuts the augite aggregate. Its form suggests fissuring of the aggregate at or above the solidus temperature resulting in rapid precipitation of feldspar from magma supersaturated in aluminium (Fortey, 1990).

The outer shell comprises coarse to pegmatitic hornblende gabbros and hornblendites. The hornblende or tremolite crystals reach up to 5cm in length and are associated with labradorite which in places breaks down to epidote and muscovite. Fine-grained hornblende basalts also occur which can be interpreted as a chilled, marginal phase of the complex. There are also small diorite bodies and sheared and mylonitic granite sheets (Fortey, 1990). Shear zones in the mafic rocks produce local zones of serpentine.

The geochemistry of three samples from the complex indicate a calc-alkaline trend (Figure 14), and, on Figure 15c, there is the possibility that the sample with lowest Cr and Ni represents the parent liquid prior to fractionation.

The Tampanchi complex represents a hornblendic, calc-alkaline plutonic complex. The ultramafic to gabbroic rocks suggest a continuum in which augite and hornblende are dominant. They appear to represent gravimetric or flow differentiation of mafic phases from an undersaturated basaltic magma. The presence of pegmatitic gabbros, the lack of orthopyroxene and the apparent concentric pattern of the complex are compatible with the presence of an Alaskan pipe complex (Taylor, 1967; Irvine, 1974). Such bodies have now been identified in the Urals and Venezuela (Murray, 1972) and Australia (Anon, 1988).

North of the Tampanchi complex, Kennerley (1980) reported a K-Ar date of 85 ± 3 Ma from a hornblendite sample near Laguna Magtayán, close to the granodiorite. Ing. D. Benalcázar (oral communication) later discovered a hornblendite complex south of the lake and a small outcrop further west by the road. Like the adjacent granodiorite, these outcrops are inliers within the Cenozoic volcanics and thus the full extent of the mafic body is not shown on the accompanying map.

Hornblendites and hornblende gabbros of Tampanchi-type are also found in outcrop close to the village of El Azul, between Tampanchi and Paute, and also upstream from Shumir, south of Paute (oral communication, Ing. L. Quevedo). Float blocks in the Río Villacruz indicate the presence of another complex south of the Río Upano along the Atillo-Macas traverse. All these occurrences are shown tentatively on the accompanying map which thus indicates five Tampanchi-type complexes forming a chain of possible Alaskan pipes cutting the metamorphic rocks of the Alao terrane. The Cordoncillo mafic complex of the El Oro area (UNDP, 1969) may be a part of this chain, which could be another manifestation of the poorly defined Late Cretaceous/Palaeocene magmatic arc.

SIX

Cordillera Real: tectonometamorphic events

Project studies along the cordillera have defined two main tectonometamorphic events. These are termed the Tres Lagunas and Peltetec events, the imprints of which are described below. Due to the presence of suspect terranes separated by faults with potential strike-slip movement, there are doubts regarding both the correlation of structures from one terrane to another and the consequent existence of a common structural history. For this reason, the terranes and boundary faults are treated separately.

TRES LAGUNAS EVENT (TRIASSIC)

This event can be postulated over the Loja terrane and Isimanchi unit of the cordillera. These Andean-trending units are for the most part bounded tectonically by younger Jurassic terranes overprinted by the Peltetec tectonometamorphic event. Although locally the polyphase structural history in the older rocks may appear to be similar to that in the younger terranes, there is sufficient evidence for an important tectonometamorphic event synchronous with the intrusion of the Tres Lagunas granite of about 228Ma, Triassic age, and common to the Chigüinda, Agoyán, Sabanilla and Isimanchi units.

The **Tres Lagunas granites** are almost everywhere foliated tectonically. In the Río Pastaza this foliation is seen to be cut by amphibolite dykes (Plate 13) which are both undeformed and xenolithic, suggesting the disruption of a late-tectonic, pre-cooling dyke intrusion. Elsewhere, the foliation in the granite is cut by undeformed tourmaline pegmatites (Plate 3b) which show every indication of being a late, post-tectonic stage of the granite. The undeformed state of these minor intrusions indicates that the Tres Lagunas (Triassic) structures were not affected by later (Peltetec) refoliation over much of the Loja terrane.

In most cases, the foliation in the Tres Lagunas granite (Plates 3b, 14a and 14c) can be related to major shear zones which have yet to be mapped out in detail along the cordillera. Even those granites which appear in the field to be undeformed show evidence of dynamic metamorphism in thin section, such as the recrystallisation of the quartz mosaic. The rocks of the shear zones exhibit complete recrystallisation and refoliation accompanied by the growth of feldspar augen and a new generation of biotite, together with muscovite, epidote, calcite and chlorite. Pale blue quartz may be found in rocks from all the dynamothermal stages. Its colour may be due to the mortar texture and internal strain of particular crystals although most do not exhibit the coloration.

a

b

Plate 13. Amphibolite xenoliths.

(a) Undeformed amphibolite within deformed, mylonitic Tres Lagunas granite, in a boulder in the Río Pastaza above Agoyán Falls (photo: J. A. A.).

(b) Detail of Plate 13a: the mylonitic fabric, but not the quartz vein, is truncated at the margin of the xenolith (photo: J. A. A.).

Many outcrops indicate that the generally steep foliation in the granite is a second (S2) shear structure which produces microcrenulations of a first-phase mylonitic foliation. This corresponds to the Type I S-C mylonites of Lister and Snoke (1984). These authors also discuss whether the intersecting fabrics relate essentially to one or two tectonic events. In the Cordillera Real it is clear that the feldspar augen and more euhedral smoky grey K-feldspar megacrysts are essentially synchronous with S2. Plunges of the augen-stretching lineation are shallow to moderate indicating an important strike-slip component in the generation of the mylonites. Between the Pastaza and Papallacta rivers, mineral lineations in the metagranite plunge to the south, and mullions and D2 fold axes in adjacent metasediments plunge to the south or north indicating a degree of rotation during deformation. With regard to the horizontal sense of shear as witnessed by tectonic transport indicators, the mylonites at Río Chalpi Chico exhibit sinistral displacements.

The **Chigüinda unit** of the Loja terrane is low grade and semipelitic and dominated on outcrop scale by fold structures picked out by massive quartzite beds. These folds are normally of local D2 age and axial planar to the generally steep and Andean-trending S2 cleavage which is a subpenetrative microcrenulation structural plane in the slaty and phyllitic rocks. The folds are tight to isoclinal in style and generally plunge to the north at shallow to moderate angles; refolded earlier D1 folds have been noted.

There is a well-defined D2 flat belt along the western margin of the Chigüinda outcrop from the Gualaceo-Limón road in the north to the Loja-Zamora road in the south, including the outcrop along the Loja-Catamayo road. Minor folds exhibit no consistent pattern of tectonic transport: at Gualaceo-Limón they are S-shaped looking north; at Loja-Zamora they are Z-shaped. Such inconsistencies suggest the presence of recumbent folds rather than separate thrust sheets. In the north, the Chigüinda unit is shown as forming part of the Cuyuja nappe complex, regarded as part of the younger Peltetec event (Figure 19). The semipelitic rocks ascribed to Chigüinda on lithology alone exhibit D2 recumbent structures similar to those of the remaining rocks of the nappe pile.

The metamorphism of the Chigüinda unit corresponds to the quartz-albite-muscovite-chlorite subfacies of the Barrovian greenschist facies within which chloritoid and stilpnomelane can also be present (Winkler, 1967) (see also Trouw, 1976). The presence of garnet and biotite and, at one locality, staurolite along the flat belt of the western margin indicates an increase in metamorphic grade up to local amphibolite-facies conditions. The metamorphic minerals are essentially syntectonic with the D2 event.

The **Agoyán unit** is dominated by pelitic schists and paragneisses of higher grade than Chigüinda, marked by a generally steep S2 schistosity. D2 minor fold axes plunge gently north at Agoyán, but further north along the Río Anatenorio, D2 quartzite rods plunge south at a moderate angle. Late, extensional, crenulation structures may be present and along the road to Monte Olivo there is a major antiform folding S2 and plunging north-east.

At most localities, metamorphism in the Agoyán unit is close to the transition from Barrovian greenschist to amphibolite facies. Almandine garnet is normally present, whilst hornblende is common in the associated Monte Olivo amphibolites. However, coarse-grained gneissose rocks with incipient migmatisation would indicate metamorphism in the upper amphibolite facies, and the presence of chloritoid indicates the greenschist facies. Kyanite was noted once, staurolite was not observed.

The **Sabanilla unit** is essentially migmatitic with the main foliation corresponding to a generally steep S2 cleavage. The Rb-Sr data points to a Triassic (Tres Lagunas) age for the Sabanilla gneisses (Figure 7b), but the K-Ar ages are mainly in the range 65-85 Ma (Figure 20) and record a younger geological event. In the east, around Valladolid, the Sabanilla gneisses are thrust eastwards over the lower-grade Isimanchi unit of ?Palaeozoic age, along the shallow-dipping Palanda fault. Along the western margin of the gneisses, near Sabanilla, steeply plunging minor folds indicate sinistral movement.

The Sabanilla gneisses have the highest metamorphic grade of the Cordillera Real rocks. They contain migmatitic gneisses which include sillimanite/kyanite-bearing streaky biotite gneisses, indicating local melting in the upper amphibolite facies, the hydrous high grade of Winkler (1976). In other lithologies, fibrous sillimanite was noted growing along the main S2 cleavage in the quartzites near Sabanilla, whilst white mica aggregates in some orthogneisses may be after cordierite. Andalusite, reported by Trouw (1976), was not confirmed. Staurolite gneisses occur to the north of Palanda over an area where muscovite and/or biotite pegmatites are common; almandine garnet is fairly common throughout the Sabanilla unit.

The **Isimanchi unit** comprises phyllites and marbles intruded by the undeformed Zamora batholith thus indicating a pre-Jurassic tectonic event. This pre-Jurassic cleavage in the Isimanchi unit becomes shallow-dipping in the west, parallel to the foliation in the Sabanilla gneisses across the Palanda thrust fault, suggesting a common tectonometamorphic event of Tres Lagunas (228 Ma) age. However, further east, phyllites attributed to the Isimanchi unit are reported to be unconformably overlain by the Piuntza unit of similar, Upper Triassic, age. The Zumba ophiolitic unit, believed to be older than the Zamora batholith, may be important in the geotectonic evolution of this sector in that it could define an important terrane boundary.

PELTETEC EVENT (UPPER JURASSIC-LOWER CRETACEOUS)

Evidence for a major tectonometamorphic event younger than Tres Lagunas is found over parts of the Cordillera Real, including the area of Peltetec. These areas contain deformed and metamorphosed rocks which on palaeontological evidence are Jurassic in age and thus younger than the Tres Lagunas event. The Peltetec event is regarded as of Upper Jurassic-Lower Cretaceous age and there are a number of metamorphic K-Ar ages to support this (Figure 20). Two are interpreted as primary metamorphic ages from Alao-Paute greenstones, whilst the others, from the Zamora, Abitagua and Azafrán plutons, are interpreted as reset ages. In the Cuenca area, the Upper Cretaceous Yunguilla Formation unconformably overlies steeply dipping metamorphic rocks of the Alao terrane, and thus provides a minimum age for the tectonic phase. Regionally the event also corresponds to the uplift and erosion of the proto-cordillera prior to the deposition of the molassic Upper Cretaceous Tena Formation. The base of the Hollín Formation (110-120 Ma) may provide a minimum age for the event. The manifestations of this event in terms of individual terranes and faults are described below from west to east across the cordillera.

Guamote terrane

These rocks contain Lower Jurassic and possibly Lower Cretaceous fossils as well as detrital blue quartz probably derived from the erosion of the S-type granites of Tres Lagunas age. The rocks are of very low grade with a slaty cleavage in the pelitic units.

Over the main Riobamba-Cuenca region this cleavage is remarkably flat except where steepened by upright D3 folds. Around Guamote it is manifested as a penetrative first cleavage axial-planar to tight or isoclinal minor folds with subhorizontal axes. The sense of movement along sheared and silicified limbs is mainly westwards, i.e. 'S-form' looking north, but structures indicating an opposite sense of tectonic transport were noted which could represent the overturned limbs of recumbent folds or nappes. 'M-form' folds representing higher-order fold closures, were also noted. Small thrust faults show westward movement. Between 1 and 2 km south of Guamote, the Pan-American highway outcrops display tectonic boudins, up to 20m across, of quartzite within ductile slates. Their long axes trend east-west which may indicate a stretching direction. However, other localities expose deformed sedimentary concretions as discoid forms within the cleavage, suggesting flattening rather than stretching as the shearing mechanism.

South of Palmira the first cleavage is refolded by a gently dipping, but steeper, crenulation cleavage with the sense of overfolding to the west.

The Ambuquí outcrop in the extreme north presents a polyphase fold complex. Dávila and Egüez (1990) propose cross folding of recumbent NW-SE trending D1 folds by a steep Andean-trending D2 phase.

The 'flat' cleavage of the type area is folded by upright, open-to-close folds with subhorizontal axes, associated in the pelitic rocks, with a subvertical crenulation cleavage. Many of the steep dips of bedding/S1/S2 lie on the limbs of such folds which exhibit wavelengths in the order of tens of metres. These folds mainly trend in the region of 70°, but another, perhaps conjugate, set was noted at 170°. They fold discordant felsic minor intrusives which cut S1/S2 and may be a Cenozoic (post-Peltetec) event.

Peltetec fault and ophiolitic mélange

The Peltetec fault is a neotectonic lineament on imagery from Patate to Cuenca, particularly striking along the Río Chambo. In the field this lineament marks a fault which at Penipe and other localities exhibits relative downthrow to the west of Upper Cenozoic volcanic formations against the metamorphic basement (Litherland and Aspden, 1992). South of Cuenca it is shown to follow the line of the former Girón fault, a prominent neotectonic structure (Winter et al., 1990), before swinging south to form the Las Aradas fault, along which Cenozoic formations are again downthrown to the west against the metamorphic basement. The Peltetec fault was thus active in Cenozoic times (p.62).

However, when this fault lineament is traced in the field over the metamorphic basement inliers between Penipe and Zula it is seen to coincide with an older fault within the basement. This older fault separates the Guamote and Alao terranes and is marked by the Peltetec ophiolitic mélange (p.42) comprising Jurassic and older elements. This is considered as one of the fundamental structures of the metamorphic basement.

In the field the 1-2 km-wide ophiolitic mélange is best exposed at Penipe, and along the Huarguallá and Zula valleys. The mélange (Figure 16) is a series of lithotectonic slices ranging in thickness from one to hundreds of metres; metamorphism is of very low grade. The rocks are generally steeply dipping, contrasting with the flat tectonics of the Guamote terrane to the west, except for the serpentinite/mafic unit at Huarguallá which dips moderately to the east. A steep cleavage is present in the more ductile lithologies and this may be truncated by the boundary faults to individual mélange slices indicating a complex tectonic history.

The extension of the Peltetec fault under the northern cordillera is uncertain. There is a weak lineament on imagery as far as Ambuquí, where rocks attributed to the Peltetec ophiolite trend north-south whilst the main cordillera trends NE-SW.

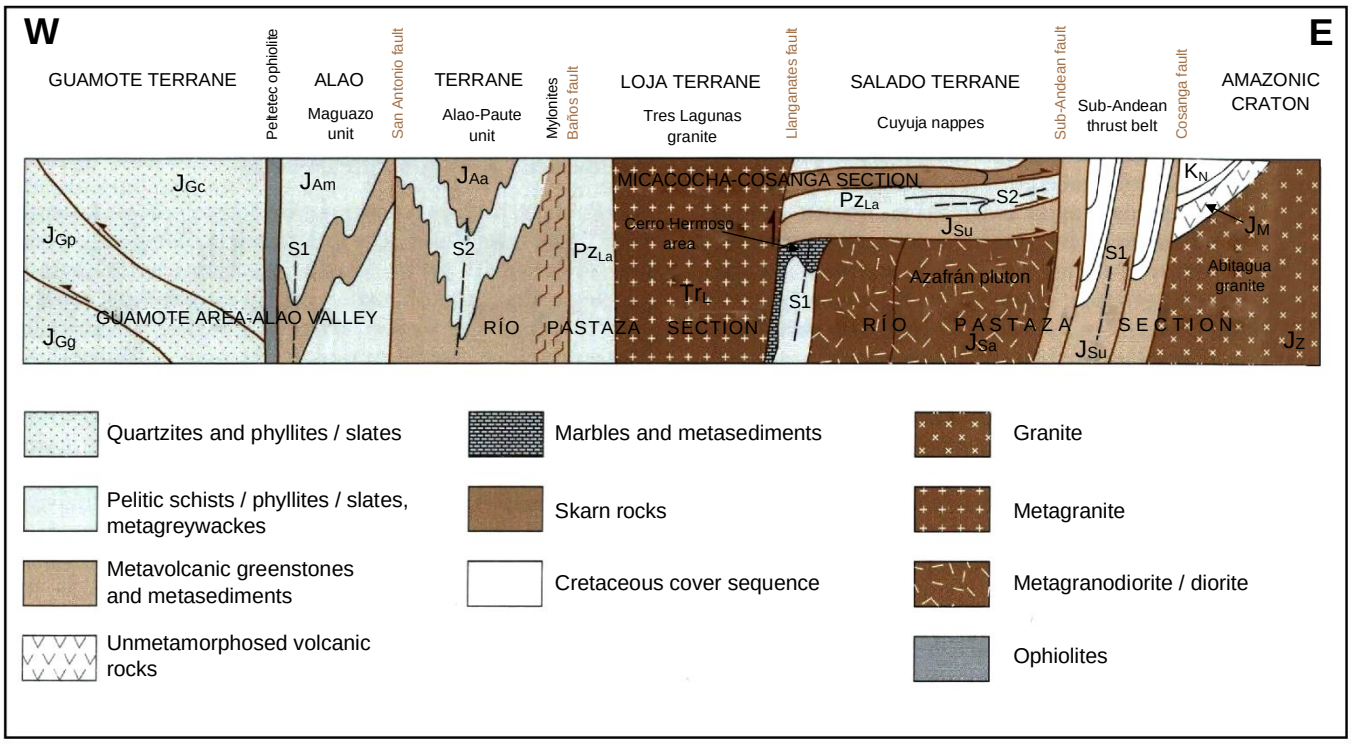

Figure 18. Schematic E-W section across the northern Cordillera Real metamorphic complex, based on the sections indicated. Stratigraphic symbols are taken from the accompanying map.

Alao terrane

The **Maguazo unit** of the type area contains very low-grade, fine-grained turbidites with sedimentary structures which can be used to determine the local 'way-up' of the sequence. Observations around Maguazo bridge (Figure 16) indicate the presence of a first-phase (D1) syncline (first recognised by B. Martin of RTZ Ltd) of probable isoclinal style with a steep axial-planar cleavage (S1) plunging gently to the south. 120km further south along the Río Paute, where the Maguazo unit yielded Jurassic microfossils, there is a similar first-phase syncline at Quebrada Totora Yacu. Detailed studies are required over the intervening ground to establish whether the syncline is continuous along the unit.

The **Alao-Paute unit** is separated from the Maguazo unit by the San Antonio fault. In the Alao valley the change is marked tectonically by the appearance of a penetrative, generally steeply dipping S2 schistosity in the Alao-Paute rocks (Figure 18), coupled with a higher metamorphic grade within the quartz-albite-epidote-chlorite subfacies of the Barrovian greenschist facies. The line of the fault is also marked by a Cenozoic felsite dyke. Eastwards, towards the Baños fault, almandine garnet and hornblende are developed within the greenschist facies. Further north along the north side of the Pastaza valley, sections show that this steeply dipping S2 cleavage or schistosity is axial-planar-to-tight D2 folds of bedding/S1 with axes plunging south-west at moderate to steep angles, and verging east. The pre-D2 disposition of bedding/S1 would seem to be subhorizontal over this sector, indicating an earlier D1 nappe phase (Figure 18).

In the south over the Río Paute type area the Alao-Paute unit is of a lower grade quartz-albite-muscovite-chlorite subfacies. Further east, almandine garnet is present in the El Pan schists (Trouw, 1976) indicating an increase in grade. A single steeply dipping cleavage is present in the massive greenstones in the west, but further east, in the El Pan schists, the steep tectonic fabric is S2 in age. Major shear zones are also present over this area; at Laguna Negra on the Atillo-Macas traverse, there are dextral movement indicators and mineral lineations plunging gently to the north.

Baños fault or shear zone

The Baños fault, previously called the Baños front in Project reports, separates the Alao and Loja terranes. It is manifested in the field as a major shear zone trending NNE-SSW within the metamorphic rocks, but, unlike the Peltetec fault, it is difficult to trace under the Cenozoic cover due to the apparent absence of neotectonic movement and resultant lack of expression on imagery.

The structure was first noted near Baños in the form of a hiatus marking both a change in lithology and increase in metamorphic grade eastwards from the present Alao terrane to the Loja terrane. Further studies showed a 2km wide shear zone west of the main lithological change near Baños Zoo. Within this zone, good exposures on the northern side of the Río Pastaza at the town of Baños show strongly sheared and lenticulated Alao-Paute greenstones and sediments. Minor drag folds exhibit an overall dextral sense of movement with their fold axes and associated mineral lineation plunging north or south at shallow to moderate angles.

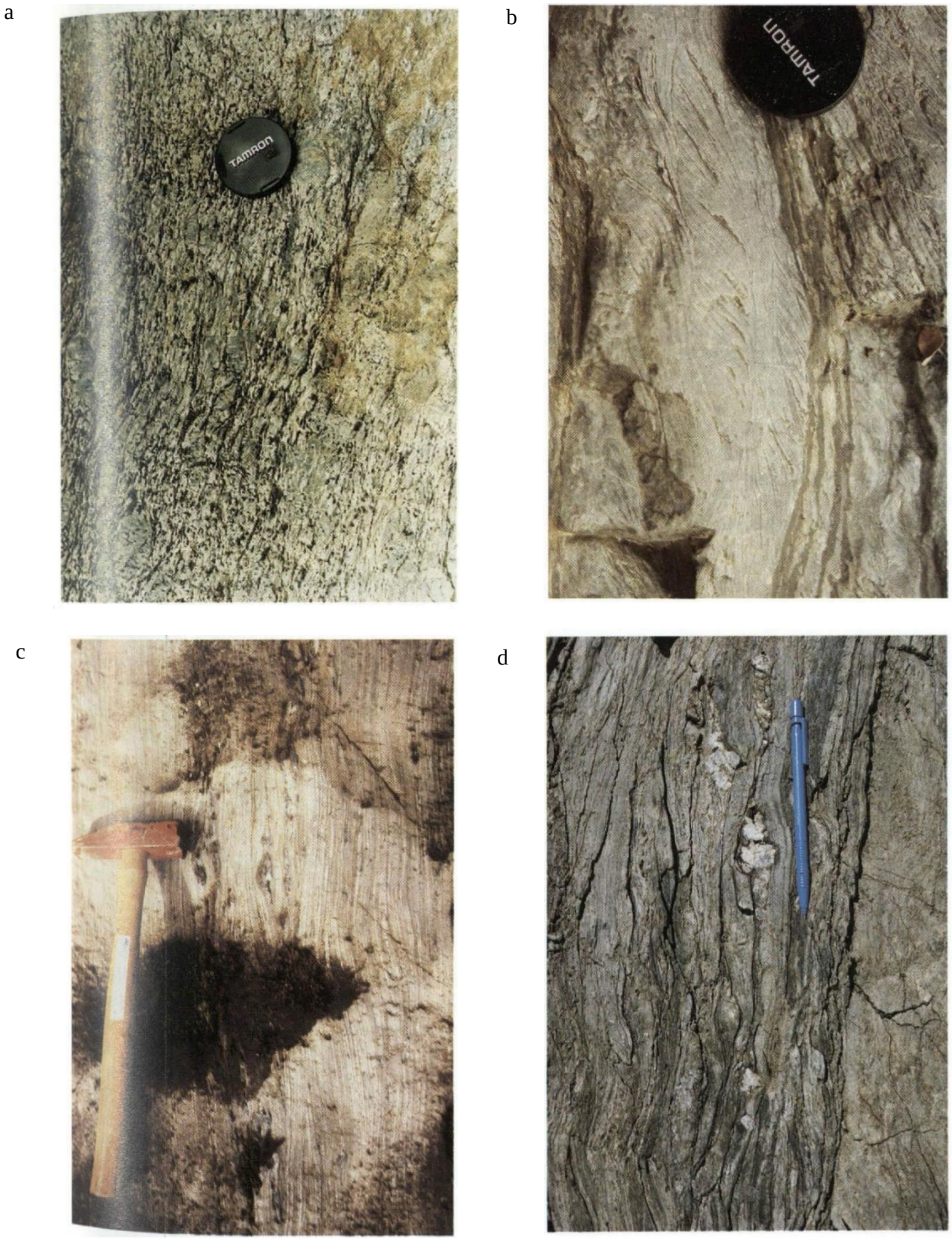

Plate 14. Baños fault or shear zone.

(a) Horizontal surface near Peggy mine showing mylonitic, K-feldspar augen gneiss of the Tres Lagunas granite (photo: J. A. A.)

(b) Dextral S-C mylonites on a horizontal surface of Alao-Paute greenstones in the Quilanga inlier (photo J. A. A.).

(c) Schistose, mylonitic Tres Lagunas granite in Río de la Burra Playa near Principal (photo: R. A. J.).

(d) Mylonitic Alao-Paute greenstones in vertical surface along the road south of Sigsig to Peggy mine (photo: J. A. A.)

Sections across the Baños fault further south show a similar tectonic pattern. Across the high watershed between the Alao and Palora rivers, the sheared metavolcanic rocks show mineral lineations plunging generally north at shallow angles. However, these lineations are steep within the 2km-wide belt of mylonitic Alao-Paute rocks along the road south of Sigsig (Plate 14d). This would indicate eastward thrusting in these west-dipping rocks. It is in this southern outcrop sector of the fault, where tectonic mixing of Loja terrane rocks, indicated on the accompanying map, can be attributed to duplex structures, although mylonites within the lenses of Tres Lagunas granites (Plate 14a and c) may relate to the older Tres Lagunas event.

In the extreme south, the Baños fault is interpreted to join the Las Aradas fault near Quilanga, where there is a small inlier of highly sheared and mylonitic greenstones (Plate 14b) with mineral lineations plunging north-east at moderate angles. This is interpreted as the southern-most extension of the Alao terrane under the Cenozoic cover. Between Sigsig and Saraguro, where the fault is largely buried by Cenozoic volcanic rocks, there is a major deflection in the interpreted course which may be axial to the Miocene Nabón basin, the outcrop trend of which is NE-SW.

To the north, the Baños fault is tentatively projected under the Cenozoic cover rocks so as to divide the Ambuquí and Monte Olivo basement areas which trend in different directions and which may represent the point of convergence of the central and eastern cordilleras of Colombia.

Salado terrane

The **Llanganates fault** forms the boundary between the Loja and Salado terranes. At the Río Cosanga sector (Figure 19) and further south, the Loja terrane is thrust eastwards over the Salado along this west-dipping fault. On the Cosanga traverse the Tres Lagunas granite is mylonitic close to the fault (Figure 19), but it is not established whether these structures belong to the Tres Lagunas or Peltetec event, or both.

The **Cerro Hermoso unit** of the type area lends itself to more detailed structural analysis due to abundant outcrop and a sequence with preserved sedimentary way-up indicators. The structure is dominated by upward-facing, first-phase folds with subhorizontal axes and a steeply dipping axial-planar cleavage, accompanied by limb faults (Figure 11). No evidence was seen for the early nappe structures suggested by Sauer (1958) and Vera and Vivanco (1983). Metamorphism is low grade, but contact metamorphism garnet, cordierite, sillimanite and andalusite were noted and attributed to effects of the adjacent Azafrán igneous phase, which is also deformed (Litherland et al., 1991).

The **Upano unit** of the type area of the Atillo-Macas traverse exhibits low-grade metamorphic rocks with a penetrative, steep, west-dipping S2 schistosity, subparallel to S1, which, on the short limbs of steep D3 monoclines, forms flat belts plicated by a steep S3 crenulation. There are suggestions of lithologic repetition in this volcanosedimentary sequence, particularly of a massive volcanoclastic greywacke unit. Such repetition would probably relate to D1/D2 thrust imbrication.

The **Azafrán unit** of Jurassic plutons exhibits sheared and less-sheared portions accompanied by mylonitic and gneissose textures, flattening of xenoliths, and progressive metamorphic recrystallisation to produce biotite and/or hornblende gneisses. Such features are common to both the Azafrán and Chingual batholiths. Along the road near Azafrán, gently plunging to subhorizontal mineral lineations have been observed which accompany S-C mylonites with a dextral sense of movement associated with steep Andean-trending shear zones. This shearing event probable corresponds to the younger, about 120 Ma, K-Ar ages from this sector (p.32). Along the Río Mulatos section of the Azafrán pluton there are abrupt changes from highly strained rocks to those which have essentially escaped deformation; small, late, epidotised feldspathic veins cut all the rocks along conjugate dextral and sinistral shears. In the Chingual pluton, along the Río Cofanes, mylonitic granodiorites exhibit a steep mineral lineation, but subhorizontal fold axes.

Cuyuja nappes

A flat schistosity was first noted by Trouw (1976) in the Cuyuja sector of the Papallacta-Baeza road section. Project studies have shown this to be related to a regional nappe complex in the north of the Cordillera Real (Litherland et al., 1992c).

The nappe complex extends for about 80km along strike and 15km across the strike of a cordillera which elsewhere shows steeply dipping metamorphic rocks. Although Cuyuja is the most accessible section, the Micacocha-Cosanga traverse (Figure 19) was geologically more rewarding, yielding a complex tectonic stratigraphy of tectonically juxtaposed lithologies from the base of the Río Cosanga at 2000m above msl to the cordilleran watershed at 4000m. These lithologies include a thick nappe sheet of semipelitic rocks similar to the Palaeozoic Chigüinda unit, Triassic granites of the Tres Lagunas unit, and Jurassic metasedimentary, metavolcanic and metaplutonic rocks belonging to the Upano and Azafrán units. Within the nappe pile there are also thin slices of serpentinite and skarn rocks which form isolated klippen along the watershed (Litherland et al., 1992a). The metamorphism in the schists falls into the quartz-albite-epidote-almandine and quartz-albite-epidote-biotite subfacies of the Barrovian greenschist facies (Trouw, 1976); kyanite was noted associated with quartz veins; garnet and chloritoid are more common.

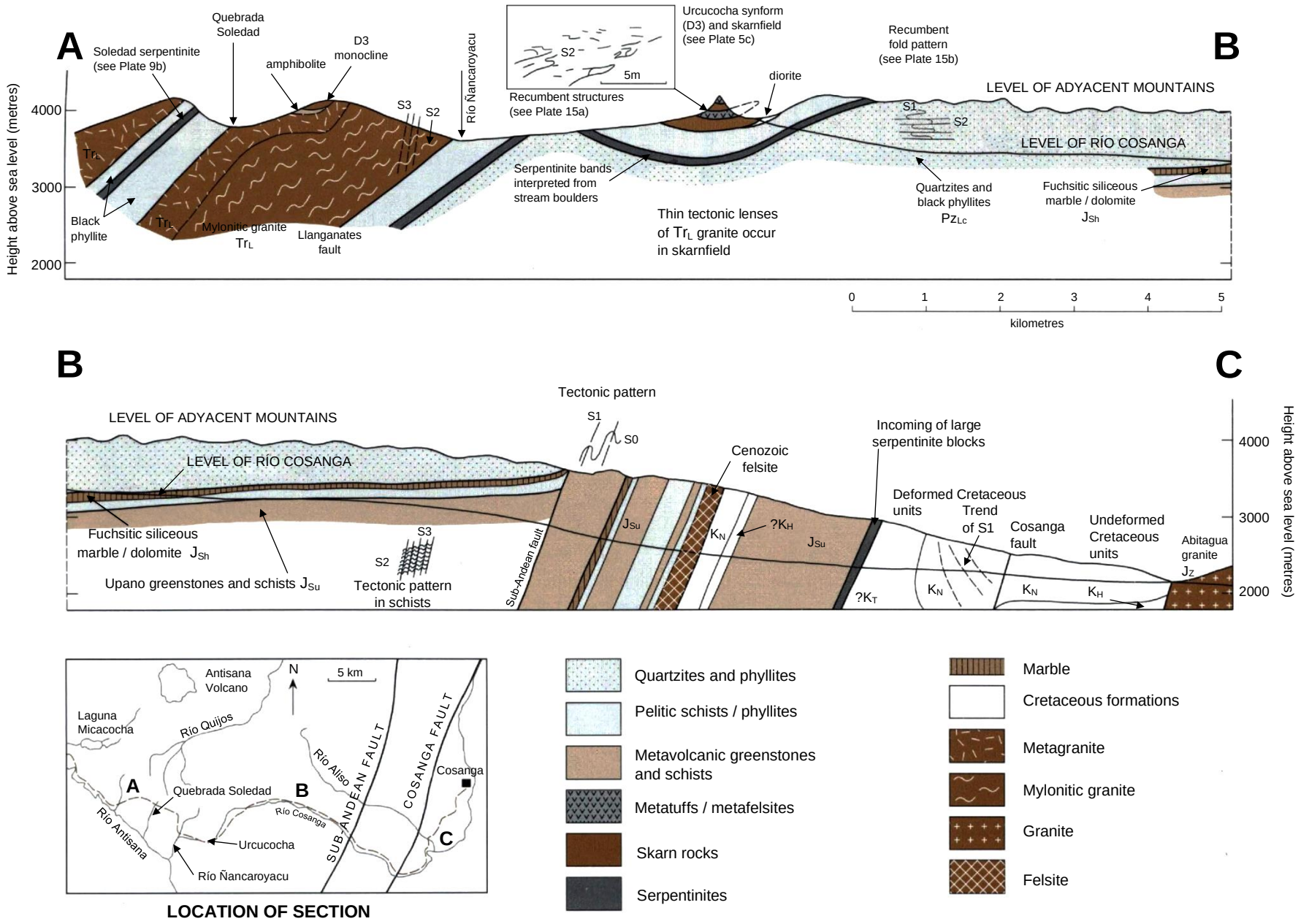

Figure 19. Geological section across the Cuyuja nappe complex from Micacocha to Cosanga, after Litherland et al. (1992c). Stratigraphic symbols are taken from the accompanying map.

The pile of nappes or thrust sheets is over 2km thick along the Río Cosanga traverse and no base is visible. Further south, however, in the area of the Río Mulatos, there is a transition from steep foliation in the river gorge (2000m above msl) to flat foliations in the El Placer skarnfield, about 1000m above the river at 3000m (Figure 13). Unfortunately, the region is heavily wooded and poorly exposed, but moderate westward foliation dips were noted at 2500m above msl suggesting that the steep schistosity curves into a roof thrust which coincides approximately with the base of the skarns. It is assumed that this roof thrust has been completely eroded further south over the steeply dipping Cerro Hermoso (Figure 11) and Río Pastaza sectors, with the possible exception of the skarn klippe at Río Verde and the marble klippe reported by Merlyn and Cruz (1986). In this respect it is important to realise that the flat nappes of Figure 19 lie along strike from the upright folds of Figure 11, and at the same altitude. The Cuyuja nappes must therefore represent tectonically high-level rocks preserved in a regional plunge depression, with the inference that such nappes have been eroded from the remainder of the cordillera.

In the schistose rocks of the Cuyuja nappes the subhorizontal schistosity is S2 in age (Figure 19) and affects a composite S0/S1 layering. There appears to be no difference in tectonic history between the rocks assigned to Jurassic units and the semipelites assigned to the Palaeozoic Chigüinda unit (Plate 15a) which should contain an earlier Tres Lagunas imprint. S2 is parallel to shear zones (Plate 19b) or a crude fracture cleavage in the massive skarns, and to the faults which divide the lithological units of the tectonic stratigraphy. These faults are postulated from the juxtaposition of lithologies of differing geological environments rather than by field observation of tectonic evidence. The metatuffs between the two skarn formations on Figure 19 exhibit 'M'-shaped fold structures (Plate 15a) consistent with a major D2 fold closure, with the skarns representing both the upright and overturned limbs.

D2 minor folds and mineral lineations both show shallow Andean-trending plunges within the S2 surface. The minor folds may exhibit both 'Z'- and 'S'-shaped structures on the same rock face (Plate 15b), and the key to the overall sense of tectonic transport lies in the morphology of Figure 19 where dips are either flat or to the west indicating movement from west to east. The same can be said for the metamorphic rocks of the cordillera as a whole.

A later Andean-trending compressional event is conspicuous over the Cuyuja nappes in the form of open folds with a steep axial-planar crenulation cleavage. One such fold is the Urcucocha synform which appears to control the disposition of the skarn klippen (Figure 19). Over the remainder of the cordillera this event is difficult to identify within the already steeply dipping rocks.

UPPER CRETACEOUS AND CENOZOIC EVENTS

It is premature to construct an ordered tectonic sequence over the Cordillera Real for this period. Many structures noted in the field are difficult to date, and there is a spread of K-Ar reset dates (Figure 20), many of which relate to partial resetting. This section merely notes some of the pertinent observations over certain sectors.

Sub-Andean thrust belt and associated structures

Field evidence around Cosanga (Figure 19) indicates two important regional faults. The Sub-Andean fault marks the eastern limit of the Cuyuja nappe complex of Peltetec age, and the Cosanga fault, the eastern limit of Andean tectonometamorphism. In between these faults, and traceable along much of the cordillera, is the Sub-Andean thrust belt, approximately 5-15km wide, which approximately corresponds to the Topo-Quijos depression of Sauer (1965), and the 'semimetamorphic' belt of the Margajitas Formation (Tschopp, 1953). Apart from the volcanosedimentary schists, now attributed to the Upano unit of Jurassic age, the Sub-Andean belt also contains rocks of the Cretaceous Hollín, Napo and Tena Formations, folded, faulted and cleaved.

The outcrop patterns along the belt indicate folding and imbricate thrusting of the Cretaceous and Upano rocks in an eastwards direction along steep limb faults. Younger, Tertiary formations of the Oriente basin were almost certainly involved, but these do not crop out over the belt, probably due to the level of erosion. Roofs to the thrusts producing duplex structures were noted in the Río Oyacachi (oral communication, P. J. Townsend).

North of the Río Oyacachi area, the belt is probably bounded westwards by the La Sofía fault. South of the Río Pastaza, over a little-studied area, the belt appears to be duplicated by the incoming of a thrust system nucleating on the eastern margin of the Abitagua granite massif, the Río Gringo thrust system (oral communication, P. Townsend). Further south over the Zamora batholith the thrust belt widens into a series of major north-south trending, ?sinistral faults which divide the essentially undeformed pluton into three tectonic segments. One of these, the La Canela fault, is associated with outcrops of cleaved Cretaceous Napo Formation along the Río Vergel, but away from the faults the Cretaceous cover sequences are little disturbed.

a

b

Plate 15. Cuyuja nappe complex.

(a) Recumbent D2 folds in siliceous metatuffs close to the summit of Urcucocha (Figure 19) (photo: M. L.).

(b) Manuel Celleri poses beside recumbent ‘M-shaped’ folds in semipelitic rocks attributed to the Chigüinda unit. This style is typical of the flat tectonic belt of the upper Río Cosanga (Figure 19) (photo: M. L.)

A generally steep, west dipping, Andean-trending, penetrative slaty cleavage is present in the pelitic fractions of the Napo and Tena Formations, associated with shallow-plunging minor folds. This cleavage may be locally folded by east-verging monoclines with the flat limbs cut by a second steep crenulation cleavage. An originally flattish first cleavage is prominent in the black slates around the bridge over the Río Abanico on the Macas road. East-dipping cleavages in the Río Cosanga (Figure 19) may relate to pop-up structures in the thrust system.

In places within the Sub-Andean belt, the tectonometamorphic history of the underlying Upano unit rocks appears to conform to that of the overlying Cretaceous units rather than of the equivalent rocks west of the Sub-Andean fault. Outcrops of Upano greenstones and greenschists around Baeza, Río Cosanga (Figure 19) and Río Negro de Pastaza exhibit a single steep penetrative cleavage with or without a later crenulation cleavage. This is accompanied by a lower metamorphic grade, of quartz-albite-muscovite-chlorite subfacies, than that found in the Cuyuja nappes. Unfortunately, no outcrop was found exposing the contact between the Upano and Cretaceous rocks in order to test this cleavage correlation. However, outcrops in the Río Salado involving massive Misahuallí volcanics as basement to the Cretaceous formations rather than the Upano unit indicate a common structural history confirming the observations of Pasquarè et al. (1990). It is possible that the steep cleavage in the thrust belt can be correlated on Figure 19 with the steep S3 crenulation cleavage which affects the Cuyuja nappes to the west and is related to the Urcucocha synform. Such a correlation would provide a mappable Cenozoic tectonic imprint over the main metamorphic complex.

However, west of Sucúa, along the Río Tutanangoza, imbricates of the essentially unmetamorphosed Hollín, Napo and Tena Formations involve basement mylonitic greenschists of the Upano unit which were clearly deformed in the Peltetec event.

These points indicate that the Sub-Andean thrust belt is a Cenozoic tectonometamorphic event with no older imprint in the basement rocks visible north of Sucúa, thus making the Sub-Andean fault the eastern limit of the Peltetec event over this area. A Neogene age for the thrusting has been proposed (Kennerley, 1980; Baldock, 1982) synchronous with the formation of structures of less intensity such as the Napo and Cutucú uplifts which occur east of the Cosanga fault.

Such an age of movement could account for the K-Ar resetting in the Chingual and Zamora batholiths (Figure 20). Detailed studies by Pasquarè et al. (1990) in the Reventador area have revealed a three-stage tectonic evolution: thrusting to the east-south-east was followed by oblique reactivation of early thrusts with directions of motion towards the east or east-north-east. The third phase involved right-lateral strike-slip faulting with directions subparallel to the old overthrust fronts. Soulas et al. (1991) indicate that the Sub-Andean thrusts are still active with dextral strike-slip faulting, as manifested by the La Sofía fault. Indeed, Tibaldi and Ferrari (1992) show this fault (their Cayambe-Chingual fault) to displace Late Pleistocene or Holocene lava flows from the Soche volcano near La Bonita. The 5 March 1987 earthquake, with an epicentre west of Reventador, was probably caused by the reactivation of the Cosanga fault.

The Sub-Andean thrust belt of Ecuador is thus typical of the Perú-Bolivia Andes where, since late-Oligocene times, most of the Andean shortening has been accommodated by underthrusting of the Amazonic craton beneath the Cordillera Real along a Sub-Andean foreland thrust belt (Soler and Sebrier, 1990).

Peltetec fault and associated structures

Around its type area the Peltetec fault is manifested on imagery as a neotectonic lineament, the Chambo lineament of Litherland and Aspden (1992), along which the Jurassic ophiolites are faulted against Neogene volcanic rocks. This lineament can be traced southwards to the Huarapungu fault of Bristow et al. (1975), axial to the Cretaceous Yunguilla basin, and thence through the Cuenca basin into the Girón fault, finally turning south to form the Las Aradas fault. This new route linking the Girón and Las Aradas faults is based on project field studies around Santa Isabel. Previously the Girón fault had been linked to the east-west-trending Jubones fault (Baldock, 1982).

Along this course the fault affects rocks of different ages. In the Río Huarapungu, the Upper Cretaceous Yunguilla Formation exhibits steep dips along the fault, with small west-dipping low-angled thrusts. Further south, the fault is axial to the Cuenca basin, a Miocene pull-apart structure (Noblet and Marocco, 1989), and the Girón basin, where the Girón fault exhibits neotectonic activity (Winter et al., 1990). In the south, the Las Aradas fault divides metamorphic basement from Cenozoic volcanic and sedimentary rocks of different ages. All these points indicate the Peltetec fault to have controlled the formation of local pull-apart basins since Cretaceous times and to have had a long history of movement during the Cenozoic.

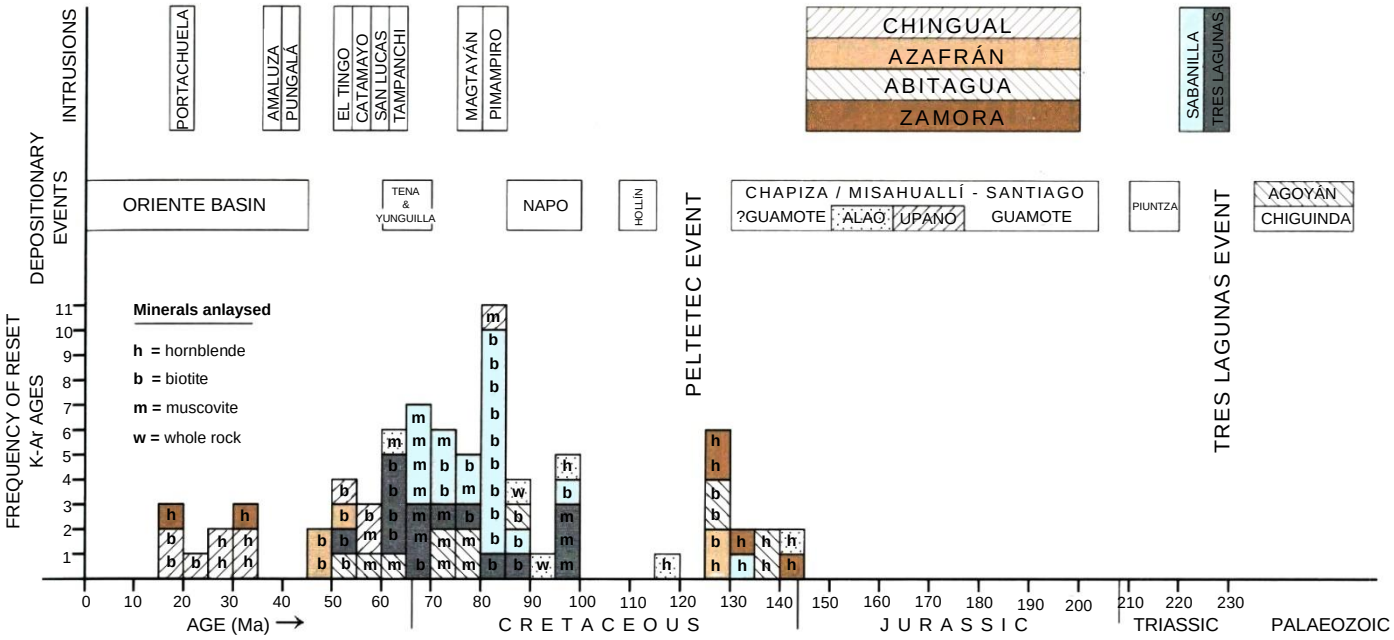

Figure 20. Reset K-Ar ages and geological events over the Cordillera Real. Ornament identifies both the primary age (right hand side) and reset ages (left hand side) for certain units.

West of the Peltetec fault, near Guasuntos, Oligocene volcanic rocks are thrust over the basement Guamote terrane slates along low-angle reverse faults dipping north-west which do not affect the overlying Miocene volcanics. This event is probably manifested as east-north-east-trending D3 open folds over the flat Guamote metamorphic rocks.

East of the Peltetec fault, the San Antonio fault exhibits Cenozoic activity: it acted as a conduit for a felsite dyke which follows the fault across the Alao valley (Figure 16). Further south Cenozoic tectonic activity is indicated along basement faults through Pilzhum and San Bartolomé, and as steep shear zones within the Early Tertiary Tampanchi mafic-ultramafic complex.

The Baños fault is regarded as a conduit for Cenozoic mineralisation (p.106) especially close to the major deflection between Sigsig and Saraguro which may have been periodically a tensional regime. The same fault may also have controlled the Nabón pull-apart basin of Miocene age.

The Cenozoic evolution of the faults controlling the inter-Andean valley probably relates to both normal and wrench faulting (Tibaldi and Ferrari, 1992). The present studies indicate that many of the neotectonically active faults of the Cordillera Real result from reactivation of older structures in the basement defined here. Litherland and Aspden (1992) have suggested that the reactivation of these old terrane boundaries, or sutures, may locally control Andean magmatism and morphology and thus be responsible for the double cordillera of the Ecuadorian Andes.

Tectonics and K-Ar resetting

Feininger's (1975) proposal that the metamorphic rocks of the Cordillera Real were Cretaceous in age and metamorphosed in the Early Tertiary was supported by Palaeocene K-Ar ages from micas of thoroughly recrystallised schists (Feininger, 1982).

Many more ages from a 50-90 Ma span have been determined by the Project from a variety of metamorphic rocks (pp. 119-120), many of which can be demonstrated to be pre-Cretaceous in age. Indeed, almost all the samples from the Tres Lagunas, Sabanilla, Agoyán and Upano units of the cordillera show these young K-Ar ages (Figure 20), whilst almost all those from the Zamora and Abitagua plutons lying east of the Cosanga fault, i.e. in the Amazonic craton, preserve their primary ages.

Cretaceous and Lower Cenozoic K-Ar dates of essentially undeformed plutons are taken as cooling ages. The Tampanchi complex, approximately 62 Ma, is locally sheared, indicating Cenozoic movement of adjacent faults, but the lack of regional penetrative tectonic fabrics in these plutons also argues against Feininger's (1975) proposal for a Lower Cenozoic regional tectonometamorphic peak. These metamorphic mineral dates are thus regarded as due to K-Ar resetting and do not represent the ages of the individual micas concerned.

Given that there was no tectonometamorphic peak to account for the reset ages, it is also unlikely that the contemporaneous plutonic phases of Pimampiro, Magtayán, Tampanchi and San Lucas (Figure 20) caused such a regional muscovite and biotite resetting. It is thus noteworthy that the resetting age corresponds to the depositional break between the Napo and Tena Formations (Figure 20), believed to represent the uplift of the Cordillera Real since the Tena redbeds are derived from the west (Baldock, 1982). Thus, the resetting may have been caused by shearing and heating related to this uplift perhaps resulting from the accretion of the Piñón terrane in the west. Alternatively, the Peltetec event could be extended, or moved, to the Upper Cretaceous, pre-Yunguilla and pre-Tena in age. What is clear is that more work is required to elucidate the details of the geological history of this period.

SEVEN

Geology of the El Oro metamorphic belt

The El Oro metamorphic belt (Figure 21) is a large inlier of metamorphic rocks located in south-west Ecuador cropping out principally in the El Oro Province. The rocks were first described by Sauer (1965) and later mapped in the east by Kennerley (1973) and in the west by Feininger (1978).

Both Sauer (1965) and Gansser (1973) pointed out the east-west strike of the El Oro metamorphic rocks, which is completely discordant with the trend of the Andes. Feininger (1978) showed them as a sandwich of schists and granites enclosing the serpentinites, blueschists and eclogites of the Raspas sector; all unconformably overlain by the Cretaceous Alamor Group.

PALAEOZOIC AND TRIASSIC ROCKS

The Palaeozoic rocks of the El Oro belt are considered (Aspden et al., 1993; Aspden, in press) to be confined to the Tahuín semipelitic division, south of the Portovelo fault, cropping out along the Cordillera de Tahuín. They form an east-west trending, 10-20 km-wide belt which can be traced continuously from the Peruvian border in the west to El Cisne in the east. The rocks have been divided on metamorphic grade into the El Tigre unit in the south and the higher-grade La Victoria unit in the north. Triassic rocks are represented by the Moromoro granites, found north and south of the Portovelo fault, and the Piedras amphibolites.

El Tigre unit (Palaeozoic)

This unit, named after the small settlement in the west of the belt, corresponds, approximately to the Capiro Formation of Kennerley (1973) and Baldock (1982). The rocks are semipelitic and low-grade, typically deeply weathered away from river sections. However, relatively fresh, semicontinuous outcrops do occur along the Arenillas-Alamor road between El Tigre and Río Puyango and also along the Portovelo-Loja road to the south of El Prado.

In the south the unit is overlain unconformably by the Cretaceous sediments of the Alamor basin (Baldock, 1982; Feininger, 1978) and this contact is particularly well exposed to the north of Río Puyango along the Arenillas-Alamor road (**6665-95737**). Further east, near El Cisne (Figure 21), the contact has been affected by a series of NNE-SSW-trending faults belonging to the Guayabal fault zone and original relationships are more difficult to establish. To the north, the contact is transitional with the higher-grade La Victoria unit, details of which are discussed below.

The age of the El Tigre unit is not well established but it is intruded and metamorphosed by the Late Triassic (228 Ma) Marcabelí pluton and is considered to be Palaeozoic. A single sample collected to the south of La Libertad (Figure 21) yielded the remains of acritarchs and spores which were assigned a pre-Devonian age (Zamora and Pothe de Baldis, 1988). Further to the south-west, along the Río Cazaderos, outside the area of the accompanying map, a sample examined by Dr. John Williams of British Petroleum Ltd. contained a 'single possible example of *Emphanisporites* and some unidentified, strongly carbonised single spore types which are either laevigate or with a low ornament of cones, spines or baculae. Though no taxa could be positively identified, this is the type of assemblage one could expect to encounter in the Early or Middle Devonian' (written communication, J. E. Whittaker). Whilst the precise relationship between this sample and the El Tigre unit is uncertain, its structural position immediately below the Cretaceous Cazaderos Formation, which forms part of the Alamor Basin sequence, suggests a correlation with the El Tigre unit. An extensive collection of material (about 40 samples) from the El Tigre unit was made during the present study but none contained datable organic remains (Owens, 1992). However, Devonian and Carboniferous fossils are found at Cerro Amotape, in northern Perú, the physical extension of Cordillera Tahuín, which is comprised of similar semipelitic rocks (Martínez, 1970; Mourier, 1988).

The El Tigre unit consists of an unmetamorphosed to weakly metamorphosed sequence of poorly sorted, immature, fine- to medium-grained, quartz-rich arkoses, feldspathic wackes and quartzites, together with interbedded lutites and siltstones. In addition to quartz and feldspar, these rocks also contain minor amounts of detrital biotite, muscovite and tourmaline. Intraformational lutite clasts, which vary from sub-millimetre to several tens of centimetres are common, especially in the coarser arenaceous beds. Sedimentary structures include graded beds, some of which have erosional bases with sole structures, flute casts, cross-laminated and parallel-laminated beds, flame structures and slump folds (Plate 16a).

Bedding dips within the east-west-trending El Tigre unit are variable but normally moderate-to-steep and generally to the north. Cleavage is developed only along faulted shale/lutite horizons, and elsewhere structures tend to be of more brittle nature.

The sedimentary structures preserved within the El Tigre unit suggest that these rocks are essentially turbiditic in origin. The absence of volcanic debris within the unit could indicate derivation from a 'passive' continental margin or cratonic source.

Figure 21. Location map for the El Oro metamorphic complex showing many of the local names referred to in the text.

La Victoria unit (Palaeozoic)

Named after the village in the west of its outcrop (Fig. 21), this unit of steeply dipping schists and gneisses corresponds roughly to the San Roque Formation (Baldock, 1982) without the orthogneiss phase; it crops out immediately to the north of the El Tigre unit. The outcrops are weathered in many places but reasonably fresh ones occur between Las Lajas and La Victoria and excellent, but semicontinuous, sections are to be found in Quebrada Primavera downstream of La Primavera, and in the Río Ingenio between Ingenio and Marcabelí. Further to the east, spectacular outcrops of the La Victoria unit occur in the Río Moromoro (Figure 21).

The contact between the La Victoria and El Tigre units is complex and in part probably gradational. It coincides with an east-west-trending tectonic zone which is marked by the incoming of a regional cleavage and/or the appearance of regional metamorphic biotite (see also Feininger, 1978). Where observed, the northern contact of the La Victoria unit with the Moromoro granites is also partly gradational but on a regional scale it corresponds with a zone of syn- to late-magmatic, dextral shearing which, especially in the east, has resulted in the complex interfingering of lithologies. Within this (Moromoro) granitoid complex the larger areas of metasediments have been assigned to the La Victoria unit.

The La Victoria unit has been affected by a single prograde temperature dominated, 'Abukuma-type' (Miyashiro, 1961), metamorphic event. In the south, near the El Tigre contact, biotite-bearing phyllites and slates are dominant but further north the phyllites may contain small porphyroblasts of sericite (?after cordierite/andalusite). Moving further north there are schists containing cordierite and/or andalusite, biotite (± muscovite), albite and quartz. Towards the contact with the Moromoro granitoid complex, fibrolite and/or sillimanite, quartz, plagioclase, muscovite, ± biotite, ± andalusite, ± cordierite, ± garnet assemblages correspond with the appearance of gneissic/migmatitic lithologies (Plate 16b).

The La Victoria unit is considered to represent the metamorphosed equivalent of the El Tigre unit. The metamorphism of these rocks took place during the Late Triassic Moromoro event.

The structure of the La Victoria unit is similar to that of the El Tigre, but, as evidenced by the metamorphic mineral assemblages, these rocks were deformed at higher temperatures. Throughout the unit, cleavage and bedding, where still recognisable, are parallel and, with notable exceptions, they are generally steeply dipping towards the north.

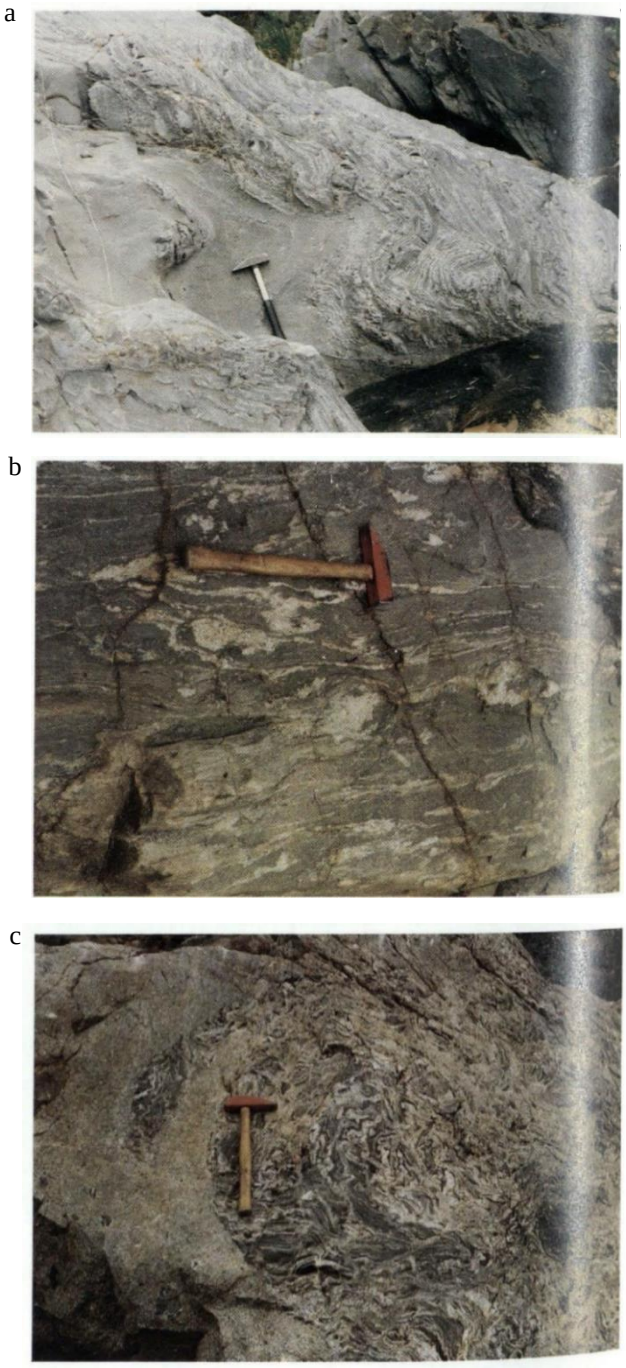

Plate 16. Progressive metamorphism in El Oro.
(a) Slump folds in slumped bed in El Tigre unit turbidites, Río Agua Negra (photo: J. A. A.).

(b) Horizontal surface of incipient migmatitic veins in La Victoria unit schists near Moromoro granite contact near San Isidro (photo: J. A. A.).

(c) High-grade La Victoria unit schists as palaeosome within Moromoro migmatitic granite near La Florida (photo: J. A. A.).

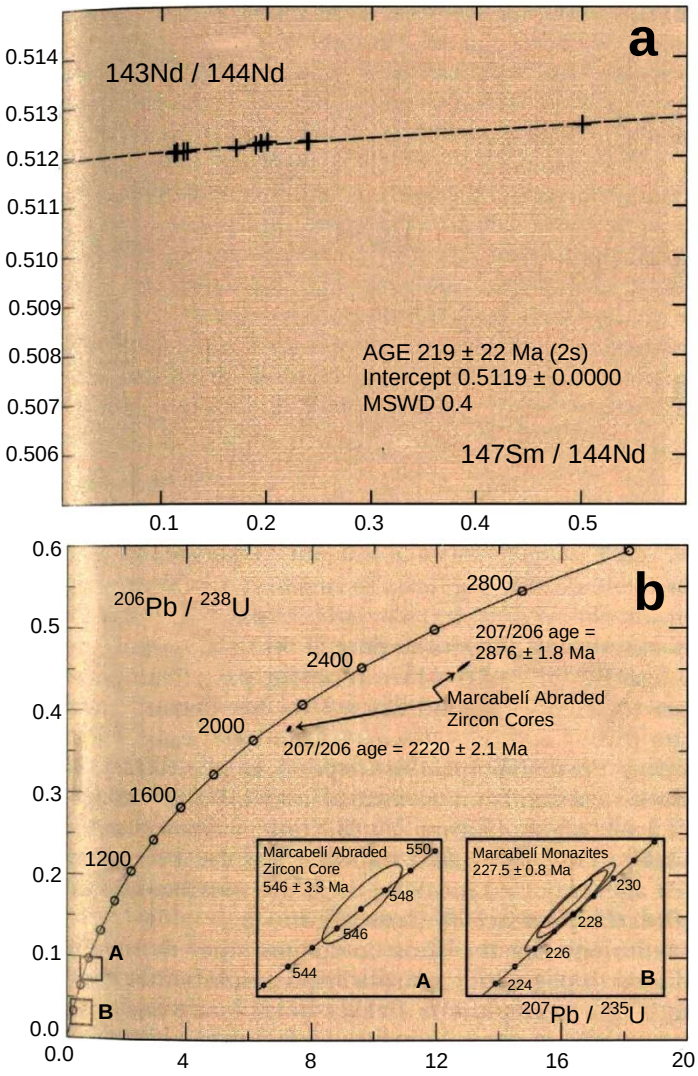

Figure 22 Geochronological plots for the Moromoro granites.

(a) Sm-Nd isochron diagram of garnet-bearing paragneissic palaeosome within the Moromoro granite; **(b)** U-Pb concordia diagram for the Marcabelí granite. The crystallisation age of 227.5 ± 0.8 Ma is given by the monazite analyses. Strongly abraided zircon cores indicate inheritance of Archaean and Proterozoic xenocrysts.

Moromoro granites (Triassic)

This complex, named after the small town of Moromoro (Figure 21) is mainly a widespread gneissic granite which can be traced from the Peruvian frontier in the west eastwards into the El Cisne area. The bulk of the Moromoro complex occurs south of the Portovelo fault; the remainder is found to the north at Limón Playa, Quera Chico and in the Manú inlier. Well-exposed sections occur in a number of north-south-trending rivers but the Quebradas Piedras and Primavera are most easily accessible. In the east, near El Cisne, the granite is truncated by the Guayabal fault zone and further west it is overlain and intruded by a volcanoplutonic complex of Tertiary age along the Portovelo fault zone. Its northern contact with the Piedras mafic complex is considered to be tectonic, but was possibly originally intrusive. The main southern contact with the La Victoria unit corresponds to a complicated zone of syn- to late-magmatic shearing which has resulted in the tectonic interfingering of the granite and metasediments.

The available K-Ar biotite and muscovite mineral ages from the granite are listed in Feininger and Silberman (1982) and on p.119. With the exception of a somewhat younger date of 189 ± 5 Ma, these ages range between 207 and 220 ± 6 Ma with a mean of 213 ± 6 Ma. In addition, a Sm/Nd whole-rock/garnet isochron age of 219 ± 2 Ma (Figure 22a) (p.120) has also been obtained from garnet-bearing paragneisses within the granite (Aspden et al., 1992c). Together these data suggest an Upper Triassic to Lower Jurassic age for the granite.

The Moromoro granites form a mixed unit that includes a number of different rock types and it is probable that with more detailed work it will be further subdivided. It consists principally of variably foliated, fine- to medium-grained, biotite, ± muscovite, ± garnet granodiorites, together with lesser amounts of migmatites and high-grade paragneisses. Texturally these granodiorites are generally heterogenous due to the presence of numerous, predominantly metasedimentary xenoliths including quartzite, pelitic schist, paragneiss and migmatite (Plate 16c). Biotite schlieren and irregular clasts of white vein quartz are common. Contact relationships between the different xenoliths and the granodiorite host vary from sharp and well-defined to extremely diffuse and ghost-like. Mineral assemblages within the metasedimentary 'restite' xenoliths are variable but include coarse sillimanite, muscovite, biotite, ± andalusite, ± cordierite and in some areas, e.g., near Santa Teresita, sillimanite ± K-feldspar + muscovite assemblages are present. Late pegmatitic dykes and apophyses composed of quartz, feldspar, ± tourmaline, ± biotite, ± muscovite are common.

The granite is variably foliated. In some areas, coarse but fairly penetrative foliations and/or discrete, ductile S-C (dextral) mylonite fabrics are preserved (Plate 17c). These zones are normally steep and trend east-west. Certain sectors, described below, are essentially unfoliated and undeformed.

The **La Florida unit** can be singled out following Feininger (1978). It consists of typically nonfoliated, medium- to coarse-grained, alkali feldspar megacrystic, biotite, ± garnet granodiorite. The pale-coloured alkali megacrysts vary in size and proportion but range up to 8cm in length and display Carlsbad twins. In marked contrast to the gneissic granites, the La Florida granodiorites are texturally homogenous with primary igneous textures. Xenoliths of quartzite, paragneiss and migmatite are common. In most cases their contacts are sharp but, in some places, they are rimmed by irregular, marginal zones of tourmaline-mica pegmatite. Dykes of leucocratic, two-mica aplite are also present.

The plutons which make up the La Florida unit occur as narrow, approximately east-trending, concordant bodies within the Moromoro gneissic granites. Contacts between these units have not been observed in the field, but irregular patches of La Florida-type granodiorites have been noted within the granites which may suggest a related origin and similar age for these granitoids.

The unfoliated **Marcabelí** and **El Prado plutons** can also be singled out from the Moromoro granites. These are the most southerly of the granites and straddle the contact between the El Tigre and La Victoria units.

The K-Ar mineral ages obtained from the Marcabelí pluton range from 193 ± 13 to 221 ± 6 Ma (p.119 and Feininger and Silberman, 1982) with a mean age of 209 Ma are in general agreement with those obtained from the Moromoro granites. Most recently, the Project has obtained a U/Pb (monazite) date of 227.5 ± 0.8 Ma for the Marcabelí pluton (written communication, S. Noble) (Figure 22b) which confirms a Late Triassic age. Old zircon cores in the samples gave inherited 207Pb/206Pb ages of 546 ± 3.3 Ma and 2876 ± 1.8 Ma, the latter indicating reworked Archaean material.

The Marcabelí and El Prado plutons are generally deeply weathered but they appear to consist mainly of medium-grained, biotite ± muscovite granodiorites. It is probable however, that both plutons are composite and include a variety of plutonic phases the nature of which, and their interrelationships, remain uncertain.

Both these plutons are relatively narrow, elongate east-west-trending bodies. Their southern contacts against the El Tigre sediments are marked by andalusite hornfels, but the northern contacts are sheared. They are essentially undeformed, but cut in places by discrete, generally steep, east-trending shear zones.

GEOCHEMISTRY

22 whole-rock analyses are available for the Moromoro granites which, together with the normative compositions and various geochemical parameters, are listed in Fortey and Gillespie (1993) and in Appendix 2.

Based on these analyses, the Marcabelí and El Prado plutons consist principally of granodiorites with lesser amounts of monzogranites, whereas the gneissic granites fall mainly within the monzogranite field but includes some quartz-rich granitoids and granodiorites (Figure 8a). Two of the geochemical plots used for the classification of granites and the distinction between those of S- and I-type character are the Al/(Na + K + Ca/2) v. SiO_2 and the K_2O v. Na_2O plots (Pitcher, 1983; Chappell and White, 1974) (Figures 8c and b). Together these plots suggest that the strongly peraluminous Moromoro granite is mainly S-type in character whereas the Marcabelí and El Prado plutons, which are geochemically similar to one another, appear to be of I-type character. However, the presence of inherited zircons at Marcabelí indicates at least some recycled material of crustal origin.

Piedras amphibolites (Triassic)

There are three east-trending, steeply dipping amphibolite belts within the El Oro metamorphic complex. The main **Piedras amphibolite,** named after a small village (Figure 21) forms a narrow, up to 3km wide, regionally persistent belt that can be traced almost continuously for approximately 60km from the Peruvian frontier into the Portovelo area. Where seen, its southern contact with the Moromoro migmatites is tectonic and its northern limit is defined by the Naranjo fault zone.

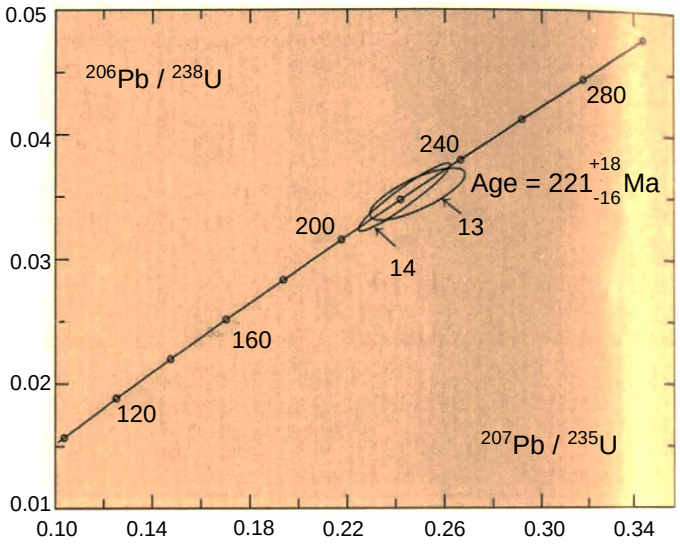

Figure 23 U-Pb zircon data for the Piedras amphibolite.

These amphibolites were considered to be of Precambrian age based on a single K-Ar amphibole (with very low potassium) determination of 743 ± 13 Ma reported by Kennerley (1980). More recently, project amphibole ages of 647 ± 37 Ma and 224 ± 3 Ma have been obtained from this unit from samples collected at the same locality near Portovelo (p.119) (Aspden et al., 1992c). The Triassic age has been confirmed by a U-Pb zircon age of 221^{+18}_{-16} Ma (Figure 23) (S. Noble, written communication). These new data indicate that the Precambrian K-Ar ages reported for these rocks are spurious and must reflect the presence of excess argon.

Lithologically the unit comprises fine- to medium-grained to pegmatitic, saussuritised amphibolites consisting of green amphibole (? relict hornblende and actinolite), plagioclase (oligoclase-andesine), epidote and minor amounts of quartz, opaques, ± sphene, ± rutile, ± clinozoisite. Mafic, hornblende-rich enclaves and, what is interpreted to represent relict igneous banding, have been observed in the Río Piedras section (**6204/95975**). Towards the Naranjo fault zone, the generally massive and weakly foliated lithologies, typical of the unit, become increasingly deformed and develop a marked, almost vertical, mineral lineation due to the growth of acicular actinolite, now largely epidotised. Elsewhere along this fault zone (e.g., **6266/95967** and **6350/95965**) more massive 'greenschists' (? retrograde amphibolites) composed of actinolite, epidote, quartz, albite, sphene, ± rutile are present. In hand specimen these rocks may resemble serpentinites due to the development of serpentine minerals on joint and fractures surfaces. In the extreme west, along the Peruvian frontier and immediately to the south of the Naranjo fault zone, a narrow, up to 100m wide, lens of serpentinite is exposed within the amphibolite. According to Feininger (1978), a similar lens is also present within the unit further to the east. The age and origin of these serpentinites is uncertain.

The **Arenillas and Taqui amphibolites** occur to the north of the Portovelo fault, forming narrow, east-west-trending, fault-bounded belts between Moromoro granitoid and younger Palenque schists. No age determinations are available for the Taqui unit but four K-Ar mineral ages ranging from 72 ± 15 Ma to 76 ± 7 Ma (p.119) exist for the Arenillas unit. These ages are considered to be reset (Aspden et al., 1992c).

The Arenillas and Taqui units consist of amphibolites which are composed essentially of hornblende and plagioclase but in thin section minor mineralogical differences are apparent. The Arenillas unit carries small amounts of clinopyroxene and the amphibole is a pleochroic brown hornblende. In contrast, clinopyroxene has not been recorded in the Taqui unit, and the amphibole, possibly in part actinolite, is pale green in colour.

GEOCHEMISTRY

Although alkali mobility may create interpretational ambiguities, the K_2O v. SiO_2 plot is a useful general classification diagram which indicates that, with the exception of the Taqui sample, the Piedras amphibolite consists of 'basalts' belonging to the low-K series (Figure 24a). In order to avoid the problem of alkali loss Winchester and Floyd (1977) suggested that altered and/or metamorphosed rocks could be classified using immobile trace-element ratios. Using the Zr/Ti v. Nb/Y plot, all the analysed samples fall within the basaltic andesite field (Figure 24b).

Geochemically the Piedras and Arenillas units appear to be virtually identical. However, on a number of plots the Taqui samples is 'anomalous' in that it is enriched in TiO_2, Sr, Zr and K_2O and possibly depleted in MgO (Aspden, in press).

In the 'spider-diagrams' (Pearce, 1983) for the Piedras, Arenillas and Taqui units (Figure 24c and d) the curves for each of the units, especially the Piedras and Arenillas, are similar and relatively flat. These shapes are typical of normal ocean ridge basalts and suggest only minor modification of original magmatic compositions. Using the discriminant plots of Pearce and Cann (1973) the majority of samples fall within the field of ocean floor basalts (Figure 14).

JURASSIC-LOWER CRETACEOUS ROCKS

With the exception of the granites and amphibolites, the metamorphic rocks north of the Portovelo fault are considered to be of Jurassic to Lower Cretaceous in age and can be subdivided, essentially, into the Palenque schist unit, containing the Palenque ophiolitic complex, and the El Oro ophiolitic complex.

Palenque unit (?Jurassic-?Lower Cretaceous)

This is the main schist division north of the Naranjo fault named after a small village (Figure 21). No single river/road section crosses the unit, but in the north, fresh and accessible exposures occur in the Río Huizho upstream of Huizho village. The schists form the bulk of the northern part of the El Oro metamorphic complex and are bounded by the Naranjo fault in the south and by the Jubones fault in the north. In the west they are buried beneath the largely unconsolidated Late Tertiary and Quaternary deposits of the coastal plain, and in the east intruded and, in part, overlain by a major Tertiary volcano-plutonic complex.

The Palenque unit consists of low- to medium-grade, dark-coloured, semipelitic, schistose phyllites and slates together with lesser amounts of quartz-sericite schists, feldspathic schists, metagreywackes, cherts, greenschists and rare amphibole (tremolite) schists. The schists, which are generally steeply-dipping, also include 'mixed' and/or 'broken', pseudoconglomeratic horizons in which lensoid clasts, up to 10cm across, of generally coarser-grained metasedimentary material, occur within a finer-grained matrix.

Mineralogically the rocks are composed of quartz, biotite, muscovite, chlorite, albite, ± graphite, ± actinolite, ± epidote, ± garnet. Late andalusite, ± cordierite, ± biotite are commonly developed as contact metamorphic minerals close to the Tertiary volcano-plutonic complex in the east.

Within the Palenque unit, the **Palenque ophiolitic complex** (Aspden et al., 1988) is represented by a number of serpentinite lenses which form small hills close to the village of Palenque. These units are composed mainly of serpentinite, but also include irregular bodies of silicified and/or black graphitic phyllites, minor cherty horizons and some metabasalts and greenschists. To the east of Aserrío black phyllites and a small inclusion of unknown dimensions composed of a heterogenous mylonitic granodiorite are associated with the serpentinite body that crops out in the Río Raspas, near its junction with the Río Colorado. Further to the west, the serpentinite which forms the small, isolated hill Ugarte contains gabbros and gabbroic pegmatites. Serpentinites are not present in the cuttings along the main highway which follows the Río Jubones, but there are some cherts and greenschists. Whole rock geochemical data plot in both the supra-subduction zone and MORB-type ophiolite fields on the Pearce et al. (1984b) diagram (Figure 17).

El Oro ophiolitic complex (Jurassic-Lower Cretaceous)

This unit has an east-west strike length of 45 km and a maximum width of about 6km. Its northern and southern limits are defined by major faults. The western part of the complex contains some of the best-known examples of high-pressure rocks in the Northern Andes and these have been previously mapped and described by Duque (1974, 1992) and Feininger (1980). In the following account the complex is subdivided into three: the Panupali, El Toro and Raspas units.

The **Panupali greenschist unit** is named after the Río Panupali which provides an almost continuously exposed section across the unit in the east. In the west these rocks are also well exposed downstream of the Tahuín dam in the Río Arenillas. The unit forms the outer 'shell' of the El Oro ophiolitic complex and has tectonic contacts with the Palenque schists and El Toro serpentinites. Originally the western part of what is here referred to as the Panupali unit was considered to be Precambrian in age and thought to form part of the Piedras mafic complex (Feininger, 1978). However, the general field relations, together with the mineralogical and geochemical evidence presented below, rule this out.

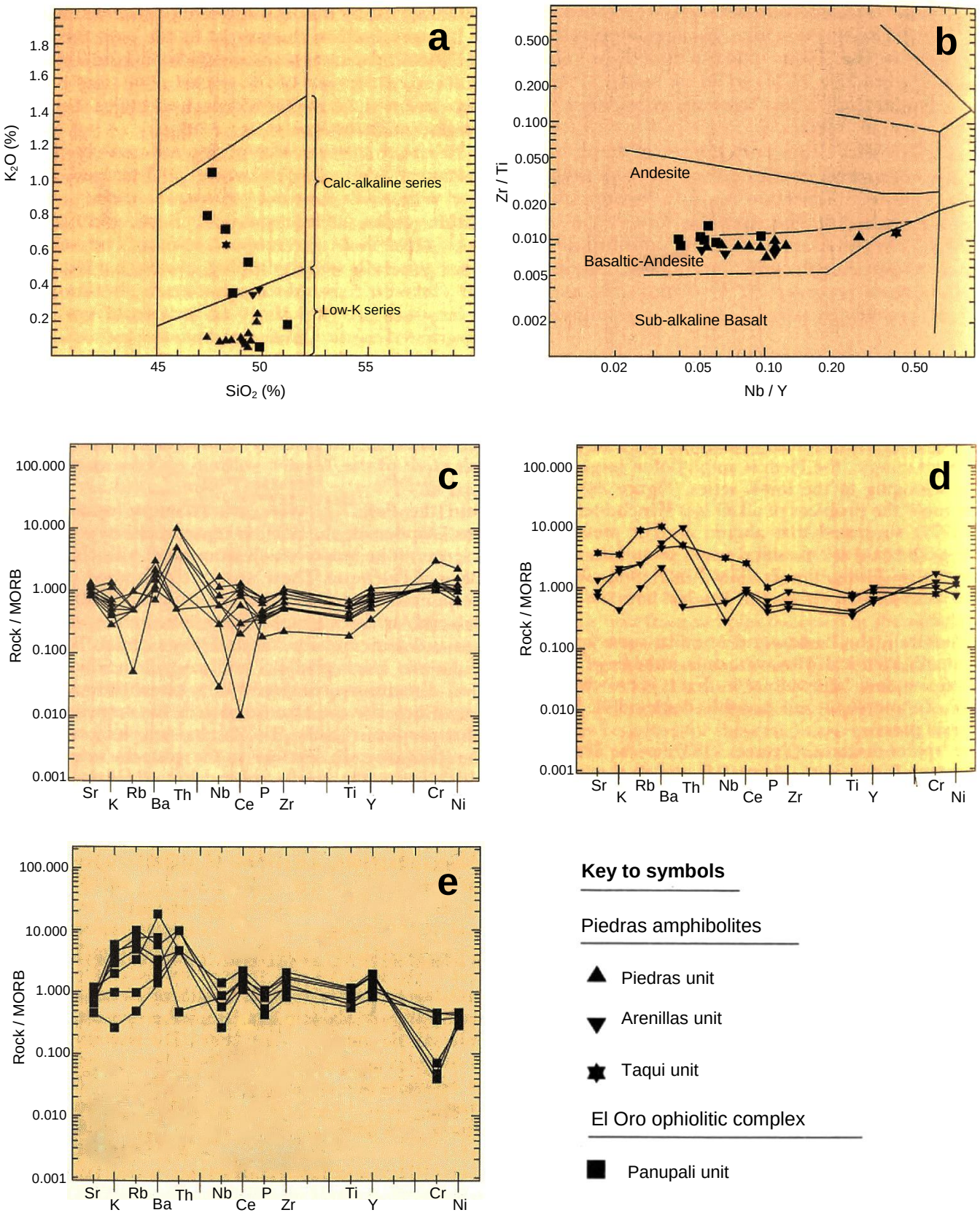

Figure 24 Geochemical plots of El Oro mafic rocks

(a) K_2O v. SiO_2 classification diagram after Ewart (1982); **(b)** Zr/Ti v. Nb /Y diagram after Winchester and Floyd (1977); ROCK/MORB normalised 'spider diagrams' after Pearce (1983) for **(c)** Piedras amphibolite, **(d)** Taqui and Arenillas amphibolites, and **(e)** Panupali unit.

The unit comprises greenschists, composed of actinolite, albite, quartz, chlorite, epidote, ± garnet, ± glaucophane, ± sphene, ± calcite, ± opaques. This assemblage, and in particular the presence of glaucophane in some samples, confirm that these rocks represent an integral part of the El Oro ophiolitic complex.

In terms of its geochemistry, seven whole-rock analyses are available from the Panupali unit which together with the normative compositions and various geochemical indices are listed in Fortey and Gillespie (1993). For comparative purposes these data have been plotted on the same diagrams as those used for the Piedras mafic complex (Figures 14 and 24). Based on these diagrams both units are broadly similar and can be classified as ocean floor (MORB) basalts/basaltic andesites. However, in spite of these similarities and with the exception of one sample, the Panupali unit stands out as a separate subgroup which, relative to the Piedras mafic complex, is depleted in MgO, Cr and Ni but enriched in Fe (total), K, Rb, Ba, Ce (but not Nb), P, Zr, Ti (> 1.5 wt%) and Y.

The **El Toro serpentinite unit** (Feininger, 1978) is well exposed in a group of quarries that are located immediately to the east of the Tahuín dam (Figure 21) in the area of El Toro. It forms an east-west trending, crescent-shaped outcrop separating, tectonically, the outer (Panupali) unit from the inner core of the Raspas unit within the El Oro ophiolitic complex.

Lithologically the El Toro unit consists of variably serpentinised, massive to schistose, medium-grained harzburgites which are composed principally of olivine, orthopyroxene, antigorite and minor amphibole. Five samples all show TiO_2 contents below detection limit and thus fall outside the field of supra-subduction zone ophiolites on the Pearce et al. (1984) diagram (Figure 17).

The **Raspas unit,** the Raspas Formation of Feininger (1978), takes its name from the Río Raspas, which following the construction of the Tahuín dam, is now only readily accessible from La Chilca in the east (Figure 21). The essentially schistose unit contains blueschists and massive eclogites. It has tectonic contacts and forms the central core of the El Oro ophiolitic complex, with an east-west-trending strike length of about 20km and a maximum width of about 3km.

A single K/Ar (phengite) determination for a pelitic schist collected from the Río Raspas gave an age of 132 ± 5 Ma (Feininger and Silberman, 1982). This date is interpreted to represent a cooling age below the blocking temperature of phengite and probably represents the age of emplacement for the El Oro ophiolitic complex.

The following lithological and petrological details of the Raspas unit are summarised from Feininger (1980) and Duque (1992). Coarse-grained pelitic schists and minor amounts of micaceous quartzites make up approximately 70 per cent of the unit. Mineralogically the schists consist of quartz, phengitic muscovite, paragonite and garnet with lesser amounts of graphite, rutile, pyrite, Mg-chloritoid and kyanite. Blueschists and eclogites occur in approximately equal proportions. The blueschists are typically fine- to medium- grained phyllites which carry small (less than 2mm) garnet porphyroblasts and can contain more than 50 per cent modal glaucophane. In addition, variable amounts of paragonite, phengite, muscovite, epidote, rutile, quartz, apatite, pyrite may be present, and secondary minerals include chlorite, sphene, albite and calcite.

The eclogites of the Raspas unit have been found as loose blocks. They are dark in colour, fine to medium grained, and variably foliated, consisting mainly of omphacite, garnet and barroisite with lesser amounts of clinopyroxene, rutile, quartz, apatite and pyrite. Layers of amphibole gneisses up to several metres thick and composed of barroisite (more than 50 per cent), garnet, zoisite, kyanite, rutile, pyrite, ± omphacite, ± paragonite, ± quartz, ± apatite, ± muscovite are associated in places with the eclogites. Minor amounts of greenschists that are mineralogically identical to those of the Panupali unit, amphibole pegmatites, garnetites (garnet more than 50 per cent) and blocks of jadeite also occur within the Raspas unit.

TECTONOMETAMORPHIC EVENTS

In contrast to the NNE-SSW regional strike of the Ecuadorian Andes the structural grain of the El Oro metamorphic complex is east-west and is dominated by the presence of numerous, generally steep, sub-parallel, anastomosing faults. In spite of the apparent uniformity of the various structural elements, the El Oro metamorphic complex comprises rocks of different ages, origins and metamorphic histories. It follows that the structures preserved must also reflect this diversity. More detailed work is required before a realistic structural/kinematic framework can be established, but nevertheless sufficient information is currently available to allow a broad distinction to be made between the Late Triassic structures, present to the south of the Naranjo fault zone, which relate to the 'Moromoro event' and those of uncertain, but younger age (?Late Jurassic-Cretaceous), which occur to the north and relate to the 'Palenque event'.

Moromoro event

In the unmetamorphosed to weakly metamorphosed **El Tigre unit** dips are variable, but normally steep-to-moderate and generally to the north. Numerous bedding-parallel faults occur throughout the rocks and, where observed, the associated lineations/slickensides are horizontal or have gentle plunges to the east or west (Plate 17a). Many of these faults are marked by irregular, concordant/discordant, quartz veins and lenses.

a

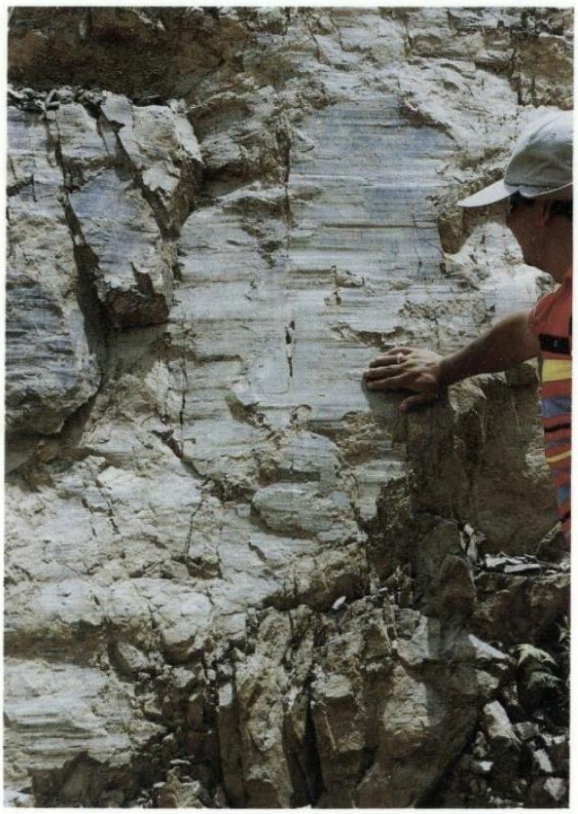

c

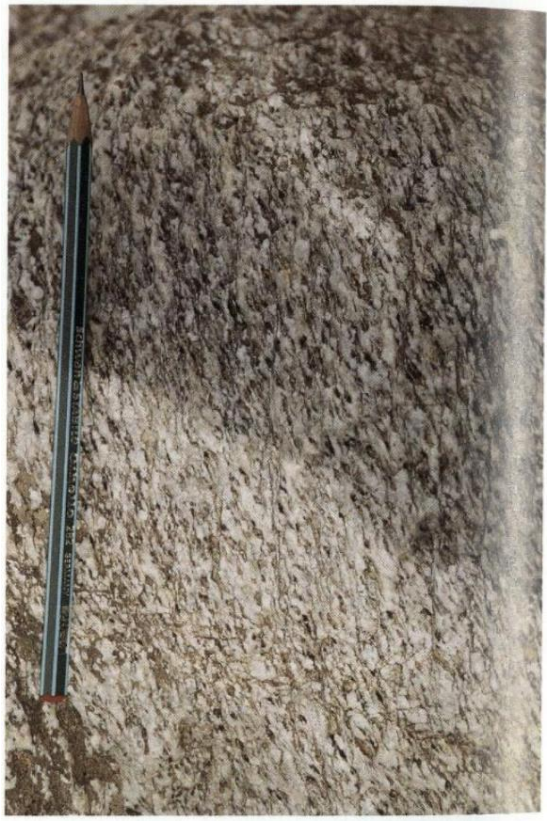

b

Plate 17 Progressive deformation in El Oro.

(a) Vertical surface showing horizontal slickensides in El Tigre unit rocks, along the road from El Tigre to Puyango (Photo: J. A. A.).

(b) Horizontal surface showing mylonitic La Victoria schists with dextrally sheared quartz vein, Quebrada Primavera, Río Piedras (photo: J. A. A).

(c) Dextral S-C mylonitic fabric in Moromoro granite (photo: J. A. A.).

In areas of high strain, zones of bedding-parallel cleavage may be developed but these are generally restricted to narrow incompetent shale/lutite horizons where a horizontal/subhorizontal, transpressional, dextral shear sense can be established in places. Elsewhere, structures tend to be of a more brittle nature, especially in the massive, quartzose horizons, where quartz-filled tensional features, some of which are demonstrably dextral, are commonly developed. These structures are typically oblique to the main, east-west, structural trend of the unit. In some areas, for example to the west of Marcabelí (**617-9581**), the El Tigre unit is overturned but it was not possible to confirm that the entire unit is inverted (cf. Feininger, 1978). Such phenomena may be associated with local thrusts/flower structures which may develop at high levels in association with regional zones of strike-slip (Sylvester, 1988) (see below).

Structurally the **La Victoria unit** is similar to the El Tigre unit, but, as evidenced by the metamorphic mineral assemblages, it was deformed at higher temperatures. Their mutual contact is a steep, complex, east-west-trending, tectonic zone across which there is an increase in both metamorphic grade and the intensity of generally subhorizontal, ductile shearing. Many S-surfaces within the La Victoria unit exhibit mineral lineations, which typically have shallow (less than 30°) plunges.

Both within the La Victoria unit and in parts of the Moromoro granitoid complex, especially in the south, there are macroscopic and microscopic kinematic indicators such as winged inclusions, boudinaged quartz veins, rotated porphyroblasts/megacrysts, tight-to-isoclinal Z-folds and/or kink bands (generally with steep-to-vertical fold axes), S-C mylonite fabrics, and mica 'fish'. All these structures give a consistent sense of dextral movement (Plate 17b). (For a review of such kinematic indicators see Hanmer and Passchier (1991)).

Much of the La Victoria unit, and parts of the El Tigre unit, consist of Type II S-C mylonites (Plate 17c) in the sense of Lister and Snoke (1984). The high fault density and its anastomosing pattern, the evidence from mineral lineations and shear sense indicators all strongly support the interpretation that, during the Moromoro event, these rocks were deformed and metamorphosed in a regional zone of dextral transpression. The dominant sense of movement was approximately horizontal and parallel to faulting, i.e. strike-slip in the sense of Sylvester (1988).

Thrusts of mylonitic schists, which are highly oblique to the regional trend of the La Victoria unit, have been mapped in the west, to the north of La Victoria and exposed along the main Arenillas road. These thrusts have a variable west-dipping, bedding-parallel cleavage with west-plunging mineral lineations. Boudinaged and sigmoidally (Z) folded quartz veins suggest tectonic transport from west to east. These structures may correspond to contractional duplexes, such as are commonly formed at restraining/compressional bends in regional zones of strike-slip faulting (Woodcock, 1986).

In the south, the east-trending **Marcabelí** and **El Prado plutons** are generally unfoliated. However, the northern part of the Marcabelí pluton is cut by a series of generally steep, dextral shear zones, and within the La Victoria unit, particularly in the west, a number of strongly foliated, isolated, faulted-bounded lenses belonging to the Moromoro granitoid complex, are present.

The main outcrop of the **Moromoro granitoid complex** is variably deformed. In some areas, coarse, but fairly penetrative foliations and/or discreet, ductile S-C (dextral) mylonite fabrics are preserved (Plate 17c). However, in many places these granitoids have an irregular or weakly developed gneissic foliation or linear fabric, due to the alignment of biotite/biotite schlieren and/or flattened and elongated xenolithic material. Elsewhere, for example in the La Florida area in the west, the La Florida pluton is unfoliated and apparently undeformed. Together these observations suggest that the magmatic activity associated with the Moromoro event may have been relatively long-lived since it appears to include a variety of syn- to late- and possibly post-tectonic plutons.

Structural dips within the elongate **Piedras amphibolite** are variable but generally steep. Its southern contact with the Moromoro granites was possibly, in part, intrusive but is now faulted. Since the amphibolites along this contact are not brecciated, nor apparently have they been significantly retrogressed, it is probable that the amphibolite was formed close to peak metamorphic conditions during the 'Moromoro event'.

In contrast, the northern margin of the same amphibolite along the Naranjo fault zone has been widely retrogressed to greenschist. In several areas, e.g. along the Río Naranjo west of Zaracay, a distinctive, banded tectonite, which normally has a strongly developed, steep-to-vertical, amphibole (actinolite), mineral lineation has been produced. Late, semi-ductile, conjugate sets of (Z) kink bands indicate downthrow to the north. These tectonites suggest that movement(s) along this segment of the Naranjo fault zone was probably dominantly of a high temperature, ductile nature. However, in the extreme west, near the Peruvian border, tectonic breccias have been observed. It is apparent that this fault zone, which defines the southern tectonic limit of the Palenque unit and the El Oro ophiolitic complex, represents an important structural break within the El Oro metamorphic complex and although the overall sense and timing of the major movement(s) are uncertain they are considered to postdate those of the Late Triassic Moromoro event.

In conclusion, the Moromoro event is represented by dextral shearing which became more ductile in the north with increasing metamorphic grade of high-temperature Abukuma-type. Rocks of highest grade are migmatitic and merge with the Moromoro granites indicating a temporal link between granite emplacement and high-grade metamorphism. This link is confirmed by the Upper Triassic ages of both the granite and metamorphic garnets (Figure 22). It therefore appears most likely that the Moromoro granite was shear-zone generated (Reavy, 1989; D' Lemos, 1992).

Palenque event

North of the Zanjón-Naranjo fault, rocks of the Palenque unit and El Oro ophiolite are thought to be of a younger Jurassic-Lower Cretaceous age, with a younger tectonometamorphic overprint, the Palenque event. However, within the Palenque schists there are bodies of amphibolite and granite interpreted as having consolidated in the Moromoro event.

Within the **Palenque unit**, the fine-grained, generally incompetent, matrix sediments have been plastically deformed and their structure is dominated by the presence of steep-to-vertical, bedding-parallel, east-west-trending faults which probably have a complex history of movement. Bedding and cleavage are parallel and dip steeply to the north or south. In thin section, S-C mylonite textures (Lister and Snoke, 1984) are common. Macroscopic, kinematic indicators and lineations are relatively rare at outcrop level but, where observed, they suggest a dextral sense of shear with fairly gentle lineation plunges.

In the south and east, strongly deformed, steeply dipping, black (± graphite) phyllonites and quartzose mylonites, silicified in places, occur sandwiched between the Naranjo fault zone and the El Oro ophiolitic complex. Dips are more variable in the west, but generally they are to the south along fault which follows the Tahuín dam.

Contacts are steep and tectonic between the matrix sediments of Palenque and the older blocks, and, in some cases subhorizontal dextral shear can be demonstrated along them. Some of these blocks of granite or amphibolite may preserve, internally, the older, ductile, Moromoro structures. In the amphibolite units in particular there are younger, irregular, brittle fractures and semibrittle, generally steep, east-west-trending shear zones. These are tentatively interpreted as forming during, or following, the incorporation of these older, competent rocks into the Palenque schists or Palenque mélange complex (Aspden, in press). Available K-Ar dates indicate that a thermal, overprinting event affected the Arenillas unit at about 74 Ma and some of these structures may relate to this event.

Few detailed structural observations are available for the **El Oro ophiolitic complex.** Mora (1988) confirmed the common occurrence of mylonitic textures in both the Panupali and Raspas units, and in the west a series of south-west-dipping imbricate thrust faults, which have southerly plunging mineral lineations, have been mapped within the Panupali unit. In spite of the general steep internal and contact structures associated with the complex, the emplacement of these rocks from their original depth of formation at a pressure of about 9kb (Duque, 1992), to their present structural level, must have involved several kilometers of dip-slip (vertical) movement. (For models of blueschist emplacement see Platt (1987)).

Structural limits of the El Oro metamorphic complex

The northern limit of the main outcrop of the El Oro metamorphic complex coincides with the Jubones fault, which was previously considered to separate the older metamorphic crust to the south from younger oceanic crust to the north (Baldock, 1982). However, since inliers of metamorphic rocks, similar to those found within the El Oro metamorphic complex, have been reported to the north of the Jubones fault (Aspden et al., 1988), it is unlikely that this structure is of such regional significance. Nevertheless, the fault is of local importance and probably has a complex history which must have included a normal component of movement with significant downthrow to the north. The fact that the Jubones fault is parallel to other east-west-trending faults within the El Oro complex may indicate a common origin but the presence of highly contorted black phyllites with numerous quartz veins and areas of silicification along its length may relate to younger movements. Structural dips are variable, but generally steep to vertical and both gentle, east- or west-plunging, and steep, north-plunging, mineral lineations have been observed.

In the east, near Uzhcurrumi, the Jubones fault is cut by undeformed Cenozoic granodiorites and similar rocks intrude the El Oro metamorphic complex along much of its eastern margin. Basement lithologies along the Portovelo fault zone have been cataclastically deformed and brecciated by younger, reactivated, normal faulting with downthrow to the north, e.g. to the south of Piñas.

In the south-east, the limit of the El Oro metamorphic complex is defined by a series of NNE-SSW-trending, 'horse-tail' faults of the Guayabal fault zone. This zone is undoubtedly complex and has probably been affected by several periods of movement which involved not only the metamorphic basement lithologies, but also those of the Cretaceous Alamor basin sequence and younger Tertiary formations and intrusions (Kennerley and Almeida, 1975). Regionally, the main Guayabal fault defines the western margin of the Neogene Catamayo 'graben' (oral communication, E. Salazar), a north-south-trending structure which separates the main outcrop of El Oro metamorphic complex from similar metamorphic lithologies of the Cordillera Real to the east (Aspden and Litherland, 1992; Kennerley and Almeida, 1975). The metamorphic rocks that have been affected by this fault zone have been cataclastically deformed and the more competent, quartz-rich lithologies are typically strongly fractured and/or brecciated. Overall, the sense of movement along the zone is thought to be dextral but it also includes an (?)eastward directed thrust component.

In the south the El Oro metamorphic complex is unconformably overlain by the Cretaceous sediments of the Alamor basin. The development of the basin was probably controlled by extensional faults, movements along which have resulted not only in the brecciation of the metamorphic basement but also, in part, the younger basinal sediments.

OTHER METAMORPHIC OCCURRENCES

There are numerous metamorphic occurrences east and north of the main El Oro complex outcrop (Figures 6 and 9), many of which were investigated by the Project.

To the east, the Manú inlier comprises foliated muscovite-biotite metagranites and pegmatites of Tres Lagunas/Moromoro type. Float blocks in the Río Manú close to the Jubones confluence exhibit these granites and semipelitic schists. Similar schists can be seen as blocks in the Río Las Palmas and Río Luis draining unmapped metamorphic inliers east and north-east of Portovelo.

North of the Río Jubones, there is a chain of poorly defined metamorphic inliers from the Mirador prospect in the south (oral communication, D. Coochey) to Chaucha in the north (INEMIN-Misión Belga, 1986) and these comprise semipelitic schists, amphibolites, gneissic granites and pegmatites; blocks derived from these inliers can be seen in the west-draining rivers at the foot of the Western Cordillera.

Further north there is an outcrop of Palenque-type schists at La Delicia on the Cañar-La Troncal highway (Egüez et al., 1988), and sheared metagranite float in the nearby Río Cañar. Blocks of blue quartz metagranite are present in Quebrada Palamá on the Huigra-El Triunfo road (Egüez et al., 1988).

There are outcrops of metagranite and amphibolite in tectonic contact with units of the Pujilí ophiolite on the western flanks of the Inter-Andean valley near Latacunga (Figure 6), whilst further north, xenoliths of metamorphic rocks have been documented from lavas of Pichincha volcano (Bruet, 1987).

EIGHT
Correlation and interpretation

PALAEOZOIC AND TRIASSIC HISTORY

Correlation

CORRELATION WITHIN ECUADOR (Figure 6). In the metamorphic belts of Ecuador, the low-grade Palaeozoic rocks of Chigüinda and El Tigre and their higher-grade equivalents of Agoyán and La Victoria, are palaeontologically constrained to the Devonian-Carboniferous periods, possibly extending into the Permian. These are metasedimentary rocks of semipelitic character typical of ensialic basins, but becoming turbiditic in the El Tigre unit of El Oro.

These Palaeozoic rocks were intruded by basaltic amphibolites and the S-type granites of Moromoro in El Oro and Tres Lagunas in the Cordillera Real. These amphibolites and granites give U-Pb ages of about 228 Ma. Since metamorphic minerals in the envelope rocks of the Moromoro granites also give Upper Triassic ages by both the K-Ar and Sm-Nd methods, the granites can be interpreted as contemporaneous with the high-grade, Abukuma-type facies metamorphism and anatexis, referred to as the Moromoro event. Over the Cordillera Real, a similar event, termed the Tres Lagunas event, has been proposed which generated the Tres Lagunas granites and migmatites of Sabanilla.

There thus seems little doubt that the El Oro and Cordillera Real metamorphic belts of Ecuador have similar Palaeozoic and Triassic histories culminating in the generation of the granites of Moromoro and Tres Lagunas.

East of the Cordillera Real, correlation becomes more difficult due to the paucity of data. The volcanosedimentary Isimanchi unit is almost certainly of Palaeozoic age and was deformed by the Triassic Tres Lagunas event. Further east along the strike, the Pumbuiza and Macuma Formations are little-deformed Palaeozoic sedimentary units. In between these outcrop areas, the Upper Triassic volcanosedimentary basin of Piuntza unconformably overlies metasedimentary rocks attributed to the Isimanchi unit. Whatever the age interpretation of these underlying rocks, there remains a problem of correlation between adjacent Upper Triassic rocks, high-grade at Sabanilla and unmetamorphosed at Piuntza.

CORRELATION INTO PERÚ. The fossiliferous Palaeozoic rocks of Cerro Amotape in northern Perú (Mourier, 1988) can be traced into the El Tigre unit of the El Oro belt. The metamorphic rocks of the Olmos arch (Cobbing et al., 1981) are contiguous with those of the Cordillera Real, but ages and field relationships are poorly understood (Mourier, 1988). However, these rocks appear to lack the Lower Palaeozoic sequences found in southern and central Perú, along with evidence for the early Hercynian (Devonian) orogeny (Laubacher and Megard, 1985).

In the Permo-Triassic, the eastern Cordillera of Perú formed the site of an ensialic rift zone characterised by the accumulation of a red-bed molasse and alkaline and peralkaline lavas of the Mitu Group (Kontak et al., 1985). These were intruded by crustally derived granites similar in age and type to those of Tres Lagunas and Moromoro. However, the granites in Perú are undeformed and not related to shear zone orogeny. In many other parts of South America such Triassic sedimentary rocks are interpreted as rift-related basins (Suárez and Bell, 1992).

CORRELATION INTO COLOMBIA. Close to the Colombian border the Cordillera Real of Ecuador bifurcates to form the Cordillera Central and Cordillera Oriental of Colombia. Over the Cordillera Oriental, or Eastern Cordillera, the Precambrian basement is overlain by metamorphosed semipelitic sediments of Lower Palaeozoic age, in turn unconformably overlain by unmetamorphosed Devonian and Carboniferous epicontinental sediments (Restrepo and Toussaint, 1988; Grosser and Prossl, 1991). This crustal block, which has been interpreted as a fragment of the Caledonian Appalachian belt of North America (Forero Suárez, 1990), has remained cratonic since Devonian times and conforms to the Amazonic craton of Ecuador in terms of post-Silurian history. However, on the National Geological Map of Colombia (1976), Precambrian rocks of the Cordillera Oriental are shown crossing the border into Ecuador, where according to the present studies, they are represented by Jurassic rocks of the Salado terrane.

The Cordillera Central of Colombia comprises semipelitic schists and amphibolites of probable Upper Palaeozoic age (McCourt et al., 1984) associated with foliated plutons of probable Triassic age (Aspden et al., 1987). These are similar to the lithologies of the Loja terrane of Ecuador and must represent its northward extension into Colombia.

IN CONCLUSION, there are recognisable tectonic domains of Palaeozoic-Triassic rocks in the northern Andes. In particular within the metamorphic belts of Ecuador, northern Perú and the Cordillera Central of Colombia, Upper Palaeozoic sedimentary rocks are affected by a Triassic Orogeny (Hall and Calle, 1982) accompanied by the generation of S-type granites. In Ecuador these rocks conform to the Loja, Amotape and Chaucha terranes of Figure 5.

Interpretation

It has been demonstrated geochronologically that the generation of the Moromoro granites was contemporaneous with the high-temperature/low pressure, Abukuma-type metamorphism which affected the Palaeozoic rocks of the El Oro belt. Moving north across this belt, low-grade metasedimentary rocks with unfoliated granites and slickensided shear zones pass into high-grade migmatitic metasedimentary rocks associated with foliated granites and dextral S-C mylonite fabrics. This demonstrates that the granites were emplaced syntectonically along a major shear zone, which formed a high-strain/high-grade belt, 10-15 km wide.

Such linear belts of shearing, high-grade metamorphism and S-type granites have been documented from the Ibero-Armorican arc (Reavy, 1989; D' Lemos et al., 1992) and models have been proposed involving frictional heating resulting in anatexis and the generation of granites from within the crust (e.g., Nicolas et al., 1977).

The interpretation of the El Oro belt can be applied to the Loja Terrane rocks of the Cordillera Real which show S-Type Tres Lagunas granites within metasedimentary rocks of low grade (Chigüinda unit), medium grade (Agoyán unit) and high grade (Sabanilla migmatites) accompanied by mylonitic textures.

There are difficulties in reconstructing the Palaeozoic-Triassic history primarily because the Amotape and Chaucha Terranes (Figure 5) are allochthonous, being separated from continental South America by the Jurassic oceanic island arc of Alao, and emplaced during Early Cretaceous times.

The 'suspect' nature of the Loja terrane also presents problems in any reconstruction. This rests upon the tectonometamorphic contrasts with the Macuma and Pumbuiza Formations, and the Piuntza unit, which is undeformed yet of similar age to the Tres Lagunas granites. If a Triassic suture zone exists along the sub-Andean belt, then it could be marked by the **Zumba ophiolite** which is probably of pre-Jurassic age. Workers in Colombia (Restrepo and Toussaint, 1988; Restrepo-Pace, 1992) have proposed such a sub-Andean suture zone through Ecuador.

The reconstruction on Figure 25a follows Aspden et al. (1992b) and shows Triassic shearing and anatexis along an ensialic rift basin to form the **Triassic metamorphic belt of the northern Andes**, fragments of which comprise the present Loja, Amotape and Chaucha terranes and the Cordillera Central of Colombia. The amphibolites of Piedras and Monte Olivo may be original mantle-derived basalt dykes related to this rifting event.

The Palaeozoic basins of the Central Andes may represent the failed arm of the early Pacific rifting which eventually separated South America from Laurentia (North America) (Dalziel, 1993) (Figure 3). However, in Perú the Palaeozoic basin was deformed and metamorphosed in the Carboniferous (Laubacher and Megard, 1985), whilst in Ecuador the equivalent event occurred in the Triassic.

According to the reconstructions of the Caribbean region (Ross and Scotese, 1988), the Permo-Triassic Pangaea united the western margin of northern México with the western margin of northern Perú. The Upper Triassic shear zone-related metamorphic belt (Figure 25a) of the northern Andes could thus mark the initial rifting which lead to the separation of Gondwana and North America and the formation of the Tethyan Ocean (Jaillard et al., 1990; Aspden et al., 1992). The belt of contemporaneous non-orogenic granites in Perú may belong to a failed arm of this event. Older, Triassic ages found over the Zamora batholith could represent magmatic activity within the rifting fragment, whilst the Triassic Piuntza basin may conform to a half-graben bordering the main rift.

However, it must also be pointed out that the Triassic metamorphic belt of the Northern Andes is a dextral shear zone which may merely represent a continuation of the dextral shift of North America *vis-à-vis* South America which opened the Pacific Ocean in the Palaeozoic (Dalziel, 1993) (Figure 3) and the Tethys Ocean in the Mesozoic (Jaillard et al., 1990). Little is known as yet regarding the movement of the smaller plates and fragments of Palaeozoic basins within this framework.

JURASSIC-LOWER CRETACEOUS HISTORY

Correlation

Metamorphic rocks of Jurassic-Lower Cretaceous age recognised in Ecuador comprise the Alao and Salado terranes and certain elements of the El Oro metamorphic belt. The Alao and Salado rocks are shown to wedge out in the south of the Cordillera Real within Ecuador. To the north, equivalents of the oceanic Alao rocks may be represented in Colombia by the Amaime Terrane (Aspden and McCourt, 1986), but the Salado Terrane, as previously noted, is shown passing into Precambrian rocks on the National Geological Map of Colombia (1976), and clearly this sector requires reinvestigation.

The Peltetec event, the main tectonometamorphic event to affect the Jurassic-Lower Cretaceous rocks of the cordillera, is correlated with the Palenque event in El Oro. This is regarded as the common imprint of the main phase of collision and accretion.

The correlation of Jurassic-Lower Cretaceous rocks over the eastern cratonic, or autochthonous area from Colombia through Ecuador to Perú, is depicted on Figure 2 of Jaillard et al. (1990) and the related plutonic activity is discussed by Aspden et al. (1987). The existence (see also Hall and Calle, 1982) of a Jurassic continental volcanic-plutonic arc which included the Zamora and Abitagua batholiths of Ecuador has been confirmed by Project geochronological studies.

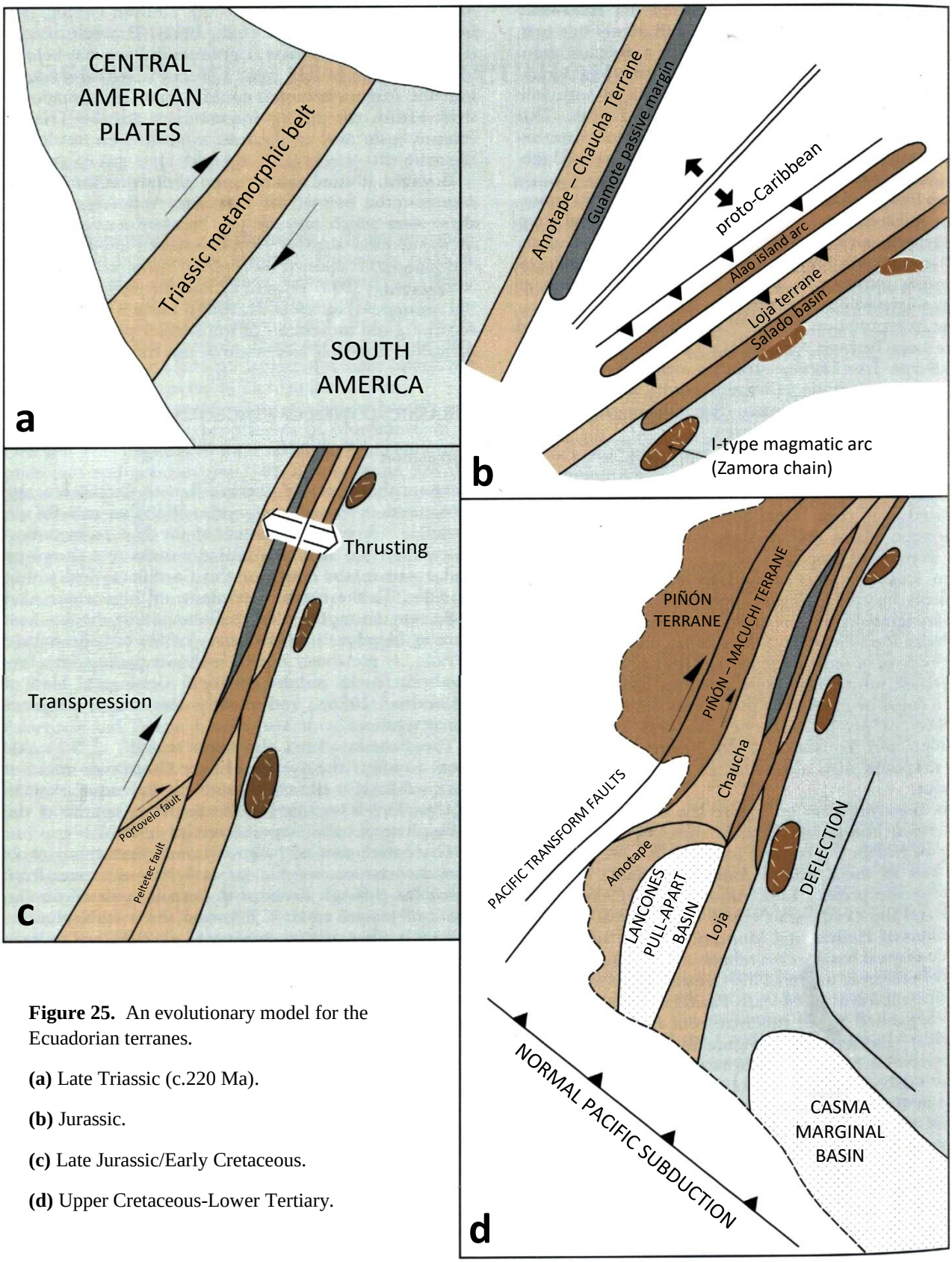

Figure 25. An evolutionary model for the Ecuadorian terranes.

(a) Late Triassic (c.220 Ma).

(b) Jurassic.

(c) Late Jurassic/Early Cretaceous.

(d) Upper Cretaceous-Lower Tertiary.

Interpretation

During the Jurassic-Lower Cretaceous period the proto-Caribbean or Tethyan ocean opened with subduction along the South American margin migrating southwards during the Jurassic and destroying a marine shelf, represented in Ecuador by the Lower Jurassic Santiago Formation (Jaillard et al., 1990). In Ecuador, this subduction phase produced the I-type batholiths of Rosa Florida, Abitagua and Zamora and their related volcanic products of the Misahuallí unit (Figure 25b).

Whilst the Abitagua-Zamora chain was previously known, and regarded as being of Jurassic age (Hall and Calle, 1982), the Project studies have established the presence of a parallel plutonic chain to the west, that of Azafrán-Chingual. These plutons are apparently similar in age and composition to Abitagua-Zamora, but are gneissic and associated with metamorphosed sedimentary and volcanic rocks of the Upano, Cuyuja and Cerro Hermoso units. Together these form the **Salado terrane**, believed to be of Jurassic age; the Upano unit may be a facies equivalent of the Misahuallí volcanics.

The status of the Salado Terrane is uncertain. The calc-alkaline nature of the analysed meta-andesites and the close spatial relationship of the Azafrán and Abitagua chains suggest that the volcanosedimentary rocks were formed in a marginal basin-type setting over continental crust as depicted on Figure 26a. The presence of clastic blue quartz in the metagreywackes suggests erosion and deposition of Tres Lagunas-Moromoro granites which would most probably have been located west of the proposed basin.

The volcanosedimentary **Alao terrane** contains fossils similar in age to the Abitagua granite (about 160 Ma), thus presenting a second magmatic arc for consideration in any plate tectonic model. Geochemically the Alao-Paute greenstones correspond to oceanic island arc basalts, which distinguishes them from those of the Upano. Furthermore, there is an eastward polarity in the four major rock belts of the Alao terrane, viz. subduction complex (Peltetec mélange), forearc (Maguazo unit), island arc (Alao-Paute unit), and backarc (El Pan unit). These can be interpreted as attenuated relics of an island arc sequence formed over an east-dipping subduction zone (Figures 25 and 26). No clastic blue quartz was noted in the Maguazo turbidites but microfossil analysis has identified the presence of reworked Ordovician acritarchs, which, presumably, were derived from an older continental source.

The **Guamote Terrane** comprises epicontinental clastic sediments with Lower Jurassic ammonites. Fossils of possible Lower Cretaceous age, if confirmed, may belong to sediments from local syn-collisional, pull-apart basins. The Guamote sediments contain clastic blue quartz, probably derived from the Tres Lagunas granites, and undeformed acid volcaniclasts. The sediments are thrust westwards over the Chaucha plate and can be interpreted as its passive margin sequence (Figures 25 and 26).

Various units of the **El Oro metamorphic belt** are ascribed a Jurassic-Lower Cretaceous age. The greenschists, blueschists, pelitic schists and eclogites of the El Oro ophiolitic complex represent the prograde products of high-pressure/low-temperature metamorphism and were probably formed in an active subduction zone for which a palaeogeothermal gradient of about 13.8°C/km has been calculated (Duque, 1992). Further north, the Palenque schists are interpreted as the matrix of a wide regional mélange belt, or accretionary complex, containing fragments derived from the Triassic metamorphic belt. It is possible that much of the Chaucha 'terrane' (Figure 5), which is largely buried by younger deposits to the north of El Oro, is comprised of such mélange rocks rather than a coherent block of the Triassic metamorphic belt.

The **Peltetec-Palenque accretion** was the main tectonometamorphic event affecting the Jurassic-Lower Cretaceous rocks. It is interpreted to represent the major accretion/collision which established the terrane mosaic of Ecuador before the addition of the Piñón terrane.

All the important faults along the metamorphic belts belong to this event. Some are interpreted as separating tectonostratigraphical terranes and can thus be regarded as 'sutures'. For example, the Peltetec and Portovelo faults contain lenses of ophiolitic rocks interpreted to represent relics of the oceanic slabs which existed between the terranes. No ophiolites were noted along the mylonitic Baños fault. Evidence exists for dextral movement along many of these faults and this strike-slip component must be borne in mind when studying Figure 26.

Figure 26b shows a structural section across the northern Cordillera Real interpreted as the collision/accretion of terranes during the Peltetec event. Extensional movements along Jurassic faults formed the Salado basin, but these were reversed during the collision. The nappe structures of Cuyuja show a tectonic mixing of rocks from different terranes along with sheets of serpentinite and skarn which are generally found close together in the tectonic pile. The dominant east-directed thrusting along the cordillera would argue for a west-dipping subduction zone at the time of the main collision, although the tectonic pattern is complicated by transpressional vectors. Fragments of Tres Lagunas granite found within the Peltetec ophiolitic mélange can be interpreted as being scraped off the Chaucha plate. Erosion has now removed the bulk of the crustal thickening represented by the nappe structures, a process of unroofing which must have started in the Lower Cretaceous, the products of which may be represented by the Lower Cretaceous top to the Chapiza unit in the Oriente (Bristow and Hoffstetter, 1977).

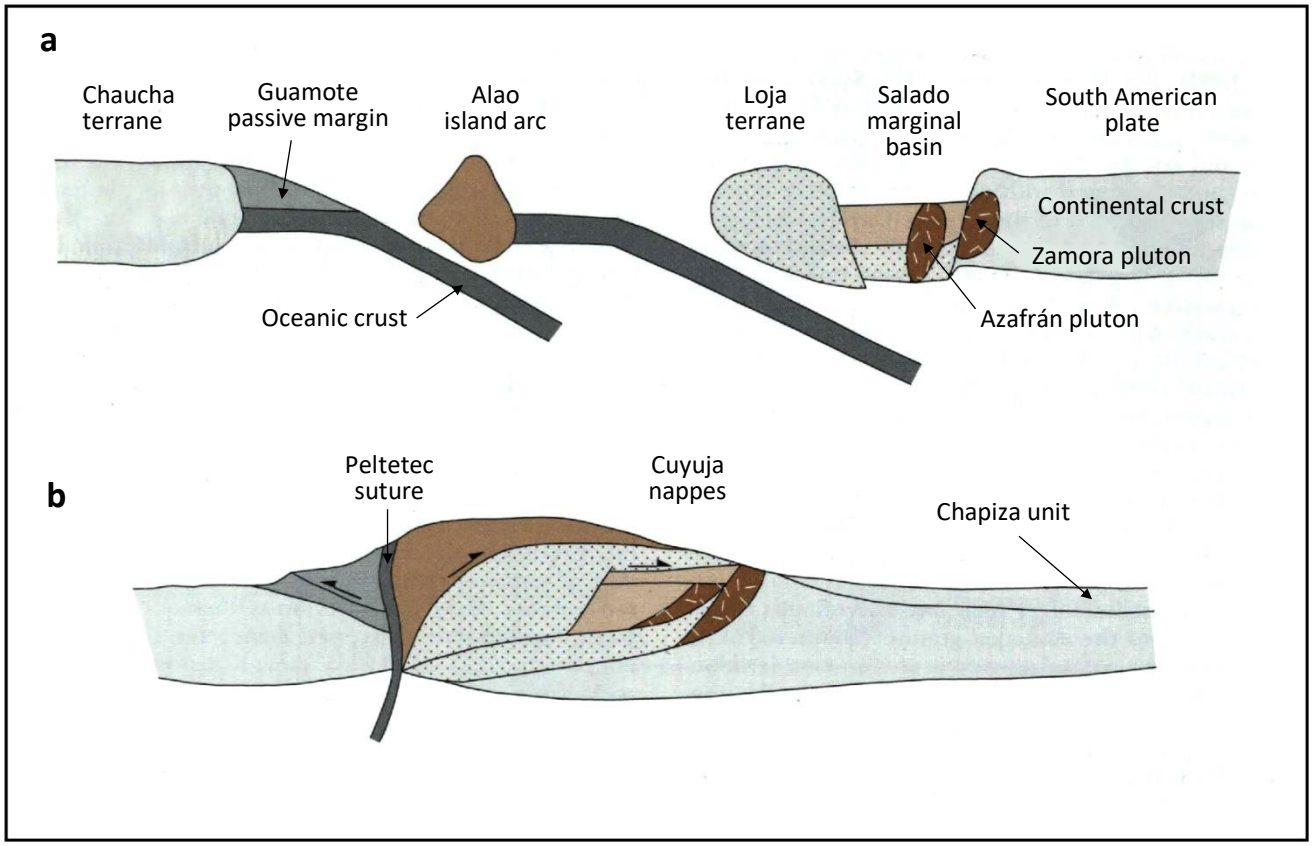

Figure 26. A two-dimensional evolutionary model for the northern Cordillera Real omitting any strike-slip motion.

(a) c. 160 Ma; **(b)** c. 135 Ma: the Peltetec event.

Figure 25c shows a transpressional terrane emplacement model for the Peltetec-Palenque event. It represents one of many scenarios. For example, Aspden (in press) indicates a mélange complex for the Chaucha terrane. It is interesting to note that Jaillard and Jacay (1989) anticipated these conclusions in their interpretation of the turbiditic Chicama basin of Tithonian (approximately 145 Ma) age of northern Perú as the infilling of a dextrally produced pull-apart basin related to the emplacement of the Amotape terrane.

LATER CRETACEOUS AND CENOZOIC HISTORY

In terms of the plate tectonics of Ecuador the most significant event following that of Peltetec-Palenque was the emplacement of the oceanic Piñón terrane. This Cretaceous crustal block forms the basement both of the Western Cordillera, where it is overlain by the Palaeocene-Eocene Macuchi island arc, and of the coastal area, overlain by Cenozoic forearc basins (Daly, 1989). Its contact with the Chaucha plate along the Pujilí fault (Figure 5) is marked by lenses of ophiolitic rocks (Litherland and Aspden, 1992).

The transpressional emplacement of this block during the late Cretaceous (Figure 25d) could account for the 50-90 Ma reset ages over the metamorphic belt of the Cordillera Real, but there are plutonic rocks over this same cordillera which would suggest a process of normal subduction during this period. There are also other models for the emplacement of the Piñón terrane (e.g., Van Thournout et al., 1992).

Figure 25d indicates the origin of the Huancabamba deflection to be the change in strike from normal Pacific subduction (NW-SE trend) of Perú to the NNE-SSW-trending Pacific transform faults which were responsible for the accretion of the Piñón terrane. It also indicates the clockwise rotation of the Amotape block to have occurred at this time.

Since the Oligocene, the terrane mosaic which constitutes Ecuador has been thrust over the subducting Nazca plate producing uplift and shortening, most of which has been accommodated by the thrusting of the Cordillera Real over the Amazonic craton along the sub-Andean thrust belt. Thus, the sub-Andean 'cratonic' front remains as fundamental as it was in the Upper Triassic and Lower Cretaceous orogenies, the buttress of any stress system.

Most of the other old 'collisional' faults, even the east-trending Portovelo fault, have been reactivated from time to time during the Cenozoic history of Ecuador. It is thought (Litherland and Aspden, 1992) that extensional episodes along such structures may have acted as conduits for the cordilleran I-type magmas resulting from the subduction of the Nazca plate. This may be important in the search for mineralised porphyry systems.

NINE

Economic geology

PROJECT MINERAL SURVEY

The mineral survey was initially based on observations along the field traverses and laboratory analysis of the samples collected. Follow-up economic studies were then undertaken over the Cordillera Real, first by Clarke and Viteri, and later by Jemielita and Bolaños. These resulted in the progressive expansion of the mineral inventory accompanied by the increasing understanding of the metallogenic history.

Approximately 600 mineralised samples have been assayed, some in the INEMIN/CODIGEM laboratory, but most in commercial laboratories overseas. In addition, 320 stream sediments, wet sieved to 175 mesh (clay and silt) size, were collected from the Cordillera Real during the routine traversing and analysed for trace elements at INEMIN laboratory. Duplicates of half of these were later analysed by an overseas commercial laboratory for a greater range of elements. One hundred and seventy-two (172) stream sediments, wet sieved to 175 mesh, were collected from the El Oro area and analysed by a commercial laboratory overseas.

The 311 heavy mineral samples collected over the Cordillera Real during the routine traversing were analysed optically by Bermúdez. Two hundred and thirty of the samples were scanned by XRF by Ms. Arauz at the Quito Polytechnic laboratory.

The analytical results obtained from these samples can be found in the relevant open-file report, referred to in this section by their open file number (p.107). These reports are accompanied by traverse maps generally on a scale of 1:50000 which show the location of sample sites and prospects and the fully assay results. In this section locations are given by UTM or conventional coordinates depending on availability.

On the accompanying metal occurrence maps, the mines and main prospects are named and the highest values from the stream-sediment and heavy-mineral samples are plotted. It can also be appreciated from these maps that the project mineral survey followed the main access routes leaving many drainage basins unsampled.

PRECIOUS METALS

Gold and silver have been mined historically from the Cordillera Real and El Oro regions and there is good potential for further discoveries.

Gold (primary)

Between 1988 and 1992 about 13 tonnes per year of gold was reportedly produced in Ecuador, about 90 per cent of which was from primary (hardrock) sources. Of these 13 tonnes, about seven originated from mines within the Zamora batholith and three from Portovelo (Figure 27). Both these mining areas are shown on the accompanying map, though neither lies in the main study belts of metamorphic rocks.

The Cordillera Real has long been recognised as a major source of alluvial gold (p.86), but little was previously known regarding primary gold sources or metallogenesis. Thus, one of the main objectives of the project was the identification of primary gold mineralisation in the cordillera; and this section deals with such occurrences and their genetic classification.

VOLCANOGENIC MASSIVE SULPHIDE GOLD MINERALISATION

Pilas mine (**78°27'30''W, 1°44'35''S**) is located on the high *páramos* south of El Altar volcano. It comprises a band of massive, granular, bedded pyrite (Plate 18b) interbedded with granular quartz and sericite schist horizons within metavolcanic greenschists and sericite schists of the Alao-Paute unit (6). The pyrite bed is at least 7m thick and about 200m long and takes the form of a fold closing to the south, with steep west-dipping axial plane, and with green chloritic schists in the core and white sericitic schists in the envelope. Values of up to 479ppb Au were obtained from pyrite samples. Mina Pilas is an example of a volcanogenic massive sulphide deposit and presents an encouraging indication for potential Au-polymetallic mineralisation in the vicinity and elsewhere within the Alao terrane, e.g., Cerro Soroche south of Osogochi where strong sulphide mineralisation is reported.

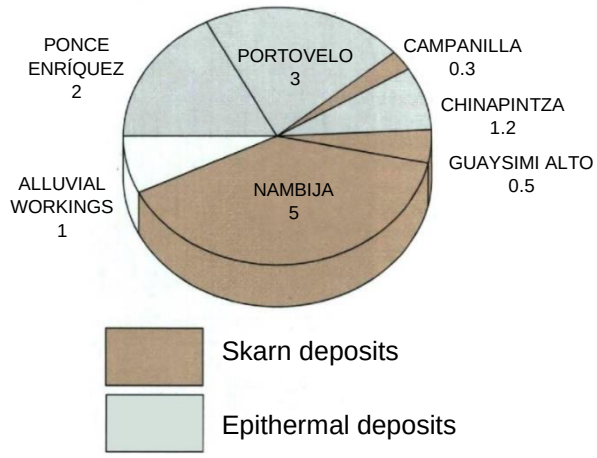

Figure 27. Approximate gold production figures in tonnes for Ecuador in 1990, from INEMIN-CODIGEM data.

a

b

Plate 18. Massive sulphides.

(a) Guarumales road surface outcrop: chlorite and sericite schists (top) and graphite schists (bottom) enclosing massive sulphides (photo: R. A. J.).

(b) Mina Pilas in the high cordillera: Richard Jemielita possess by the granular, bedded and folded, massive pyrite.

Guarumales prospect (**7780-97154**) (Plate 18a) is interpreted as another polymetallic volcanogenic massive sulphide deposit (p.95) occurring in metavolcanic and metasedimentary rocks similar to those at Pilas. Values of up to 2.5ppm Au were recorded (6).

VOLCANIC-HOSTED EPITHERMAL GOLD MINERALISATION

Anomalous gold values were obtained from epithermal-style mineralisation in Cenozoic volcanic and volcanoclastic lithologies of the Inter-Andean valley which lap onto the metamorphic basement on the high cordillera.

At **Cuchil prospect** (**78°48'W, 3°05'20''S**) near Sigsig, Au values of up to 4ppm were obtained (6) from a chalcedonic breccia within variously silicified, clay-altered and/or iron-oxide-(brown)-stained, porphyritic rhyolite lavas and breccias. The mineralised zone is a red-brown-stained, vuggy, grey, silicified rhyolite porphyry breccia with disseminated pyrite which forms a bed overlain by cream-coloured, rhyolite breccia. Similar rhyolites were observed in the outcrops west of Cuchil.

Also, near Sigsig, the **Loma Quipal prospect** (**78°47'W, 3°03'30''S**) has yielded gold and copper assay values (oral communication, A. Carter). The geology comprises andesite-dacite volcanic and volcaniclastic rocks overlying sheared Tres Lagunas granite. Alteration and mineralisation comprise weakly to moderately silicified and, in places, clay-altered host with disseminated pyrite in places. Blocks of porous and gossanous, acid-leached volcanic rocks with hematite, jarosite, quartz and alunite are present, in places stained by copper sulphate. Accessory gold values are reported from the nearby epithermal silver mine of San Bartolomé (p.94) whilst Pilzhum silver mine has ore grades of 3.2ppm Au (INEMIN-Misión Belga, 1988).

At **Cerro Colorado** (**78°55'W, 3°15'S**), an acid-leached, silicified, gossanous, porphyry breccia (Plate 23b) assayed up to 4.3ppm Au (6). Mineralisation comprises narrow, epithermal veins which cut the basement schistose granite of Tres Lagunas, and form wider zones of silicification within the overlying dacitic volcanic and volcaniclastic lithologies.

At **Cerro Pucurcu Grande** (**78°34'45''W, 2°19'35''S**), epithermal gold indications yield values up to 64ppm Au (6). The geology is dominated by Cenozoic lavas and volcanoclastic rocks which unconformably overlie steeply dipping metavolcanic and metasedimentary rocks of the Alao terrane. Cerro Pucurcu (Red Mountain) Grande is red in colour due to oxidisation of the disseminated pyrite-bearing feldsparphyric porphyry of which the mountain is composed and covers an area of about 3km^2.

More intense, but localised, alteration occurs in the surrounding region. These include the north-west slopes of Cerro Tintillay, to the east, where a narrow valley contains boulders of white-grey, altered and silicified andesite porphyry and breccia with fine- to medium-grained disseminated pyrite and chalcopyrite. Slightly further east, mineralisation also occurs west of Laguna Verde Cocha and nearby in the vicinity of Quebrada Yuracyacu, and also further north close to Atillo. Further mineralisation is suggested by names on the topographic sheet such as Cerro Pucurcu Chico and Quebrada de Minas, which were not visited during this survey.

Several newly discovered prospects of porphyry-related polymetallic epithermal vein, intrusive breccia and disseminated gold-silver mineralisation occur within the Zamora batholith. These prospects are related either to young Cenozoic intrusives or porphyries cogenetic with the host batholith. The **Chinapintza mining area** (**7690-95520**) is characterised by a suite of polymetallic epithermal quartz veins hosted in tuffs, feldspar porphyries and coarse-grained granodiorite of the Zamora batholith (3). Values of up to 363ppm Au were obtained (3) but average grade is estimated at 50 g/t (Gemuts et al., 1992). The mineralisation affects the Cretaceous Hollín Formation and is thus of Cenozoic age (oral communication, D. Coochey). The nearby **Biche prospect** (**7695-95515**) comprises sulphide-mineralised diatremes and intrusive breccia pipes cutting sulphide-rich (pyrite and sphalerite), silicified and quartz-veined, dacite-rhyolite tuffs and lava flows. Mineralised samples yield up to 10.9ppm Au (Gemuts et al., 1992). The nearby Pangui and Santoré prospects are breccia pipes; Tres Cerritos is an intrusive stockwork, and Jardín del Cóndor, a sinter deposit (oral communication, D. Coochey). Another prospect of probable epithermal origin occurs at Sangola (oral communication, P. Jeffcock). At the **Piuntza mine** (**78°52'30''W, 4°07'30''S**) gold mineralisation is associated with a central breccia and a network of quartz-sulphide veinlets cutting a quartz-feldspar porphyry plug. Values of gold from Project samples are up to 7.3ppm (3).

In the extreme south of the Zamora batholith, the **Los Planes prospect** (**78°59'W, 4°38'30''S**) consists of a series of quartz veins and quartz stockworks hosted by strongly weathered and argillised tuffs and andesite lavas which overlie the batholith. A sample of dense quartz stockwork yielded 233ppm Au (3). West of Los Planes in the Río Mayo, there are narrow copper-bearing veins in the Zamora batholith, one of which yielded 1.1ppm Au (3).

Over the El Oro area, the currently active Portovelo mining district corresponds to a porphyry-related epithermal polymetallic vein system (INEMIN-Misión Belga, 1988; Van Thournout et al., 1991), and other epithermal deposits occur to the north such as Ligzhu and Gañarín (Gemuts et al., 1992).

PORPHYRY-RELATED GOLD MINERALISATION

Fierro Urcu (79°19'44''W, 3°41'04''S) is a porphyry-related copper-molybdenum and precious metal vein prospect on the west of the Cordillera Real. Abandoned adits in the area follow polymetallic veins exploited in colonial times. Country rocks are Cenozoic andesitic to rhyolitic volcanic and volcaniclastic rocks intruded by dykes and plugs of granodiorite. The veins comprise milky quartz with tourmaline, pyrite, chalcopyrite, molybdenite and traces of enargite, stibnite and other sulphides. Values of up to 22ppm Au have been obtained from vein samples and an estimate of 53.5 million tonnes of mineralised rock containing 0.3ppm Au and 0.2 per cent Cu has been proposed (INEMIN-Misión Belga, 1988). Nearby, the **Loma del Loro prospect** (**79°16'20''W, 3°39'45''S**) exposes extensive clay-altered dacite porphyry (6) where values of up to 0.8ppm Au were obtained (6) from sulphide-mineralised, clast-supported, dacite porphyry intrusive breccia within the quartz-feldsparphyric dacite pluton. In the same area an intrusive breccia east of **Cerro Puglla** (**79°15'40''W, 3°37'20''S**) assays up to 0.2ppm Au and is characterised by silicified and pyritised porphyry clasts, in places with pink, crystalline alunite. Other gold prospects, believed to be porphyry-related, include those discovered recently at Mozo and Chachahuayco.

Peggy mine is characterised by polymetallic porphyry-related mineralisation yielding gold values up to 2.7ppm, but is dominated by silver content (p.95). To the east, in the vicinity of the confluence of the Río Santa Bárbara and Río Ayllón, quartz-arsenopyrite boulders from the river assay up to 5.2ppm Au. In the same area, a quartz vein containing arsenopyrite, pyrite and other sulphides has been mined about 500m downstream from the junction on the east bank of the **Río Santa Bárbara** (**78°44'W, 3°07'15''S**). Values between 46.5 and 635ppm Au have been obtained from this site (3). About 1km upstream from this junction, both banks of the **Río Ayllón** have hard-rock workings producing gold from a 50cm-thick quartz-pyrite-chalcopyrite-arsenopyrite vein which intrudes the basement schists of the Chigüinda unit. Such vein mineralisation at Santa Bárbara and Ayllón may be a gold-rich distal zone (Jones, 1992) related to the Peggy mine porphyry.

Porphyry-related gold mineralisation within the Zamora batholith is reported from El Hito where a copper-molybdenum system is developed within the batholith, both being overlain by Hollín Formation quartzites (oral communication, D. Coochey). Gold was panned in creeks draining the northern part of the prospect (Gemuts et al., 1992). Another Cu-Mo porphyry occurs at La Esperanza, whilst Jurassic porphyry-gold-type systems occur at Augusta (Gemuts et al., 1992), and probably at Shamataka and Cerro Quemado. In certain cases, it is unclear whether the mineralisation is Jurassic or Cenozoic in age.

Over the El Oro region, possible porphyry-related mineralisation has been recognised in the Cerro Pelado area, where there are several active and abandoned mines. At **El Guayabo mine** (**6275-96055**) the country rock comprises steeply dipping, sheared, fine-grained, black phyllites and quartzose schists of the Palenque unit, cut by a semiconcordant vein, 50-100cm wide, composed of quartz, arsenopyrite and pyrite with average gold assays of 7ppm (7). This deposit may be of shear-zone-hosted type. The nearby recently discovered **Cerro Pelado mine** (**6278-95062**) is located in flat-lying rhyodacitic volcanic rocks with the mineralisation related to a breccia pipe (7).

GOLD SKARN MINERALISATION

The gold skarnfield of **Nambija** (Salazar, 1988; Clarke (3); (5); (6); McKelvey, 1991; Litherland et al., 1992) within the Zamora batholith, is presently the most economically important occurrence of gold mineralisation in Ecuador (Figure 27). The Nambija deposit was worked during colonial and pre-colonial times (Navarro, 1986), but was only rediscovered in 1982, and has since become the site of a modern gold rush, producing, by primitive and wasteful means (Plate 19a), about 30 tonnes of gold up to 1991. The Nambija mining area is about 1km long and 100m wide and of unknown depth. Gold is often visible in hand specimen, and some skarn pockets yield grades up to 400ppm Au.

The skarns occur as pockets within a strip of the Triassic Piuntza unit which forms a north-south-trending hill range about 30km long and 2km wide. The strip is interpreted as a roof pendant of the Jurassic Zamora batholith which underlies the surrounding area of lower relief. The Piuntza unit comprises marbles, sandstones andesitic-dacitic lavas and tuffs. Over the Nambija skarn-field, gold-bearing skarns have been mined at Fortuna, Cambana, Campanilla, Nambija, Guaysimi and Sultana del Cóndor, from north to south along the central part of the hill outcrop.

At **Campanilla** the Piuntza unit is well exposed in mine workings. The plutonic phase of the Zamora batholith is exposed at lower altitudes, but the critical contact between the two has not been studied. The stratigraphic sequence has a maximum thickness of a few hundred metres and comprises coarse- and fine-grained beds interpreted as volcaniclastic breccias and tuffs respectively. The beds are intruded in places by basic dykes and small monzonite porphyry dykes and plugs of possible Tertiary age; magnetite blocks have been noted in adjacent streams. The skarnification and gold mineralisation appear to be controlled by north-east-trending brittle faults intersecting the major north-trending faults. The mineralised structures are subvertical and cut the open-folded Triassic sequence. The extent of the mineralisation away from the faults is controlled by the stratigraphy, with lateral skarnification wider in fine calcareous tuff beds and narrower in the coarser breccias. Ore shoots form where late veins intersect these skarn rocks.

a

b

Plate 19. Skarn mineralisation (see also Plate 5).

(a) The El Playón sector of the Nambija mining camp: exploitation of gold skarn pockets (photo: R. A. J.).

(b) Boulder in the Río Mulatos of massive, pink grandite skarn cut by shear zone with quartz veining and weak mineralisation. The boulder is probably derived from the El Placer field (photo: M. L.).

At the Nambija and Campanilla mines gold mineralisation occurs as nuggets, blebs or fine disseminations associated with quartz-carbonate-adularia veins within the skarn rocks (see p.27 for skarn petrography); although traces of gold have been noted in host breccias (McKelvey, 1991). The veins with native gold are narrow discontinuous 'sweats' with white to grey, translucent and massive quartz. In thin section this quartz is clear, unstrained and poikilitic and formed at epithermal temperatures (Plate 22c). Such veining and accompanying gold mineralisation is characteristic of late-stage alteration of grandite-rich skarns (Meinert, 1988) and thus does not have to be explained by a later, post-Jurassic, thermal event. Pyrite, magnetite and chalcopyrite are fairly common and galena and sphalerite have also been noted, but the deposit is essentially poor in base metals compared to the nearby epithermal deposits such as Chinapintza. Silver, too, is low, with an average Ag:Au ratio in assays of 1:20 (3), a ratio similar to that noted in the gold analysis (Table 4).

A second, but ill-defined, approximately north-trending skarn belt also occurs in the Zamora batholith east of Nambija. It encompasses the María Elena banded magnetite-rich skarn and the Napintza and Congüime deposits (Gemuts et al., 1992; oral communication, D. Coochey).

There are enormous volumes of rock in the **northern skarnfields** of the Cordillera Real (p.33), but significant gold values have yet to be proved. Up to 15ppm Au was analysed from skarn blocks in the Río Mulatos derived from the El Placer and Inga skarnfields (1), but though these values were confirmed elsewhere, chips from the same samples yielded no gold. Little or no gold was panned from the Río El Placer and upper Río Mulatos; and the highest value obtained from rock samples from the El Placer field was 46ppb Au (2). This would indicate the El Placer field to be essentially barren.

Other northern skarnfields may be more promising. L. Torres (oral communication) has identified Au-Ag mineralisation in the Inga skarnfield which may be the source of the Río Cedroyacu placer gold. Further north, a sphalerite-mineralised boulder in the Río Quijos, above the Papallacta confluence, and possibly derived from the Urcucocha field, gave 0.5ppm Au (4). There may be skarnfields around Oyacachi (Litherland et al., 1992b), where gold is reported to have been worked; and mineralised skarn rocks may be the source of the Cofanes goldfield in the extreme north of the cordillera.

GRANODIORITE INTRUSION-RELATED GOLD MINERALISATION

Lithologies of the Guamote Terrane are intruded in the **Río Quishpe** (**78°32'W, 1°49'30''S**) by the Tertiary Alao granodiorite pluton which hosts auriferous polymetallic vein mineralisation (6). Around **Río Ishpingo** (**78°37'30''W, 3°01'S**), a sulphide-mineralised biotite granodiorite which intrudes the Chigüinda unit yielded up to 319ppb Au (6). Other gold values were found from Amaluza and Río Isimanchi (6).

MESOTHERMAL QUARTZ-GOLD VEIN MINERALISATION

In the south of the Cordillera Real, at **Cera**, gold has been mined from narrow, quartz-ankerite-pyrite veins in sheared black and grey schists of the Chigüinda unit (6). East of Loja, Wolf (1892) described similar mineralisation from Cerritos de Calvario. At Masanamaca, between Vilcabamba and Yangana, gold has been worked from quartz veins in black and grey schists of the Chigüinda unit along the **Quebrada de Minas** (Wolf, 1892). A mine was visited with a similar geological setting along the **Río Chiriguana** (**79°09'W, 4°21'15''S**) (6). At Chigüinda (p.97), a 2km-wide section of grey mica schists is hydrothermally altered and pyritised (6); values of up to 1 ppm Au were obtained at one locality.

Curiayana mine (**78°28'45''W, 1°51'30''S**), near Alao, follows two narrow quartz veins, 15cm wide, which cut the Alao-Paute greenschists. Sulphides occur near the walls of the veins and include pyrite, chalcopyrite, sphalerite and galena. Free gold was obtained from the oxidised veins. Wallrock alteration is absent or inconspicuous, but the veins are oxidised and show brown iron staining. This mineralisation is considered to be polymetallic, hydrothermal vein type (6).

In El Oro, alluvial and hard-rock gold are worked intermittently at **Sacachispas mine** (**79°46'W, 3°20'45''S**). The host rock consists of weathered, sericite quartz schists of the Palenque unit which carry concordant and discordant irregular quartz veins and stringers containing iron oxides and minor quantities of free gold (7).

The widespread occurrence of massive, mesothermal vein quartz as boulders and pebbles in auriferous gravels (p.87), terrace alluvium and sedimentary formations strongly suggests that much of the alluvial gold of the cordillera is derived from mesothermal vein quartz mineralisation. This is especially apparent over the Shincata-Betas sector (p.87).

OTHER GOLD MINERALISATION

Gold has been reported from **mafic-ultramafic complexes**. Free gold was reported by a private company from the Tampanchi complex (**7618-97082**), and one sample of unmineralised pyroxenite, collected for petrographic studies, gave 176ppb Au (3). A little gold was analysed from the serpentinites at Peltetec and Huarguallá (1), but this has not been confirmed by reanalysis.

Gold was panned from streams draining west from the **pegmatite belt** (**77°46'45''W, 0°32'N**) south-east of San Gabriel (4). One rock sample yielded 69ppb Au (6).

At **Monte Olivo** prospect (**77°52'45''W, 0°23'35''N**), a prominent 10m-wide roadside exposure of white-yellow-red-brown-coloured and hydrothermally altered amphibolite of the Monte Olivo unit forms a feature across the valley. Alteration is sericitic and kaolinitic. No sulphides were noted, but channel samples assayed up to 0.45 ppm Au.

Gold (secondary)

Alluvial gold (Plate 22a and b) is widespread in the drainage systems of the Cordillera Real and has been exploited since pre-colonial times, and almost all the small towns of the eastern foothills can trace their origins to Spanish mining settlements (Holloway, 1932; Navarro, 1986). Artisanal miners still exploit these rivers (Pillajo, 1982; Pillajo and Báez, 1986; 6) using relatively primitive methods (Plates 20 and 21). Production is in the region of 500 kg/yr. Gold is also won from palaeoplacer deposits. Details of these secondary goldfields can be found in Jemielita and Bolaños (6).

PALAEOPLACER DEPOSITS

Gold is found in coarse clastic sedimentary formations of Late Cretaceous and Cenozoic age within and east of the Cordillera Real. In the east, the Tena, Tiyuyacu, Arajuno, Chambira and Mera Formations of the Oriente (Pillajo and Báez, 1983; 6) are deposits related to stages of uplift and erosion of the gold-bearing metamorphic basement of the cordillera. Gold has also been noted in the Middle Cretaceous Hollín Formation quartzites near Chinapintza (oral communication, D. Coochey), but this may be derived from the weathering of the metamorphic rocks of the Amazonic craton (Wilkinson, 1982).

Gold was panned from the Tena Formation and studies made of the **Tiyuyacu Formation** during the present survey (6). South of Puerto Napo the Eocene Tiyuyacu sediments comprise poorly lithified beds of purple-brown, coarse sands and gravels, dominated by rounded, well-sorted pebbles of massive, white, mesothermal vein quartz, as well as grey microcrystalline quartz and mica schist. This unit, with a strike length of over 300km, is considered to be an important potential source of alluvial gold in the Oriente east of the accompanying maps, and perhaps the only source in certain rivers with no drainage link to the cordillera, e.g., Cushimi and Payamino (Pillajo and Báez, 1983).

In the Cordillera Real at the headwaters of the **Ríos Shincata-Betas** (**79°02'W, 3°28'S**), there are palaeo-river terraces which are rich in gold and have a long history of exploitation (Wolf, 1892). Pre-colonial, possible pre-Inca workings are common, and mechanised and artisanal mining is presently active. The terraces are perched tens of metres above the present river and comprise poorly sorted, and poorly to well-bedded, mature, unlithified, quartz-tourmaline pebble gravels or conglomerates. These deposits, the Bestión Formation of Pillajo and Báez (1983) (Plate 20b), contain pebbles of rounded, black tourmaline mixed with those of pure mesothermal vein quartz, and quartz pebbles containing needles and masses of black tourmaline are common. The tourmaline pebbles are named *piedras tibias* (warm stones) by the miners who take their presence as an indication of gold-bearing material. The gold is bright golden yellow, irregular shaped to subrounded, thin, flat plates, pellets and rods (6) and its morphology suggests a proximal source (Grant et al., 1991). The pebbles are derived from mesothermal quartz veins similar to those noted cutting the nearby schists. The quartz-tourmaline association is thus common to the palaeo-river terrace alluvial deposits and the basement-hosted veins.

Quartz and tourmaline pebbles occur commonly in alluvium from the Río San Antonio, east-north-east of Saraguro, through the Shincata-Betas headwaters area north-east to the Río Minas, east of Gima, a distance of 50km along the strike. It appears that over this strike length, which is close to the trace of the Baños fault, tourmaline occurs only in those quartz veins which cut the Tres Lagunas granite.

Another palaeoplacer occurs at **Nayumbi** (**7645-95380**) in the east of the Zamora batholith area where a 200-300m-thick auriferous palaeo-alluvial deposit is preserved in a Tertiary graben structure (oral communication, D. Coochey).

ALLUVIAL GOLD

In the Cordillera Real, the alluvial gold is worked in active river sediments and incised river terraces (Plate 20a and c). The deposits are generally narrow and elongate (Pillajo and Báez, 1983) and occupy steeply incised river valleys. The volume of auriferous material is usually small and the sediments are polymictic and very immature; large boulders are common. Only artisanal methods are used to extract this gold and it is unlikely that large-scale commercial dredging operations would be economical in these areas.

Eastwards, away from the steep slopes of the cordillera, flatter terrace areas are auriferous in places. The Río Palora-Río Sangay area (**78°08'W, 1°52'S**) is characterised by wide terraced valleys (Plate 21a) with gold workings in the polymict terrace gravels which appear to lack large boulders. An extensive horizon of volcanic lahar from Sangay Volcano underlies the alluvium and provides a 'false bed' to the auriferous gravels. These may cover several square kilometres and may be amenable to dredging operations. Extensive auriferous alluvial terraces also occur around Tena (Plate 21b) (6).

Table 3 summarises some of the results of the detailed Project studies (6) considering only the area of the accompanying maps. The data indicate rivers and areas of alluvial gold production together with an indication of source-rock metallogenesis based on field observations. Thus, for the Cordillera Real a mesothermal quartz vein source predominates, whilst for the Cordillera del Cóndor and El Oro, skarn-, epithermal- and porphyry-related mineralisation is more important.

Gold analysis

Gold analyses over the Cordillera Real and El Oro have been undertaken by Wolf (1892) and this project (Beddoe-Stephens, 1987; 1989; Styles et al., 1992). One of the objectives of the present work was to characterise gold grains from bedrock and alluvial sources to establish whether variations in gold may be used to 'fingerprint' primary sources. Samples from primary and alluvial sources have been analysed for morphological studies, and quantitative electron microprobe analysis of gold grains and their contained inclusions have been undertaken, together with microchemical mapping of the primary gold where available.

a

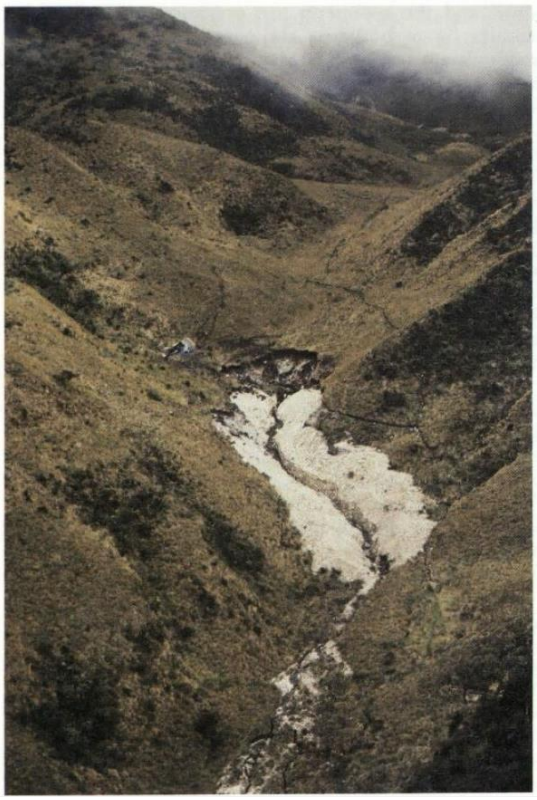

b

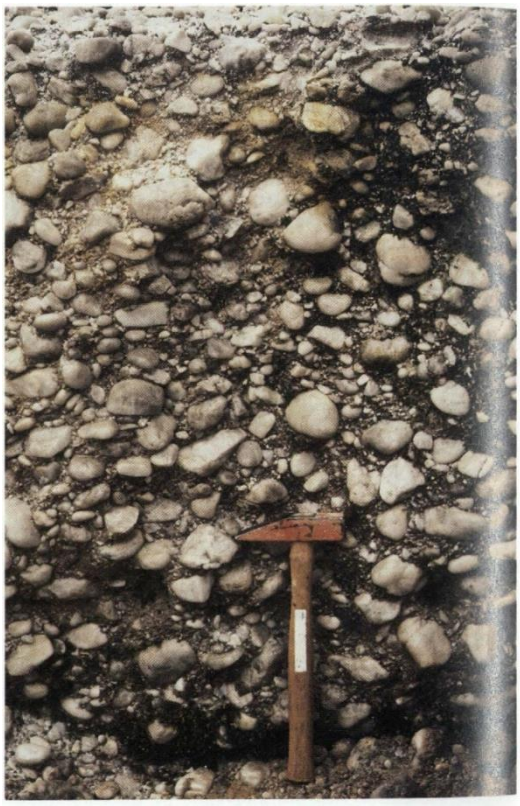

c

Plate 20. Secondary gold in the highlands.

(a) Alluvial/colluvial gold workings west of the cordillera watershed on the *páramos* of Matango/Río Minas (photo: R. A. J.).

(b) Details of Bestión Formation of Pillajo and Báez (1983), west of the confluence of the Ríos Betas and Shincata: pebble gravels of vein quartz ± tourmaline ± gold (photo: R. A. J.).

(c) View east along upper reaches of Río San Francisco, east of Gualaceo: placer gold workings on south bank river (photo: R. A. J)

a

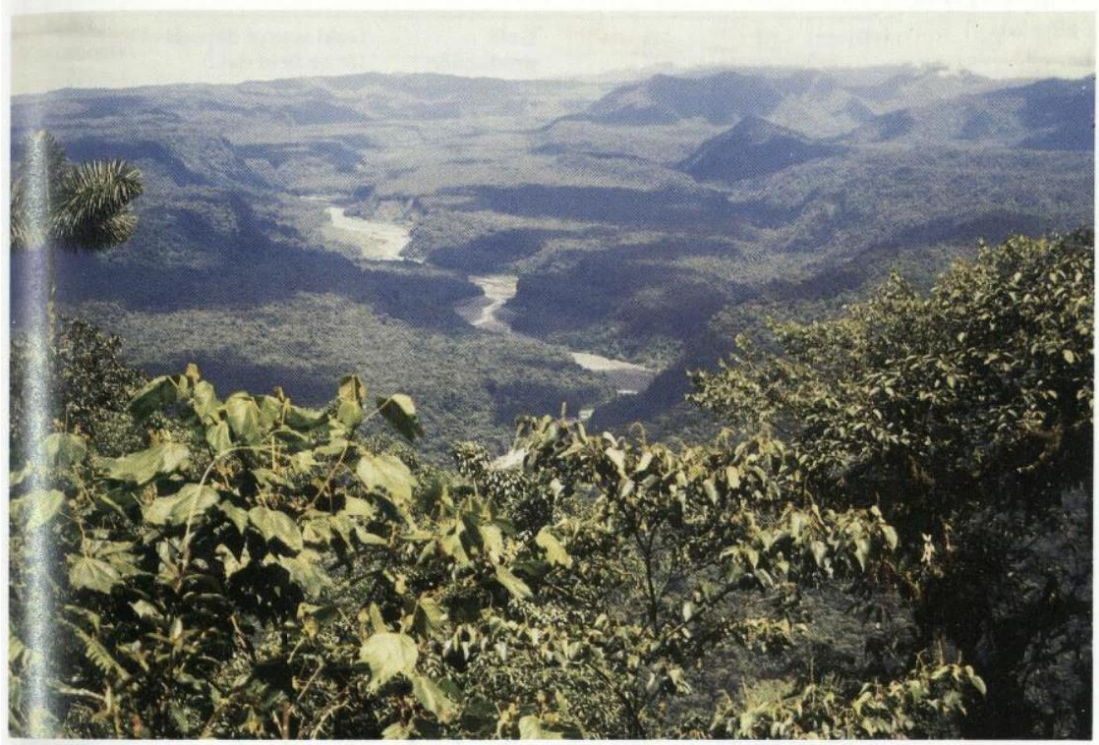

b

Plate 21. Alluvial gold in the lowlands.

(a) View south showing the wide, auriferous, terraced valley of the Río Sangay from the Palora/Sangay river confluence (photo: R. A. J.).

(b) Family group washing gold in the Sardinas area of the Río Jatunyacu (photo: R. A. J.).

Table 3. Summary of alluvial gold deposits

River (north-to-south)	**Gold production**			**Gold source deposit (**from field data)					
	Substantial	Moderate to low	Little or no	Massive sulphide	Epithermal	Porphyry-related	Skarn-related	Granodiorite-related	Mesothermal vein
Northern Cordillera Real									
Chingual			x			x	x		x
El Dorado			x			x			x
Cofanes-Aguarico		x					x		x
Oyacachi			x			x			x
Quijos			x			x	x		x
Cosanga			x				x		x
Verdeyacu			x			x	x		x
Cedroyacu-Chalupas		x				x	x		x
Mulatos-Jatunyacu		x	x			x	x		x
Central Cordillera Real									
Llushín		x				x			●
Palora		x		x		x			●
Quishpe		x						●	
Alao			x	x		x		x	x
Upano-Abanico		x		x				x	●
Paute		x	x	x	x	x		x	x
Negro-Tayuso	x	x	x		x	x			x
Yanganza		x				x			x
South-Central Cordillera Real									
Collay		x			x				●
San Francisco		x							●
Ishpingo		x						x	●
Gualaceño		x							●
Shío		x			●				
Santa Bárbara-Ayllón		x				●			x
Sangurima-Blanco	x	x				x			●
Moriré-Cuyes		x				x			●
Amarillo		x				x			●
Shincata-Betas	x	x							●
Yacuambí		x				x			x
Southern Cordillera Real									
Zamora		x							●
Malacatus			x		x				●
Jorupé			x						●
Piscopamba			x						●
Numbala			x			x			x
Vergel		x			●				
Palanda			x			x			x
Mayo		x				x			x
Isimanchi			x			●		x	x
Sangolá			x		●				
Cordillera del Cóndor									
Zamora	x	x	x			x	●		x
Bomboscara			x			x			x
Jamboe			x			●			
Nambija		x					●		
Nangaritza	x	x	x		●	x	x		
Cambana		x					●		
El Oro									
Jubones		x			x	x			
Caluguro	x					●			
Naranjo		x				x			x
Amarillo		x			●				

● major component

The analyses of primary gold indicates that silver content is low in skarns but increases in porphyry-related and epithermal gold (Table 4). This supports the correlation of Ag content with crustal maturity (Boyle, 1977), with the Ag/Au ratio rising in younger and shallower metal deposits.

Table 4 shows, for the Cordillera Real, a high component of low-Ag alluvial grains which probably correspond to mesothermal gold, since skarns are absent over most of the source areas.

Tables 3 and 4 thus both indicate, from different criteria, that mesothermal and porphyry gold predominates in the Cordillera Real. However, in the Cordillera del Cóndor although the low-Ag gold is skarn-related, the alluvial gold collected only 1km downstream from Campanilla mine is observed to be already mixed with gold from higher crustal levels or lower temperature veins at Campanilla (Table 4). The gold from Río Piuntza, however indicates that the Piuntza prospect is not skarn-related.

Table 4. Variations in gold composition

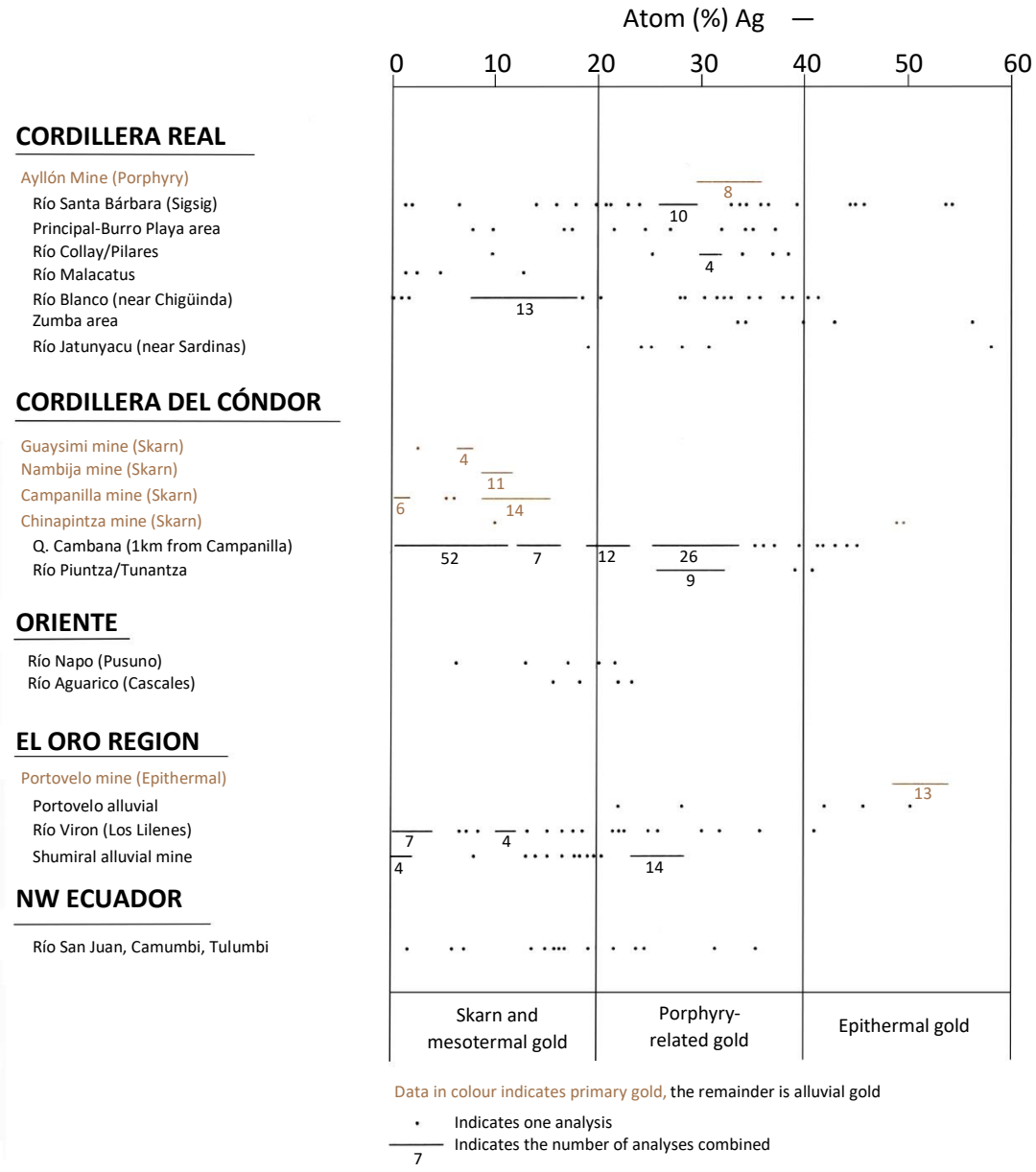

Samples from Portovelo mine in the El Oro region are indicative of epithermal gold, yet the alluvial gold from Los Lilenes draining Cerro Pelado, and Shumiral draining the Ponce Enríquez deposit (not on the area of accompanying map), have a remarkable high content of low-Ag gold which can only be explained by the presence of mesothermal veins, since no skarns have been reported.

The study of inclusions in alluvial gold from Campanilla (Styles et al., 1992) shows them to be representative of the source region. They comprise both the base metals seen in the bedrock samples and the rarer Bi and Ag-Au tellurides (Plate 22e). However, the microchemical mapping of gold grains showed a lack of internal chemical variation. This may be due to the gold at Campanilla forming at temperatures where internal variation is readily destroyed by annealing of Au-Ag alloys.

Silver (Ag)

Since colonial times, hard-rock mining in the Cordillera Real has been dominated by silver production. No figures are available but several locations, e.g., Cubillín, Tungurahua, Condorazo and Pilzhum are mentioned in Navarro (1986). Occurrences of silver mineralisation are also indicated on the DGGM/INEMIN/CODIGEM geological map sheets Nos. 56, 72 and 73, and in Ribadeneira (1960) and Goossens (1972a). Many new occurrences are noted here.

Silver occurs widely as an accessory metal in gold and/or silver polymetallic mineral deposits and prospects. High silver values are usually related to hydrothermal mineralisation and alteration associated with andesite to rhyolite porphyry intrusions and volcanic to volcaniclastic rocks. The mineralisation ranges from mesothermal to epithermal in character, the latter type generally being preserved only in the younger Tertiary deposits.

a

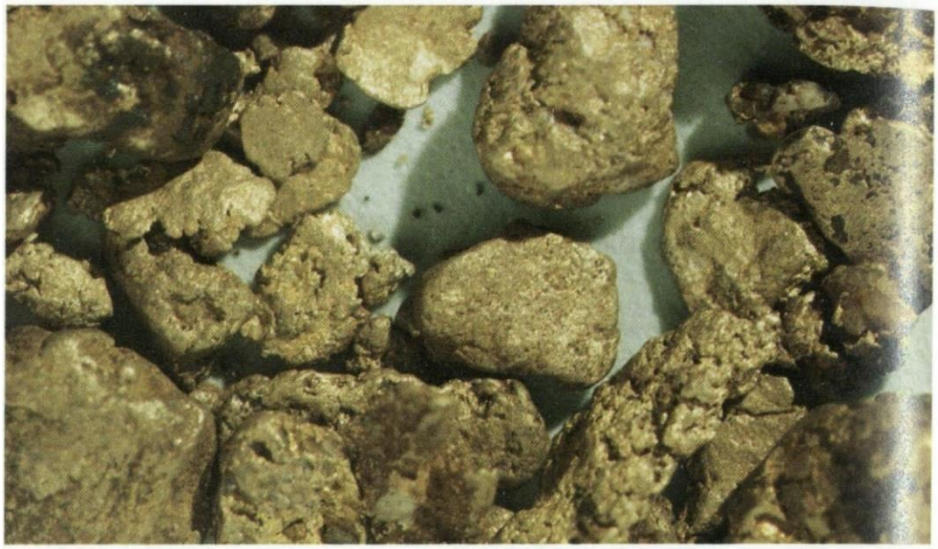

b

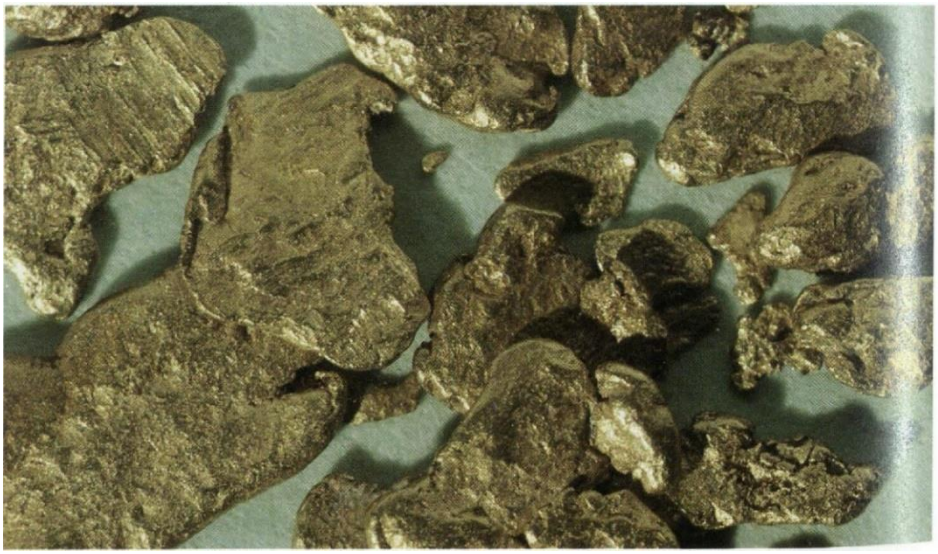

c

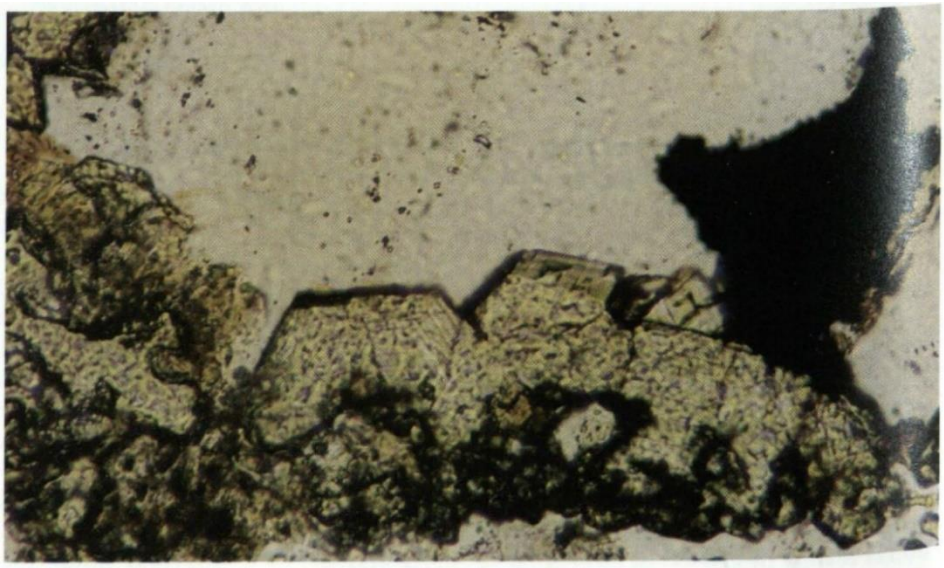

Plate 22 Gold grains.

(a) Irregular-shaped, coarse alluvial gold from 1km downstream from Campanilla mine in Quebrada Cambana (×9).

(b) Flat, platy alluvial gold with distal source from the Río Jatunyacu (×9).

(c) Photomicrograph of gold (opaque) adjacent to garnet at the contact between quartz vein and country rock in rock sample from Campanilla mine (×210).

(d) Hair-like gold grains in vugs in quartz in rock sample from Portovelo (×42).

(e) Reflected light micrograph of gold (gold colour) and types of bismuth telluride (pale yellow) in rock sample from Campanilla (×60).

(f) Reflected light micrograph of alluvial gold grain, from Río Blanco near Chigüinda, with inclusion of galena with arsenopyrite (×300).

For details of (c)-(f) see Styles et al. (1992).

d

e

f

VOLCANIC-HOSTED EPITHERMAL SILVER MINERALISATION

San Bartolomé mine (**78°51'26''W, 3°00'50''S**) was discovered during the UNDP survey (Fozzard, 1985). At present it is an operating mine (Puig and Pazmiño, 1990) as opposed to a small-scale working. Mineralisation occurs within fine- to coarse-grained Tertiary andesitic porphyry lava flows, and is hosted within fracture veins, 5 to 10 cm wide, and veinlets. These are of steep and flat types and trend dominantly east-north-east. The main silver mineral is freibergite, a silver-rich tetrahedrite, along with sphalerite, pyrite, marcasite, galena, chalcopyrite, sulphosalts, arsenopyrite, native arsenic, pyrrhotite, boulangerite, polybasite, pearcite, sternbergite, pyrargyrite, freieslebenite and native gold. Reserves are estimated at 100000 tonnes with average grades of 560 g/t Ag, 0.55 g/t Au, 0.57% Pb and 1.86% Zn (UNDP, 1972; INEMIN-Misión Belga, 1988; 6).

Pilzhum mine (**7482-97072**) presently abandoned, has long been known as a silver-producing area (Wolf, 1892; Spindler and Herrera, 1959; INEMIN-Misión Belga, 1988; 6). The country rock is a quartz andesite or dacite porphyry stock of Upper Cenozoic age. Mineralisation occurs within 23 known veins occupying a 3×2 km area; the principal veins are up to 600m long. Mineralisation is complex epithermal type with pyrite, chalcopyrite, galena, sphalerite, enargite, tetrahedrite, proustite, bornite, chalcocite and covellite; reported grades are 1500 g/t Ag, 3.2 g/t Au and 2% Cu. The mineral system is large and the economic potential good for the discovery of further veins and breccia-hosted and porphyry-type mineralisation (6).

Other epithermal prospects carrying silver values include Chinapintza (p.83) with up to 250ppm reported (3); Los Planes (p.83) with 62ppm Ag (3); and Piuntza (p.83) with 38ppm Ag (3). High Ag values are also associated with altered and mineralised dacite-rhyolite porphyry intrusions and associated intrusive breccias such as Loma del Loro (p.84) with 11ppm Ag (6), Cerro Puglla (p.84) with 0.4ppm Ag (6), Río Collay (**78°39'45''W, 2°53'S**) with 13.1ppm Ag (6), and Gima-Cerro Colorado (p.83) with 6.8ppm Ag (6). In addition, high Ag values occur in altered and mineralised andesite to rhyolite porphyry, volcanic and volcaniclastic rocks at Cuchil (p.83) with 1.7 ppm Ag (6), Principal (**78°43'15''W, 3°02'10''S**) with 0.9ppm Ag (6), Cerro Pucurcu Grande (p.83) with 1.8ppm Ag (6), and Atillo (**78°32'45''W, 2°10'25''S**) with 0.3ppm Ag (6). The colonial Cubillín and Tungurahua deposits cited by Navarro (1986) are probably of this type.

Over the El Oro area there are many gold and silver epithermal prospects. At the Portovelo mining area (Van Thournout et al., 1991) reserves are estimated as 120000 tones at 63ppm Ag (Delbridge and Robertson, 1992).

OTHER SILVER MINERALISATION

Volcanogenic massive sulphide mineralisation at the Guarumales prospect (p.95) gave values of up to 400ppm.

Porphyry-related silver mineralisation has been identified at Fierro Urcu (p.83) which was exploited in colonial times for silver and gold. Silver assay values up to 1464ppm have been reported (INEMIN-Misión Belga, 1988). Peggy mine (p.95) carries significant silver values, many mineralised samples exceeding 50 ppm Ag (6) and values of up to 222ppm have been reported (3). East of Peggy mine, the Ayllón-Santa Bárbara workings (p.84) yielded values greater than 50ppm Ag (6) reaching 246ppm (3). At Río Isimanchi (**6784-94720**) 49ppm Ag was recorded (3). The Cerro Pelado mining area of El Oro is porphyry-related (p.84) and shows high silver values in streams (below).

Granodiorite-related silver mineralisation shows the following maximum values: 28.9ppm Ag from Ishpingo (p.86) (6); 5.5ppm Ag from a mineralised zone along the Amaluza granodiorite (**78°34'05''W, 2°35'20''S**) (6); and 0.3ppm Ag from close to the Colimbo pluton west of Macas (**78°12'20''W, 2°15'50''S**) (6).

Shear zone-hosted silver mineralisation at Laguna Negra, near Atillo (**78°30'W, 2°10'20''S**), gave 0.9ppm Ag (6), and in the Chigüinda deposit (p.97) 1ppm Ag was recorded (6).

Skarn-related silver mineralisation is present at Nambija and an assay of 17ppm Ag was recorded. One of the remarkable features of this deposit, however, is the low proportion of silver to gold (Table 4). Over the northern skarnfields, values reach 5.8ppm Ag at El Placer (**78°12'30''W, 1°00'30''S**), whilst the Zn-mineralised block in the Río Quijos, possibly derived from the Urcucocha field, gave 2.8ppm Ag (4). Likewise, the Zn-mineralised 'skarn' from Quebrada La Industria (**2181-00454**), derived, possibly, from an undiscovered field near La Bonita, gave 2ppm Ag (4).

SILVER STREAM GEOCHEMISTRY

High silver values from 5 to 15.2 ppm in the El Oro area correspond to the sectors of known mineralisation of Cerro Pelado and the La Tigrera mining area to the north of the accompanying map. Over the Cordillera Real, values are rarely greater than 1ppm Ag.

BASE METALS

Base metals have been worked at Peggy mine, and lead and zinc are presently being exploited as a by-product of the San Bartolomé silver mine. The metals are mostly concentrated in polymetallic veins, breccias and stratiform deposits.

Numerous other indications and occurrences of copper, lead and zinc have been noted as single metals or polymetallic mineralisation (Goossens, 1969; 1972a, and geological map sheets). Many more have been located during the present survey.

Copper (Cu), lead (Pb) and zinc (Zn)

VOLCANOGENIC MASSIVE SULPHIDE Cu-Pb-Zn MINERALISATION

This primary stratiform mineralisation (Hutchinson, 1980) is believed to be manifested at **Guarumales prospect**, where black, grey and green, steeply dipping schists of the Upano unit on the east bank of the Río Paute contain an approximately 60m section of strongly mineralised schists and massive polymetallic sulphides exposed as iron-oxide-stained rocks in a roadcut (Plate 18a) (6). The mineralised rock is principally white and green mica schists with fine- to medium-grained disseminated pyrite; massive sulphide beds range from 10cm bands of granular, bedded and folded, polymetallic sulphides (pyrite, chalcopyrite, galena and other sulphides) to metre-thick beds of massive pyrite. Assay values range up to 1.32% Cu, 7.97 % Pb and 12.62% Zn, together with high or anomalous Au, Ag, As, Sb, Bi, Cd, Ba, Mo, W and Sn. To the north, in the same Upano unit, along the Río Upano, traces of copper mineralisation were noted in four volcaniclastic greywacke localities (1) which may be a tectonically repeated formation.

Greenstones and metasediments similar to the Upano unit are found to the west as the Alao terrane. At Mina Pilas (p.81), no base metal values were recorded (6), but the mineralisation is considered to be a volcanogenic massive sulphide, and could indicate potential for base metals elsewhere in the Alao-Paute and El Pan units. South of Pilas there are reports of strong sulphide mineralisation at Cerro Soroche (**78°32'30''W, 2°20'S**) near Osogochi. Cu mineralisation, of possible stratabound type, has also been noted in the volcanosedimentary rocks of the Maguazo unit near Quebrada Totora Yacu (Río Paute) (2).

VOLCANIC-HOSTED EPITHERMAL Cu-Pb-Zn MINERALISATION

This type of mineralisation has been recognised in Tertiary volcanic rocks at various localities. At the San Bartolomé silver mine (p.94) lead and zinc are currently mined as a by-product; copper mineralisation occurs in the Pilzhum silver mine (p.94). At **Cerro Minas-Malacatus** (**79°16'13''W, 4°13'16''S**), Wolf (1892) reported galena, silver, zinc, and fluorspar at Cerro de Santa Cruz (Cerro Minas), where silver and gold values are associated with zinc and copper sulphides (6) in an epithermal intrusive breccia with fluorite-bearing trachyte dykes. The Osogochi-Atillo mineralised volcanic rocks assay up to 2730ppm Cu (6), and a sample of mineralised dacite at Río Tintas near Principal yielded 7189 ppm Cu (3).

In the Chinapintza gold mining area (p.83), in the Cordillera del Cóndor, a suite of Cu-Pb-Zn-bearing epithermal quartz veins within granodiorite, tuffs and feldspar porphyries yield values of up to 0.04% Cu, 0.11% Pb and 5.27% Zn associated with Au and Ag, and sphalerite, argentiferous galena, pyrite, pyrrhotite and chalcopyrite have been identified (3). The nearby prospects of Santoré, Tres Cerritos, Pangui and Biche (p.83) are similar in type (oral communication, D. Coochey; Gemuts et al., 1992).

PORPHYRY-RELATED Cu-Pb-Zn MINERALISATION

Peggy mine (**78°46'23''W, 3°05'45''S**) (3; 6; de Coster, 1987: INEMIN-Misión Belga, 1988) is a mineralised sector within an area where a suite of undeformed quartz-feldspar porphyry dykes and stocks intrude strongly deformed and mylonitic megacrystic biotite granite of the Tres Lagunas suite. Mineralisation in the 'Peggy vein' (Plate 23a) comprises a porphyry-related, mesothermal polymetallic pebble dyke about 10m thick. There is also a mineralised intrusive breccia pipe, dominated by country rock schist fragments, exposed for 35m in a roadcut 1.5km north of Peggy mine (Plate 23c) (6). Mineralised breccia dykes and veins were also noted in the mining area. The mineralisation is complex, polymetallic, vein/stockwork and mineralised breccia, with the following ore minerals reported: chalcopyrite, pyrrhotite, arsenopyrite, pyrite, marcasite, stannite, cassiterite, sphalerite, native bismuth, bismuthinite, wolframite and galena. Cu and Zn assay up to 2% and Pb to 1%, and these metals have been mined this century.

Close to Peggy are the Ayllón-Santa Bárbara workings (p.84) which assay up to 2113ppm Cu, 17300ppm Pb and 30700ppm Zn (6). Fierro Urcu (p.83), near Saraguro, is a porphyry-related Cu-Mo and precious-metal prospect. Further south, Los Juanes south of Catamayo was reported by Wolf (1892) as a porphyry related copper deposit. To the south, **Uritohauser** (**79°21'40''W, 3°51'10''S**) is a porphyry-related Pb-Zn prospect close to the contact between a granodiorite intrusion and andesitic volcanic rocks. Mineralisation occurs as quartz veins associated with disseminated galena, sphalerite, pyrite and chalcopyrite (INEMIN-Misión Belga, 1988). In the extreme south, the Río Isimanchi prospect gave values of up to 3626ppm Cu, 1318ppm Pb and 10457ppm Zn (6).

The **El Hito** porphyry copper prospect (**7690-95440**) is located in the south-east of the area where coarse-grained porphyritic granite is intruded by quartzfeldspar and hornblende-pyroxene porphyries. Alteration comprises an outer propylitic halo with an inner sericite-pyrite core (Gemuts et al., 1992).

In the El Oro sector there are many polymetallic prospects related to porphyry intrusions including the Cerro Pelado area (p.84) and the Zaruma-Portovelo mining district (INEMIN-Misión Belga, 1988; Van Thournout et al., 1991).

a

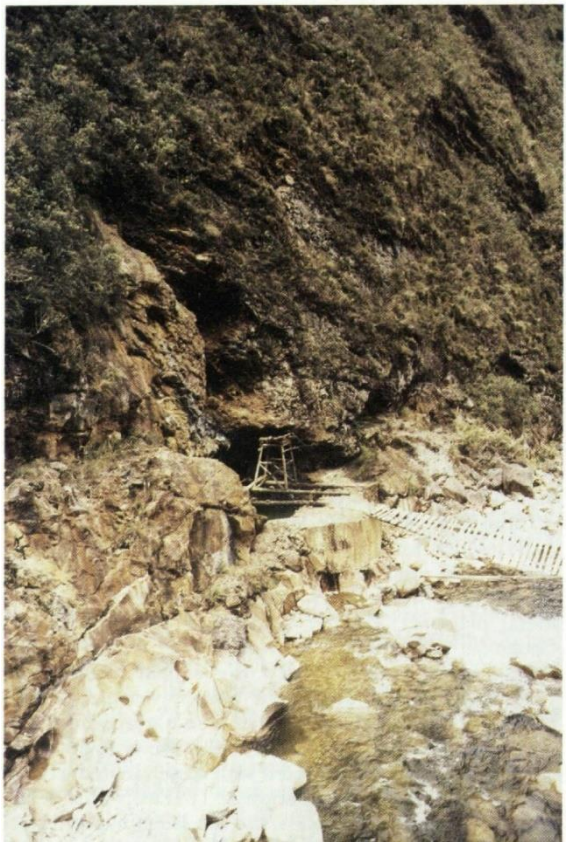

b

c

Plate 23 High level mineralisation.

(a) View NW to Peggy mine with massive Tres Lagunas granite in the foreground and mineralised, sheared granite in the mine area (photo: R. A. J.).

(b) Gima-Cerro Colorado epithermal prospect: a silicified, pyritised, acid-leached, porphyry breccia (photo R. A. J.).

(c) Malachite-stained fracture cutting intrusive breccia in road-level adit in east bank of Río Santa Bárbara, Quebrada Reote, Peggy mine area (photo: R. A. J.).

SKARN-RELATED Cu, Pb, Zn MINERALISATION

In the Zamora batholith, both the Zumbi and María Elena prospects are reported as magnetite-copper-gold skarns (oral communication, A. Hirtz). At the Campanilla mine, coarse blocks of chalcopyrite and pyrite were discovered in 1991 (oral communication, A. Rogers). Chalcopyrite, sphalerite and galena have been reported from Nambija (McKelvey, 1991).

In the northern skarnfields of the Cordillera Real, small Cu-Pb-Zn mineralisation is visible in many places (Plate 19b) particularly in the El Placer field (p.34) where assays yielded up to 1347ppm Cu (from a tourmalinite), 278 ppm Pb and 4279 ppm Zn (2). Zn up to 578 ppm (3) is elevated in the Urcucocha field (Figure 19), and blocks in the Río Quijos of quartz-calcite vein material probably from this same source assayed up to 7189ppm Zn (4). Further north samples from the Sara Urcu skarnfield (**1717-99888**) yielded values up to 591 ppm Zn (3), and in the extreme north, a block of garnet hornfels from Quebrada La Industria (**2181-00454**) gave 4% Zn (4). Thus, of the three major base metals, copper appears to be associated with the Nambija fields, and zinc with the northern fields.

GRANODIORITE INTRUSION-RELATED Cu-Pb-Zn MINERALISATION

In the Río Ishpingo area, along the Gualaceo-Limón road (p.86), 2346ppm Cu was recorded from a sample of hydrothermally altered and pyritised granodiorite of the Ishpingo pluton (6). The Alao pluton shows traces of Cu mineralisation in the Alao Valley (Figure 16) (2) and also in Quebrada Quishpe to the north (p.86) where chalcopyrite and malachite occur in auriferous veins (6). In the same region the Agua Santa mine (Figure 16) is a small copper deposit (6) possibly related to the adjacent Pungalá pluton. There is also a 200m mineralised zone in the Amaluza pluton (6). The plutons of Ishpingo, Pungalá and Amaluza have all been dated at about 40 Ma, and the Alao pluton may be the same age.

Cu traces have been noted in the Jurassic Azafrán pluton along the Río Oyacachi (3). Similar traces were noted in the Cretaceous Pimampiro granodiorite (1), whilst Cu-Zn mineralisation occurs in granite sheets cutting metamorphic rocks nearby (1, 6). There are many occurrences of base metal mineralisation in the Zamora batholith away from the main gold regions; a vein in the Rosa Florida monzonite gave 0.1% Cu and 0.1% Zn (4).

Cu-Pb-Zn MINERALISATION IN MESOTHERMAL QUARTZ VEINS

Numerous polymetallic prospects and showings related to mesothermal quartz veins cut the metamorphic rocks, a number of which can be demonstrated to be shear zone hosted. In the north of the Cordillera Real traces were noted in the Cofanes shear zone (4); in the Upano greenstones near the Oyacachi/Santa María confluence (Plate 4b) (3,6); and near Laguna Atillo (6). Small Cu-Zn mineralisation and an old working are present in the rocks of Cerro Hermoso (Figure 11) (2).

At the headwaters of the Río Palora, the legendary **Condorazo mine** (**78°24'50''W, 1°44'05''S**) (Navarro, 1986) is located (6) close to the Baños shear zone. The steeply dipping vein is somewhat discontinuous but can be traced along strike for more than 200m and is semiconcordant with the host rock of sheared Tres Lagunas granite. Along strike to the south are the series of Cu-Pb-Zn veins which make up the El Placer prospect (1, 4), a sample of which assayed at 3170ppm Pb (4). Along strike to the north there are Zn-Cu-bearing veins near the Agoyán tunnel (1) in an alteration zone which crosses to the south bank of the Río Pastaza (6). To the west there are polymetallic veins at Cruzacta and Curiayana mines near Alao (6).

At the **Chigüinda prospect** (**78°43'45'W, 3°12'40''S**) there are variably altered and mineralised mica schists of the Chigüinda unit for about 2km along the road between Chigüinda and Río Blanco bridge (6). Mineralisation comprises fracture coatings and quartz veins with sulphides which include galena, sphalerite and molybdenite; assay values range up to 224ppm Cu, 2030ppm Pb and 216ppm Zn (6). Vein quartz textures are generally vuggy, indicating epithermal-mesothermal conditions, but milky-white, massive vein quartz also occurs. It is not clear whether the mineralisation is shear zone- or porphyry-related.

OTHER Cu-Pb-Zn MINERALISATION

Small copper mineralisation was noted in the serpentinites of the Peltetec unit in the Huarguallá Valley (Figure 16); one sample assayed at 1.5% Cu (1). There are reports of copper mineralisation in the Tampanchi mafic-ultramafic complex.

Weak galena mineralisation was noted in marbles close to metavolcanics of the Isimanchi unit on the trail from Valladolid to El Porvenir (2).

Cu-Pb-Zn STREAM GEOCHEMISTRY

The highest copper anomalies of 8067 ppm and 2629 ppm come from streams in the El Oro area draining south into the Río Jubones from the La Tigrera, La Playa and La Banda prospects which lie outside the accompanying map. Other elevated Cu-Pb-Zn clusters are close to the Cerro Pelado and Cerro Azul prospect areas, with highest values of 296ppm Pb and 292ppm Zn.

The highest copper value in the Cordillera Real was registered as 865ppm in a western tributary of the Río Yacuambí. A stream close by gives 605ppm Cu and 394ppm Pb. A value of 740ppm Zn is recorded from a west-draining tributary of the Río Paute where this river flows north. There are other values of Zn >200ppm from streams similarly draining westwards along this stretch (see also anomalies on DGGM geological sheet No 72). The highest value for lead over the cordillera is 435ppm from a stream close to Peggy mine.

Cadmium (Cd)

Samples from Peggy mine assayed up to 2650ppm Cd (3), and this appears to be the first recorded cadmium occurrence in the Cordillera Real. Assays from the Guarumales prospect (p.95) gave up to 730ppm Cd, and from Chinapintza, 410ppm Cd. The Zn mineralised sample from Quebrada La Industria assayed at 494ppm Cd.

The highest stream-sediment value for cadmium of 10.8ppm comes from a north-flowing tributary of the Río Paute. A stream close by gave 6.4ppm Cd and both are associated with high zinc.

METALLOIDS AND MERCURY

There are small workings for antimony and mercury, and some potential for bismuth over the Peggy Mine area.

Antimony (Sb)

El Antimonio mine is located in the Cerro Pelado area of El Oro in Quebrada Guayabo (**6272-95043**). The main abandoned adit is located within the granular-textured, sheared granite of Limón Playa (7). The mineralised vein is about 40cm wide and comprises massive and vuggy quartz with coarse stibnite. Float blocks of tourmaline breccia are common. The area was mined by the Ecuaba Company for antimony, but gold assays of up to 14ppm have been obtained from the vein.

Loma Larga Mine is in the El Oro area near the village of Loma Larga in the upper reaches of Quebrada Lozumbe (about **6450-95880**). The mine was being rehabilitated in 1991. Samples from waste dumps comprise vein quartz with massive to crystalline vuggy stibnite hosted in quartzite. The country rocks are quartzites and sheared granites of the Moromoro unit (7). Similar stibnite-bearing quartz veins have been reported from Quebrada El Oso, a tributary of the Río Moromoro.

In the Cordillera Real, the antimony minerals boulangerite, polybasite and freieslebenite were reported from San Bartolomé (UNDP, 1972), and antimony sulphosalts are present at Pilzhum (Wolf, 1892; Goossens, 1972a). Values of up to 4900ppm Sb were assayed from quartz-arsenopyrite veins from the Santa Bárbara-Río Ayllón area (3); boulangerite and bournonite were noted. In the adjacent Peggy mine area, Sb values of up to 207ppm were found in mineralised rocks, and 244ppm in samples from the Quebrada Reote nearby (6).

Also in the Cordillera Real, values of up to 1228 ppm Sb were assayed from the massive sulphide of Guarumales (6) (p.95), and up to 402ppm Sb from the Río Isimanchi prospect in the extreme south.

Values over the detection limit of 5ppm are plotted for antimony on the accompanying maps. The highest stream sediment values are close to the known Sb mineralisation in El Oro reaching a maximum of 286ppm. In the Cordillera Real the highest value, 171ppm, is from the Peltetec stream draining the main ophiolite.

Arsenic (As)

Arsenopyrite is common in mineralised samples from the Peggy Mine area in the Cordillera Real. It is also common upstream in the Santa Bárbara-Ayllón area nearby where it is associated with precious and base metals; assays yielded in excess of 2000ppm As (3, 6). This mineralisation is considered to be mesothermal and is probably porphyry-related (6). A value of 1143 ppm As was obtained from a sample of coarse clast-supported, pyritised dacite breccia at Loma del Loro prospect, near Saraguro (p.84). Samples from the volcanogenic massive sulphide prospect at Guarumales (p.95) have yielded As values over 2000ppm (6). Other assays are listed (6) from rocks associated with hydrothermally altered and mineralised dacite-rhyolite porphyries and volcanics, and from granular biotite-hornblende granodiorite intrusions and their hornfelsed aureoles.

The highest stream sediment value over the cordillera is 537ppm near Peggy Mine. However, in El Oro, three samples are in the region of 2000ppm As, one from the Río Santa Rosa and the others from the Río Caluguro/Viron. In general, over the El Oro belt there appears to be a good correlation between arsenic and gold and the highest values were recorded from samples near the contact between the metamorphic complex and Cenozoic igneous rocks, in particular the Cerro Pelado and Cerro Cangrejos mining areas.

Bismuth (Bi)

This metal has been noted in tetrahedrite at Pilzhum (Putzer and Schneider, 1958) and as a native bismuth and bismuthinite at the Peggy mine (de Coster, 1986). Project mineral samples from this mine yielded up to 5800ppm Bi (3, 6). Values of up to 56ppm Bi have been assayed from mineralised samples elsewhere.

The highest bismuth value in stream sediments over the Cordillera Real is 83ppm from the Peltetec stream draining the ophiolite (**7717-97946**). Values reach 104ppm in El Oro where high values are found around the Cerro Pelado mine.

Mercury (Hg)

Ribadeneira (1960) reports mercury mineralisation at Cerro Huaizhun near the town of Azogues (Azogue is Spanish for mercury). This location was previously mined for mercury (Chacón, 1986), probably from epithermal mineralisation. It is shown on DGGM geological sheet No. 73NW, cited by Goossens (1972a), and was part of an area studied by the UNDP (1972). Wolf (1892) reports native mercury from the alluvium in the Collay area (**78°40'W, 2°53'S**).

Tellurium (Te)

The Peltetec stream yielded a stream-sediment value of 123ppm Te. Over El Oro, three stream sediments in the Cerro Pelado area gave 28-47 ppm Te.

METALS RELATED TO MAFIC-ULTRAMAFIC INTRUSIONS

No mining of these metals has been undertaken but several mafic-ultramafic intrusions have been discovered and the occurrences of related metals are listed below. Economic potential is considered to be low.

Platinum group metals (PGM)

Alluvial gold and platinum concessions were held between 1900 and 1920 in the Río Pindilig-Río Cochicorral area, east of Azogues (Navarro, 1986, Vol. 3, Appendix). These rivers drain eastwards across the Tampanchi mafic-ultramafic complex recognised by the Project (2; Pozo, 1990) which is a probable source for the alluvial platinum and possibly the gold reported from this area. Subsequent commercial surveys have yielded values of up to 1980ppb Pt and 2568ppb Pd from pan concentrates, and 205ppb Pt and 260ppb Pd from soils (oral communication, A. Hirtz).

Chromium (Cr)

Chromite has been identified in ultramafic rocks from the Cordillera Real (4) but assays show values of up to 4079ppm which are normal for ophiolites worldwide (Hutchison, 1983). Chromite blocks have been reported from the hills near Río Zula (**78°40'W, 2°15'S**) (oral communication, A. Hirtz) and fuchsite (chrome muscovite) has been noted in ultramafic rocks, quartzites and impure marbles.

Higher values in stream sediments and pan concentrates can generally be related to mafic-ultramafic complexes (see accompanying maps). At Tampanchi, pan concentrates yielded up to 9842ppm Cr and soils 4863ppm (oral communication, A. Hirtz). A stream-sediment value of 1820 ppm from Quebrada Las Palmas (**6112-96045**) of the El Oro sector can be related to the El Toro serpentinite (7).

Nickel (Ni)

Like chromium, the nickel assays of ultramafic rocks from the region, which range up to 2000ppm, are normal for ophiolites worldwide. Quartz veins with reddish weathering material cutting the Guamote terrane quartzites at Ambuquí gave 742ppm Ni (1).

Quebrada Las Palmas (El Oro) carries a stream sediment value of 1696ppm Ni coincident with the Cr anomaly (above). The stream draining the Peltetec ophiolite at Peltetec gave 759ppm Ni.

Sauer (1965) reported 1.5% Ni from ophiolites in the 'Río Mulatos'. These outcrops are now believed to occur in the present Río Parcayacu, upstream from the Mulatos confluence, but this section was not traversed by the Project.

The rapid rate of uplift and erosion of the Cordillera Real does not permit the stabilisation of a tropical laterite weathering profile and the subsequent formation of nickeliferous laterites.

Cobalt (Co)

An assay of 236ppm Co was detected from a skarn block in the Río Quijos above the Papallacta confluence (**8372-99520**) (3). Cobalt ranges from 100-150ppm in ultrabasic rocks (p.124).

For stream sediments, higher Co values are coincident with those of Cr-Ni (above). Thus Quebrada Las Palmas (El Oro) yielded 164ppm Co, and the Peltetec stream 56ppm.

Vanadium (V)

Vanadium shows a range of 239-409ppm in samples of the Panupali amphibolite from El Oro (p.133). Vanadium values of 334ppm and 289ppm were assayed from those skarn rocks with high molybdenum in the Urcucocha skarnfield (3). A value of 326ppm was recorded from a Zamora granitoid and 244ppm V from a garnet granite near Oyacachi (4). The highest stream-sediment value of 606ppm V was analysed from Quebrada Curispe, a tributary of the Yacuambí. High vanadium values from stream sediments were also found from the Río Vergel sector in the south-east of the Cordillera Real.

Titanium (Ti)

An occurrence of titanium mineralisation is mentioned on the DGGM Cordillera Real geological sheet No. 71. Large, brownish red rutile crystals up to 4cm in length are found isolated in pegmatised gneiss east of Monte Olivo, an occurrence classed as a mineral curiosity only (5). High stream sediment Ti values of up to 1.04% correspond to the high vanadium values of the Río Vergel area (above).

FERROUS METALS

No large deposits of these metals are known; there are small manganese workings.

Iron (Fe)

Iron-bearing minerals have been reported on the following Cordillera Real geological sheets of DGGM/INEMIN/CODIGEM:

Goethite No. 86
Magnetite No. 71
Pyrite Nos. 57, 72, 75, 85, 90, 96, 99, 100, 101, 102
Glauconite No. 102
Limonite No. 96

Magnetite is common in the skarnfields of the cordillera. In the south, the Zumbi and María Elena prospects are both essentially magnetite-Cu-Au skarns, whilst those in the northern cordillera have been classified as the calcic magnetite type of Einaudi et al. (1981). There are magnetite float blocks in streams draining the southern skarnfields, e.g., Quebrada Cambana near Nambija (6), whilst the names of the adjacent Quebradas Hierro and Fierro both translate as 'iron streams'. No large float blocks of magnetite-rock have been noted in streams draining the northern skarnfields.

Magnetite float blocks occur in the Río Yacuambí. Some are derived from the Ríos Espadilla and Campana Urcu which form the Río Ortega tributary (4). Others come from the Río Cambana tributary further downstream and are associated with pyritic hornfels rocks (2). Magnetite float was also noted in the Río Ayllón (6). Veins of specular hematite are reported from the hills west of Cerro Pan de Azúcar and west of Limón (oral communication, L. Torres).

Large quantities of magnetite octahedra occur as black sand in the Río Arenillas, downstream from the Tahuín dam in El Oro (7). The magnetite is probably derived from the weathering of the serpentinised harzburgites of the El Toro unit, but is unlikely to be of commercial interest.

Pyrite occurs widely and is well developed in the volcanogenic massive sulphide deposits of Mina Pilas and Guarumales (Plate 18).

Manganese (Mn)

Manganese occurrences are mentioned on Cordillera Real geological sheets Nos. 55 and 96. Small Quaternary deposits of manganese wad are associated with carbonated water springs in the Río Pun valley near El Carmelo in the extreme north of the cordillera (6).

In the El Oro area there is an abandoned manganese working sometimes referred to as Sacachispas Mine (**6365-96296**). The country rock consists of silicified metasediments of the Palenque mélange. The 'mine', according to Harrington (1957), consisted of lenses of quartz that contain appreciable quantities of massive, pink rhodonite and black psilomelane. The largest lens was about 6×2 m, and there is probably no commercial interest except, possibly, for ornamental purposes.

GRANITE-RELATED METALS

No mining for these metals has been undertaken. During the Project traces of tin and tungsten mineralisation have been discovered related to a regional chain of S-type granites, but there are no indications of deposits of commercial interest.

Molybdenum (Mo)

Molybdenum mineralisation is mentioned on Cordillera Real geological sheets Nos. 39, 56, 72 and 73. Molybdenite has been identified at several locations, in places associated with ferrimolybdite.

Mo mineralisation was discovered in the northern skarnfields (3): from the summit of the Urcucocha field east to Urcucocha (Figure 19) the exposure wall (Plate 5c) comprises mainly massive green epidote skarn with a subhorizontal fracture foliation. Fine disseminated molybdenite, associated with hairline veinlets of carbonate, together with larger, up to 1cm, pyrite crystals, are present in the outcrop over a lateral distance of over 2m, but probably less than 10m. Assays show values of 5092ppm and 3383ppm Mo. This mineralisation was discovered along the only traverse so far undertaken across this skarnfield. Other northern skarnfields have Mo indications: a sample from Sara Urcu gave 556ppm Mo (4), whilst the highest value from the El Placer field was 113ppm Mo (2).

There are several Mo indications in the extreme north of the cordillera, including a number of Mo values greater than 10ppm in stream sediments. About 3km east of Monte Olivo, in the Río San Miguel (**77°50'10''W, 0°23'15''N**), an exposure of brown-yellow, iron-oxide-stained rock is related to a deformed and discordant, massive quartz vein containing abundant pyrite and, less commonly grains of molybdenite with its characteristic yellow alteration product ferrimolybdite (6). The vein is tens of centimetres thick and an assay of 964ppm Mo was recorded. In the same river close to Monte Olivo there are boulders of pegmatite with molybdenite and chalcopyrite, and granular feldspar rock with coarse blebs of pyrite and molybdenite (6, INEMIN-Misión Belga, 1988). It is not clear whether these Mo showings have any relationship to the pegmatites found over this area east of Monte Olivo. Molybdenite flakes were also noted in small quartz veins cutting the mafic (gabbro pegmatite) contact zone of the Chingual pluton along the old road from Santa Bárbara to La Bonita (1). Further south, Ribadeneira (1960) reports molybdenite in pegmatites near Hacienda Ilade, Río Anzu.

In the south, molybdenite flakes occur in **massive white vein quartz** cutting strongly altered mica schists at one locality within an approximately 2km-wide altered and mineralised zone termed the Chigüinda prospect (p.97). An assay of 4396 ppm Mo was obtained from one sample (6). Further south molybdenite was noted in vuggy quartz veins in a similarly altered and mineralised zone along the San Antonio road south-east of Yangana (6). In the nearby Río Chiriguana, a value of 107ppm Mo was obtained from a sample of iron-oxide-stained schist with coarse vuggy vein quartz and pyrite (6).

Fierro Urcu is a porphyry-related Cu-Mo and precious-metal vein prospect, 14km south-west of Saraguro (p.83). Molybdenite occurs in a quartz vein (*veta ancha*) associated with other sulphides and sulphosalts (INEMIN-Misión Belga, 1988). Traces of molybdenite are also reported from the Uritohauser prospect further south (p.95) associated with fault-hosted, Pb-Zn mineralisation (INEMIN-Misión Belga, 1988).

Other locations yielding Mo values include the following: up to 76ppm Mo from the Guarumales VMS prospect (6), up to 90ppm Mo from the sulphide-mineralised and altered Ishpingo granodiorite along the Gualaceo-Limón road (6); up to 118ppm Mo for mineralised samples from the Peggy Mine area; and up to 56ppm Mo from altered and pyritised dacite porphyry volcanics in the Cerro Pucurcu Grande-Atillo areas (6).

In the Cordillera Real, the highest molybdenum, stream sediment value is 122ppm Mo from the Quebrada Napurca, Río Yacuambí (**78°51'W, 3°45'30''S**). Of the other Mo values from stream sediments and heavy minerals plotted on the accompanying map, there is an interesting cluster from samples collected from streams draining north into the Río Isimanchi in the extreme south. These possibly relate to mineralisation in high-level felsitic phases within the Portachuela pluton. In El Oro the highest stream-sediment value was 128ppm Mo from Río Mollepungu.

Tin (Sn)

Tin mineralisation is mentioned on Cordillera Real geological map sheets Nos. 55 and 75.

Cassiterite and stannite have been reported from the Peggy Mine area (de Coster, 1986) and cassiterite has been recovered from nearby stream sediments. Project assay values from the mine area range up to 7684ppm Sn (3).

Cassiterite and scheelite are abundant in pan concentrates from the Río Pichinal east of Saraguro (3, 6), an occurrence discovered by the UNDP (1972). Cassiterite does not occur in adjacent tributaries of the Río Casaturu. The occurrence is likely to be related to localised veins, pegmatites or disseminations associated with the adjacent Tres Lagunas S-type granite.

Tourmaline pegmatite samples from the Monte Olivo belt south-east of San Gabriel, east of Río Minas, gave 17 and 33ppm Sn (4), whilst a value of 63ppm Sn is reported from a sample of muscovite-tourmaline 'greisen' from the headwaters of the Río Cuyes (3).

There are a number of values of Sn greater than 20ppm in stream sediment and 10-120 ppm in heavy minerals. When plotted on the accompanying maps, these can almost all be related to the Tres Lagunas/ Moromoro granites. Worldwide, tin mineralisation in similar S-type granites is common.

Tungsten (W)

Tungsten mineralisation is mentioned on Cordillera Real geological map sheets Nos. 55, 58 and 75.

Tungsten occurs in mineralised samples from the Peggy Mine area with assay values up to 5979 ppm W (3). Wolframite was identified comprising 60-70% ferberite.

Values of up to 444ppm W were obtained from samples from the Guarumales volcanogenic massive sulphide prospect (p.95). A value of 59ppm W was obtained from an iron-oxide-stained, green-grey-coloured schist boulders from the Río Agua Clara, about 10km west of Santa Bárbara in the extreme north of the Cordillera Real (6).

There is a stream sediment anomaly of 600ppm W from Quebrada Napurca, a tributary of the Río Yacuambí, and one of 405ppm from the Río Mollepungu in the El Oro sector (**6494-96340**) (7).

Other tungsten occurrences are found as scheelite in pan concentrates (4). Plots of samples with more than 100 grains fall into a cluster in the Río Oyacachi-Río Papallacta sector of the northern Cordillera Real and straddling the contact of the Tres Lagunas and Chigüinda units in the south. The scheelite is probably derived from the Tres Lagunas granite and/or the enclosed younger porphyries.

RARE METALS

Traces of these metals are noted, but potential for major deposits is thought to be poor.

Rare-earth elements

Goossens (1972a) reported a possible heavy-mineral stream sediment occurrence of thorianite from the Río Verde near Baños.

Heavy-mineral concentrates show, by XRF analysis, a cluster of higher caesium, thorium, yttrium (and rubidium) in streams draining north into the Río Isimanchi in the south of the area. These may relate to high-level mineralisation within the Portachuela pluton.

Yttrium in stream sediments ranges up to 64ppm. Lanthanum reaches 54ppm over the Cordillera Real, but is higher in the El Oro sector with a highest value of 432ppm in Quebrada Canoas (**6050-95942**) (7). The higher lanthanum values in El Oro may reflect the presence of REE-enriched minerals such as monazite, probably derived from the Moromoro granites.

In rocks, the highest Ce (105ppm), Y (62ppm) and Th (30ppm) values come from granites (p.134). It is interesting to note that a dioritic phase of the Tampanchi mafic-ultramafic complex shows the highest lanthanum (44ppm) and elevated Ce and Th. A value of 38ppm Th was recorded from a mineralised polymetallic vein from the El Placer prospect area near Alao, and 30ppm Th from a Sara Urcu skarn rock (4).

Niobium (Nb)

Higher niobium coincides with higher REE in pan concentrates along the traverse across the Portachuela pluton (above).

NON-METALLIC AND INDUSTRIAL MINERALS

No new major occurrences of non-metallic and industrial minerals have been noted, but the inventory below may be useful for further investigations.

Asbestos

Small blocks of tremolite asbestos and small veins of antigorite asbestos are commonly associated with the serpentinites in the northern Cordillera Real. At the base of the main (Peltetec) serpentinite in the Huarguallá valley (Figure 16) there is a 5m unit within which slip-fibre chrysotile asbestos is well developed (2). This passes up into more massive serpentinite in which the asbestos forms a vein stockwork. In the same area, along the Alao road to the north, loose blocks contain small veins of blue asbestos.

Barytes/barium

Barytes of hydrothermal origin is presently worked in the Río Bomboiza area, with a production in the region of 6000 tonnes per year (Delbridge and Robertson, 1992).

Barium mineralisation is also mentioned on the Cordillera Real geological sheet No. 72. Wolf (1892) reported baryte from the Pilzhum silver mine where it was confirmed to occur as fine to coarse platy crystals in epithermal veins.

High Ba values have been obtained from samples from the following epithermal mineralisation (6): Satunsaray-Cuchil (841ppm); Collay (450ppm); Loma Quipal (1002ppm); and Cerro Colorado-Gima (758ppm). Samples of porphyry-related mineralisation also yield Ba values (6): Peggy Mine (437ppm); Loma del Loro (439ppm); and Cerro Puglla (408ppm). A value of 1105ppm Ba was recorded in a sample from the Guarumales massive sulphide prospect (6); whilst a mineralised mylonitic granodiorite from near La Bonita gave 442ppm Ba (4).

The highest barium value from stream sediments was 860ppm from upstream in the Río Chicana (**78°49'W, 3°40'30''S**). This coincides with the highest barium peak of the XRF analysis of heavy minerals.

Carbonate

Travertine has been worked at Zula and Baeza, and other occurrences are mentioned on DGGM/INEMIN/CODIGEM geological sheets and noted on project field maps.

Limestones and marbles are found in the Cordillera Real. Black limestones are abundant in the Napo Formation along the Sub-Andean belt. Great thicknesses of marble, blue to off-white in colour, belonging to the Isimanchi unit, occur on the east bank of the Río Isimanchi; south of Isimanchi town; and to the east of Valladolid on the trail to Porvenir (2). Accessible marble bands also occur along the Ríos Paute, Zula and Negro, west of Méndez (2). White marble float blocks occur in the Río Diviso (3). The Cerro Hermoso black marbles form part of a 500m sequence (2). Impure fuchsitic dolomites occur in the Río Cosanga (3).

Small calcite veins are ubiquitous, especially in the greenstones. In the Huarguallá valley canal section (Figure 16) calcite crystals up to 30×20×20 cm in size can be obtained (1), but these are not of Iceland Spar quality.

Corundum

Goossens (1972a) mentions a report by Yantis (1943) of disseminated corundum in an altered syenite located at Ludo about 8km south-east of San Bartolomé. This occurrence has not been confirmed.

Diatomite

Occurrences are recorded on geological sheets Nos. 56, 57 and 71; Goossens (1972a) mentions a diatomite occurrence near Loja.

Feldspar

Feldspar is mined at the Jerusalem Mine, 1-2km south of the town of Marcabelí in El Oro (**6220-95800**). The workings are located within the Marcabelí granite and consist of weathered, leucocratic, pegmatitic feldspar veins which are extracted for use in the ceramic industry by Cerámica Andina CA. Approximately 4000 to 5000 tonnes of material are removed annually, and reserves are estimated at about 80000 tonnes (7).

In the Cordillera Real, feldspar is noted on geological sheets Nos. 75 and 76. Feldspar-rich rocks include the quartz monzonites and quartz syenites of the Rosa Florida pluton, and various microfeldspathic dykes and sheets, aplogranites, aplites and pegmatites mentioned in Project field reports. These are unlikely to be of economic interest.

Fluorite

This mineral has been described from Cerro de Santa Cruz (Cerro Minas) near Malacatus (Wolf, 1892; Goossens, 1972a). Samples of purple fluorite were found at Cerro Minas (p.95) (6) associated with vein quartz and as irregular but smaller masses within a trachyte dyke.

Garnet

Garnet is a commonly occurring mineral and local inhabitants sometimes refer to it as 'ruby', but no large gem-quality garnets have been noted.

Garnet rock of high purity can be found in the Nambija area and northern skarnfields. Boulders of garnetite were noted in the Río Blanco (Chigüinda) and the confluence of the Ríos Ayllón and Santa Bárbara (7).

Euhedral, idioblastic garnets, up to 3cm in size, are present in float blocks in the Río Collanes which drains into the Río Palora from the north. Local reports indicate that garnets ('rubies') up to 5cm in size can be panned from Quebrada Culebrillas near La Bonita.

Gemstones and mineral curiosities

Brownish red **rutile** megacrysts up to 4cm in size and green, semitranslucent, euhedral **zoisite** crystals were noted from the pegmatites east of Monte Olivo (3). There is an occurrence of sky-blue **lazulite** (Fe, Mg-aluminophosphate) at the headwaters of the Río Sardinas Chico (Van Thournout and Piedra, 1986), and blocks, presumably from this source, can be seen in the Río Quijos below Borja.

In El Oro **topaz** has been recognised, in thin section (7), in a leucocratic, two-mica phase of the Marcabelí granite on the south bank of the Río Puyango (**6172-957766**), and also in a phase of the El Prado pluton in Quebrada Usulaca (**6514-95838**). In the Cordillera Real, topaz has been noted in the heavy-mineral study (4). Two occurrences from headwaters/watershed of the Río Sangurima are just north of the greisen/pegmatite zone at the Río Cuyes headwaters, and a greisen source is likely.

Tourmaline (black schorl) is common in pegmatites and in quartz veins hosted by sheared Tres Lagunas granite in the Saraguro to Gima areas; no gemstone-quality crystals were noted.

Accounts of **emeralds** have yet to be confirmed geologically. Claims for the existence of a lost emerald mine located in the sub-Andean area of the Río Bermejo north of the Río Aguarico are detailed in a magazine article (Krippene, 1960), and, apparently, supported by a mining claim lodged with the Ministry of Mines. Such a location, if confirmed, could represent an extension of the Colombian emerald fields (e.g. Muzo) found in contact aureoles around Tertiary intrusives cutting Napo Formation equivalents, recognised by the accompanying presence of pyrite, barite and fluorite. However, a more recent claim of emeralds in pegmatites in the Quito newspaper *La Hora* (17-19 Feb. 1992) cites a location close to Chunchi, in the Sierra, a great distance from the nearest Napo Formation outcrop.

Graphite

Goossens (1972a) lists the graphite occurrences in Ecuador, and some in the Cordillera Real are noted on geological map sheets Nos. 56 and 57. Exploitation is reported near Sevilla de Oro (CLIRSEN, 1985). Graphitic or carbonaceous shales, slates, phyllites and schists are common throughout the cordillera. Enriched zones were noted on Project field maps but no extensive high-grade deposits were found.

Gypsum

The mineral is mined locally from the Tertiary rocks of the Malacatus basin. Occurrences in the Cordillera Real are noted on geological sheets Nos. 57, 73, 96 and 102. Veins of fibrous anhydrite occur in sulphur- and pyrite-mineralised rhyolite breccias at the Shucos (Tixán) sulphur mine (6).

Hot springs

The occurrences and chemical compositions of thermal waters are reviewed in Grys et al. (1970) and Goossens (1972a). Hot springs are also noted on geological map sheets Nos. 71, 86 and 88.

There is a line of east-draining hot springs east of those shown on the map of Grys et al. (1970). From north to south these occur at Oyacachi, Papallacta, Baños and El Placer (headwaters of Río Palora). These springs lie close to the Baños fault and relatively close to the volcanic centres of Chacana, Antisana, Tungurahua and El Altar respectively.

Kaolin and other clay minerals

The occurrences of kaolin, bentonite and other clays in Ecuador are reviewed by Goossens (1972a). In the cordillera, occurrences are recorded on geological sheets Nos. 73, 75 and 96.

Plastic clays used in the manufacture of sanitary ware are worked in the Plan de Milagro area near Limón where the illite deposits have been formed by weathering of the adjacent metamorphic rocks.

The Tertiary sedimentary basins of Cuenca and Loja contain deposits of kaolin and bentonite exploited since pre-colonial times for local ceramic industries. The clays are associated with acid intrusive and pyroclastic rocks. Small-scale workings for kaolinite were noted in the Shincata-Bestión area (6) and production has also been reported from the Puyo and Azogues areas (Goossens, 1972a; Stoll, 1962).

Within the metamorphic rocks, weathered, kaolinitic deposits derived from feldspar-rich intrusions are common, and some are noted in Project field maps and reports. In El Oro there are many small-scale workings which exploit the weathering products of the Marcabelí granite for brick and tile making, particularly around the towns of Balsas and Marcabelí (7).

Magnesite

Small veins of magnesite are common in the serpentinites of Peltetec, the northern cordillera and Tampanchi; but they are of no economic interest.

Mica

Small one- or two-mica pegmatites are found along the Cordillera Real, but mica crystals reach up to 5cm across and are of no economic interest.

Ornamental stone

Many new occurrences with ornamental stone potential have been discovered. These include the blue quartz-grey feldspar granites of Tres Lagunas, the ‘black granites’ (megacrystic gabbros) of Tampanchi, the pink syenites of Rosa Florida, the green/pink/black rocks of the northern skarnfields, green and black serpentinites, blue or black marbles, and many granitoid plutons. Orbicular diorite boulders were noted in the Río San Miguel near Monte Olivo (6), but their source was not traced. Travertine is used as a building and ornamental stone.

Phosphate rocks

The occurrence and economic potential of phosphate rocks in Ecuador are reviewed by Wilkinson (1982) and Boujo et al. (1984). The most significant phosphate deposits occur within the Napo Formation to the east of the Cordillera Real. Within the metamorphic belt, a river block of apatite-rich metagranite collected east of Papallacta (2) gave 2.25 per cent P_2O_5, but this has no economic significance.

Quartz and silica minerals

Rock crystal and massive quartz veins occur but no potentially commercial deposits are known. Quartzites of the Cretaceous Hollín Formation have economic potential for glass manufacture and some workings are reported near Limón and Indanza. Pure Hollín Formation quartzites crop out along the right bank of the Río Chuchumbleza (4). Other silica minerals, e.g., geyserite, opal and jasper, are noted by Goossens (1972a) and Ribadeneira (1960).

Sillimanite minerals

Both sillimanite and kyanite have been noted in places, but their occurrence is of academic interest only.

Sulphur

Along the western flanks of the Cordillera Real there are sulphur deposits and indications associated with young volcanic rocks. The Shucos Mine at Tixán (**78°49'W, 2°08'30''S**) produced native sulphur associated with rhyolite lavas and breccias; the nearby Chunchi district is characterised by extensive hydrothermal alteration and is said to contain native sulphur mineralisation; minor amounts of sulphur associated with zones of pyritic alteration are present within the volcanic formations between Atillo and Laguna Atillo.

At Malacatus, Goossens (1972a) reports sulphur and gypsum impregnations in Tertiary coal seams. Other occurrences in the cordillera are noted on geological map sheets Nos. 71, 96 and 97.

Talc

Some talc and steatite showings in the Cordillera Real are described by Ribadeneira (1960). Talc schists and talcose serpentinites were noted by the Project associated with the newly discovered serpentinites, but no large deposits are present.

ENERGY MINERALS

The following occurrences of energy minerals are noted, but the overall potential is poor.

Coal

Coal/lignite reserves occur in the Miocene sedimentary basins of Cuenca, Loja and Malacatus (Stoll, 1962; UNDP, 1969). The largest known deposit is at Biblián in the Cuenca basin. Coal and/or lignite occurrences are mentioned on geological sheets Nos. 75, 87, 101 and 102.

Oil

Asphalt occurrences are mentioned on geological sheets Nos. 101 and 102. The bulk of Ecuador's oil reserves are located in Cretaceous formations of the Oriente region, east of the Cordillera Real. In the Sub-Andean belt bordering the Oriente, bituminous black shales from the Napo Formation, which when hammered gave a smell of petroleum, were noted as river blocks in the Ríos Chingual, Salado and Vergel (3, 4). Bituminous mudstones from the Tertiary Malacatus basin gave a total hydrocarbon yield of 60-80 kg/tonne (2).

Uranium

Uranium occurrences are noted on geological map sheets Nos. 100, 101 and 102. In the extreme north of the Cordillera Real, Vera (1980) reported a band of uriniferous phosphate in the Napo Formation, and a project scintillometer survey confirmed the radioactive anomaly (320cps) (4). Close by, a value of 19ppm U was recorded from a Cu-mineralised gneissic block in the Río Condué (4), and 13ppm U from a tourmaline pegmatite from the belt south-east of San Gabriel (4).

Most field samples including those from pegmatites were examined in the office under a portable gamma ray scintillometer, but no anomalously high counts were noted.

Various weak radiometric anomalies, mostly below 300cps, were determined in the Cordillera Real during a national uranium survey (Carrión and Villalba, 1981; Severne et al., 1978). Some relate to small Cu mineralisations in the Zamora batholith along the Zamora-Cumbaratza road; others were found along the Río Paute between Amaluza and Méndez. Uranium stream sediment anomalies up to 5ppm were detected in the Río Jamboe, east of Zamora, which drains the Zamora batholith. Uranium anomalies were also found in the freshwater Miocene sediments of the Cuenca, Loja and Malacatus basin (Carrión and Villalba, 1981; Severne et al., 1978).

DISCUSSION AND CONCLUSIONS

Mineral potential and metallogenesis

Ecuador is part of the Pacific Rim, a global belt of important mineralisation. The present studies have revealed a history of subduction, accretion, transpression and magmatism which is not typical of the classic Andean model but more in keeping with North American Cordilleran areas such as Alaska (Goldfarb et al., 1986) and British Columbia (McMillan et al., 1986). The different types of mineralisation are discussed below, starting with the oldest (Table 2), with reference to the geological framework and their individual mineral potential.

S-type granites can be important sites of tin-tungsten mineralisation (Hutchison, 1982). The Tres Lagunas and Moromoro granites of Ecuador are Triassic in age and broadly S-type in character. Various showings of tin and tungsten can be related to them as can occurrences of tourmaline pegmatites and topaz, but there is no indication of major mineralisation. This lack of major mineralisation may be due to the post-Triassic uplift such that the less productive mesozonal and migmatitic catazonal levels of mineralisation are now exposed. Preserved high-level sectors, such as the Marcabelí granite, may have more potential.

Volcanogenic massive sulphide (VMS) deposits are important producers of base metals, with significant by-products of precious metals and other elements. They are exploration targets within Pacific Rim accretionary terrane complexes such as Alaska (Goldfarb et al., 1986) and British Columbia (McMillan et al., 1986). The recognition in the Cordillera Real at Pilas and Guarumales of VMS mineralisation in the metamorphosed Jurassic volcanic arcs of Alao and Salado is thus noteworthy, and these terranes, accreted/deformed during the Peltetec collision, must now be considered as highly prospective for VMS deposits. Large areas underlain by rocks of the Alao and Salado terranes remain unexplored, in particular the area of around Cerro Soroche (**78°32'30''W, 2°20'S**), the highest metamorphic peak, close to Cerro Tintillay on the accompanying map.

Mineralised skarns are a notable feature of the region and many new discoveries have been made. All the skarnfields are the result of Jurassic granodiorite batholiths intruding volcanosedimentary sequences. At Nambija the important gold skarns are autochthonous and the protolith comprises the Triassic Piuntza unit, of continental rift basin origin, which appears to be present only within the confines of the batholith. In tectonic contrast to the Nambija fields, the northern Cordillera skarns are allochthonous and formed during the Peltetec accretion/collision. The deformed Azafrán batholith is the structural base of this chain of skarn klippen of calcic magnetite type derived from an island arc volcanosedimentary sequence. Great tonnages of skarn rock with polymetallic and molybdenum indications remain to be explored over the watershed of the northern Cordillera Real.

Mesothermal vein mineralisation is usually hosted by shear zone structures and is typical of Archaean greenstone environments (Colvine et al., 1988) and Phanerozoic transpressional accretionary margins (Nesbitt and Muehlenbachs, 1988). It has not been widely recognised in the Andes. However, in the Cordillera Real and El Oro, massive mesothermal quartz veins are common throughout the metamorphic rocks and are probably related to high-strain, brittle-ductile shear zones, confined, in the main, to the Upper Triassic Tres Lagunas-Moromoro event and the Lower Cretaceous Peltetec-Palenque event. Some veins may be even younger. Gold, and stibnite in El Oro, have been noted in these veins which may have formed at crustal depths of 2-10km (Colvine et al., 1988). However, much of this material has now been eroded as indicated by the boulders and pebbles of massive vein quartz in Late Cretaceous and Cenozoic sedimentary formations in the Cordillera Real and the Oriente. The mesothermal veins are regarded as the major source of alluvial gold in the Cordillera Real, but the potential for economic primary mineralisation is low.

I-type granitoid plutons may be associated with sulphide mineralisation, especially the Early Tertiary granular granodiorite stocks of Ishpingo, Amaluza, Colimbo, Pungalá and Alao. These may represent the deeper levels of mineralised porphyry systems in which the altered and mineralised intrusions and their host rocks represent substantial tonnages of rock with significant polymetallic potential.

Mafic-ultramafic complexes have been discovered throughout the area. Many of these have been interpreted as slices of oceanic crust, others as younger intrusions of Alaskan type. No major mineralisation has been noted in these bodies but there are gold and PGM indications at Tampanchi.

Porphyry-related deposits and related types of mineralisation are of worldwide importance, reflecting the large tonnages of metals amenable to economic exploitation which they contain. The greatest concentration of copper porphyry deposits and associated mineralisation occurs around the Pacific Rim, notably in Chile (Sillitoe, 1993). Two ages or porphyry-related deposits occur within the Project area. There are Cu-Mo and Au porphyries within, and probably cogenetic with, the Jurassic Zamora batholith (Gemuts et al., 1992). This Cordillera del Cóndor area has been subjected to minimal tectonic uplift since Jurassic times compared to the Cordillera Real and has thus preserved these high-level deposits. Younger, Cenozoic porphyries, high-level I-type magmas generated during the Miocene-Recent subduction of the Nazca plate, are found in the area particularly on the western flanks of the Cordillera Real and in El Oro. Mineralisation ranges in character from disseminated sulphides and stockworks, to intrusive breccias and discrete veins, and usually polymetallic. There may be an element of control along ancient structures such as the Baños fault. Mineral potential is good.

Epithermal deposits are an important source of gold and silver and have been an exploration target around the Pacific Rim for many years (Sillitoe, 1993). Volcanic-hosted epithermal mineralisation occurs in the Jurassic Zamora batholith area. Gemuts et al. (1992) regard the mineralisation as cogenetic, but other reports suggest that the Chinapintza porphyry-related epithermal system intrudes the Cretaceous formations and is thus of Tertiary age. The main belt of epithermal Au-Ag mineralisation is related to the porphyries of the Cordillera Real and occurs mostly within andesitic to rhyolitic, volcanic and volcaniclastic lithologies of the Miocene Pisayambo volcanic Formation which replaces the Quaternary 'Tarqui Formation' on the new national map (Litherland et al., 1993a). Within this belt, there is a line of epithermal silver prospects from Tungurahua and Cubillín in the north to Pilzhum and San Bartolomé in the south. The mineralogy and textures in these silver deposits are typical of the deeper epithermal ('bonanza lode') environment. Gold is more prominent as the Baños fault is approached and there is considerable potential for major deposits in these poorly explored areas.

Secondary gold deposits of palaeoplacer and alluvial type have formed since Late Cretaceous times by the erosion of primary gold deposits, particularly the mesothermal veins of the metamorphic basement. These deposits are the easiest targets for exploitation, and potential is considerable especially in the east where the Tiyuyacu Formation is considered to be an important palaeoplacer and source of alluvial gold. Studies in the Río Shincata-Río Betas area of the Cordillera Real identified terraces comprising quartz-tourmaline pebble gravels derived from a local mesothermal auriferous quartz-tourmaline vein source.

The **metallogenic history** (Table 2) of the metamorphic belts of Ecuador is not dissimilar to those parts of the Pacific Rim where suspect terranes have been identified. S-type granites, with tin-tungsten potential, were developed in Triassic shear zones along with auriferous and stibnite-bearing quartz veins. During the Jurassic, the subduction-related, I-type Zamora batholith hosted mineralisation of skarn and epithermal type. This was followed by transpressional accretion of continental and island arc terranes carrying volcanogenic massive sulphides, accompanied by the generation of further shear zone hosted mesothermal quartz veins. The Cenozoic history of the metamorphic belts is marked by generations of subduction-related I-type intrusions of Andean type, the older ones exposing granodiorite-related polymetallic mineralisation, and the younger, porphyry-related and epithermal precious- and base-metal mineralisation.

Structural controls and mineral belts

Many workers, e.g., Goossens (1972b) and Paladines (1989) interpret the siting of major mineral deposits in Ecuador to the intersection of Andean-trending and transverse, east-west-trending structures. The transverse trend of the El Oro complex is presently interpreted as the result of block rotation along the Peltetec suture, it being noteworthy that the trend stops at the Peltetec-Girón-Las Aradas fault and does not transect the Cordillera Real.

Major structural controls on the evolution of the Ecuadorian Andes during the Tertiary appear to relate to the rejuvenation of old faults or terrane boundaries (Figure 5) resulting from the subduction of the Farallón/Nazca plates. Of the main terrane boundaries in the Cordillera Real, the Baños fault has most frequently been cited as a linear control of gold mineralisation, the ‘Collay-Shincata gold belt’ (2). Further studies (3, 6) have shown that age and type of mineralisation varies along this belt. The mesothermal, shear-zone-hosted, Au-quartz-tourmaline veins which supply the Bestión formation of Shincata-Betas are reportedly concentrated close to the Baños fault, or shear zone (6). Later, in the Cenozoic, the Baños fault appears to have been a conduit for porphyry-related and epithermal Au mineralisation, especially close to the major fault deflection between Sigsig and Saraguro, which may have been a tensional jog during Cenozoic rejuvenations.

This hypothesis has resulted in the prospection of this belt by private companies. It must be stated, however, that between Sigsig and Saraguro the Baños fault is buried by volcanic formations capable of carrying epithermal deposits, which elsewhere in the Cordillera Real, have long since been eroded.

The case for rejuvenated basement faults acting as ‘conduits’ for Tertiary porphyries can be demonstrated in the Alao valley, where the trace of the San Antonio fault, which locally separates the Mesozoic metamorphic units of Maguazo and Alao-Paute, is followed by a silicified porphyry dyke up to 500m wide (Figure 16) of Cenozoic age. It is interesting to note that the Cenozoic Pilzhum prospect is interpreted to straddle the same fault further south.

Other structural controls are apparent. In the El Oro area, high-level porphyries and associated epithermal mineralisation are present in the Cenozoic volcanic cover rocks north of the Portovelo fault, but such mineralised rocks are absent to the south, presumably removed by erosion. In the cratonic area of the Zamora batholith, the orientation of the roof pendants of skarn rocks is controlled by north-trending faults. Later, in the Cenozoic, porphyry intrusions and related epithermal mineralisation was concentrated at the intersections of these and younger NW-SE-trending faults (oral communication, D. Coochey).

With regard to Andean metallogenesis, Sillitoe (1972) suggested that parallel metallogenic belts related to Mesozoic-Cenozoic I-type magmas reflected the increasing depth of the underlying subduction zone away from the continental margin. Difficulties in tracing such belts through Ecuador can now be explained by the suspected allochthonous status of the Andean basement due to Late Mesozoic-Early Tertiary accretionary events.

Frutos (1982) suggested that the metallogenic belts of the Central Andes were indicative of a pre-Andean metallogenic inheritance. He cites the observations of Schneider and Lehmann (1977) that the magmatic-related Mesozoic and Cenozoic tin deposits of Bolivia occur over Silurian synsedimentary cassiterite enrichments of the Bolivia basin. A similar inheritance is indicated in Ecuador in that the tin-bearing Cenozoic porphyry system of the Peggy Mine area is hosted in the tin-bearing Tres Lagunas Triassic granites of the Cordillera Real (Plate 23a).

REFERENCES

1. NUMBER REFERENCES OF PROJECT OPEN-FILE REPORTS

These refer to the seven major reports and accompanying maps covering the Project which are on open file in English at BGS, Keyworth, UK, and in Spanish at CODIGEM, Quito, Ecuador.

1. LITHERLAND M. (compiler). (1987) First annual report (for 1986-1987) of the Cordillera Real Geological Research Project, Ecuador. Open-File Report of the British Geological Survey, Keyworth (in English) and of INEMIN, Quito (in Spanish). 245 pp.

2. LITHERLAND M. (compiler). (1988) Second annual report (for 1987-1988) of the Cordillera Real Geological Research Project, Ecuador. Open-File Report of the British Geological Survey, Keyworth (in English) and of INEMIN, Quito (in Spanish). 346 pp.

3. LITHERLAND M. (compiler). (1989) Third annual report (for 1988-1989) of the Cordillera Real Geological Research Project, Ecuador. Open-File Report of the British Geological Survey, Keyworth (in English) and of INEMIN, Quito (in Spanish). 346 pp.

4. ASPDEN J.A. (compiler). (1990) Fourth annual report (for 1989-1990) of the Cordillera Real Geological Research Project, Ecuador. Open-File Report of the British Geological Survey, Keyworth (in English) and of INEMIN, Quito (in Spanish). 300 pp.

5. LITHERLAND M., ASPDEN J.A., BERMÚDEZ R., VITERI F., and POZO M. (1990) The geology and mineral potential of the Cordillera Real, Ecuador. Open-File Report of the British Geological Survey, Keyworth (in English) and of INEMIN, Quito (in Spanish). 111pp.

6. JEMIELITA R.A. and BOLAÑOS J. (1993) Mineralization, mineral potential and metallogenesis of the Cordillera Real of Ecuador. Open-File Report of the British Geological Survey, Keyworth (in English) and of INEMIN, Quito (in Spanish). 220pp.

7. ASPDEN J.A., BONILLA W. and DUQUE P. (1993) The geology and economic mineral potential of the El Oro metamorphic complex. Open-File Report of the British Geological Survey, Keyworth (in English) and of INEMIN, Quito (in Spanish). 121pp.

2. UNPUBLISHED PROJECT-RELATED REPORTS

La mayoría de estos reportes, de consultores del Proyecto, son incluidos como apéndices en los reportes de arriba, y/o están disponibles en el BGS, Keyworth, UK.

ATHERTON M.P. (1987) Petrographic study of rocks from the Tres Lagunas granite suite. *Report for BP Petroleum*. 3pp. (also in Reference No. 2 above).

BEDDOE-STEPHENS B. (1987) A pilot examination of alluvial and in situ gold and platinum from Ecuador. *British Geological Survey Mineralogy and Petrology Research Group Report*, No. 87/3. 27 pp (also in Reference No.1 above).

BEDDOE-STEPHENS B. (1989) Mineralogical examination and analysis of samples from Ecuador. *British Geological Survey Mineralogy and Petrology Research Report,* No. WG/89/1R. 33 pp. (also in Reference No. 3 above).

BRITISH GEOLOGICAL SURVEY (1989) Conodont investigation by Nottingham University of ten BGS samples from Ecuador. *British Geological Survey Technical Report*, No. WH/89/13/R. 6 pp (also in Reference No. 3 above).

CLARKE M.G.C. (1988) Visit report on work completed on three mineral belts in the Cordillera Real, Ecuador. *British Geological Survey Report,* No. WC/88/29/R. 15 pp (also in Reference No. 3 above).

CLARKE M.G.C. (1989) Contribution to the understanding of the mineral potential of the southern Ecuadorian Andes. *British Geological Survey Report,* No. WC/89/12/R. 49 pp (also in Reference No. 3 above).

DANGERFIELD J. (1988). Petrography of some granites from the Cordillera Real, Ecuador. *British Geological Survey Technical Report,* No. WG/88/17/R. 25 pp (also in Reference No. 3 above).

DANGERFIELD J. (1989) Petrology of some granitic rocks and a suite of mainly volcanic altered rocks from the Cordillera Real, Ecuador. *British Geological Survey Technical Report,* No. WG/89/9/R. 20 pp (also in Reference No. 3 above).

FORTEY N.J. (1990) Petrographic data and course notes for the Cordillera Real Project, Ecuador. *British Geological Survey Technical Report,* No. WG/90/14/R. 67 pp (also in Reference No. 4 above).

FORTEY N.J., and GILLESPIE M.R. (1993) Assessment of geochemical analyses of igneous rocks from Ecuador. *British Geological Survey Technical Report,* No. WG/93/3/R. 174 pp

HARRISON S.M. (1989). Report on a visit to Ecuador Geochronology sampling, Phase II. *British Geological Survey Technical Report,* No. WC/89/10/R. 18 pp (also in Reference No. 4 above).

HARRISON S.M. (1990) Radiometric ages (Rb-Sr, K-Ar, and Sm-Nd) for rocks from the Cordillera Real, Ecuador: Phase II. *British Geological Survey Technical Report,* No. WC/90/12/R. 29 pp (also in Reference No. 4 above).

HOWARTH M.K. and IVIMEY-COOK H.C. (1991) A Lower Jurassic, probably Sinemurian, ammonite from the vicinity of Guamote, Ecuador. *British Geological Survey Technical Report,* No. WC/91/211/R. 3 pp.

IVIMEY-COOK H.C. (1988) Cretaceous ammonites from the province of Zamora Chinchipe in SE Ecuador. *British Geological Survey Technical Report,* No. WH/88/416/R. 2 pp (also in Reference No. 3 above).

IVIMEY-COOK H.C. and MORRIS N.J. (1989). Triassic bivalves from the province of Zamora Chinchipe in SE Ecuador. *British Geological Survey Technical Report,* No. WC/89/28/R. 2 pp (also in Reference No. 3 above).

IVIMEY-COOK H.C. and MORRIS N.J. (1989) Sinemurian ammonites from the Santiago Formation, Ecuador. *British Geological Survey Technical Report*, No. WH/89/85/R. 3 pp (also in Reference No. 3 above).

IXER R. (1988) Heavy mineral analysis of samples from the Río Mulatos. *Report for BP Minerals International.* 38 pp. (also in Reference No.2 above)

MOLYNEUX S.G. (1988a) Palynological analysis of samples from Ecuador. *British Geological Survey Technical Report,* No. WC/88/320/R. 2 pp (also in Reference No. 3 above).

MOLYNEUX S.G. (1988b) Palynological analysis of samples from the Maguazo Division, Río Jadán, Ecuador. *British Geological Survey Technical Report,* No. WH/88/341/R. 2 pp (also in Reference No. 3 above).

MOLYNEUX S.G. (1988c) Palynological analysis of samples from the Palenque cherts, Río Palenque, Ecuador. *British Geological Survey Report,* No. WH/88/342/R. 2 pp (also in Reference No. 3 above).

OWENS B. (1992) Palynological investigation of samples collected by M. Woods, 1991. *British Geological Survey Technical Report,* No. WH/92/157/R. 34 pp (also in Reference No. 3 above).

PATTERSON C. (1990) Report on fossil fish from Laguna de Atillo, Ecuador. *British Geological Survey Technical Report,* No. WH/90/54/R. 4 pp (also in Reference No. 4 above).

RIDING J.B. (1988) A palynological investigation of a sample from the Maguazo Division, Río Jadán, Ecuador. *British Geological Survey Technical Report,* No. WH/88/347/R. 3 pp (also in Reference No. 3 above).

RIDING J.B. (1989a) A palynological investigation of nine rock samples from Ecuador (Maguazo unit). *British Geological Survey Technical Report,* No. WH/89/361/R. 4 pp (also in Reference No. 4 above).

RIDING J.B. (1989b) A palynological investigation of six rock samples from Ecuador (Chiguinda unit). *British Geological Survey Technical Report,* No. WH/89/345/R. 4 pp (also in Reference No. 4 above).

RIDING J.B. (1991) A palynological investigation of six rock samples from Ecuador (Guamote unit). *British Geological Survey Technical Report,* No. WH/91/192/R. 3 pp.

RUNDLE C.C. (1987a) Reconnaissance potassium-argon ages from the Cordillera Real, Ecuador. *British Geological Isotope Geology Unit Report,* No.87/5. 4 pp (also in Reference No. 1 above).

RUNDLE C.C. (1987b) Rb-Sr analysis of rocks collected in May/June 1987 for the ODA-funded Cordillera Real Project, Ecuador. *Natural Environment Research Council Isotope Geology Centre Report,* No.87/1. 52 pp (also in Reference No. 2 above).

RUNDLE C.C. (1988) Potassium-argon ages for minerals from the Cordillera Real, Ecuador. *Natural Environment Research Council Isotope Geology Centre Report,* No. NIGC/87/7. 20 pp (also in Reference No. 3 above).

SHEPHERD T.J. (1988) Fluid inclusion studies on rocks from the Nambija and Portovelo areas. 5pp. (also in Reference No. 2 above).

STYLES M.T., PÉREZ-ÁLVAREZ M., BLAND D.J., WETTON P., and NADEN J. (1992) Characterisation of gold from Ecuador. *British Geological Survey Technical Report,* No. WG/92/48. 65 pp.

THOMAS J.E. (1989) Palynology of two samples from the Zamora Chinchipe province of SE Ecuador. *British Geological Survey Technical Report,* No. WH/89/89/R. 4 pp (also in Reference No. 3 above).

THOMPSON A. (1987) Petrography of eight samples from the Río Mulatos. *Report for BP Minerals International.* 12 pp. (also in Reference No. 1 above).

WARRINGTON G. (1987) Palynological report on samples from Ambato and Chimborazo, Ecuador. *British Geological Survey Technical Report,* No. PD/87/262/R. 3 pp.

WILKINSON I.P. (1992) Calcareous microfaunas from a suite of samples from Ecuador-Cordillera Occidental. *British Geological Survey Technical Report,* No. WH/92/121/R. 3 pp.

WILLIAMS P.J. (1987) Petrology of rocks from the Río Mulatos area, Ecuador. *Report for BP Minerals International.* 37 pp. (also in Reference No. 2 above).

WOODS M.A. and MORRIS N.J. (1992) Identification and interpretation of collections of macrofossils from Ecuador. *British Geological Survey Technical Report,* No. WH/92/72/R. 5 pp.

3. PROJECT-RELATED PUBLICATIONS

ASPDEN J.A. (In press) The El Oro metamorphic complex, Ecuador. *Overseas Geology and Mineral Resources,* No. 67.

ASPDEN J.A., FORTEY N.J., LITHERLAND M., VITERI F., and HARRISON S.H. (1992a) Regional S-type granites in the Northern Andes. *Abstracts of the International Geological Congress, Kyoto,* No. 2, 536.

ASPDEN J.A., FORTEY N.J., LITHERLAND M., VITERI F., and HARRISON S.H. (1992b) Regional S-type granites in the Ecuadorian Andes: possible remnants of western Gondwana breakup. *Journal of South American Earth Sciences,* Vol. 6, No. 3, 123-132.

ASPDEN J.A., HARRISON S.H., and RUNDLE C.C. (1992c) New geochronological control for the tectono-magmatic evolution of the metamorphic basement, Cordillera Real and El Oro Province of Ecuador. *Journal of South American Earth Sciences,* Vol. 6, No. 1/2, 77-96.

ASPDEN J.A., IVIMEY-COOK H.C. (1992) Nuevos Datos Paleontológicos del Centro y Sureste del Ecuador. (New palaeontological data from Central and Southeastern Ecuador). *Boletín Geológico Ecuatoriano,* Vol. 3, 33-42.

ASPDEN J.A., LITHERLAND M. (1987) Ophiolitic rocks from the Cordillera Real of Ecuador: their regional significances within the context of the Northern Andes. *Terra Cognita,* Vol 7, No. 2-3, 419.

ASPDEN J.A., LITHERLAND M. (1992) The geology and Mesozoic collisional history of the Cordillera Real, Ecuador. 187-204 in Andean Geodynamics. OLIVER R.A., et al. (editors). *Tectonophysics,* Vol. 205.

ASPDEN J.A., LITHERLAND M., DUQUE P., SALAZAR E., BERMÚDEZ R., and VITERI F. (1987) Un nuevo cinturón ofiolítico en la Cordillera Real, Ecuador, y su posible significación regional. [A new ophiolitic belt in the Cordillera Real, Ecuador, and its possible regional significance.] Politécnica, Quito, *Monografía de Geología,* Vol 5, Part XII, No. 2, 81-93.

ASPDEN J.A., LITHERLAND M., and SALAZAR E. (1988) Una interpretación preliminar de la historia colisional del centro y sur de Ecuador y posibles controles para la geología cenozoica y de mineralización polimetálica. [A preliminary interpretation of the collisional history of central and southern Ecuador and possible controls for Cenozoic geology and polymetallic mineralisation.] Politécnica, Quito. *Monografía de Geología,* Vol. 6, Part XIII, No. 3, 49-75.

ASPDEN J.A., RUNDLE C.C., and BERMÚDEZ R. (1991) Nueva información de la edad del batolito de Abitagua en el Oriente Ecuatoriano, por el método Rb/Sr. [New Information on the age of the Abitagua batholith in eastern Ecuador by the Rb-Sr method.]. *Boletín Geológico Ecuatoriano,* Vol. 2, 139-142.

ASPDEN J.A., LITHERLAND M., VITERI F., BERMÚDEZ R., and HARRISON S. (1990) Edades radiométricas del batolito de Zamora-Río Mayo. [Radiometric ages from the Zamora-Río Mayo batholith.] *Boletín Geológico Ecuatoriano,* Vol. 1, No 1, 85-88.

EGÜEZ A., and ASPDEN J.A. (1993) The Mesozoic-Cenozoic evolution of the Ecuadorian Andes. *Abstract of the Symposium on Andean Geodynamic,* Oxford, 179-181.

JEMIELITA R.A., ASPDEN J.A., and LITHERLAND M. (1992). The metallogenesis and mineral potential of the eastern Cordillera of Ecuador. *Abstracts of the Mineral Deposit Studies Group Annual Meeting, Aberdeen,* p. 11.

LITHERLAND M. and ASPDEN J.A. (1990) Evidence for pre-Cretaceous collision in Ecuador. 199-201 in *Colloques et Seminaires, Symposium International Geodynamique Andine, Grenoble.* (Paris: ORSTOM).

LITHERLAND M. and ASPDEN J.A. (1992) Terrane boundary reactivation: a control on the evolution of the Northern Andes. *Journal of South American Earth Sciences,* Vol. 5, No. 1. 71-76

LITHERLAND M., ASPDEN J.A. and EGÜEZ A. (1993) The geotectonic evolution of Ecuador in the Phanerozoic. *Abstract of the Symposium on Andean Geodynamic, Oxford,* 215-218.

LITHERLAND M., BERMÚDEZ R., and FORTEY N. (1992a) Las Ofiolitas de Peltetec y su significado en la Evolución Geológica del Ecuador. [The Peltetec ophiolite and its significances in the geological evolution of Ecuador.] *Boletín Geológico Ecuatoriano,* Vol. 3, No. 1, 43-46.

LITHERLAND M., FORTEY N., and BEDDOE-STEPHENS B. (1992b) Newly discovered Jurassic skarnfields in the Ecuadorian Andes. *Journal of South American Earth Sciences,* Vol. 6, No. 1/2, 67-75.

LITHERLAND M., POZO M., and BERMÚDEZ R. (1992c) El Complejo de Napas de Cuyuja de la Cordillera Real, Ecuador. [The Cuyuja nappe complexo f the Cordillera Real, Ecuador.] *Boletín Geológico Ecuatoriano,* Vol. 3, No. 1, 57-62.

LITHERLAND M. and TOWNSEND P.J. (1991) La Geología del Cerro Hermoso de los Llanganates. [The geology of Cerro Hermoso of the Llanganates]. *Boletín Geológico Ecuatoriano,* Vol. 2, 47-52.

LITHERLAND M., and ZAMORA A. (1991) A terrane configuration for the Northern Andes. *Comunicaciones de la Universidad de Chile, Santiago,* Vol. 42, 122-126.

LITHERLAND M., ASPDEN J.A., and EGÜEZ A. (1993a) National geological map of Ecuador, scale 1: 1 million. (Keyworth, Nottingham: British Geological Survey and Quito: CODIGEM.).

LITHERLAND M., ASPDEN J.A., and EGÜEZ A. (1993b) National tectono-metallogenic map of Ecuador, scale 1: 1 million. (Keyworth, Nottingham: British Geological Survey and Quito: CODIGEM.).

POZO M. (1990) Complejo ultramáfico Tampanchi. [Tampanchi ultramafic complex.] *Minería Ecuatoriana,* No. 2, 35-37.

4. OTHER REFERENCES

ALY S. (1980) Petrologische Untersuchungen plutonischer Gesteine von Ecuador. [Petrological investigations of plutonic rocks in Ecuador.] Unpublished thesis, University of Tübingen.

Annon (1988) Alaskan/Ural ultramafic complexes in the Canadian Cordillera. *The Gangue,* No. 26, Sept. 1988, 3-4.

ASPDEN J.A. and McCOURT W.J. (1986) Mesozoic oceanic terrane in the Central Andes of Colombia. *Geology*, Vol. 14, 415-418.

ASPDEN J.A., McCOURT W.J. and BROOK M. (1987) Geometric control of subduction-related magmatism: the Mesozoic and Cenozoic plutonic history of Western Colombia. *Journal of the Geological Society of London*, Vol. 144, 893-905.

BALDOCK J.W. (1982) *Geology of Ecuador: explanatory bulletin of the National Geological Map of the Republic of Ecuador*. (Quito: Dirección General de Geología y Minas).

BALDOCK J.W. (1985) The Northern Andes: a review of the Ecuadorian Pacific margin. 181-217 in *The Pacific Ocean*. Vol. 7A of *The ocean basins and margins*. NAIRN, A.E.M. et al. (editors). (New York: Plenum Press).

BANKWILL H.R., PAREDES F.I., and ALMEIDA J.P. (1991) Relations of intra-crustal delamination, stratigraphy and oil prospectivity, Oriente basin, Ecuador. *Petromine International, Quito,* No 4, 7-24.

BARBERI F., COLTELLI M., FERRARA G., INNOCENTI F., NAVARRO J.M., and SANTACROCE R. (1988) Plio-Quaternary volcanism in Ecuador. *Geological Magazine*, Vol. 125, No. 1, 1-14.

BERGER J.P., (1986) Dinoflagellates of the Callovian-Oxfordian boundary of the Liesberg-Dorf Quarry (Berner-Jura, Switzerland). *Neues Jahrbuch für Geologie un Paläontologie*, Vol. 172, 331-355.

BOUJO A., VERA R., ALABOUVETTE B., PRIAN J.P., GRANDA B. and MALDONADO P. (1984) Proyecto fosfatos [Phosphate Project]. Dirección General de Geología y Minas – BRGM-CIEPER, Quito (Unpublished).

BOYLE R.W. (1979) The geochemistry of gold and its deposits. *Bulletin of the Geological Survey of Canada*, No 280.

BRISTOW C.R. (1973) *Guide to the geology of the Cuenca Basin, southern Ecuador.* (Quito: Ecuadorian Geological and Geophysical Society).

BRISTOW C.R. and HOFFSTETTER R. (1977) *Lexique stratigraphique international (*2nd edition). (Paris : Centre National de la Recherche Scientifique).

BRISTOW C.R. and PARODIZ J.J. (1982) The stratigraphical paleontology of the Tertiary non-marine sediments of Ecuador. *Bulletin of Carnegie Museum of Natural History,* No. 19.

BRISTOW C.R., LONGO R. and GUEVARA S. (1975) Mapa geológico del área de Cañar. [Geological map of the Cañar área]. Dirección General de Geología y Minas, Quito.

BRUET F. (1987) Los xenolitos en las lavas de los volcanes de Quito, República de Ecuador. [Xenoliths in the lavas of Quito´s volcanoes, Ecuador] *Politécnica, Quito,* Vol. XII, No. 2, 113-128.

CARRIÓN J. and VILLALBA F. (1981) Investigaciones uraníferas en el Ecuador. [Uranium investigations in Ecuador]. *Politécnica, Quito,* Vol. VI, No. 4, 85-117.

CASE J.E., BARNES J., PARIS G., GONZALES H. and VINA A. (1973) Trans-Andean geophyisical profile, southern Colombia. *Bulletin of the Geological Society of America*, Vol. 84, 2895-2904.

CHACÓN Z.J. (1986) Historia de la minería en Cuenca. [History of mining in Cuenca]. Universidad de Cuenca, Instituto de Investigaciones Sociales (IDIS).

CHAPPELL B.W. and WHITE A.J.R. (1974) Two contrasting granite types. *Pacific Geology*, Vol. 8, 173-174.

CLIRSEN (1985) Inventario de Recursos Mineros del Ecuador, Hoja Azogues. [Mineral resource inventory for Ecuador: Azogues sheet]. Centro de Levantamientos Integrados de Recursos Naturales, Quito, (unpublished).

COBBING E.J., PITCHER W.S., WILSON J.J, BALDOCK J.W., TAYLOR W.P., McCOURT W. and SNELLING N.J. (1981) The geology of the Western Cordillera of northern Perú. *Overseas Memoir of the Institute of Geological Sciences*, No. 5. 143 pp.

COLONY R.J. and SINCLAIR J.H. (1932) Metamorphic and igneous rocks of eastern Ecuador. *Annals of the New York Academy of Sciences*, Vol. 34, 1-53.

COLVINE A.C., FYON J.A., HEATHER K.B., SOUSSAN MARMONT, SMITH P.M. and TROOP D.G. (1988) Archean lode gold deposits in Ontario. *Ontario Geological Survey Miscellaneous Paper*, No. 139.

CONEY P.J., JONES D.L. and MONGER J.W.H. (1980) Cordilleran suspect terranes. *Nature, London*, Vol. 288, 329-333.

DALMAYRAC B., LAUBACHER G. and MAROCCO R. (1980) *Géologie des Andes Péruviennes.* [Geology of the Peruvian Andes]. (Paris : Office de la Recherche Scientifique et Technique Outre-Mer).

DALZIEL I.W.D. (1993) The origin and early history of the Pacific margin of South America: their influence on the development of the Andean Cordillera. *Abstracts of the Symposium on Andean Geodynamics*, Oxford, 505-508.

DALY M.C. (1989) Correlation between Nazca / Farallón plate kinematics and forearc basin evolution in Ecuador. *Tectonics*, Vol. 8, No. 4, 769-790.

DÁVILA F. and EGÜEZ A. (1990) Análisis de la deformación en el basamento de la cuenca del Chota: Grupo Ambuquí. [Deformation analysis in the basement of the Chota basin: Ambuquí Group]. *Boletín Geológico Ecuatoriano*, Vol. 1, No. 1, 39-52.

DE COSTER A. (1987) Metallogenetic study of the mineralisation at San Bartolomé and Sigsig. Internal Report, Musee Royal de l'Afrique Centrale, Brussels (Unpublished).

DE GRYS A., VERA J., and GOOSSENS P.J. (1970) A note on the hot springs of Ecuador. *Geothermics Special Issue for UN Symposium on the development and utilisation of geothermal resources, Pisa 1970*, Vol. 2, Part 2, 1400-1404.

DELBRIDGE C.G., and ROBERTSOM A. (1992) Ecuador Mineral Industry Profile. Delbridge-Robertson Associates, UK. (Unpublished).

DE LOCZY L. (1968) Geotectonic evolution of the Amazon, Parnaiba and Paraná basins. *Anais da Academia Brasileira de Ciencias*, Vol. 40, 231-249.

DEWEY J.F. and BIRD J.M. (1970) Mountain belts and new global tectonics. *Journal of Geophysical Research*, Vol. 75, 2625-2647.

D'LEMOS R.S., BROWN M. and STRACHAN R.A. (1992) Granite generation, ascent and emplacement within a transpressional orogen. *Journal of the Geological Society of London*, Vol. 149, Part 4, 487-490.

DUQUE P. (1974) Petrogénesis de unas rocas metamórficas de alta presión en la Provincia de El Oro, Ecuador. [Petrogenesis of some high-pressure metamorphic rocks from the El Oro Province, Ecuador]. Unpublished thesis, Escuela Politécnica Nacional, Quito. 66 pp.

DUQUE P. (1992) Condiciones de formación de las rocas metamórficas de alta presión de la formación Raspas. [Conditions of formation of the high-pressure metamorphic rocks of the Raspas formation]. *Boletín Geológico Ecuatoriano*, Vol. 3, No. 1, 63-78.

EGÜEZ A., CAJAS M. and DÁVILA F. (1988). Distribución de terrenos oceánicos alóctonos y de terrenos continentales en la Cordillera Occidental del Ecuador: evidencias en las geotravesías Otavalo-Selva Alegre y Cañar-La Troncal. [The distribution of allochthonous oceanic and continental terranes in the Cordillera Occidental of Ecuador: evidence from the Otavalo-Selva Alegre and Cañar-La Troncal geotraverses]. Politécnica, Quito. *Monografía de Geología*, Vol. 6, Part XIII, No. 3. 101-136.

EINAUDI M.T., MEINERT L.D. and NEWBERRY Y. (1981) Skarn deposits. *Economic Geology 75th Anniversary Volume*, 317-391.

EVERNDEN J. (1961) Edades absolutas de algunas rocas ígneas en Bolivia. [Absolute ages of some Bolivian igneous rocks]. *Noticiero Sociedad Geológico Boliviano*, Vol. 2, 3.

EWART A. (1982) The mineralogy and petrology of Tertiary – Recent orogenic volcanic rocks: with special reference to the andesitic basaltic composition range. 25-87 in *Andesites*. THORPE R.S. (editor). (Chichester: John Wiley).

FEININGER T. (1975) Origin of petroleum in the Oriente of Ecuador. *Bulletin of the American Association of Petroleum Geologists*, Vol. 57, No.7, 1166-1175.

FEININGER T. (1978) Mapa geológico de la parte occidental de la Provincia de El Oro. [Geological map of the western part of the El Oro Province]. (Quito: Escuela Politécnica Nacional).

FEININGER T. (1980) Eclogite and related high-pressure regional metamorphic rocks from the Andes of Ecuador. *Journal of Petrology*, Vol. 21, 107-140.

FEININGER T. (1982) The metamorphic 'basement' of Ecuador. *Bulletin of the Geological Society of America*. Vol. 93, 87-92.

FEININGER T. (1987) Allochthonous terrane in the Andes of Ecuador and northwestern Perú. *Canadian Journal of Earth Sciences*, Vol. 24, 266-278.

FEININGER T. and BRISTOW C.R. (1980) Cretaceous and Paleogene geologic history of coastal Ecuador. *Geologische Rundschau*, Vol. 69, Part 3, 849-874.

FEININGER T. and SEGUIN M.K. (1983) Simple Bouguer gravity anomaly field and the inferred crustal structure of continental Ecuador. *Geology*, Vol. 11, 40-44.

FEININGER T. and SILBERMAN M.L. (1982) K-Ar geochronology of basement rocks on the northern flanks of the Huancabamba Deflection, Ecuador. *Open File Report, United States Geological Survey*, No. 82-206.

FORERO SUÁREZ A. (1990) The basement of the Eastern Cordillera, Colombia: An allochthonous terrane in northwestern South America. *Journal of South American Earth Sciences*, Vol. 3, No. 2/3, 141-151.

FOZZARD P.M. (1985) San Bartolomé, Ecuador. 115-116 in *Discoveries of epithermal precious metal deposits. Case histories of mineral discoveries.* HOLLISTER V.F. (editor). (Society of Mining Engineers, USA).

FRUTOS J. (1982) Andean metallogeny related to the tectonic and petrologic evolution of the cordillera: some remarkable points. 493-507 in *Ore genesis, the state of the art.* G.S. AMSTUTZ et al. (editors). (Berlin: Springer-Verlag).

FULP S.F. and WOODWARD L.A. (1990) Epithermal gold deposits remobilized from Precambrian volcanogenic sulfide source during late Cenozoic continental rifting. *Geology*. Vol. 18, 179-182.

GANSSER A. (1973) Facts and theories on the Andes. *Journal of the Geological Society of London*, Vol. 129. 93-131.

GEMUTS I., LÓPEZ G. and JIMÉNEZ F. (1992) Gold deposits of southern Ecuador. *Society of Economic Geologists Newsletter*, Oct. 1992, No. 11, 1 and 13-16.

GERTH H. (1955). Der Geologische Bau der sudamerikanischen Kordillere. [The geological structure of the South American Cordillera]. (Berlin: Borntraeger).

GEYER O.F. (1974) Der Unterjura (Santiago Formation) von Ekuador. [The Lower Jurassic (Santiago Formation) of Ecuador] *Neues Jahrbuch Paläontologie Monatshefte*, Vol. 9, 525-541.

GOLDFARB R.J., NELSON S.W., BERG H.C. and LIGHT T.D. (1986) Distribution of mineral deposits in the Pacific Border Ranges and coast mountains of the Alaskan Cordillera. 19-41 in *Exploration in the North American Cordillera*. ELLIOT I.L. and SMEE B.W. (editors). Association of Exploration Geochemists, Geoexpo/86, P.

GOOSSENS P.J. (1968) La geología de la costa ecuatoriana entre Manta y Guayaquil. [The Geology of the Ecuadorian coast between Manta and Guayaquil]. *Boletín Estudios Geológicos Servicio Nacional Geológico-Minero,* No. 1, 5 – 17.

GOOSSENS P.J. (1969) Mineral Index Map, Republic of Ecuador. UN – Dirección General de Geología y Minas, Quito.

GOOSSENS P.J. (1972a) *Los yacimientos e indicios de los minerales metálicos y no metálicos de la República del Ecuador.* [*The metallic and non-metallic deposits and showings of Ecuador*]. Departamento de publicaciones, Universidad de Guayaquil.

GOOSSENS P.J. (1972b) Metallogeny in the Ecuadorian Andes. *Economic Geology,* Vol. 67, 458-468.

GOOSSENS P.J. and ROSE W.I. (1973. Chemical composition and age determination of tholeiitic rocks in the Basic Igneous Complex, Ecuador. *Bulletin of the Geological Society of America,* Vol. 84, 1043-1052.

GRANT A.H., LAVIN O.P. and NICOL I. (1991) The morphology and chemistry of transported gold grains as an exploration tool. *Journal of Geochemical Exploration,* Vol. 40, 73-94.

GROSSER J.R. and PROSSL K.F. (1991) First evidence of the Silurian in Colombia: palynostratigraphic data from the Quetame massif, Cordillera Oriental. *Journal of South American Earth Sciences*, Vol. 4, No. 3, 231-238.

HALL M. and CALLE J. (1982) Geochronological control for the main tectono-magmatic events of Ecuador. *Earth Science Review*, Vol. 10, 215-239.

HANMER S. and PASSCHIER C. (1991) Shear-zone indicators: a review. *Geological Survey of Canada, Paper*, No. 90-17, 72pp.

HARRINGTON J. (1957) Varios aspectos de las investigaciones de las posibilidades mineras en las provincias de Azuay y Cañar. [Various aspects of mineral potential investigations in Azuay and Cañar provinces]. *Servicio Nacional de Geología y Minas, Quito, Report H,* No. 665-1. (Unpublished).

HARTNADY C.J.H. (1991) About turn for supercontinents. *Nature, London,* London, Vol. 352. 476-478.

HERBERT H. (1977) Petrochemie und Ausgangmaterial von Grünschiefern aus der E-Kordillere Ecuadors. [Petrochemistry and origin of the greenschists from the Eastern Cordillera of Ecuador]. *Fortschritte der Mineralogie*, Vol. 55, No. 1.

HERBERT H. (1983) Die kristallinen Gesteine aus der nördlichen Hälfte der E-Kordillere Ecuadors. [The crystalline rocks of the northern half of the Eastern Cordillera, Ecuador]. *Geotektonische Forschungen*, Vol. 65, 1-77.

HERBERT H. and PICHLER H. (1983) K-Ar ages of rocks from the Eastern Cordillera of Ecuador. *Zeitschrift der deutschen Geologischen Gesellschaft*, Vol. 134, 483-493.

HOFFMANN P. (1991) Did the breakout of Laurentia turn Gondwanaland inside-out? *Science, New York,* Vol. 252, 1409-1412.

HOLLOWAY H.L. (1932) Gold in Ecuador. *Mining Magazine* (April), Vol. 46, No. 4, 219-223.

HUTCHINSON R.W. (1980) Massive base metal sulphide deposits as guides to tectonic evolution. 659-694 *in* The continental crust and the mineral deposits. Strangeway, D.W. (editor). *Geological Association of Canada Special Paper,* No. 20, 659-684.

HUTCHISON C.S. (1982) The various granitoid series and their relationship to W and Sn mineralisation. 87-114 *in* Symposium on Tungsten Geology (HEPWORTH J.V. and ZHANG YU HONG (editors). ESCAP/RMRDC Bandung, Indonesia.

HUTCHISON C.S. (1983) Economic deposits and their tectonic setting. (London: Macmillan).

INEMIN-MISIÓN BELGA (1986) Informe Chaucha [Chaucha report] Instituto Ecuatoriano de Minería, Quito. 311 pp. (Unpublished).

INEMIN-MISIÓN BELGA (1988) Inventario, clasificación y metalogenia de las mineralizaciones polimetálicos en el Ecuador [Inventory, classification and metallogeny of polymetallic mineralisation in Ecuador]. Instituto Ecuatoriano de Minería, Quito. 334 pp. (Unpublished).

IRVINE T.N. (1974) Petrology of the Duke Island ultramafic complex, southeastern Alaska. *Memoir of the Geological Society of America Memoir,* No. 138. 240 pp.

ISHIHARA S. (1977) The magnetite-series and ilmenite-series of granitic rocks. *Mining Geology,* Vol. 27, 293-305.

JAILLARD E. and JACAY J. (1989) Les “couches Chicama” du Nord du Pérou : Colmatage d’un bassin né d’une collision oblique au Tithonique. [The “Chicana beds” of northern Perú: in-filling of a trough originated by oblique collision during Tithonian times]. *Comptes Rendus Hebdomadaire des Séances de l’Académie des Sciences de Paris,* (II), Vol. 308, 1459-1465.

JAILLARD E., SOLER P., CARLIER G. and MOURIER T. (1990) Geodynamic evolution of the northern and central Andes during early to middle Mesozoic times: a Tethyan model. *Journal of the Geological Society of London*, Vol. 147, Part 6, 1009-1022.

JAMES D.E. (1984) Quantitative models for crustal contamination in the Central and Northern Andes. 124-137 in *Andean magmatism: chemical and isotopic constraints.* HARMON R.S. and BARREIRO B.A. (editors). (Nantwich UK: Shiva).

JONES B.K. (1992) Application of metal zoning to gold exploration in porphyry copper systems. *Journal of Geochemical Exploration,* Vol. 43, 127-155.

JONES D.L., HOWELL D.G., CONEY P.J. and MONGER J.W.H. (1983) Recognition, character, and analysis of tectonostratigraphic terranes in western North America. 21-35 in *Accreted terranes in the Circum-Pacific regions.* HASHIMOTO M. and UYEDA S. (editors). (Tokyo: Terra Scientific Publishing Company).

KENNERLEY J.B. (1971) Geology of the Llanganates area, Ecuador. *Report of the Institute of Geological Sciences (Overseas Division),* No. 21.

KENNERLEY J.B. (1973) Geology of the Loja Province. *Report of the Institute of Geological Sciences (Overseas Division),* No. 23.

KENNERLEY J.B. (1980) (posthumous) Outline of the geology of Ecuador. *Overseas Geology and Mineral Resources,* No. 55.

KENNERLEY J.B. and ALMEIDA L. (1975) Mapa geológico del área de Loja. [Geological map of the Loja area]. Dirección General de Geología y Minas, Quito.

KONTAK D.J., CLARK A.H., FARRAR E. and STRONG D.F. (1985) The rift-associated Permo-Triassic magmatism of the Eastern Cordillera: a precursor to the Andean orogeny. 36 – 44 in *Magmatism at a plate edge.* (PITCHER W.S. et al. (editors). (London: Blackie).

KRIPPENE K. (1960) A fortune in emeralds. *Argosy,* June 1960, 30-107.

KROONENBERG S.B. (1982) A Grenvillian granulite belt in the Colombian Andes and its relation to the Guiana Shield. *Geologie en Mijnbouw,* Vol. 61, 325-333.

LAUBACHER G. and MEGARD F. (1985) The Hercynian basement: a review. 29-35 in *Magmatism at a plate edge.* PITCHER W.S., et al. (editors). (London: Blackie).

LAVENU A. and NOBLET C. (1990) Análisis sedimentológico y tectónico de la cuenca intramotañosa terciaria de Cuenca. [Sedimentological and tectonic analysis of the Tertiary intramontane basin of Cuenca]. *Boletín Geológico Ecuatoriano,* Vol. 1, No. 1, 11-26.

LAVENU A., NOBLET C., BONHOMME M.G., EGÜEZ A., DUGAS F. and VIVIER G. (1992) New K-Ar age dates of Neogene and Quaternary volcanic rocks from the Ecuadorian Andes: Implications for the relationship between sedimentation, volcanism and tectonics. *Journal of South American Earth Sciences,* Vol. 5 No. 3/4, 309-320.

LE BAS M.J., LE MAITRE R.W., STRECKEISEN A. and ZANETTIN B. (1986) A chemical classification of volcanic rocks based on the total alkali-silica diagram. *Journal of Petrology,* Vol. 27, 745-750.

LEBRAT M., MEGARD F., and DUPUY C. (1985) Pre-orogenic volcanic assemblages and position of the suture between oceanic terranes and the South American continent in Ecuador. *Zentralblatt für Geologie Paläontologie,* Teil I, Vol. 9/10, 1207-1214.

LEHMANN B. and HARMANTO (1990) Large-scale tin depletion in the Tanjungpandan tin granite, Belitung Island, Indonesia. *Economic Geology,* Vol. 85, 99-111.

LIDDLE R.A. and PALMER K.V.W (1941) The geology and palaeontology of the Cuenca – Azogues – Biblián region, provinces of Cañar and Azuay, Ecuador. *Bulletin of the American Palaeontologist,* Vol. 26, No. 100, 357-418.

LITHERLAND M., ANNELLS R.N., DARBYSHIRE D.P.F., FLETCHER C.J.N., HAWKINS M.P., KLINCK B.A., MITCHELL W.I., O' CONNOR E.A., PITFIELD P.E.J., POWER G., and WEBB B.C. (1989) The Proterozoic of eastern Bolivia and its relationship to the Andean mobile belt. *Precambrian Research,* Vol. 43, 157-174.

LITHERLAND M., KLINCK B.A., O' CONNOR E.A. and PITFIELD P.E.J. (1985). Andean-trending mobile belts in the Brazilian Shield. *Nature, London,* Vol. 314, 345-348.

LITHERLAND MARTIN (2015) Inca Treasure. Poems from the Andes of Ecuador. Smashwords Edition ֍.

LISTER G.S. and SNOKE A.W. (1984) S.C mylonites. *Journal of Structural Geology,* Vol. 6, 617-638.

MARTÍNEZ M. (1970) Geología del basamento paleozoico en las montañas de Amotape y posible origen del petróleo en las rocas paleozoicas del noreste de Perú. [The Palaeozoic basement Geology of the Amotape mountains and the possible origin of petroleum in the Palaeozoic rocks of northeast Perú]. 1er Congreso Latinoamericano de Geología, Lima, Vol. 2, 105-138.

MCCOURT W.J., ASPDEN J.A. and BROOK M. (1984) New geological and geochronological data from the Colombian Andes: continental growth by multiple accretion. *Journal of the Geological Society of London,* Vol. 141, 831-845.

MACINNES H. (1984) *Beyond the Ranges* (London: Victor Gollanz).

MCKELVEY G.E. (1991) Interest shown in Nambija gold deposits, Zamora province, Ecuador. *Mining Engineering,* December 1991, 1412-1414.

MCMILLAN W.J., PANTELEYEV A. and HOY T. (1986) Mineral deposits in British Colombia: A review of their tectonic settings. 1-18 in *Exploration in the North American Cordillera.* ELLIOT I.L. and SMEE B.W. (editors). Association of Exploration Geochemists, Geoexpo/86, P.

MEINERT L.D. (1988) Gold in skarn deposits – a preliminary overview. *Proceedings of 7th Quadrennial IAGOD Symposium,* 363-374.

MERLYN M. and CRUZ M. (1986) Informe técnico de la comisión realizada al área central de los Llanganates. [Technical report on the commission to the central Llanganates area]. *Report of the Instituto Ecuatoriano de Minería,* No. 6452/86. (Unpublished).

MIYASHIRO A. (1961) Evolution of metamorphics belts. *Journal of Petrology,* Vol. 2, 277-311.

MORA I.M. (1988) Petrología estructural de la Formación Raspas, Provincia de El Oro. [Structural petrology of the Raspas Formation, El Oro Province). Unpublished thesis, Escuela Politécnica, Quito. 159 pp.

MOURIER T. (1988) La transition entre Andes marginales et Andes cordillèraines à ophiolites : évolution sédimentaire, magmatique et structurale du relais de Huancabamba. [Sedimentation, tectonism and magmatism along the transition between Cordilleran and marginal Andes of Huancabamba]. Unpublished thesis, University of Paris Sud. 281 pp.

MOURIER T., LAJ C., MEGARD F., ROPERCH P., MITOUARD P. and FARFÁN-MEDRANO A. (1988) An accreted continental terrane in northwestern Peru. *Earth and Planetary Science Letters,* Vol. 88, 182-192.

MURRAY C.G. (1972) Zoned ultramafic complexes of the Alaskan type: feeder pipes of andesitic volcanoes. *Memoir Geological Society of America,* Vol. 132, 313-335.

NAVARRO M. (1986) Investigación histórica de la minería en el Ecuador. [Historical investigation of mining in Ecuador]. (Quito: Instituto Ecuatoriano de Minería).

NESBITT B.E. and MUEHLENBACHS K. (1986) Genetic implications of the association of mesothermal gold deposits with major strike slip fault systems. University of Rolla, North American Conference on Tectonic Controls of Ore Deposits, 57-66.

NICOLÁS A., BOUCHEZ J.L., BLAISE J. and POIRIER J.P. (1977) Geological aspects of deformation in continental shear zones. *Tectonophysics,* Vol. 42, 55-73.

NOBLET C. and MAROCCO R. (1989) Lacustrine megaturbidites in an intermontane strike-slip basin: the Miocene Cuenca basin of south Ecuador. International Symposium on Intermontane Basins: Geology and Resources, Chiang Mai, Thailand, 282-293.

PALADINES A. (1989) Zonificación geotectónica y metalogenia del Ecuador. [Geotectonic zoning and metallogeny in Ecuador] Instituto Ecuatoriano de Minería, Quito. 192 pp.

PASQUARE G., TIBALDI A. and FERRARI L. (1990) Relationships between plate convergence and tectonic evolution in the Ecuadorian active thrust belt. 365-387 in *Critical aspects of plate tectonic theory*. (Athens: Theophrastos Publications).

PEARCE J.A. (1983) Role of the subcontinental lithosphere in magma genesis at active continental margins. 230-272 in *Continental basalts and mantle xenoliths*. HAWKSWORTH C.J. and NORRY M.J. (editors). (Nantwitch, UK: Shiva).

PEARCE J.A. and CANN J.R. (1973) Tectonic setting of basic volcanic rocks determined using trace elements. *Earth and Planetary Science Letters*, Vol. 19, 290-300.

PEARCE J.A., HARRIS N.B.W. and TINDLE A.G. (1984a). Trace element discrimination diagrams for the tectonic interpretation of granitic rocks. *Journal of Petrology*, Vol. 5, 956-983.

PEARCE J.A., LIPPARD S.J. and ROBERTS S. (1984b) Characteristics and tectonic significance of supra-subduction zone ophiolites. 77-96 *in* Marginal basin geology. KOKELAAR B.P. and HOWELLS M.F. (editors). *Special Publication of the Geological Society of London*, No. 16.

PICHLER H. and ALY S. (1983) Neue K-Ar-Alter plutonischer Gesteine in Ecuador. [New K-Ar dates of plutonics rocks in Ecuador]. *Zeitschrift der Deutschen Geologischen Gesellschaft*, Vol. 134, 495-506.

PITCHER W.S. (1983) Granite type and tectonic environment. 19-40 in *Mountain building processes.* HSU K. (editor). (London: Academic Press).

PILLAJO E. (1982) Origen del oro aluvial en el Ecuador. [The origin of alluvial gold in Ecuador]. *Flysch*, Vol. 3, 48-73.

PILLAJO E. and BÁEZ N. (1983) Mapa del potencial aurífero aluvial de la República del Ecuador. [Alluvial gold potential map for Ecuador]. Dirección General de Geología y Minas, Quito (Unpublished).

PLATT J.P. (1987) The uplift of high pressure-low temperature metamorphic rocks. *Philosophical Transactions of the Royal Society of London*, Vol. A.321, 87-102.

PUIG C. and PAZMIÑO H. (1990) Desarrollo minero de San Bartolomé. [The mineral Development of San Bartolomé]. *Minería Ecuatoriana*, No. 2, 21-24.

PUTZER A. and SCHNEIDER A. (1958) Informe sobre investigaciones de yacimientos en el Ecuador. [Report on mineral investigations in Ecuador] Misión Alemana-Servicio Nacional de Geología y Minas, Quito. (Unpublished).

RAMOS V.A. (1989) The birth of southern South America. *American Scientist*, Vol. 77, 444-450.

REAVY R.J. (1989) Structural controls on metamorphism and syntectonic magmatism: the Portuguese Hercynian collision belt. *Journal of the Geological Society of London*, Vol. 146, Part 4, 649-658.

RESTREPO J.J. and TOUSSAINT J.F. (1988) Terranes and continental accretion in the Colombian Andes. *Episodes*, Vol. 11, No. 3, 189-193.

RESTREPO-PACE P.A. (1992) Petrotectonic characterization of the Central Andean Terrane, Colombia. *Journal of South American Earth Sciences*, Vol. 5, No. 1, 97-116.

RIBADENEIRA J.A. (1960) Varios minerales. [Various minerals]. *Servicio Nacional de Geología y Minas, Archivo Técnico*, No. 139-2 (Unpublished).

RIDING J.B. (1987) Dinoflagellate cyst stratigraphy of the Nettleton Bottom borehole (Jurassic: Hettangian to Kimmeridgian), Lincolnshire, England. *Proceedings of the Yorkshire Geological Society*, Vol. 46, 231-266.

ROPERCH P., MEGARD F., LAJ C., MOURIER T., CLUBE T. and NOBLET C. (1987) Rotated oceanic blocks in western Ecuador. *Geophysical Research Letters*, Vol. 14, No. 5, 558-561.

ROSS M.I. and SCOTESE C.R. (1988) A hierarchical tectonic model of the Gulf of México and Caribbean region. *Tectonophysics*, Vol. 155, 139-168

SALAZAR E. (1988) Nambija: conocimiento geológico y mineralógico hasta el presente. [Nambija: present geological and mineralogical knowledge]. Internal Report, Instituto Ecuatoriano de Minería, Quito. (Unpublished).

SALAZAR E., CILSO E. and DIAZ L. (1986) Mapa geológico de la Hoja San Gabriel. [Geological map of the San Gabriel sheet]. Instituto Ecuatoriano de Minería, Quito.

SAUER W. (1950) Mapa geológico del Ecuador 1:1500000. [Geological map of Ecuador 1:1500000]. (Quito: Universidad Central and Dirección de Minería).

SAUER W. (1957) El mapa geológico del Ecuador. Memoria explicativa. [Geological map of Ecuador; explanatory report]. (Quito: Universidad Central).

SAUER W. (1958) El Cerro Hermoso de los Llanganates en el Ecuador. [Cerro Hermoso of the Llanganates in Ecuador]. *Boletín Instituto Científico Nacional, Quito*, Vol. 8, No. 75, 465-499.

SAUER W. (1965) *Geología del Ecuador*. [*Geology of Ecuador*] (Quito: Ministerio de Educación).

SCHNEIDER H.J. and LEHMANN B. (1977) Contribution to a new genetic concept of the Bolivian tin province. 153-168 in *Time and stratabound or deposits*. (Berlin: Springer-Verlag).

SEVERNE B., PEÑAHERRERA P.F. and FIALLOS V.S. (1978) Uranium exploration in Ecuador. International Atomic Energy Agency-AG-162/12, 179-189.

SHACKLETON R.M., RIES A.C., COWARD M.P. and COBBALD P.R. (1979) Structure, metamorphism and geochronology of the Arequipa Massif of coastal Perú. *Journal of the Geological Society of London*, Vol. 136, 195-214.

SHEPPARD G. and BUSHNELL G.H.S. (1933) Metamorphic rocks of the eastern Andes near Cuenca, Ecuador. *Geological Magazine*, Vol. 70, 321-330.

SILLITOE R.H. (1972) Relation of metal provinces in western America to subduction of oceanic lithosphere. *Bulletin of the Geological Society of America*, Vol. 83, 813-818.

SILLITOE R.H. (1993) Gold and copper metallogeny of the Central Andes – past, present and future exploration objectives. *Economic Geology*, Vol. 87, 2205-2216.

SOLER P. and SEBRIER M. (1990) Nazca slab retreat versus compressional deformation in the Central Andes since Late Oligocene times. 187-190 in *Colloques et Séminaires, Symposium International Géodynamique Andine, Grenoble* (Paris : ORSTOM).

SOULAS J., EGÜEZ A., YÉPEZ J. and PÉREZ H. (1991) Tectónica activa y riesgo sísmico de los Andes ecuatorianos en el extremo sur de Colombia. [Active tectonics and seismic risks of the Ecuadorian Andes and southern Colombia]. *Boletín Geológico Ecuatoriano,* Vol 2, No. 1, 3-12.

SPINDLER J.P. and HERRERA J.I. (1959) Reconocimiento geológico del Cerro Pilzhum y de la zona Taday-Pindilig. [Reconnaissance Geology of Cerro Pilzhum and the Taday-Pindilig area]. *Report Misión geológica-minera Franco-Ecuatoriana, Quito,* No. 7. (Unpublished).

STEIGER R.H. and JAEGER E. (1977) Subcommission on Geochronology: convention on the use of decay constants in geo- and cosmo-chronology. *Earth and Planetary Sciences Letters,* Vol. 36, 356-362

STOLL W.C. (1962) Notes on the mineral resources of Ecuador. *Economic Geology,* Vol. 57, No. 5, 799-805.

STOREY B.C. (1993) The changing face of late Precambrian and early Palaeozoic reconstructions. *Journal of the Geological Society of London,* Vol. 150, Part 4, 665-668.

STRECKEISEN A. (1976). To each plutonic rock its proper name. *Earth Science Reviews,* Vol. 12, 1-33.

SUÁREZ M. and BELL C.M. (1992) Triassic rift-related sedimentary basins in northern Chile (24°-29°S). *Journal of South American Earth Sciences,* Vol. 6, No. 3, 109-121.

SYLVESTER A.G. (1988) Strike-slip faults. *Bulletin of the Geological Society of America,* Vol. 100, 1666-1703.

TAYLOR H.P. (1967) The zoned ultramafic complexes of southeastern Alaska. 97-121 in *Ultramafic and related rocks.* WYLLITE P.J. (editor). (New York: Wiley).

TIBALDI A. and FERRARI L. (1992) Latest Pleistocene-Holocene tectonics of the Ecuadorian Andes. 109-126 *in* Andean geodynamics. OLIVER R.A., VATIN-PÉRIGNON N. and LAUBACHER G. (editors). *Tectonophysics,* Vol. 205.

TROUW R. (1976) *Cuatro cortes por la faja metamórfica de la Cordillera Real, Ecuador*. [*Four traverses across the metamorphic belt of the Cordillera Real, Ecuador*]. (Guayaquil: Escuela Politécnica del Litoral).

TSCHOPP H.J. (1948) Geologische Skizze von Ekuador. [Geological sketch of Ecuador]- *Bulletin de l'Association. Suisse de Géologie Ingénieur et Petrologie,* Vol. 15, No. 48, 14-15.

TSCHOPP H.J. (1953) Oil explorations in the Oriente of Ecuador. *Bulletin of the American Association of Petroleum Geologists,* Vol. 37, No. 10, 2303-2347.

TSCHOPP H.J. (1956) Upper Amazon Basin geological province. 253-267 *in* Handbook of South American geology. *Memoir of the Geological Society of America,* Vol. 65.

UNDP (1969) Survey of metallic and nonmetallic minerals. *Technical Reports, UN Development Programme, New York,* Nos. 1-3

UNDP (1972) Survey of metallic and nonmetallic minerals (Phase II). *Technical Reports, UN Development Programme, New York,* Nos. 12-17.

VAN THOURNOUT F., HERTOGEN J. and QUEVEDO L. (1992) Allochthonous terranes in northwestern Ecuador. 205-222 *in* Andean geodynamics. OLIVER R.A., VATIN-PÉRIGNON N. and LAUBACHER G. (editors). *Tectonophysics,* Vol. 205.

VAN THOURNOUT F. and PIEDRA J. (1986) Informe sobre la zona de Sardinas, Provincia de Napo. [Report on the Sardinas area, Napo Province]. Instituto Ecuatoriano de Minería. (Unpublished).

VAN THOURNOUT F., VALENZUELA G., MERLYN M. and SALEMINK J. (1991) Portovelo: mineralización epitermal en relación con una caldera riolítica. [Portovelo: epithermal mineralisation related to a rhyolitic caldera]. *Boletín Geológico Ecuatoriano,* Vol. 2, No. 1, 13-26.

VERA R. (1980) La fosforita uranífera, Río Chingual, Provincia del Napo. [The uraniferous phosphate, Río Chingual, Napo Province]. *Politécnica, Quito,* Vol. V, No. 2, 47-55.

VERA R. and VIVANCO G. (1983) Estudio Estructural del Cerro Hermoso de los Llanganates. [Structural study of Cerro Hermoso of the Llanganates]. III Congreso Ecuatoriano de Ingenieros geológicos, de minas y petróleos, Quito, 1-15.

WASSON T. and SINCLAIR J.H. (1923) Geological explorations east of the Andes in Ecuador. *Bulletin of the American Association of Petroleum Geologists,* Vol. 11, No. 12, 1253-1281.

WINCHESTER J.A. and FLOYD P.A. (1977) Geochemical discrimination of different magma series and their differentiation products using immobile elements. *Chemical Geology,* Vol. 20, 325-343.

WILKINSON A. (1982) Exploration for phosphate in Ecuador. *Transactions of the Institution of Mining and Metallurgy,* Vol. 91, B130-B145.

WINKLER H.G.F. (1967) *Petrogenesis of metamorphic rocks* (2nd edition). (New York: Springer-Verlag).

WINKLER H.G.F. (1976) *Petrogenesis of metamorphic rocks* (4th edition). (New York: Springer-Verlag).

WINTER Th., IGLESIAS R. and LAVENU A. (1990) Presencia de un Sistema de fallas activas en el sur del Ecuador. [A system of active faults in southern Ecuador]. *Boletín Geológico Ecuatoriano,* Vol. 1, No. 1, 53-68.

WOLF T (1892) Geografía y geología del Ecuador. [Geography and geology of Ecuador]. (Leipzig: Brockhaus)

WOODCOCK N.H. (1986) The role of strike-slip faults at plate boundaries. *Philosophical Transactions of the Royal Society of London,* Vol. A.317. 13-29.

WOOLLAM R. and RIDING J.B. (1983) Dinoflagellate cyst zonation of the English Jurassic. *Report of the Institute of Geological Sciences*, No. 83/2.

ZAMORA A. and POTHE DE BALDIS E. (1988) Nuevos aportes al conocimiento del Paleozoico del Ecuador. [New contributions to the understanding of the Palaeozoic of Ecuador]. *Minería Ecuatoriana,* INEMIN, Quito, Vol. 1, 54.

ZEIL W. (1979) The Andes, a geological review. (Berlín: Gebrüder Borntraeger).

APPENDIX 1

Geochronological data

LOCATION AND DESCRIPTION OF SAMPLES

Sample no.	Rock type(s)	Area	Map Sheet*	Grid reference
Garnet gneisses, Agoyán unit				
CCR/87/11A-E	Garnet biotite muscovite schists/gneisses	Baños-Puyo road	Baños (c)	7939-8458 7918-8457
Garnet gneisses/amphibolite, Agoyán unit, Papallacta				
CCR/87/4	Biotitic amphibolite	Papallacta village	Papallacta (c)	8184-99596
CRSH/891A	Garnet amphibolite	Float block, Río Chalpi Grande	Papallacta (c)	8246-99608
CRSH/89/1B-C	Garnet biotite ± muscovite gneisses	Float block, Río Chalpi Grande	Papallacta (c)	8246-99608
Sabanilla unit garnet gneisses/amphibolite, Valladolid				
CCR/87/24A	Amphibolite	North of Valladolid	Valladolid	7079-94983
CCR/87/24B	Muscovite pegmatite	North of Valladolid	Valladolid	7079-94984
CCR/87/24C	Muscovite pegmatite	South of Valladolid	Valladolid	7075-94935
CCR/87/24D	Biotite pegmatite	Near Palanda	Valladolid	7074-94868
CRSH/89/10A-D	Garnet-bearing gneisses/migmatites	Float blocks, Río Valladolid	Valladolid	7075-94976
Sabanilla unit orthogneisses, Loja-Zamora road				
CCR/87/23A-H	Biotite orthogneisses	East of Sabanilla	Loja Norte	7199-9562 7199-95588
CRSH/89/12A-C	Biotite orthogneisses	East of Sabanilla	Loja Norte	7199-95587
CRSH/89/12D-J	Migmatitic biotite orthogneisses	East of Sabanilla	Loja Norte	7197-95600
FV57/FV58	Biotite orthogneisses	East of Sabanilla	Loja Norte	7194-95614
Tres Lagunas unit orthogneisses, south of Sigsig				
CCR/87/14A-D	Biotite orthogneisses + igneous xenolith (14C)	Float blocks, Río Santa Bárbara, Peggy Mine	Sigsig	7476-96578
Tres Lagunas unit orthogneisses north margin of Malacatus Basin				
CRSH/89/11A-F	Biotite ± muscovite ± tourmaline granitic orthogneisses	Quebrada La Picota	Nambacola	6917-95396
CRSH/89/11G-J	Biotite ± muscovite ± tourmaline granitic orthogneisses	Quebrada Cobalera	Nambacola	6914-95399
Tres Lagunas unit orthogneisses, Tres Lagunas, east of Saraguro				
CRSH/89/14A-K	Biotite ± muscovite orthogneisses ± aplitic variant (14K)	Río Negro	Saraguro	c. 712-9604
Piedras unit amphibolite				
CRSH/89/5A-B	Amphibolites	Arenillas bridge	Arenillas	6049-96072
Piedras unit, Portovelo amphibolite				
CRSH/89/8A-B	Amphibolites	West of Portovelo	Zaruma	8519-95882
La Victoria unit garnet gneisses				
CRSH/89/6A-E	Garnet-biotite gneisses and felsic pegmatites	Río Piedras north of La Bocana	La Avanzada	6213-95955
La Victoria unit pegmatitic gneisses				
CRSH/89/7A-B	Biotite-muscovite granite and muscovite tourmaline pegmatite	Río El Negro south of La Bocana	Marcabelí	6218-95911
CRSH/89/19	Muscovite-tourmaline pegmatite	Float Block, Río Piedras at La Bocana	Marcabelí	6219-95927

Sample no.	Rock type(s)	Area	Map Sheet*	Grid reference
Marcabelí pluton				
CRSH/89/4A-E	Biotite-muscovite granites	Balsas quarry	Marcabelí	6308-95837
CRSH/89/4F-J	Biotite-muscovite granites	Southwest of Marcabelí	Marcabelí	6188-95775
Zamora batholith				
CCR/87/16A-H	Hornblende granodiorites/hornblende diorites + felsic vein (16D)	La Paz area	Yantzaza	7362-95864 7369-95845
CCR/87/17	Hornblende diorite	Float block, Qda. Curishpe, south of La Paz	Yantzaza	7368-95845
CCR/87/18	Porphyritic hornblende-feldspar andesite	Float block, Qda. Curishpe, south of La Paz	Yantzaza	7368-95845
CCR/87/19	Hornblende granodiorite	Qda. Maycunantza, south of La Paz	Yantzaza	7351-95830
CCR/87/20	Hornblende-biotite granodiorite	South of La Paz	Yantzaza	7340-95783
CCR/87/21A-J	Hornblende-biotite granodiorites + felsic vein (21C) + partially digested xenolith (21D)	South of Qda. Chapintza	Guaysimi	7660-95530
		Paquisha area		7652-95540
CCR/87/22A-F	Pink porphyritic biotite-hornblende (?) monzogranites + hornblende microdiorite (22F)	Río Pituca area and Río Jambue	Zamora	7294-95428 7288-95432
CCR/87/25	Porphyritic hornblende andesite dyke	Palanda-Zumba road	Río Mayo	7074-94804
CCR/87/26A-E	Hornblende-biotite granodiorites/diorites	Palanda-Zumba road	Río Mayo	7074-94809 7075-94781
CRSH/89/13A-B	Hornblende diorites	Río Chicana east of La Paz	Yantzaza	7432-95930
FV60	Porphyritic hornblende granodiorite/diorite	Float block from Guaysimi south of Paquisha	Guaysimi	7575-95527
RM1	Hornblende-biotite granodiorite	Río Mayo	Zumba	7144-94536
FV681	Hornblende-biotite granodiorite	East of Palanda	Valladolid	7218-94880
FV485	Hornblende-biotite granodiorite	Qda. de Los Derrumbes east of Valladolid	Valladolid	7175-94972
Abitagua batholith				
CCR/87/5A-I	Hornblende-biotite granodiorites+felsic material	Cosanga-Tena road (c.55 km north of Tena)	Cosanga (c)	---------
CCR/87/6A, B, D, G-K	Hornblende-biotite granodiorites+felsic vein material	Baños-Puyo road	Mera (c)	8131-98442 8127-98444
CCR/87/6C, E, F	Pink porphyritic hornblende-biotite granodiorites	Baños-Puyo road	Mera (c)	8148-98405 8127-98444
CCR/87/7	Hornblende andesite dike	Baños-Puyo road	Mera (c)	8147-98404
ADML5	Hornblende granodiorite	Float block, Río Zúñag, Baños-Puyo road	Mera (c)	8127-98444
CCR/87/8A-I	Leucogranites ± aplite vein (8I) ± quartz-feldspar pegmatite (8C)	Baños-Puyo road	Baños (c)	8058-98448 8039-98449
CCR/87/9	Biotite granodiorite	Baños-Puyo road	Baños (c)	8039-98450
CCR/87/10A-B	Hornblende-biotite diorites	Baños-Puyo road	Baños (c)	8009-8452
ADML4	Hornblende-biotite diorites	Float block in Río Verde, Baños-Puyo road	Baños (c)	8009-8452
Chingual batholith, Santa Bárbara-La Bonita Road				
CCR/87/2A-J	Biotite orthogneisses	North-west of Pimampiro	Huaca (c)	8869-100605 8871-100595

Sample no.	Rock type(s)	Area	Map Sheet*	Grid reference
Sacha pluton				
CCR/87/3	Hornblende-biotite diorite	Qda. Tungurahua	Huaca (c)	8834-100690
Pimampiro pluton				
CCR/87/1A	Hornblende granodiorite	Near Mataqui	Pimampiro	1744-00420
CCR/87/1C	Hornblende granodiorite	Quebrada Manzanal	Pimampiro	1785-00438
Magtayán pluton				
CCR/87/13A-C	Hornblende-biotite diorites and hornblende gabbro (13B)	Osogochi area	Totoras	7678-97580 7621-97520
Ishpingo pluton, Cuenca-Limón road				
FV83	Biotite granodiorite	-	Principal (c)	7650-96663
San Lucas pluton				
CCR/87/28A-C	Pink porphyritic biotite granodiorites	Quebrada Tuntún	Santiago	6933-95849
FV11	Hornblende granodiorite	Quebrada Bucashi	Santiago	6928-95857
FV15	Hornblende-biotite granodiorite	-	Las Juntas	6948-95785
FV34	Biotite granodiorite	Quebrada El Gallo	Loja Norte	6985-95740
Tampanchi mafic igneous complex				
CRSH/89/17A-C	Hornblende gabbro, pegmatitic hornblendites and hornblende basalt	-	Cola de San Pablo	7625-97080
Catamayo pluton				
CCR/87/29A-B	Biotite granodiorite	Loja-La Toma road	Catamayo (La Toma)	-
Pichinal pluton				
CRSH/89/15	Biotite granodiorite	Río Pinchinal	Saraguro	7045-95999
Pungalá pluton				
CCR/87/12A-C	Hornblende biotite granodiorites	-	Guamote and Riobamba	7680-97965 7680-98000
Portachuela batholith, track from Jimbura to Zumba				
CCR/87/27A-B	Biotite felsic porphyry	-	Laguna Cox	6773-94723
CCR/87/27C-G	Hornblende-biotite granodiorites and diorites	-	Laguna Cox	6755-94744 6745-94765

* 1:50000 Topographic Sheet, published by Instituto Geográfico Militar Quito;

(c) indicates uncontrolled topographic base map without contours (censal)

Rb-Sr ANALYTICAL DATA

Sample no.	Rb (ppm)	Sr (ppm)	$\frac{^{87}Rb}{^{86}Sr}$	$\frac{^{87}Sr}{^{86}Sr}$
Sabanilla unit orthogneisses, near Zamora				
CRSH/89/12A	106.2	188.7	1.6714	0.71801
CRSH/89/12B	97.8	207.8	1.3973	0.71690
CRSH/89/12C	83.7	182.5	1.3628	0.71686
CRSH/89/12D	82.8	178.6	1.3767	0.71671
CRSH/89/12E	104.0	204.9	1.5065	0.71717
CRSH/89/12F	100.3	191.3	1.5575	0.71740
CRSH/89/12G	117.5	209.9	1.6629	0.71742
CRSH/89/12H	87.9	188.6	1.3848	0.71671
CRSH/89/12I	82.7	176.2	1.3946	0.71670
CRSH/89/12J	73.5	214.5	1.0175	0.71596
CCR/87/23A	123	204	1.747	0.71788
CCR/87/23B	110	197	1.601	0.71774
CCR/87/23C	45.2	201	0.6521	0.71436
CCR/87/23D	128	208	1.768	0.71776
CCR/87/23E	119	210	1.633	0.71682
CCR/87/23F	128	192	1.931	0.71716
CCR/87/23G	96.3	231	1.205	0.71546
CCR/87/23H	121	124	2.833	0.72173
Tres Lagunas unit orthogneisses				
CRSH/89/11A	124.5	142.0	2.6054	0.71922
CRSH/89/11B	124.6	138.3	2.6795	0.71994
CRSH/89/11C	129.5	133.8	2.8755	0.71967
CRSH/89/11D	117.5	144.6	2.4150	0.71883
CRSH/89/11E	126.1	137.1	2.7307	0.71975
CRSH/89/11F	131.9	168.0	2.3324	0.71871
CRSH/89/11G	138.7	99.5	4.1415	0.72156
CRSH/89/11H	134.3	131.1	3.0438	0.72075
CRSH/89/11I	135.1	129.4	3.0908	0.72082
CRSH/89/14A	189.7	95.0	5.9439	0.72867
CRSH/89/14B	174.8	106.9	4.8606	0.72590
CRSH/89/14C	186.7	93.3	5.9499	0.72893
CRSH/89/14D	182.7	102.0	5.3283	0.72839
CRSH/89/14E	175.1	97.3	5.3507	0.72684
CRSH/89/14G	186.3	97.7	5.6710	0.72905
CRSH/89/14H	197.0	85.8	6.8323	0.73043
CRSH/89/14I	173.7	103.2	5.0067	0.72579
CRSH/89/14J	169.8	109.9	4.5905	0.72520
CRSH/89/14K	144.7	102.1	4.1989	0.72379
Abitagua batholith				
CCR/87/5A	159	22.7	20.42	0.75183
CCR/87/5B	85.9	285	0.8717	0.70652
CCR/87/5C	156	26.3	17.29	0.74410
CCR/87/5D	87.0	259	0.9730	0.70677
CCR/87/5E	160	23.4	19.85	0.74963
CCR/87/5F	66.5	421	0.4574	0.70560
CCR/87/5G	92.3	389	0.6868	0.70620
CCR/87/5H	103	327	0.9044	0.70664
CCR/87/5I	150	54.1	8.016	0.72298
CCR/87/6B	132	428	0.8886	0.70667
CCR/87/6D	130	98.5	3.821	0.71348
CCR/87/6G	225	15.2	43.31	0.80394
CCR/87/6H	105	355	0.8319	0.70670
CCR/87/6I	93.1	382	0.7041	0.70615
CCR/87/6J	235	10.3	67.85	0.86170
CCR/87/6K	54.9	959	0.1659	0.70494

Sample no.	Rb (ppm)	Sr (ppm)	$\frac{^{87}Rb}{^{86}Sr}$	$\frac{^{87}Sr}{^{86}Sr}$
Zamora batholith, La Paz area				
CCR/87/16D	82.6	46.2	5.190	0.71840
CCR/87/16E	42.7	247	0.5469	0.70609
CCR/87/16F	51.1	238	0.6231	0.70622
CCR/87/16G	14.9	374	0.1160	0.70499
CCR/87/16H	26.1	270	0.2802	0.70530
Zamora batholith, Paquisha area				
CCR/87/21A	66.2	391	0.4904	0.70631
CCR/87/21B	70.7	367	0.5582	0.70665
CCR/87/21D	63.9	432	0.4281	0.70629
CCR/87/21E	79.1	391	0.5844	0.70668
CCR/87/21F	96.7	339	0.8275	0.70734
CCR/87/21G	62.8	364	0.4993	0.70635
Zamora batholith, Río Pituca area				
CCR/87/22A	105	373	0.8170	0.70660
CCR/87/22B	71.8	181	1.139	0.70770
CCR/87/22C	103	387	0.7701	0.70645
CCR/87/22D	107	385	0.8054	0.70649
CCR/87/22E	96.8	388	0.7213	0.70640
CCR/87/22F	59.2	674	0.2545	0.70460
Zamora batholith, Palanda area				
CCR/87/26A	58.6	329	0.5161	0.70617
CCR/87/26B	56.0	335	0.4848	0.70612
CCR/87/26C	53.5	325	0.4863	0.70599
CCR/87/26D	47.3	359	0.3821	0.70592
CCR/87/26E	42.4	353	0.3476	0.70578
Azafrán batholith				
CCR/87/8A	100	86.5	3.345	0.71029
CCR/87/8B	127	70.8	4.817	0.71291
CCR/87/8D	109	77.1	4.074	0.71160
CCR/87/8E	110	75.5	4.229	0.71171
CCR/87/8F	111	71.0	4.495	0.71223
CCR/87/8G	111	80.5	3.984	0.71147
CCR/87/8H	104	60.3	5.004	0.71309
Chingual batholith				
CCR/87/2B	38.2	467	0.2368	0.70414
CCR/87/2C	44.4	353	0.3640	0.70450
CCR/87/2D	43.6	335	0.3999	0.70460
CCR/87/2E	31.6	517	0.1766	0.70406
CCR/87/2F	30.6	507	0.1748	0.70402
CCR/87/2G	31.2	507	0.1779	0.70413
CCR/87/2J	44.7	417	0.3106	0.70428
CCR/87/2J	46.6	405	0.3326	0.70433
San Lucas Pluton				
CCR/87/28A	130	123	3.049	0.70703
CCR/87/28B	154	79.9	5.561	0.70887
CCR/87/28C	82.2	263	0.9165	0.70536

K-Ar analytical data and calculated ages

Sample no.	K (%)	$^{40}Ar_{atm}$ (%)	$^{40}Ar_{rad}$ (nl/g)	Age (Ma)
Garnet gneisses, Agoyán				
CCR/87/11B (mica)	0.135	95.3	0.421	78 ± 33
CCR/87/11D (mica)	0.156	94.6	0.457	74 ± 27
CCR/87/11E (mica)	0.472	79.1	1.413	75 ± 7
Garnet gneisses, amphibolite, Papallacta				
CCR/87/4 (hb)	0.612	19.3	9.563	363 ± 9
‡		39.0	9.794	371 ± 10
CRSH/89/1A (hb)	0.294	76.51	4.301	342 ± 23
‡	0.294	44.89	3.815	306 ± 10
CRSH/89/1B (bt)	5.817	27.13	243.146	844 ± 20
‡	5.741	9.29	253.597	881 ± 44
CRSH/89/1C (msc)	6.965	50.93	20.373	74 ± 3
Sabanilla unit garnet gneisses, Valladolid				
CCR/87/24A (hb)	0.584	64.6	3.012	128 ± 6
‡		71.4	3.178	135 ± 8
CCR/87/24A (bt)	5.38	40.8	16.30	76 ± 3
CCR/87/24B (msc)	8.36	54.8	22.48	77 ± 3
CCR/87/24C (msc)	7.39	51.4	21.6	65 ± 2
CCR/87/24D (bt)	7.09	12.6	20.35	72 ± 2
CCR/89/10A (msc)	6.54	43.85	17.809	69 ± 2
CCR/89/10A (bt)	7.02	28.51	23.672	85 ± 2
CCR/89/10C (msc)	6.50	58.22	18.926	73 ± 3
CCR/89/10C (bt)	7.20	23.56	23.274	81 ± 2
CCR/89/10D (bt)	7.41	32.83	24.085	82 ± 2
Sabanilla unit orthogneisses, Loja-Zamora road				
CCR/87/23D (bt)	7.81	25.7	25.44	82 ± 3
CCR/87/23E (bt)	7.64	22.9	24.93	82 ± 3
CCR/87/23F (bt)	7.58	31.3	24.69	82 ± 3
CRSH/89/12A (msc)	6.09	33.14	15.841	66 ± 2
CRSH/89/12A (bt)	7.82	32.67	26.348	84 ± 3
CRSH/89/12C (msc)	5.72	50.44	14.86	66 ± 2
CRSH/89/12C (bt)	7.78	15.23	26.784	86 ± 2
FV57 (bt)	5.96	27.3	19.7	83 ± 2
FV58 (bt)	6.46	24.6	24.9	97 ± 3
Tres Lagunas unit orthogneisses, south of Sigsig				
CCR/87/14A (bt)	6.03	41.6	19.5	81 ± 3
CCR/87/14D (bt)	6.10	55.0	20.83	86 ± 4
Tres Lagunas unit orthogneisses, Malacatus basin				
CRSH/89/11A (msc)	7.45	44.87	29.642	100 ± 3
CRSH/89/11A (bt)	7.43	85.80	18.996	65 ± 9
CRSH/89/11B (msc)	7.32	18.07	28.793	99 ± 3
CRSH/89/11B (bt)	7.43	67.56	18.531	63 ± 3
CRSH/89/11F (msc)	7.75	32.59	30.615	99 ± 3
CRSH/89/11F (bt)	7.26	46.30	18.827	65 ± 2
Tres Lagunas unit, Tres Lagunas, Saraguro				
CRSH/89/14D (msc)	6.29	61.01	16.812	68 ± 3
CRSH/89/14D (bt)	7.22	25.96	17.619	62 ± 2
CRSH/89/14E (msc)	8.13	36.11	23.584	73 ± 2
CRSH/89/14E (bt)	7.09	33.25	14.109	50 ± 2
CRSH/89/14F (msc)	7.77	47.33	21.186	69 ± 2
CRSH/89/14F (bt)	7.26	43.42	17.725	62 ± 2
Arenillas amphibolites				
CRSH/89/5A (hb)	0.370	91.23	1.062	72 ± 15
CRSH/89/5B (hb)	0.358	76.17	1.051	74 ± 6
‡	0.358	81.36	1.080	76 ± 7

Sample no.	K (%)	$^{40}Ar_{atm}$ (%)	$^{40}Ar_{rad}$ (nl/g)	Age (Ma)
Piedras complex, Portovelo amphibolites				
CRSH/89/8A (hb)	0.07	88.72	0.602	224 ± 34
CRSH/89/8B (hb)	0.05	75.43	1.389	647 ± 37
La Victoria unit, garnet gneisses				
CRSH/89/6B (bt)	6.26	28.24	54.375	211 ± 6
CRSH/89/6C (msc)	7.04	11.08	61.822	213 ± 6
CRSH/89/6D (msc)	5.68	14.82	48.492	207 ± 6
La Victoria unit, pegmatitic gneisses				
CRSH/89/7A (msc)	8.45	32.94	76.941	220 ± 6
CRSH/89/7A (bt)	7.47	8.67	66.548	216 ± 6
CRSH/89/19 (msc)	8.51	15.30	65.994	189 ± 5
Marcabelí pluton				
CRSH/89/4A (msc)	8.405	9.72	74.353	214 ± 6
CRSH/89/4A (bt)	7.497	72.05	61.798	201 ± 12
CRSH/89/4H (msc)	6.997	74.92	55.487	193 ± 13
CRSH/89/4H (bt)	7.651	7.06	70.042	221 ± 6
Zamora batholith				
CCR/87/16C (hb)	0.371	88.5	2.009	134 ± 21
CCR/87/16H (hb)	0.289	71.8	2.107	178 ± 10
CCR/87/17 (hb)	0.277	40.6	1.776	191 ± 10
CCR/87/18 (hb)	0.168	71.9	1.602	230 ± 14
CCR/87/19 (hb)	0.205	50.2	1.581	188 ± 6
CCR/87/20 (hb)	0.591	40.1	4.356	126 ± 4
CCR/87/20 (bt)	2.34	37.3	15.77	166 ± 5
CCR/87/21A (hb)	0.99	64.0	6.134	153 ± 10
CCR/87/21A (bt)	3.93	25.7	24.32	153 ± 4
CCR/87/21G (hb)	0.971	45.6	6.036	153 ± 12
CCR/87/21G (bt)	5.16	25.3	32.78	156 ± 5
CCR/87/22B (bt)	4.7	20.8	34.2	178 ± 5
CCR/87/22E (hb)	0.32	64.2	2.363	181 ± 14
CCR/87/25 (hb)	0.382	34.7	2.208	143 ± 7
CCR/87/26B (hb)	0.499	78.8	3.562	175 ± 14
CCR/87/26B (bt)	4.19	24.1	29.34	172 ± 5
CCR/87/26C (hb)	0.549	78.6	4.172	186 ± 14
CCR/87/26C (bt)	5.21	38.7	39.87	187 ± 6
CCR/87/26E (hb)	0.375	78	2.688	176 ± 13
CCR/87/26E (bt)	2.13	34.1	15.53	178 ± 5
CRSH/89/13A (hb)	0.17	63.96	1.331	193 ± 9
CRSH/89/13B (hb)	0.16	81.95	1.230	187 ± 17
FV60 (hb)	0.570	35.7	3.49	151 ± 5
RM1 (hb)	0.593	59.3	3.161	132 ± 5
RM1 (bt)	4.64	15.9	19.29	104 ± 3
FV681 (hb)	0.916	22.5	5.708	153 ± 5
FV681 (bt)	5.67	23.5	34.53	150 ± 4
FV485 (hb)	0.481	37.6	3.247	166 ± 5
FV485 (bt)	4.04	52.0	28.73	174 ± 6
Abitagua batholith				
CCR/87/5G (hb)	0.849	58.9	4.638	135 ± 8
CCR/87/6A (hb)	0.569	56.6	3.512	152 ± 7
‡		65.3	3.806	164 ± 10
CCR/87/6A (bt)	0.537	73.1	2.724	126 ± 12
CCR/87/7 (hb)	0.323	57.8	2.206	168 ± 8
‡		59.8	2.298	174 ± 8
ADML5 (hb)	0.755	47.6	5.21	169 ± 6

K-Ar analytical data and calculated ages (*continued*)

Sample no.	K (%)	$^{40}Ar_{atm}$ (%)	$^{40}Ar_{rad}$ (nl/g)	Age (Ma)
Azafrán batholith				
CCR/87/8E (bt)	2.54	57.5	4.706	47 ± 2
CCR/87/9 (bt)	5.914	37.2	11.79	51 ± 2
‡		50.3	11.38	49 ± 2
CCR/87/10A (hb)	0.995	64.9	5.145	128 ± 7
CCR/87/10A (bt)	5.02	27.9	25.96	128 ± 4
CCR/87/10B (hb)	0.827	40.0	5.777	171 ± 5
CCR/87/10B (bt)	5.296	14.5	38.02	176 ± 5
ADML4 (hb)	0.757	26.9	5.26	171 ± 5
Chingual batholith				
CCR/87/2C (bt)	6.95	64.5	5.399	20 ± 1
CCR/87/2E (bt)	7.81	54.1	5.672	19 ± 1
‡	6.41	69.1	4.821	19 ± 1
Sacha pluton				
CCR/87/3 (hb)	0.679	73.4	0.904	34 ± 4
‡		63.8	0.816	31 ± 3
CCR/87/3 (bt)	6.629	60.4	6.536	25 ± 1
Pimampiro pluton				
CCR/87/1A (hb)	0.363	59.8	1.172	81 ± 3
‡		77.8	1.142	79 ± 6
CCR/87/1A (bt)	4.27	46.9	14.18	84 ± 3
CCR/87/1C (hb)	0.371	54.4	1.341	91 ± 3
‡		62.3	1.389	94 ± 4
CCR/87/1C (bt)	4.72	21.6	13.71	73 ± 2
‡		58.2	13.73	73 ± 4
Magtayán pluton				
CCR/87/13A (hb)	1.04	51.2	3.066	74 ± 3
CCR/87/13A (bt)	4.08	76.8	10.95	68 ± 5
CCR/87/13B (hb)	0.409	60.1	1.397	86 ± 5
‡		63.5	1.446	89 ± 4
CCR/87/13C (hb)	0.996	47.3	3.139	79 ± 3
Ishpingo pluton, Cuenca-Limón road				
FV83 (bt)	2.31	46.4	3.52	39 ± 4
San Lucas pluton				
CCR/87/28A (bt)	7.18	13.7	16.08	57 ± 2
CCR/87/28B (bt)	7.62	36.9	17.57	58 ± 2
FV11 (bt)	4.84	35.0	9.85	52 ± 2
‡		37.7	9.71	51 ± 2
FV15 (hb)	0.702	69.8	1.82	66 ± 4
‡		63.8	1.70	61 ± 4
FV34 (bt)	6.83	35.8	15.8	59 ± 2
Tampanchi mafic igneous complex				
CRSH/89/17A (hb)	0.53	63.40	1.386	66 ± 3
CRSH/89/17B (hb)	0.51	71.69	1.229	61 ± 4
CRSH/89/17C (wr)	0.12	88.29	0.276	61 ± 10
Catamayo pluton				
CCR/87/29A (bt)	7.18	13.7	16.08	57 ± 2
CCR/87/29B (bt)	7.62	36.9	17.57	58 ± 2
Pichinal pluton				
CRSH/89/15 (bt)	7.11	27.9	15.27	54 ± 4
Pungalá pluton				
CCR/87/12A (hb/bt)	0.264	76.3	0.471	45 ± 4
CCR/87/12B (hb/bt)	1.969	51.9	3.276	42 ± 2
CCR/87/12C (hb)	1.25	53.2	2.080	42 ± 2
CCR/87/12C (bt)	5.07	38.2	8.298	42 ± 1
Portachuela batholith				
CCR/87/27C (bt)	6.56	81.2	3.109	12 ± 1
‡		67.3	3.101	12 ± 1
CCR/87/27C (hb)	0.839	94.3	0.670	20 ± 1
CCR/87/27C (bt)	6.21	77.7	4.055	17 ± 1
CCR/87/27F (hb)	0.508	90.9	0.469	24 ± 5
CCR/87/27F (bt)	6.38	67.2	4.645	19 ± 1
CCR/87/27G (bt)	6.94	61.4	4.893	18 ± 1

The ages were calculated using the decay constants of Steiger and Jaeger (1977)

‡ duplicate analysis
atm atmosphere
bt biotite
hb hornblende
msc muscovite
rad radiogenic
wr whole rock

Sm-Nd analytical data for the La Victoria gneisses

Sample no.	Sm (ppm)	Nd (ppm)	$\frac{^{147}Sm}{^{144}Nd}$	$\frac{^{143}Nd}{^{144}Nd}$
CRSH/89/6A (wr)	5.59	30.63	0.1102	0.512075
CRSH/89/6A (gt)	4.56	14.52	0.1898	0.512220
CRSH/89/6B (wr)	7.63	37.41	0.1232	0.512132
CRSH/89/6B (gt)	6.62	23.54	0.1700	0.512170
CRSH/89/6C (wr)	6.33	34.64	0.1105	0.512074
CRSH/89/6C (gt)	4.22	10.73	0.2377	0.512280
CRSH/89/6D (wr)	7.92	40.13	0.1193	0.512111
CRSH/89/6D (gt)	5.53	16.74	0.1997	0.512245
CRSH/89/6E (wr)	7.23	38.83	0.1126	0.512099
CRSH/89/6E (gt)	4.83	14.93	0.1956	0.512237

wr whole rock
gt garnet

APPENDIX 2

Geochemical data

Locations of analysed samples

Sample No.	Units or area	Locality/Sheet	Grid reference
Ultramafic rocks: El Oro province			
JR363A	Piedras	Arenillas sheet	5908-95973
JR363B	Piedras	Arenillas sheet	5908-95973
RB035G	Palenque	S. Rosa del Oro sheet	6369-96271
JR303	Palenque	S. Rosa del Oro sheet	6333-96244
JR305	Palenque	S. Rosa del Oro sheet	6347-96236
JR397	Palenque	Chilla sheet	6395-96248
JR398	Palenque	Chilla sheet	6395-96248
JR400	Palenque	Chilla sheet	6395-96249
JR231	El Toro	La Avanzada sheet	6286-96033
JR284	El Toro	La Avanzada sheet	6184-96045
JR335	El Toro	Arenillas sheet	6044-96033
JR341	El Toro	La Avanzada sheet	6110-96000
JR342	El Toro	La Avanzada sheet	6110-96000
JR343	El Toro	La Avanzada sheet	6110-96000
JR346	El Toro	Arenillas sheet	6107-95993
Peltetec Ophiolitic Complex: Cordillera Real			
MN61C	Peltetec	Río Blanco road section	7750-98253
MN63	Peltetec	Alao road section	7716-97946
MN65A	Peltetec	Huarguallá irrigation canal	7713-97923
MN61A	Peltetec	Río Blanco road section	7750-98253
MN61B	Peltetec	Río Blanco road section	7750-98253
MN64A	Peltetec	Alao road section	7716-97946
MN64B	Peltetec	Alao road section	7716-97946
MN65C	Peltetec	Huarguallá irrigation canal	7713-97923
Greenstone rocks: Cordillera Real			
MN1A	Maguazo	Cuenca-Limón road	7417-96849
MN1B	Upano	Baeza-Papallacta road	8439-99498
MN1C	Upano	Baeza-Papallacta road	8364-99531
AP01	Alao-Paute	Gualaceo sheet	7428-96843
AP02	Alao-Paute	Gualaceo sheet	7428-96843
AP03	Alao-Paute	Gualaceo sheet	7486-96796
AP04	Alao-Paute	Córdova sheet	7521-96784
AP05	Alao-Paute	Córdova sheet	7221-96784
AP06	Alao-Paute	Córdova sheet	7519-96778
AP07	Alao-Paute	Córdova sheet	7519-96778
AP08	Alao-Paute	Córdova sheet	7524-96776
AP09	Alao-Paute	Córdova sheet	7523-96778
AP10	Alao-Paute	Córdova sheet	7527-96768
AP11	Alao-Paute	Guachapala sheet	7501-96939
AP12	Alao-Paute	Guachapala sheet	7501-96939
AP13	Alao-Paute	Guachapala sheet	7411-96844
AP14	Alao-Paute	Guachapala sheet	7534-96947
AP15	Alao-Paute	Guachapala sheet	7534-96947
AP16	Alao-Paute	Guachapala sheet	7503-96942
AP17	Alao-Paute	Guachapala sheet	7504-96943
AP18	Alao-Paute	Guachapala sheet	7521-96955
AP19	Alao-Paute	Guachapala sheet	7526-96956
AP20	Alao-Paute	Guachapala sheet	7526-96956

Sample No.	Units or area	Locality/Sheet	Grid reference
Tampanchi Complex: Cordillera Real			
MN68	Tampanchi	Cola de S. Pablo sheet	7618-97802
MN69	Tampanchi	Cola de S. Pablo sheet	7618-97802
MN70	Tampanchi	Cola de S. Pablo sheet	7618-97802
Amphibolites: El Oro province			
JR148	Piedras	Zaruma sheet	6532-95889
JR149	Piedras	Zaruma sheet	6529-95888
JR150	Piedras	Zaruma sheet	6523-95885
JR203	Piedras	Paccha sheet	6395-95961
JR206	Piedras	La Avanzada sheet	6349-95964
JR217	Piedras	La Avanzada sheet	6250-95969
JR271	Piedras	La Avanzada sheet	6267-95967
JR275	Piedras	La Avanzada sheet	6205-95974
JR276A	Piedras	La Avanzada sheet	6207-95969
JR339	Piedras	Arenillas sheet	6008-95965
JR349	Piedras	Arenillas sheet	6070-95960
JR295	Arenillas	La Avanzada sheet	6178-96066
JR333	Arenillas	Arenillas sheet	6049-96095
JR347	Arenillas	Arenillas sheet	6064-96061
JR384	Arenillas	Chilla sheet	6582-96285
JR270	Panupali	La Avanzada sheet	6232-95983
JR298	Panupali	Paccha sheet	6398-95968
JR301B	Panupali	La Avanzada sheet	6353-95980
JR357	Panupali	Arenillas sheet	6096-96003
JR358	Panupali	Arenillas sheet	6096-96003
JR359	Panupali	Arenillas sheet	6095-96003
JR360	Panupali	Arenillas sheet	6094-96009
Granitic rocks: El Oro province			
GR01	Marcabelí	Río Puyango	8167-95767
JR54G	Marcabelí	Marcabelí sheet	6324-95859
SH4A	Marcabelí	Marcabelí sheet	6308-95837
SH4C	Marcabelí	Marcabelí sheet	6308-95837
SH4E	Marcabelí	Marcabelí sheet	6308-95837
SH4I	Marcabelí	Marcabelí sheet	6188-95775
JR70G	Marcabelí	Marcabelí sheet	6179-95773
JR323A	El Prado	Zaruma sheet	6610-95785
JR323B	El Prado	Zaruma sheet	6610-95785
JR324	El Prado	Zaruma sheet	6610-95785
JR326A	El Prado	Zaruma sheet	6595-95785
JR326B	El Prado	Zaruma sheet	6595-95785
JR111	Moromoro	Marcabelí sheet	6218-95904
JR280A	Moromoro	La Avanzada sheet	6129-95954
JR280B	Moromoro	La Avanzada sheet	6129-95954
JR281A	Moromoro	La Avanzada sheet	6125-95956
JR281B	Moromoro	La Avanzada sheet	6125-95956
JR283	Moromoro	La Avanzada sheet	6152-95969
JR329	Moromoro	Zaruma sheet	6398-95921
JR330	Moromoro	Zaruma sheet	6398-95921
JR331	Moromoro	Zaruma sheet	6398-95921
JR332	Moromoro	Zaruma sheet	6398-95921
Granitic rocks: Cordillera Real I-types			
CR16D	Zamora	Yantzaza sheet	3690-8534
CR16E	Zamora	Yantzaza sheet	3691-8531
CR16F	Zamora	Yantzaza sheet	3692-8440
CR16G	Zamora	Yantzaza sheet	3692-8440
CR16H	Zamora	Yantzaza sheet	3692-8440
CR21A	Zamora	Guaysimi sheet	6598-5302
CR21B	Zamora	Guaysimi sheet	6598-5302

Sample No.	Units or area	Locality/Sheet	Grid reference
Granitic rocks: Cordillera Real (continued)			
CR21D	Zamora	Guaysimi sheet	6598-5302
CR21F	Zamora	Guaysimi sheet	6551-5329
CR5A	Abitagua	Cosanga sheet	8570-9282
CR5C	Abitagua	Cosanga sheet	8570-9282
CR5D	Abitagua	Cosanga sheet	8570-9282
CR5F	Abitagua	Cosanga sheet	8555-9286
CR5I	Abitagua	Cosanga sheet	8540-9286
CR6B	Abitagua	Mera sheet	8131-8441
CR6E	Abitagua	Mera sheet	8127-8444
CR6G	Abitagua	Mera sheet	8127-8444
CRGJ	Abitagua	Mera sheet	8127-8444
CR6K	Abitagua	Mera sheet	8127-8444
CR8A	Azafrán	Baños sheet	8058-8448
CR8B	Azafrán	Baños sheet	8049-8445
CR8D	Azafrán	Baños sheet	8045-8444
CR8E	Azafrán	Baños sheet	8042-8444
CR8F	Azafrán	Baños sheet	8039-8449
CR8H	Azafrán	Baños sheet	8039-8449
Granitic rocks: Cordillera Real S-types (Tres Lagunas Suite)			
GSH9B	Valladolid	Yangana sheet	0551-0632
SH9E	Valladolid	Yangana sheet	0551-0632
SH9I	Valladolid	Yangana sheet	0495-0551
SH9J	Valladolid	Valladolid sheet	0761-9745
CR23A	Sabanilla	Loja Norte sheet	1990-5870
CR23B	Sabanilla	Loja Norte sheet	1990-5870
CR23C	Sabanilla	Loja Norte sheet	1985-5940
CR23H	Sabanilla	Loja Norte sheet	1978-6235
SH11A	Malacatos	Numbacola sheet	9172-3940
SH11C	Malacatos	Numbacola sheet	9172-3940
SH11D	Malacatos	Numbacola sheet	9172-3940
SH11E	Malacatos	Numbacola sheet	9172-3940
SH11F	Malacatos	Numbacola sheet	9172-3940
SH11H	Malacatos	Gonzanamá sheet	8948-3852
SH16A	Peggy Mine area	Sigsig sheet	4765-5768
SH16B	Peggy Mine area	Sigsig sheet	4765-5768
SH16C	Peggy Mine area	Sigsig sheet	4765-5768
SH16D	Peggy Mine area	Sigsig sheet	4765-5768
SH14A	Saraguro	Saraguro sheet	1285-0522
SH14B	Saraguro	Saraguro sheet	1285-0522
SH14D	Saraguro	Saraguro sheet	1285-0522
SH14G	Saraguro	Saraguro sheet	1285-0522
SH14H	Saraguro	Saraguro sheet	1285-0522
SH14I	Saraguro	Saraguro sheet	1285-0522
SH14J	Saraguro	Saraguro sheet	1315-0475
SH14K	Saraguro	Saraguro sheet	1315-0475
JR385	Baños	Baños sheet	(Río Pastaza between Agoyán Dam and Falls)
JR386	Baños	Baños sheet	

ANALYTICAL RESULTS

ULTRAMAFIC ROCKS: EL ORO PROVINCE

Sample Area / Unit Lithology		JR363A Piedras ultramafic	JR363B Piedras ultramafic	RBO35G Palenque ultramafic	JR303 Palenque ultramafic	JR305 Palenque ultramafic	JR397 Palenque ultramafic	JR398 Palenque ultramafic	JR400 Palenque ultramafic
Major element (fused bead data)									
SiO_2	wt%	40.86	41.11	40.69	40.16	41.19	40.73	41.33	41.69
TiO_2	wt%	0.00	0.00	0.00	0.00	0.00	0.00	0.00	0.00
Al_2O_3	wt%	1.30	1.14	3.13	2.51	1.38	1.36	1.86	1.49
Fe_2O_3t	wt%	8.55	8.62	8.09	8.31	7.44	7.83	7.46	6.96
MnO	wt%	0.10	0.10	0.12	0.11	0.08	0.09	0.10	0.09
MgO	wt%	37.12	38.05	36.44	36.38	38.50	39.11	37.50	39.03
CaO	wt%	0.52	0.18	1.23	0.83	0.03	0.17	0.47	0.05
Na_2O	wt%	0.00	0.00	0.02	0.00	0.00	0.00	0.00	0.00
K_2O	wt%	0.01	0.01	0.06	0.01	0.01	0.01	0.01	0.01
P_2O_5	wt%	0.01	0.00	0.02	0.00	0.00	0.00	0.00	0.01
LOI	wt%	11.66	11.49	10.80	11.85	11.58	11.63	11.30	11.53
Total	**wt%**	**100.13**	**100.70**	**100.60**	**100.16**	**100.21**	**100.93**	**100.03**	**100.86**
Trace element (pressed pellet data)									
V	ppm	40	50	67	63	33	38	49	39
Cr	ppm	3026	3051	2461	3167	2823	3093	3103	3187
Co	ppm	131	136	111	118	132	125	124	118
Ni	ppm	1867	1785	1405	1629	1789	1791	1617	1537
Cu	ppm	16	26	21	44	6	nd	5	3
Zn	ppm	39	47	38	51	46	37	41	31
Rb	ppm	1	nd	2	1	nd	1	2	2
Sr	ppm	3	2	2	6	1	2	14	4
Y	ppm	nd	nd	2	1	nd	nd	1	nd
Zr	ppm	1	4	2	1	nd	1	3	1
Nb	ppm	nd	nd	nd	nd	nd	nd	1	nd
Mo	ppm	1	nd	2	nd	1	nd	nd	nd
Ag	ppm	nd	nd	1	nd	nd	nd	nd	nd
Sn	ppm	nd	nd	nd	nd	nd	nd	0	nd
Sb	ppm	nd	nd	1	6	6	1	1	2
Ba	ppm	23	16	22	27	17	10	17	38
La	ppm	nd	nd	1	nd	nd	nd	0	nd
Ce	ppm	17	5	5	13	19	13	6	14
Pb	ppm	1	nd	1	1	2	1	nd	2
Th	ppm	nd	1	1	nd	nd	1	2	nd
U	ppm	nd	nd	nd	nd	nd	nd	nd	nd
As	ppm	2	6	1	11	20	2	6	5
W	ppm	3	2	2	3	2	3	5	3
Bi	ppm	nd	nd	1	nd	nd	nd	nd	nd

ppm = parts per million; nd = not detected

ANALYTICAL RESULTS (*continued*)

ULTRAMAFIC ROCKS: EL ORO PROVINCE

Sample Area / Unit Lithology		JR231 El Toro ultramafic	JR284 El Toro ultramafic	JR335 El Toro ultramafic	JR341 El Toro ultramafic	JR342 El Toro ultramafic	JR343 El Toro ultramafic	JR346 El Toro ultramafic
Major element (fused bead data)								
SiO_2	wt%	38.21	42.06	40.61	41.17	41.34	41.15	41.30
TiO_2	wt%	0.01	0.05	0.00	0.00	0.00	0.00	0.00
Al_2O_3	wt%	1.17	3.22	1.68	1.75	1.92	1.14	1.08
Fe_2O_3t	wt%	7.86	7.98	8.63	8.58	8.34	8.47	9.01
MnO	wt%	0.10	0.12	0.12	0.12	0.12	0.12	0.12
MgO	wt%	38.53	35.65	38.38	39.53	39.54	41.86	43.73
CaO	wt%	0.87	2.60	0.03	1.57	1.47	1.15	0.78
Na_2O	wt%	0.00	0.04	0.00	0.06	0.04	0.03	0.13
K_2O	wt%	0.01	0.02	0.00	0.01	0.01	0.00	0.01
P_2O_5	wt%	0.04	0.05	0.00	0.02	0.02	0.03	0.02
LOI	wt%	13.85	8.02	11.36	7.10	7.84	6.42	4.68
Total	**wt%**	**100.65**	**99.81**	**100.81**	**99.91**	**100.64**	**100.37**	**100.86**
Trace element (pressed pellet data)								
V	ppm	44	70	56	48	46	42	37
Cr	ppm	3083	2898	2940	3053	3034	3062	3311
Co	ppm	122	102	132	127	128	135	142
Ni	ppm	1685	1262	1531	1645	1654	1791	1883
Cu	ppm	5	55	37	13	3	11	3
Zn	ppm	31	52	49	37	37	36	44
Rb	ppm	nd	nd	nd	nd	1	nd	nd
Sr	ppm	2	10	1	5	5	3	2
Y	ppm	nd	1	nd	nd	nd	nd	nd
Zr	ppm	nd	nd	2	1	nd	nd	1
Nb	ppm	nd	1	nd	nd	nd	nd	nd
Mo	ppm	nd	nd	nd	nd	nd	1	nd
Ag	ppm	nd	2	nd	1	1	2	2
Sn	ppm	nd	nd	nd	nd	nd	nd	nd
Sb	ppm	5	4	1	nd	nd	nd	nd
Ba	ppm	12	15	11	16	17	13	18
La	ppm	nd	nd	nd	nd	nd	nd	nd
Ce	ppm	12	nd	19	10	nd	nd	4
Pb	ppm	1	3	nd	2	nd	nd	5
Th	ppm	1	1	nd	nd	1	nd	1
U	ppm	nd	nd	nd	nd	nd	nd	nd
As	ppm	7	292	14	10	3	4	2
W	ppm	5	5	2	3	3	1	3
Bi	ppm	1	nd	nd	nd	nd	nd	nd

ppm = parts per million; nd = not detected

ANALYTICAL RESULTS (*continued*)

PELTETEC OPHIOLITIC COMPLEX: CORDILLERA REAL

Sample Area / Unit Lithology		MN61C Río Blanco ultramafic	MN64B Peltetec gabbro	MN65A Huarguallá ultramafic	MN61A Río Blanco basalt	MN61B Río Blanco gabbro	MN63 Peltetec ultramafic	MN64A Peltetec gabbro	MN65C Huarguallá basalt
Major element (fused bead data)									
SiO_2	wt%	39.58	45.13	38.97	48.47	45.55	47.01	48.34	48.58
TiO_2	wt%	0.09	0.81	0.09	1.58	1.51	0.00	0.15	0.85
Al_2O_3	wt%	2.36	10.88	1.82	13.71	16.47	0.46	14.58	12.01
Fe_2O_3t	wt%	7.85	11.70	11.30	11.89	10.56	7.94	6.80	11.32
MnO	wt%	0.14	0.17	0.12	0.20	0.19	0.05	0.15	0.16
MgO	wt%	34.16	13.88	36.31	8.13	10.79	33.97	11.17	11.81
CaO	wt%	2.77	10.64	0.17	8.97	9.42	0.34	12.93	8.82
Na_2O	wt%	0.00	1.37	0.00	2.16	2.40	0.00	1.41	2.58
K_2O	wt%	0.01	0.07	0.01	0.08	0.04	0.01	0.40	0.39
P_2O_5	wt%	0.06	0.09	0.06	0.17	0.15	0.03	0.10	0.15
LOI	wt%	13.65	5.27	11.72	5.20	3.85	9.71	4.27	3.77
Total	**wt%**	**100.67**	**100.01**	**100.57**	**100.56**	**100.93**	**99.52**	**100.30**	**100.44**
Trace element (pressed pellet data)									
V	ppm	48	258	104	274	221	20	139	237
Cr	ppm	2269	1164	3187	166	373	2858	516	810
Co	ppm	94	56	146	38	40	125	36	47
Ni	ppm	1601	212	1750	61	166	1448	211	157
Cu	ppm	3	32	297	55	55	10	29	133
Zn	ppm	33	142	46	82	42	40	31	61
Rb	ppm	nd	nd	nd	nd	nd	nd	4	6
Sr	ppm	19	34	4	133	122	1	21	67
Y	ppm	2	13	1	29	30	nd	3	14
Zr	ppm	7	38	nd	85	83	nd	3	42
Nb	ppm	nd	2	nd	2	2	nd	nd	2
Mo	ppm	nd	2	nd	nd	3	nd	3	2
Ag	ppm	nd	2	2	2	3	nd	3	2
Sn	ppm	nd	nd	nd	nd	nd	nd	nd	nd
Sb	ppm	nd	nd	3	nd	nd	nd	nd	nd
Ba	ppm	8	35	27	56	39	12	48	380
La	ppm	2	5	1	6	4	0	1	5
Ce	ppm	12	6	2	8	1	11	1	12
Pb	ppm	nd	1	1	nd	nd	nd	nd	nd
Th	ppm	1	1	nd	1	nd	nd	nd	1
U	ppm	nd	nd	nd	nd	nd	nd	nd	nd
As	ppm	21	1	1	1	3	nd	nd	3
W	ppm	nd	nd	2	2	1	1	2	nd
Bi	ppm	nd	nd	nd	nd	nd	nd	nd	nd

ppm = parts per million; nd = not detected

ANALYTICAL RESULTS (*continued*)

GREENSTONE ROCKS: CORDILLERA REAL

Sample Area / Unit Lithology		MN1A Maguazo basaltic	MN1B Upano basaltic	MN1C Upano andesitic	AP01 Alao-Paute andesitic	AP02 Alao-Paute andesitic	AP03 Alao-Paute basaltic	AP04 Alao-Paute basaltic	AP05 Alao-Paute andesitic
Major element (fused bead data)									
SiO_2	wt%	53.96	53.40	59.59	56.33	58.92	50.74	49.76	54.75
TiO_2	wt%	0.69	0.79	0.63	1.17	1.15	0.87	0.97	0.83
Al_2O_3	wt%	15.21	17.54	16.56	15.52	14.87	17.39	17.10	16.59
Fe_2O_3t	wt%	8.49	8.03	5.16	11.14	10.60	9.06	9.79	7.91
MnO	wt%	0.13	0.16	0.09	0.19	0.19	0.17	0.11	0.14
MgO	wt%	8.54	3.98	3.02	3.45	3.39	6.42	8.29	5.95
CaO	wt%	5.68	5.21	4.32	4.71	3.30	9.39	7.92	7.36
Na_2O	wt%	1.44	2.87	3.84	4.30	4.85	1.79	0.95	3.52
K_2O	wt%	1.25	2.67	1.96	0.11	0.23	1.47	2.21	0.17
P_2O_5	wt%	0.12	0.41	0.20	0.34	0.30	0.27	0.24	0.20
LOI	wt%	4.84	5.32	4.63	3.28	3.15	3.35	3.58	2.96
Total	**wt%**	**100.35**	**100.38**	**100.00**	**100.54**	**100.95**	**100.92**	**100.92**	**100.38**
Trace element (pressed pellet data)									
V	ppm	182	144	86	107	103	200	221	174
Cr	ppm	109	12	74	8	nd	107	154	69
Co	ppm	27	19	15	20	21	22	31	22
Ni	ppm	35	10	27	6	2	51	75	33
Cu	ppm	69	5	34	39	63	67	78	44
Zn	ppm	59	144	63	104	99	67	65	58
Rb	ppm	11	73	31	2	3	52	46	4
Sr	ppm	173	409	264	78	78	589	338	272
Y	ppm	13	14	9	25	25	17	18	14
Zr	ppm	33	116	85	56	56	48	50	56
Nb	ppm	nd	7	5	2	2	4	6	6
Mo	ppm	nd	nd	2	2	3	1	2	nd
Ag	ppm	1	2	1	3	2	3	2	2
Sn	ppm	nd	nd	nd	nd	nd	nd	nd	nd
Sb	ppm	nd	4	1	nd	nd	2	nd	1
Ba	ppm	422	779	479	75	90	554	600	86
La	ppm	4	29	11	4	5	12	12	11
Ce	ppm	12	57	30	9	14	36	29	25
Pb	ppm	4	14	5	nd	nd	nd	1	nd
Th	ppm	1	4	3	1	nd	4	6	4
U	ppm	nd	nd	nd	nd	nd	nd	nd	nd
As	ppm	3	8	nd	nd	2	7	1	nd
W	ppm	nd	nd	nd	3	2	2	2	2
Bi	ppm	nd	nd	nd	nd	nd	nd	nd	nd

ppm = parts per million; nd = not detected

ANALYTICAL RESULTS (*continued*)

GREENSTONE ROCKS: CORDILLERA REAL

Sample Area / Unit Lithology		AP06 Alao-Paute basaltic	AP07 Alao-Paute basaltic	AP08 Alao-Paute andesitic	AP09 Alao-Paute basaltic	AP10 Alao-Paute basaltic	AP11 Alao-Paute basaltic	AP12 Alao-Paute basaltic	AP13 Alao-Paute andesitic
Major element (fused bead data)									
SiO_2	wt%	51.43	48.44	58.41	51.49	51.32	51.93	26.95	57.82
TiO_2	wt%	1.22	0.80	1.44	0.77	1.08	0.82	0.53	0.97
Al_2O_3	wt%	16.58	16.95	14.89	16.70	15.99	16.06	11.44	15.25
Fe_2O_3t	wt%	11.54	10.95	10.31	10.33	8.87	9.38	4.62	5.19
MnO	wt%	0.19	0.20	0.18	0.22	0.18	0.05	0.20	0.10
MgO	wt%	5.45	6.24	3.11	6.48	5.05	7.54	3.73	1.85
CaO	wt%	7.61	11.87	6.88	6.86	9.12	8.33	27.14	14.07
Na_2O	wt%	4.87	2.51	3.11	4.87	4.80	1.12	0.78	0.39
K_2O	wt%	0.11	0.36	0.04	0.05	0.09	0.72	2.09	0.20
P_2O_5	wt%	0.14	0.25	0.30	0.07	0.13	0.25	0.20	0.38
LOI	wt%	1.28	1.52	1.53	2.24	4.07	4.00	21.41	4.05
Total	**wt%**	**100.42**	**100.09**	**100.20**	**100.08**	**100.70**	**100.20**	**99.09**	**100.27**
Trace element (pressed pellet data)									
V	ppm	252	272	150	226	203	188	131	130
Cr	ppm	5	59	6	115	26	146	69	5
Co	ppm	30	32	19	32	31	29	10	8
Ni	ppm	10	17	4	25	19	45	18	5
Cu	ppm	78	190	17	101	111	80	56	24
Zn	ppm	62	78	118	102	65	64	33	24
Rb	ppm	2	3	1	1	1	14	36	7
Sr	ppm	117	432	164	126	215	271	251	155
Y	ppm	21	13	27	15	19	16	11	25
Zr	ppm	60	28	73	36	53	52	28	96
Nb	ppm	2	2	3	nd	nd	4	2	3
Mo	ppm	1	1	2	nd	2	4	1	3
Ag	ppm	3	4	2	2	3	2	4	2
Sn	ppm	nd	nd	nd	nd	nd	nd	nd	nd
Sb	ppm	nd	nd	nd	1	nd	nd	nd	1
Ba	ppm	43	115	40	117	36	204	623	87
La	ppm	4	5	6	4	6	15	6	21
Ce	ppm	11	17	10	7	11	33	14	50
Pb	ppm	nd	nd	nd	2	1	2	nd	1
Th	ppm	nd	1	1	1	2	6	1	10
U	ppm	nd	2	nd	nd	1	1	1	2
As	ppm	nd	nd	nd	3	7	nd	1	nd
W	ppm	2	1	1	nd	2	1	1	5
Bi	ppm	1	nd	nd	nd	nd	nd	1	nd

ppm = parts per million; nd = not detected

ANALYTICAL RESULTS (*continued*)

GREENSTONE ROCKS: CORDILLERA REAL

Sample Area / Unit Lithology		AP14 Alao-Paute basaltic	AP15 Alao-Paute basaltic	AP16 Alao-Paute basaltic	AP17 Alao-Paute basaltic	AP18 Alao-Paute basaltic	AP19 Alao-Paute basaltic	AP20 Alao-Paute basaltic
Major element (fused bead data)								
SiO_2	wt%	46.33	52.07	51.02	50.78	51.14	49.90	49.51
TiO_2	wt%	0.74	0.77	0.78	0.92	0.81	0.78	0.72
Al_2O_3	wt%	14.38	15.11	16.77	17.73	14.94	14.68	13.92
Fe_2O_3t	wt%	8.85	8.83	8.98	8.98	8.75	8.95	8.39
MnO	wt%	0.08	0.07	0.13	0.18	0.16	0.16	0.15
MgO	wt%	11.45	11.50	6.26	4.66	8.65	8.45	10.07
CaO	wt%	9.41	5.22	9.92	8.78	9.67	12.11	12.69
Na_2O	wt%	1.75	1.60	1.72	3.27	3.28	1.54	1.00
K_2O	wt%	0.74	0.24	0.53	1.07	0.14	0.36	0.85
P_2O_5	wt%	0.08	0.10	0.34	0.26	0.09	0.11	0.22
LOI	wt%	6.15	4.72	3.73	3.27	2.28	3.01	2.88
Total	**wt%**	**99.96**	**100.23**	**100.18**	**99.90**	**99.91**	**100.05**	**100.40**
Trace element (pressed pellet data)								
V	ppm	225	236	180	218	178	186	183
Cr	ppm	506	262	161	6	288	472	390
Co	ppm	37	35	23	22	34	32	32
Ni	ppm	98	62	58	13	69	136	100
Cu	ppm	66	53	76	93	77	64	71
Zn	ppm	56	55	65	66	56	52	49
Rb	ppm	12	4	14	29	3	6	14
Sr	ppm	136	122	261	227	48	311	257
Y	ppm	12	14	17	18	16	16	14
Zr	ppm	30	33	53	44	43	40	35
Nb	ppm	2	2	3	3	1	2	3
Mo	ppm	3	1	4	3	1	nd	2
Ag	ppm	2	2	2	2	2	2	3
Sn	ppm	nd	nd	nd	nd	nd	nd	nd
Sb	ppm	nd	nd	nd	nd	nd	nd	nd
Ba	ppm	95	39	246	543	104	237	272
La	ppm	1	5	11	12	4	5	12
Ce	ppm	nd	8	25	26	8	6	21
Pb	ppm	3	3	4	nd	nd	nd	nd
Th	ppm	1	nd	4	4	1	1	4
U	ppm	1	1	1	1	1	nd	2
As	ppm	nd	2	2	1	1	nd	1
W	ppm	2	1	4	nd	1	nd	nd
Bi	ppm	1	nd	1	nd	1	1	nd

ppm = parts per million; nd = not detected

ANALYTICAL RESULTS (*continued*)

TAMPANCHI COMPLEX: CORDILLERA REAL

Sample Area / Unit Lithology		MN68 Tampanchi Pyroxenite	MN69 Tampanchi ultramafic	MN70 Tampanchi diorite
Major element (fused bead data)				
SiO_2	wt%	47.63	39.10	52.99
TiO_2	wt%	0.53	0.09	0.63
Al_2O_3	wt%	5.72	1.16	20.73
Fe_2O_3t	wt%	11.36	10.72	3.56
MnO	wt%	0.19	0.18	0.07
MgO	wt%	15.85	34.32	4.09
CaO	wt%	14.74	3.46	9.85
Na_2O	wt%	0.63	0.02	4.45
K_2O	wt%	0.23	0.02	0.68
P_2O_5	wt%	0.17	0.08	0.31
LOI	wt%	2.30	11.20	1.73
Total	**wt%**	**99.35**	**100.35**	**99.09**
Trace element (pressed pellet data)				
V	ppm	217	45	79
Cr	ppm	321	1805	84
Co	ppm	52	130	11
Ni	ppm	85	636	28
Cu	ppm	165	3	14
Zn	ppm	45	44	27
Rb	ppm	3	1	21
Sr	ppm	65	26	1508
Y	ppm	8	nd	8
Zr	ppm	8	1	132
Nb	ppm	1	nd	9
Mo	ppm	2	nd	1
Ag	ppm	3	1	1
Sn	ppm	nd	nd	nd
Sb	ppm	nd	nd	1
Ba	ppm	64	19	1429
La	ppm	4	nd	44
Ce	ppm	6	nd	97
Pb	ppm	1	nd	7
Th	ppm	1	1	18
U	ppm	nd	nd	nd
As	ppm	1	1	nd
W	ppm	nd	1	1
Bi	ppm	nd	nd	1

ppm = parts per million; nd = not detected

ANALYTICAL RESULTS (*continued*)

AMPHIBOLITES: EL ORO PROVINCE

Sample Area / Unit Lithology		JR148 Piedras amphibolite	JR149 Piedras amphibolite	JR150 Piedras amphibolite	JR203 Piedras amphibolite	JR206 Piedras amphibolite	JR217 Piedras amphibolite	JR271 Piedras amphibolite
Major element (fused bead data)								
SiO_2	wt%	48.01	47.37	49.35	48.32	48.98	49.35	49.76
TiO_2	wt%	1.72	1.66	1.39	0.95	1.39	1.17	1.35
Al_2O_3	wt%	13.77	15.78	16.19	16.51	14.14	14.90	14.65
Fe_2O_3t	wt%	11.33	10.76	8.80	8.62	10.80	9.92	10.69
MnO	wt%	0.19	0.17	0.15	0.14	0.23	0.18	0.26
MgO	wt%	9.15	8.44	8.06	9.38	8.89	8.54	8.58
CaO	wt%	10.68	10.90	11.43	11.74	10.48	11.83	10.82
Na_2O	wt%	2.73	2.88	2.82	2.31	2.82	2.59	2.60
K_2O	wt%	0.08	0.11	0.13	0.09	0.11	0.05	0.20
P_2O_5	wt%	0.21	0.17	0.20	0.10	0.13	0.13	0.12
LOI	wt%	2.21	1.95	1.88	2.12	2.32	1.81	1.63
Total	**wt%**	**100.08**	**100.19**	**100.40**	**100.28**	**100.29**	**100.47**	**100.66**
Trace element (pressed pellet data)								
V	ppm	250	231	195	154	237	204	235
Cr	ppm	325	250	290	323	264	290	271
Co	ppm	34	33	30	38	33	35	36
Ni	ppm	114	87	98	144	60	88	61
Cu	ppm	279	184	3	14	54	6	122
Zn	ppm	64	68	32	49	84	57	125
Rb	ppm	nd	1	2	1	1	1	1
Sr	ppm	95	124	150	127	105	96	104
Y	ppm	32	27	22	16	27	21	24
Zr	ppm	93	99	88	52	74	61	72
Nb	ppm	4	3	6	1	2	2	2
Mo	ppm	nd	2	3	1	1	nd	2
Ag	ppm	3	3	3	2	3	3	3
Sn	ppm	nd	nd	nd	nd	nd	nd	nd
Sb	ppm	nd	nd	nd	nd	1	nd	nd
Ba	ppm	31	34	60	24	34	21	35
La	ppm	6	6	7	4	4	4	1
Ce	ppm	13	11	9	nd	3	2	12
Pb	ppm	1	nd	nd	nd	nd	nd	3
Th	ppm	2	1	nd	1	2	nd	nd
U	ppm	nd	nd	nd	nd	nd	1	1
As	ppm	4	15	1	nd	1	nd	4
W	ppm	4	3	2	1	nd	3	1
Bi	ppm	nd	nd	nd	nd	nd	nd	nd

ppm = parts per million; nd = not detected

ANALYTICAL RESULTS (*continued*)

AMPHIBOLITES: EL ORO PROVINCE

Sample Area / Unit Lithology		JR275 Piedras amphibolite	JR275A Piedras amphibolite	JR339 Piedras amphibolite	JR349 Piedras amphibolite	JR295 Piedras amphibolite	JR333 Piedras amphibolite	JR347 Piedras amphibolite
Major element (fused bead data)								
SiO_2	wt%	49.20	49.47	49.78	48.56	49.08	49.84	49.56
TiO_2	wt%	0.90	0.99	0.92	0.48	1.81	0.95	1.07
Al_2O_3	wt%	15.68	15.61	15.76	15.92	14.19	16.49	16.01
Fe_2O_3t	wt%	9.18	9.64	8.92	6.51	12.23	8.70	9.49
MnO	wt%	0.15	0.16	0.15	0.11	0.19	0.14	0.16
MgO	wt%	8.65	8.53	8.41	11.51	8.23	7.84	7.12
CaO	wt%	12.38	11.78	11.73	12.88	11.07	12.72	14.15
Na_2O	wt%	2.54	2.58	3.03	1.71	2.74	2.16	2.08
K_2O	wt%	0.07	0.09	0.24	0.09	0.08	0.38	0.35
P_2O_5	wt%	0.09	0.10	0.11	0.05	0.17	0.11	0.14
LOI	wt%	1.71	1.61	1.50	2.51	0.98	0.75	0.62
Total	**wt%**	**100.55**	**100.56**	**100.55**	**100.33**	**100.77**	**100.08**	**100.75**
Trace element (pressed pellet data)								
V	ppm	182	185	172	104	294	175	203
Cr	ppm	340	330	348	764	253	422	307
Co	ppm	37	37	36	35	37	34	33
Ni	ppm	88	67	102	200	66	125	98
Cu	ppm	3	32	44	5	48	26	48
Zn	ppm	47	49	55	38	65	58	66
Rb	ppm	1	2	1	2	2	5	5
Sr	ppm	96	138	136	96	89	105	165
Y	ppm	18	19	16	10	31	18	20
Zr	ppm	47	52	49	20	82	44	52
Nb	ppm	2	1	nd	1	2	2	1
Mo	ppm	1	nd	4	nd	nd	nd	3
Ag	ppm	3	2	3	4	4	4	4
Sn	ppm	nd	nd	nd	nd	nd	nd	nd
Sb	ppm	nd	nd	nd	nd	1	nd	nd
Ba	ppm	25	44	41	14	43	95	109
La	ppm	3	0	2	1	3	4	3
Ce	ppm	8	6	3	10	9	9	10
Pb	ppm	nd	1	nd	2	3	3	nd
Th	ppm	1	nd	nd	1	nd	2	1
U	ppm	1	2	nd	nd	nd	1	1
As	ppm	4	3	3	4	1	1	2
W	ppm	1	1	1	1	3	2	2
Bi	ppm	nd	nd	nd	nd	nd	1	nd

ppm = parts per million; nd = not detected

ANALYTICAL RESULTS (*continued*)

AMPHIBOLITES: EL ORO PROVINCE

Sample Area / Unit Lithology		JR384 Arenillas amphibolite	JR270 Panupali amphibolite	JR298 Panupali amphibolite	JR301B Panupali amphibolite	JR357 Panupali amphibolite	JR358 Panupali amphibolite	JR359 Panupali amphibolite	JR360 Panupali amphibolite
Major element (fused bead data)									
SiO_2	wt%	48.27	49.33	49.90	48.60	48.21	47.57	47.34	51.31
TiO_2	wt%	1.96	1.87	1.47	2.92	2.72	2.80	2.60	1.57
Al_2O_3	wt%	16.54	14.49	13.66	14.10	12.94	13.30	12.71	12.98
Fe_2O_3t	wt%	11.24	13.18	11.02	15.22	17.01	17.26	16.49	12.66
MnO	wt%	0.17	0.21	0.16	0.16	0.23	0.30	0.25	0.17
MgO	wt%	6.64	5.73	8.32	5.49	5.09	4.43	5.77	5.74
CaO	wt%	11.26	10.10	8.33	7.89	8.70	8.36	7.27	8.68
Na_2O	wt%	3.00	2.87	3.82	3.72	2.93	3.21	3.94	4.46
K_2O	wt%	0.64	0.54	0.05	0.36	0.73	1.06	0.81	0.18
P_2O_5	wt%	0.28	0.24	0.12	0.29	0.28	0.29	0.22	0.15
LOI	wt%	0.56	2.42	3.24	1.84	2.04	1.73	2.46	1.30
Total	**wt%**	**100.56**	**100.98**	**100.09**	**100.59**	**100.88**	**100.31**	**99.86**	**99.20**
Trace element (pressed pellet data)									
V	ppm	202	265	239	384	365	409	377	257
Cr	ppm	202	91	114	19	12	12	10	120
Co	ppm	33	35	35	33	39	46	44	31
Ni	ppm	101	36	42	26	35	34	29	38
Cu	ppm	17	36	83	48	10	35	58	39
Zn	ppm	86	105	61	119	143	165	132	87
Rb	ppm	18	10	1	7	15	20	12	2
Sr	ppm	440	125	53	140	89	96	77	102
Y	ppm	27	34	25	52	60	58	51	37
Zr	ppm	134	107	77	189	170	165	156	122
Nb	ppm	11	2	1	5	3	3	2	2
Mo	ppm	nd	nd	nd	1	2	1	nd	3
Ag	ppm	4	3	4	4	4	5	5	4
Sn	ppm	nd	nd	nd	nd	4	4	1	nd
Sb	ppm	nd	nd	nd	nd	2	nd	nd	nd
Ba	ppm	201	52	27	375	167	123	71	36
La	ppm	9	3	2	7	7	5	8	3
Ce	ppm	26	12	13	22	15	14	16	17
Pb	ppm	4	nd	nd	nd	1	2	2	3
Th	ppm	1	2	1	1	nd	2	1	1
U	ppm	nd	1	nd	nd	nd	nd	nd	nd
As	ppm	18	1	6	1	7	5	4	5
W	ppm	5	2	2	4	5	5	2	1
Bi	ppm	nd	nd	nd	nd	nd	nd	1	nd

ppm = parts per million; nd = not detected

ANALYTICAL RESULTS (*continued*)

GRANITIC ROCKS: EL ORO PROVINCE

Sample Area / Unit Lithology		GR01 Marcabelí granite	JR54G Marcabelí granite	SH4A Marcabelí granite	SH4C Marcabelí granite	SH4E Marcabelí granite	SH4I Marcabelí granite	JR70G Marcabelí granite	JR323A El Prado granite
Major element (fused bead data)									
SiO_2	wt%	76.75	66.40	72.04	71.87	72.73	71.98	72.18	70.72
TiO_2	wt%	0.03	1.00	0.49	0.45	0.54	0.34	0.32	0.47
Al_2O_3	wt%	13.53	14.71	14.17	14.37	13.60	14.67	14.72	14.56
Fe_2O_3t	wt%	0.96	5.62	3.20	3.15	3.58	2.57	2.54	3.41
MnO	wt%	0.04	0.10	0.07	0.07	0.07	0.06	0.06	0.06
MgO	wt%	0.10	2.45	0.99	1.02	1.10	1.10	1.14	1.66
CaO	wt%	0.39	4.41	1.82	2.15	1.94	2.23	2.32	2.35
Na_2O	wt%	4.39	3.23	3.14	3.37	2.94	3.74	3.72	3.15
K_2O	wt%	3.94	1.68	3.04	2.63	2.93	2.76	2.79	3.09
P_2O_5	wt%	0.05	0.20	0.16	0.16	0.12	0.11	0.10	0.14
LOI	wt%	0.5	0.71	0.92	0.96	0.84	0.79	0.76	0.79
Total	**wt%**	**100.68**	**100.51**	**100.04**	**100.2**	**100.39**	**100.35**	**100.65**	**100.4**
Trace element (pressed pellet data)									
V	ppm	1	83	46	44	57	40	30	41
Cr	ppm	35	58	37	31	32	25	29	40
Co	ppm	nd	13	na	na	na	na	6	8
Ni	ppm	1	16	12	9	12	12	8	21
Cu	ppm	1	19	17	6	6	9	8	14
Zn	ppm	20	62	55	54	58	42	35	50
Rb	ppm	158	60	132	123	132	118	110	136
Sr	ppm	17	144	123	123	104	104	99	114
Y	ppm	28	24	27	23	25	25	22	13
Zr	ppm	49	217	166	167	188	119	116	164
Nb	ppm	7	7	8	9	10	7	6	8
Mo	ppm	nd	1	na	na	na	na	nd	nd
Ag	ppm	nd	2	na	na	na	na	nd	nd
Sn	ppm	1	nd	na	na	na	na	nd	4
Sb	ppm	nd	nd	na	na	na	na	nd	1
Ba	ppm	292	248	492	276	385	444	338	308
La	ppm	10	18	9	9	12	4	13	14
Ce	ppm	28	38	41	34	43	42	41	44
Pb	ppm	18	12	18	16	17	15	14	21
Th	ppm	5	5	7	7	10	7	7	7
U	ppm	3	1	na	na	na	na	3	1
As	ppm	nd	nd	na	na	na	na	0	2
W	ppm	2	2	na	na	na	na	2	2
Bi	ppm	nd	1	na	na	na	na	nd	nd

ppm = parts per million; nd = not detected; na = not analysed

ANALYTICAL RESULTS (*continued*)

GRANITE ROCKS: EL ORO PROVINCE

Sample Area / Unit Lithology		JR323B El Prado granite	JR324 El Prado granite	JR326A El Prado granite	JR326B El Prado granite	JR111 Moromoro granite	JR280A Moromoro granite	JR280B Moromoro granite	JR281A Moromoro granite
Major element (fused bead data)									
SiO_2	wt%	70.29	62.94	70.67	71.94	73.08	73.56	71.52	73.31
TiO_2	wt%	0.46	0.60	0.44	0.45	0.37	0.74	0.73	0.62
Al_2O_3	wt%	14.70	16.30	14.54	14.62	14.42	11.13	11.90	12.97
Fe_2O_3t	wt%	3.30	5.88	3.01	3.12	2.58	5.40	5.74	5.06
MnO	wt%	0.06	0.10	0.07	0.07	0.05	0.12	0.16	0.13
MgO	wt%	1.58	2.80	1.17	1.21	0.96	2.14	2.27	1.51
CaO	wt%	2.35	5.43	1.94	2.09	1.62	1.60	1.42	1.07
Na_2O	wt%	3.19	2.94	3.34	3.35	2.92	1.82	1.75	1.68
K_2O	wt%	3.11	1.98	3.65	3.35	3.22	2.38	2.42	2.59
P_2O_5	wt%	0.15	0.12	0.16	0.17	0.11	0.23	0.09	0.09
LOI	wt%	0.74	0.66	0.59	0.51	1.09	0.73	1.09	1.46
Total	**wt%**	**99.93**	**99.75**	**99.58**	**100.88**	**100.42**	**99.85**	**99.09**	**100.49**
Trace element (pressed pellet data)									
V	ppm	42	107	33	38	39	83	94	74
Cr	ppm	45	46	31	37	55	83	85	100
Co	ppm	9	15	6	7	5	15	18	13
Ni	ppm	18	10	9	9	7	36	35	16
Cu	ppm	15	26	7	9	9	19	20	18
Zn	ppm	52	89	53	56	41	88	83	63
Rb	ppm	138	72	154	154	101	92	91	80
Sr	ppm	120	274	139	132	184	129	119	131
Y	ppm	15	20	21	23	20	23	25	28
Zr	ppm	169	130	152	159	117	187	216	275
Nb	ppm	7	5	9	8	7	13	13	11
Mo	ppm	nd	3	nd	nd	nd	nd	1	nd
Ag	ppm	nd	4	nd	nd	nd	nd	1	nd
Sn	ppm	3	1	5	6	nd	nd	nd	nd
Sb	ppm	2	1	nd	1	nd	nd	nd	nd
Ba	ppm	315	438	325	323	565	759	810	807
La	ppm	15	16	16	16	16	12	25	26
Ce	ppm	48	36	40	47	40	36	60	66
Pb	ppm	17	36	20	22	30	12	9	24
Th	ppm	7	8	8	7	9	6	10	13
U	ppm	nd	1	1	1	1	3	3	1
As	ppm	1	4	2	2	0	3	3	5
W	ppm	2	4	5	5	5	2	2	3
Bi	ppm	nd	nd	nd	nd	1	nd	nd	nd

ppm = parts per million; nd = not detected

ANALYTICAL RESULTS (*continued*)

GRANITE ROCKS: EL ORO PROVINCE

Sample Area / Unit Lithology		JR281B Moromoro granite	JR283 Moromoro granite	JR329 Moromoro granite	JR330 Moromoro granite	JR331 Moromoro granite	JR332 Moromoro granite
Major element (fused bead data)							
SiO_2	wt%	70.21	64.71	72.64	69.19	76.78	80.36
TiO_2	wt%	0.76	0.74	0.35	0.62	0.37	0.33
Al_2O_3	wt%	14.27	17.05	14.68	14.92	12.25	10.59
Fe_2O_3t	wt%	5.34	6.35	2.59	4.11	2.88	2.41
MnO	wt%	0.09	0.12	0.05	0.07	0.05	0.04
MgO	wt%	1.76	2.40	0.77	1.35	0.83	0.64
CaO	wt%	1.61	2.28	2.11	2.14	0.78	0.64
Na_2O	wt%	2.13	2.21	3.99	3.75	1.88	1.81
K_2O	wt%	2.66	2.71	2.81	2.33	2.56	2.42
P_2O_5	wt%	0.11	0.08	0.25	0.35	0.14	0.17
LOI	wt%	1.59	1.88	0.82	1.15	1.49	0.92
Total	**wt%**	**100.53**	**100.53**	**101.06**	**99.98**	**100.01**	**100.33**
Trace element (pressed pellet data)							
V	ppm	93	115	25	44	42	31
Cr	ppm	77	100	29	36	55	47
Co	ppm	15	14	5	8	8	6
Ni	ppm	22	23	4	11	11	7
Cu	ppm	36	14	0	11	14	7
Zn	ppm	68	85	35	60	42	42
Rb	ppm	89	92	83	118	99	89
Sr	ppm	168	198	128	126	81	89
Y	ppm	29	34	13	18	20	16
Zr	ppm	236	218	115	194	212	251
Nb	ppm	11	11	8	11	8	5
Mo	ppm	1	nd	nd	nd	nd	nd
Ag	ppm	1	1	1	nd	nd	nd
Sn	ppm	nd	nd	3	2	3	2
Sb	ppm	1	nd	nd	nd	nd	nd
Ba	ppm	736	553	197	114	364	287
La	ppm	29	33	13	9	22	17
Ce	ppm	70	70	42	28	57	46
Pb	ppm	22	20	28	24	17	15
Th	ppm	14	16	5	3	9	6
U	ppm	1	3	nd	2	3	1
As	ppm	3	2	2	4	3	4
W	ppm	2	5	4	3	4	3
Bi	ppm	nd	nd	nd	nd	nd	nd

ppm = parts per million; nd = not detected

ANALYTICAL RESULTS (*continued*)

GRANITIC ROCKS: CORDILLERA REAL

Sample Area / Unit Lithology		CR16D Zamora I-type	CR16E Zamora I-type	CR16F Zamora I-type	CR16G Zamora I-type	CR16H Zamora I-type	CR21A Zamora I-type	CR21B Zamora I-type	CR21D Zamora I-type	CR21F Zamora I-type
Major element (fused bead data)										
SiO_2	wt%	78.50	65.79	67.36	50.60	54.70	65.22	65.09	53.94	64.97
TiO_2	wt%	0.07	0.43	0.39	1.01	0.68	0.41	0.44	0.63	0.42
Al_2O_3	wt%	12.32	15.26	15.28	19.14	17.41	16.53	16.05	18.59	16.19
Fe_2O_3	wt%	0.53	2.42	2.08	4.66	3.08	2.03	2.03	3.10	1.85
FeO	wt%	0.20	2.32	2.05	4.58	4.63	2.14	2.24	4.73	2.18
MnO	wt%	0.04	0.11	0.10	0.13	0.13	0.09	0.08	0.20	0.12
MgO	wt%	0.01	1.69	1.39	4	4.90	1.52	1.57	3.93	1.76
CaO	wt%	0.35	4.23	4.07	9.20	8.09	4.82	4.24	7.07	2.71
Na_2O	wt%	5.31	4.07	3.99	3.82	3.37	3.78	3.88	4.24	4.08
K_2O	wt%	2.49	1.81	1.95	0.56	0.96	2.18	2.44	1.54	3.12
P_2O_5	wt%	0.07	0.10	0.10	0.11	0.12	0.15	0.14	0.20	0.13
LOI	wt%	0.27	1.34	1.34	1.94	2.02	1.14	1.47	1.86	2.28
Total	**wt%**	**100.16**	**99.57**	**100.10**	**99.75**	**100.09**	**100.01**	**99.67**	**100.03**	**99.81**
Trace element (pressed pellet data)										
S	ppm	85	88	87	385	217	93	99	126	125
Cl	ppm	391	607	552	699	560	354	420	425	366
Ba	ppm	118	781	722	173	307	583	842	595	1133
Rb	ppm	85	46	51	13	24	66	70	63	98
Sr	ppm	48	250	242	374	270	392	368	431	339
Pb	ppm	7	6	5	9	5	7	6	10	13
Th	ppm	38	6	6	2	0	6	8	0	7
Zr	ppm	136	89	99	40	71	92	93	91	90
Nb	ppm	8	5	5	4	5	6	6	7	7
Y	ppm	19	19	17	16	24	17	16	29	18
V	ppm	9	105	88	326	211	64	91	169	76
Cr	ppm	21	16	13	15	36	31	17	14	16
Ni	ppm	4	6	5	12	27	7	6	12	6
Cu	ppm	3	23	20	31	35	6	5	14	6
Zn	ppm	9	30	33	36	46	29	32	59	51
Ga	ppm	11	14	14	18	17	15	16	21	14
La	ppm	25	7	4	3	3	10	6	1	7
Ce	ppm	41	11	23	11	16	16	6	3	14
Nd	ppm	9	16	26	11	17	8	11	9	11

ppm = parts per million

ANALYTICAL RESULTS (*continued*)

GRANITIC ROCKS: CORDILLERA REAL

Sample Area / Unit Lithology		**CR5A Abitagua I-type**	**CR5C Abitagua I-type**	**CR5D Abitagua I-type**	**CR5F Abitagua I-type**	**CR5I Abitagua I-type**	**CR6B Abitagua I-type**	**CR6E Abitagua I-type**	**CR6G Abitagua I-type**
Major element (fused bead data)									
SiO_2	wt%	77.65	77.57	73.28	68.64	76.97	65.40	74.71	75.57
TiO_2	wt%	0.06	0.06	0.23	0.35	0.07	0.54	0.14	0.13
Al_2O_3	wt%	12.65	12.53	14.12	16.10	12.65	16.41	13.39	12.65
Fe_2O_3	wt%	0.47	0.62	0.88	1.25	0.49	1.39	0.81	1.10
FeO	wt%	0.29	0.28	0.93	1.60	0.33	2.32	0.92	0.65
MnO	wt%	0.08	0.08	0.05	0.09	0.03	0.09	0.07	0.07
MgO	wt%	0.01	0.01	0.33	0.75	0.01	1.17	0.17	0.10
CaO	wt%	0.38	0.39	1.62	3.02	0.62	3.23	0.58	0.47
Na_2O	wt%	3.87	3.80	3.82	4.73	3.95	3.51	3.94	3.77
K_2O	wt%	4.47	4.41	3.69	2.63	4.44	5.08	4.66	5.07
P_2O_5	wt%	0.03	0.03	0.09	0.14	0.03	0.19	0.05	0.03
LOI	wt%	0.32	0.35	0.65	0.89	0.28	0.69	0.61	0.21
Total	**wt%**	**100.28**	**100.13**	**99.69**	**100.19**	**99.87**	**100.02**	**100.05**	**99.82**
Trace element (pressed pellet data)									
S	ppm	80	80	86	79	82	150	126	159
Cl	ppm	227	215	204	430	242	373	327	171
Ba	ppm	144	173	1515	1342	143	1218	407	39
Rb	ppm	163	161	87	66	154	134	166	236
Sr	ppm	24	27	261	425	55	432	108	16
Pb	ppm	18	18	10	10	20	20	15	40
Th	ppm	17	14	4	3	19	5	16	30
Zr	ppm	71	71	111	141	93	207	140	175
Nb	ppm	10	10	5	5	8	11	10	16
Y	ppm	18	18	11	12	21	22	28	44
V	ppm	7	0	22	29	1	52	8	7
Cr	ppm	24	23	26	17	26	22	18	39
Ni	ppm	2	2	3	2	2	5	3	142
Cu	ppm	0	0	4	11	3	22	3	23
Zn	ppm	23	21	41	40	20	53	32	55
Ga	ppm	13	14	13	14	11	17	12	10
La	ppm	2	19	10	7	31	27	28	40
Ce	ppm	29	40	10	12	58	38	58	101
Nd	ppm	8	11	5	13	13	22	25	46

ppm = parts per million; nd = not detected

ANALYTICAL RESULTS (*continued*)

GRANITIC ROCKS: CORDILLERA REAL

Sample Area / Unit Lithology		CR6J Abitagua I-type	CR6K Azafrán I-type	CR8A Azafrán I-type	CR8B Azafrán I-type	CR8D Azafrán I-type	CR8E Azafrán I-type	CR8F Azafrán I-type	CR8H Azafrán I-type
Major element (fused bead data)									
SiO_2	wt%	75.67	57.30	76.04	76.37	76.52	76.33	76.20	75.88
TiO_2	wt%	0.13	0.61	0.12	0.13	0.12	0.11	0.11	0.08
Al_2O_3	wt%	12.86	20.07	13.09	13.02	12.87	13.00	12.97	13.16
Fe_2O_3	wt%	0.66	2.08	0.67	0.43	0.56	0.54	0.52	0.62
FeO	wt%	0.72	3.86	0.47	0.53	0.47	0.53	0.53	0.44
MnO	wt%	0.05	0.16	0.09	0.08	0.08	0.10	0.10	0.11
MgO	wt%	0.10	1.79	0.06	0.08	0.10	0.07	0.03	0.03
CaO	wt%	0.54	5.94	0.83	0.82	0.52	0.75	0.73	0.54
Na_2O	wt%	3.84	4.75	3.93	3.85	4.02	3.96	3.96	4.34
K_2O	wt%	5.09	2.14	4.36	4.46	4.31	4.42	4.42	4.29
P_2O_5	wt%	0.03	0.32	0.04	0.04	0.04	0.04	0.04	0.04
LOI	wt%	0.26	0.83	0.42	0.41	0.42	0.39	0.40	0.32
Total	**wt%**	**99.95**	**99.85**	**100.12**	**100.22**	**100.03**	**100.24**	**100.01**	**99.85**
Trace element (pressed pellet data)									
S	ppm	88	104	82	88	80	84	85	82
Cl	ppm	467	301	202	147	206	233	221	232
Ba	ppm	74	1385	747	457	571	675	638	746
Rb	ppm	242	52	103	130	110	112	114	109
Sr	ppm	12	955	90	78	80	78	74	63
Pb	ppm	19	13	13	13	14	11	11	18
Th	ppm	22	0	9	13	11	11	15	11
Zr	ppm	158	159	95	81	79	91	98	99
Nb	ppm	16	8	12	14	13	12	17	14
Y	ppm	37	19	13	14	14	15	19	18
V	ppm	3	73	10	14	1	7	0	4
Cr	ppm	21	15	17	23	18	25	22	27
Ni	ppm	2	6	2	3	2	2	3	1
Cu	ppm	3	12	0	2	0	0	1	1
Zn	ppm	22	84	32	25	24	23	22	27
Ga	ppm	12	19	13	13	11	13	12	12
La	ppm	42	12	5	1	5	16	8	11
Ce	ppm	80	41	8	7	18	29	12	21
Nd	ppm	26	19	5	7	13	15	9	8

ppm = parts per million

ANALYTICAL RESULTS (*continued*)

GRANITIC ROCKS: CORDILLERA REAL (TRES LAGUNAS SUITE)

Sample Area / Unit Lithology		SH9B Valladolid S-type	SH9E Valladolid S-type	SH9I Valladolid S-type	SH9J Valladolid S-type	CR23A Sabanilla S-type	CR23B Sabanilla S-type	CR23C Sabanilla S-type	CR23H Sabanilla S-type
Major element (fused bead data)									
SiO_2	wt%	74.20	73.77	73.09	72.47	71.32	71.42	78.34	73.21
TiO_2	wt%	0.51	0.53	0.48	0.51	0.74	0.71	0.54	0.50
Al_2O_3	wt%	12.93	13.71	13.41	14.17	12.93	13.15	10.09	13.22
Fe_2O_3	wt%	0.89	0.77	0.48	0.61	0.53	0.16	0.32	0.57
FeO	wt%	2.95	2.89	2.96	3.23	3.70	3.78	2.13	2.94
MnO	wt%	0.08	0.05	0.10	0.06	0.06	0.06	0.07	0.10
MgO	wt%	1.34	1.04	1.27	1.15	1.93	1.75	1.09	1.36
CaO	wt%	0.59	0.54	1.23	1.04	2.23	2.38	3.74	1.47
Na_2O	wt%	1.75	1.45	2.51	2.02	2.24	2.40	1.44	2.30
K_2O	wt%	3.22	3.15	3.28	3.28	3.03	2.63	1.11	3.14
P_2O_5	wt%	0.14	0.16	0.17	0.18	0.17	0.20	0.16	0.16
LOI	wt%	1.44	1.92	1.04	1.47	1.05	1.10	0.74	1.03
Total	**wt%**	**100.04**	**99.98**	**100.02**	**100.19**	**99.93**	**99.74**	**99.77**	**100.00**
Trace element (pressed pellet data)									
S	ppm	93	95	299	369	133	146	252	353
Cl	ppm	207	181	199	114	129	122	92	93
Ba	ppm	1007	532	733	582	589	479	236	651
Rb	ppm	141	143	131	139	125	112	46	125
Sr	ppm	76	86	134	118	206	201	205	127
Pb	ppm	25	20	23	31	20	15	7	19
Th	ppm	7	9	9	10	9	9	8	7
Zr	ppm	135	191	160	157	258	232	295	183
Nb	ppm	10	11	10	12	14	14	10	11
Y	ppm	21	23	22	26	29	25	23	23
V	ppm	84	80	77	87	103	91	49	78
Cr	ppm	84	87	104	77	58	59	47	64
Ni	ppm	197	174	207	150	24	23	15	19
Cu	ppm	13	10	18	13	11	12	19	19
Zn	ppm	66	74	76	67	73	71	42	65
Ga	ppm	15	18	17	18	15	16	11	15
La	ppm	9	3	15	12	20	23	12	9
Ce	ppm	29	21	26	42	51	42	47	33
Nd	ppm	25	14	16	23	19	24	32	22

ppm = parts per million

ANALYTICAL RESULTS (*continued*)

GRANITIC ROCKS: CORDILLERA REAL (TRES LAGUNAS SUITE)

Sample Area / Unit Lithology		SH11A Malacatus S-type	SH11C Malacatus S-type	SH11D Malacatus S-type	SH11E Malacatus S-type	SH11F Malacatus S-type	SH11H Malacatus S-type	SH16A Peggy S-type	SH16B Peggy S-type
Major element (fused bead data)									
SiO2	wt%	70.20	70.52	69.85	69.97	68.51	70.01	71.01	70.99
TiO_2	wt%	0.71	0.68	0.72	0.64	0.75	0.71	0.55	0.55
Al_2O_3	wt%	13.67	13.64	13.53	13.98	14.10	13.87	13.67	13.73
Fe_2O_3	wt%	0.95	0.72	0.86	0.72	0.99	0.78	0.65	0.82
FeO	wt%	3.52	3.59	3.73	3.39	3.80	3.69	2.58	2.52
MnO	wt%	0.10	0.10	0.10	0.10	0.10	0.12	0.11	0.09
MgO	wt%	1.65	1.57	1.73	1.52	1.83	1.70	1.15	1.13
CaO	wt%	1.96	1.87	1.95	1.89	2.26	1.51	1.82	1.85
Na_2O	wt%	2.46	2.44	2.33	2.71	2.42	2.39	2.45	2.59
K_2O	wt%	3.18	3.25	3.14	3.19	3.28	3.44	4.21	3.82
P_2O_5	wt%	0.18	0.17	0.17	0.17	0.17	0.17	0.16	0.17
LOI	wt%	1.54	1.55	1.59	1.51	1.60	1.64	1.32	1.58
Total	**wt%**	**100.12**	**100.10**	**99.70**	**99.79**	**99.81**	**100.03**	**99.68**	**99.84**
Trace element (pressed pellet data)									
S	ppm	884	744	1275	1211	481	811	298	306
Cl	ppm	104	104	92	93	104	95	133	163
Ba	ppm	818	818	861	781	844	982	1024	660
Rb	ppm	128	132	121	129	134	138	150	158
Sr	ppm	146	136	147	139	171	133	132	114
Pb	ppm	22	20	22	23	18	37	45	33
Th	ppm	14	12	13	11	11	13	12	13
Zr	ppm	193	197	200	168	210	197	178	175
Nb	ppm	11	12	11	11	13	12	11	12
Y	ppm	33	32	34	29	31	30	32	35
V	ppm	100	101	94	97	107	105	65	55
Cr	ppm	107	95	101	89	99	92	39	35
Ni	ppm	212	217	199	206	210	180	13	12
Cu	ppm	23	29	24	16	23	19	13	13
Zn	ppm	78	81	77	69	81	148	51	60
Ga	ppm	20	17	17	16	17	19	14	15
La	ppm	29	29	29	23	20	23	21	15
Ce	ppm	54	52	58	54	66	60	35	73
Nd	ppm	23	30	19	28	35	33	12	47

ppm = parts per million

ANALYTICAL RESULTS (*continued*)

GRANITIC ROCKS: CORDILLERA REAL (TRES LAGUNAS SUITE)

Sample Area / Unit Lithology		**SH16C Peggy S-type**	**SH16D Saraguro S-type**	**SH14A Saraguro S-type**	**SH14B Saraguro S-type**	**SH14D Saraguro S-type**	**SH14G Saraguro S-type**	**SH14H Saraguro S-type**	**SH14I Saraguro S-type**
Major element (fused bead data)									
SiO_2	wt%	71.38	71.09	71.88	70.89	72.74	73.16	71.40	71.18
TiO_2	wt%	0.58	0.59	0.55	0.55	0.53	0.45	0.52	0.53
Al_2O_3	wt%	13.47	13.56	13.55	14.28	13.30	13.44	13.87	13.68
Fe_2O_3	wt%	0.90	0.86	0.76	0.91	0.45	0.50	0.74	0.79
FeO	wt%	2.60	2.70	2.57	2.38	2.62	2.20	2.53	2.48
MnO	wt%	0.09	0.10	0.08	0.07	0.07	0.06	0.07	0.07
MgO	wt%	1.24	1.20	1.03	1.04	0.96	0.79	1.01	1.04
CaO	wt%	1.63	1.82	1.65	1.73	1.47	1.41	1.54	1.59
Na_2O	wt%	2.46	2.59	2.53	2.85	2.49	2.55	2.66	2.49
K_2O	wt%	3.92	3.56	4.05	4.17	4.44	4.53	4.17	4.33
P_2O_5	wt%	0.16	0.17	0.18	0.18	0.19	0.19	0.20	0.19
LOI	wt%	1.46	1.52	1.23	1.17	0.96	1.01	1.23	1.20
Total	**wt%**	**99.89**	**99.76**	**100.06**	**100.22**	**100.22**	**100.29**	**99.94**	**99.57**
Trace element (pressed pellet data)									
S	ppm	443	279	351	353	316	223	407	366
Cl	ppm	101	157	145	118	113	166	150	132
Ba	ppm	723	641	535	775	659	756	481	809
Rb	ppm	171	153	196	181	189	192	206	181
Sr	ppm	115	116	95	109	104	98	86	105
Pb	ppm	25	22	21	24	27	26	23	26
Th	ppm	13	14	15	13	12	10	14	16
Zr	ppm	181	188	185	169	177	155	179	178
Nb	ppm	12	12	13	13	12	10	13	12
Y	ppm	34	38	41	40	40	34	40	38
V	ppm	64	70	57	57	57	52	59	46
Cr	ppm	39	38	35	33	37	32	37	34
Ni	ppm	13	15	13	14	11	12	15	12
Cu	ppm	13	13	14	10	12	10	12	12
Zn	ppm	58	59	63	61	52	52	71	62
Ga	ppm	16	16	16	14	14	15	18	15
La	ppm	15	18	12	18	18	15	15	12
Ce	ppm	57	44	64	58	56	38	54	59
Nd	ppm	37	25	30	30	30	18	29	29

ppm = parts per million

ANALYTICAL RESULTS (*continued*)

GRANITIC ROCKS: CORDILLERA REAL (TRES LAGUNAS SUITE)

Sample Area / Unit Lithology		SH14J Saraguro S-type	SH14K Saraguro S-type	JR385 Baños S-type	JR386 Baños S-type
Major element (fused bead data)					
SiO_2	wt%	71.95	68.49	72.23	73.04
TiO_2	wt%	0.54	0.99	0.36	0.31
Al_2O_3	wt%	13.62	14.24	14.36	14.07
Fe_2O_3	wt%	0.89	1.89	2.39	2.12
FeO	wt%	2.29	2.74	Na	Na
MnO	wt%	0.06	0.09	0.03	0.02
MgO	wt%	1.04	1.25	0.77	0.66
CaO	wt%	1.58	2.84	2.29	2.08
Na_2O	wt%	2.50	3.56	3.19	3.07
K_2O	wt%	4.51	2.53	3.60	3.80
P_2O_5	wt%	0.19	0.28	0.13	0.14
LOI	wt%	1.09	1.06	1.16	1.09
Total	**wt%**	**100.26**	**99.96**	**100.51**	**100.40**
Trace element (pressed pellet data)					
S	ppm	388	363	na	na
Cl	ppm	141	130	na	na
Ba	ppm	874	259	595	669
Rb	ppm	176	151	113	113
Sr	ppm	111	104	187	184
Pb	ppm	28	23	9	9
Th	ppm	16	22	10	10
Zr	ppm	184	343	142	136
Nb	ppm	12	16	7	7
Y	ppm	38	62	26	24
V	ppm	54	89	28	25
Cr	ppm	32	65	8	6
Ni	ppm	13	208	5	4
Cu	ppm	16	8	8	6
Zn	ppm	57	85	20	17
Ga	ppm	15	19	na	na
La	ppm	21	31	18	16
Ce	ppm	49	105	51	44
Nd	ppm	25	47	na	na

ppm = parts per million; na = not analysed

GEOLOGICAL INDEX

Pages in bold are those containing the main description of the item

ISBN 0-85272-239-7

Natural
Environment
Research
Council